# Biomechanical form and function in primate seed predators: Common solutions for similar mechanical challenges?

Emily M. Hunter

PhD in Human Sciences

The University of Hull and the University of York

The Hull York Medical School

March 2021

## Abstract

Seed predation, as seen in a diverse range of primate species, is a specialist diet in which seeds are accessed via the breakdown of stress-resistant external protective layers. This diet is considered mechanically challenging, requiring high forces and wide gapes to successfully fracture seed casings and gain access to nutrients. It is expected that seed predators will possess anatomical features which facilitate the breakdown of large, hard items. The biomechanical function of seed predator morphology relative to other primates is not known, nor is it known if members of this group converge on the same morphologies. This study examines the masticatory morphology of a diverse range of primate seed predators by combining 1) geometric morphometrics and convergence testing, 2) biomechanical modelling and 3) direct physical testing of tooth performance.

Comparisons between different seed predator masticatory morphologies demonstrate some convergence in shape, but other factors including body size, prognathism, and dental morphology appear to enable different solutions to the same mechanical problem. Smaller-bodied seed-predators primarily show adaptations for high mechanical advantage, while larger-bodied seed predators have large muscle cross-sectional area but low mechanical advantage. The dentition of some seed predators requires less force to fracture hard brittle seeds than non-seed predators. Surprisingly, some non-seed predators also possess features which are advantageous to hard food consumption, while one intensive seed predator has poor performance on nearly all measurements.

This study suggests no common solution for seed predation, but instead proposes multiple morphologies capable of meeting the demands of this diet. Results presented here also highlight the need to consider the masticatory system as a whole, as both muscle force capacity and dental occlusal surface impact food breakdown. Without considering these different components of the masticatory apparatus it is not possible to fully appreciate the potential for functional equivalence in this system.

# Table of contents

## List of figures

## List of tables

# Acknowledgements

## Author's Declaration

I confirm that this work is original and that if any passages or diagrams have been copied from academic papers, books, the internet or any other sources these are clearly identified by the use of quotation marks and the references is fully cited. I certify that, other than where indicated, this is my own work and does not breach the regulations of HYMS, the University of Hull or the University of York regarding plagiarism or academic conduct in examinations. I have read the HYMS Code of Practice on Academic Misconduct, and state that this piece of work is my own and does not contain any unacknowledged work from any other sources.

# Chapter 1 - Introduction and Literature review

## 1.1 Introduction

In biological systems form and function are considered to be closely linked (Wainwright, 2009). Masticatory morphology is no exception. Animals have to consume sufficient food to meet their nutritional needs, so anatomical features which can optimise their ability to sense, capture, access, and break down the foods should be advantageous. Specialisation of organisms towards specific food sources is often considered one of the major causes of evolution in form and function (Herrel et al., 2008; Grossnickle, 2020). Within the animal kingdom such specialisations can be seen in the diversity of beak shapes in waterfowl (Olsen, 2017), head shape in natricine snakes (Herrel et al., 2008), and rodent masticatory muscle configuration (Cox et al., 2012). These features affect feeding performance and so are often considered adaptations to particular dietary niches.

Primates live in a range of different environments, from open savannahs to dense rain forests. Their diets vary in their physical properties and access challenges, including such diverse examples as tough grasses in *Theropithecus gelada,* gnawing for exudate extraction in *Callithrix jacchus*, hunting and eating a range of small vertebrates in *Cebus capucinus*, and seeds encased in large, hard shells as seen in *Cacajao calvus* (Dunbar and Dunbar, 1974; Eng et al., 2009; Norconk et al., 2013; de Oliveira et al., 2014). These primates all possess features which enable, and perhaps enhance, their food processing capabilities such as internal muscle architecture geared for high force and wide gape bites in *Callithrix jacchus* or the enamel shearing crests on the dentition of *Theropithecus gelada* which efficiently comminute grass particles (Eng et al., 2009; Venkataraman et al., 2014). However, the extent to which primates are morphologically adapted to their diets is a large area of scientific study and debate (Ross and Iriarte-Diaz, 2014, 2019; Terhune, Cooke, et al., 2015; Berthaume et al., 2020). The relationship between masticatory form and function is highly complex, constrained by variables such as phylogeny and non-feeding behaviours, making it extremely challenging to predict function from form (Wainwright, 2009; Ross and Iriarte-Diaz, 2014). For a species to consume a given diet, especially one which is mechanically challenging, it would have to possess the correct tools to do so. Without sufficient jaw opening or ample bite force to break down a food item, the individual would simply fail to

consume it. What we do not know however is, when presented with the same challenge, will primates solve dietary constraints in the same way: do some primates converge in form and/or functional performance? Are there many primate morphologies which consume the same food type? These questions also have applications beyond the fields of biomechanics and anatomy as extant species are often used as models for predicting fossil hominin diets (Wroe et al., 2005c; Elton, 2006; Daegling et al., 2011; Thiery et al., 2017). As such, an improved understanding of how masticatory form relates to dietary adaptations could also inform predictive models on extinct species.

There are many studies of masticatory form and function primates (e.g. Hylander, 1979; Daegling and Mcgraw, 2007; Eng et al., 2009; Berthaume et al., 2010; Terhune et al., 2015; Ross et al., 2016, 2017; Taylor et al., 2018). These studies have examined how masticatory form alters kinematics (Ross et al., 2017), bone strain (Hylander, 1979; Daegling and W Scott McGraw, 2007), mechanical advantage (Taylor et al., 2018), gape (Eng et al., 2009), quantified morphology and related them to dietary groups (Terhune, Cooke, et al., 2015), and tested how food breaks down differently based on dental morphology (Berthaume et al., 2010). Crucially however, these studies make an omission as they mainly study the lever system (jaws and muscles), or the morphology of the teeth in isolation, and very few have directly studied the breakdown performance of the dentition. A more holistic understanding, considering both muscle configuration and the dental morphology in the context of food breakdown, provides an opportunity for a more complete understanding of primate adaptations for feeding.

It is possible that dietary extremists provide especially clear examples of form-function links to meet the demands of their exceptional diets. A diet consisting of hard, stress-resistant objects such as seeds is a mechanically challenging extreme, yet this challenge is met by primate seed predators of differing sizes, sexes, and morphologies across the phylogeny (Norconk et al., 2013). How these primates achieve this feat is not fully understood.

## 1.2 The masticatory system

The oral cavity is the part of the masticatory system which serves as the entry point of food into the digestive system. It is the pathway by which nutrients are accessed, generally by the comminution of food particles to a size that they may be swallowed (Kay, 1975; Lucas, 2004;

Chen, 2009; Moore, 2014). In mammals the basic elements of the masticatory apparatus comprise the upper and lower jaw (skeletal elements) which house the mandibular and maxillary teeth. Masticatory muscles attach between the mandible and cranium (Hylander, 2006; Moore, 2014). These muscles generate forces used to move the mandible and produce an effective biting force at the teeth (Hylander, 2006; Moore, 2014).

## 1.2.1 Skeletal components of the masticatory apparatus

The bony mandible and cranium are connected via the left and right temporomandibular joint (TMJ). The anatomy of these skeletal structures varies widely in size and shape within mammals and among primates (Fig. 1.1). The TMJ is a bilateral modified hinge-type synovial joint and is formed by the articular surface of the temporal bone of the cranium and the condyles of the mandible, which are enclosed by an articular capsule (Hylander, 2006). Between these surfaces of the joint sits an articular disc of fibrocartilage which assists in distributing loads during feeding (Hylander, 2006). TMJ anatomy facilitates the rotation and translation of the mandible, but the degree of movement and subsequent kinematics of the mandible has been shown to vary significantly in different species (Lucas, 2004; Hylander, 2006).

**Figure 1.1 Diverse morphologies in mammalian cranio-mandibular skeletal form. Showing, from top left:** *Crocruta crocruta*, **the spotted hyena; Equus ferus, the horse;** *Chrotopterus auritus*, **the big-eared woolly bat;** *Papio anubis*, **the olive baboon;** *Gorilla gorilla*, **the western gorilla, and** *Saimiri sciureus*, **the squirrel monkey. Images not to scale.** *Image sources, from top left: Klaus Rassinger for the Museum Wiesbaden under a CC BY-SA-3.0 license (https://commons.wikimedia.org/wiki/File:Crocuta_crocuta_02_MWNH_249.jpg); public domain (https://commons.wikimedia.org/wiki/File:Cr%C3%A2ne_cheval.jpg); Santana and Cheung, 2016; Johnston, 2003; Didier Descouens for the Museum de Toulouse, distributed under a CC BY-SA 4.0 license (https://de.wikipedia.org/wiki/Datei:Gorilla_gorilla_skull.jpg); Berkovitz and Shellis, 2018.*

## 1.2.2 Muscles of mastication

In primates, the primary muscles involved in mastication, often collectively referred to as the muscles of mastication or jaw adductors, are masseter, temporalis, medial and lateral pterygoid (Hylander, 2006). Numerous other muscles also play smaller but still significant roles in feeding by stabilising and optimising the masticatory system, and include muscles of the tongue, face, and neck (Lucas, 2004; Moore, 2014). As reflected by the range in mammalian cranio-mandibular skeletal morphologies, masticatory muscles vary in their external anatomy; positions relative to the teeth and TMJ, orientation, shape and size (Fig. 1.2). The masseter is typically a relatively quadratic muscle with deep and superficial heads which have an origin along the zygomatic arch and attach along the mandibular angle (Hylander, 2006). The action of this muscle is primarily to elevate the mandible. The temporalis muscle also plays a key role in elevating the mandible, as well as closing and retracting the mandible (Lucas, 2004; Hylander, 2006; Moore, 2014). The temporalis has a broad, triangular fan-like shape originating along the vault of the skull and an insertion from

the coronoid process of the mandible and the anterior border of the mandibular ramus (Hylander, 2006; Moore, 2014). The medial and lateral pterygoids are deep to the masseter and temporalis and both attach to the medial surface of the mandible (Moore, 2014). The medial pterygoid primarily works with masseter to elevate the mandible, originating on the medial surface of the lateral pterygoid plate and attaching to the medial mandibular angle (Moore, 2014). The lateral pterygoid has an origin on the lateral surface of the pterygoid plate and inserts on the mandibular condyle (Moore, 2014). This muscle works to stabilise the mandible in feeding while also contributing to mandibular protrusion (Hylander, 2006). As a group these muscles work to rotate the jaw upwards during feeding and provide multiple lines of action at different angles for evenly applied forces during biting (Crompton, 1962; Lucas, 2004). The relative position, orientation, and size of the masticatory muscles varies between species, affecting a wide range of biomechanical parameters including bite force and gape (see 1.6.1.2 and 1.6.4; Maynard Smith and Savage, 1957; Ross and Iriarte-Diaz, 2019). The position of the muscles in relation to the bite point (teeth) and the jaw joints (fulcrum) results in a third-class lever, and a change in the relative position of the masticatory muscles affects leverage in feeding (see 1.6.1.1; Maynard Smith and Savage, 1957; Hylander, 1975; Ross and Iriarte-Diaz, 2019). Muscle internal architecture also varies between mammal species, including a wide range of variation within primates (Eng et al., 2009). Variation in internal properties such as muscle fibre length and pennation angle can affect the force a muscle is able to generate (see 1.6.1.2; Eng et al., 2009; Taylor et al., 2019).
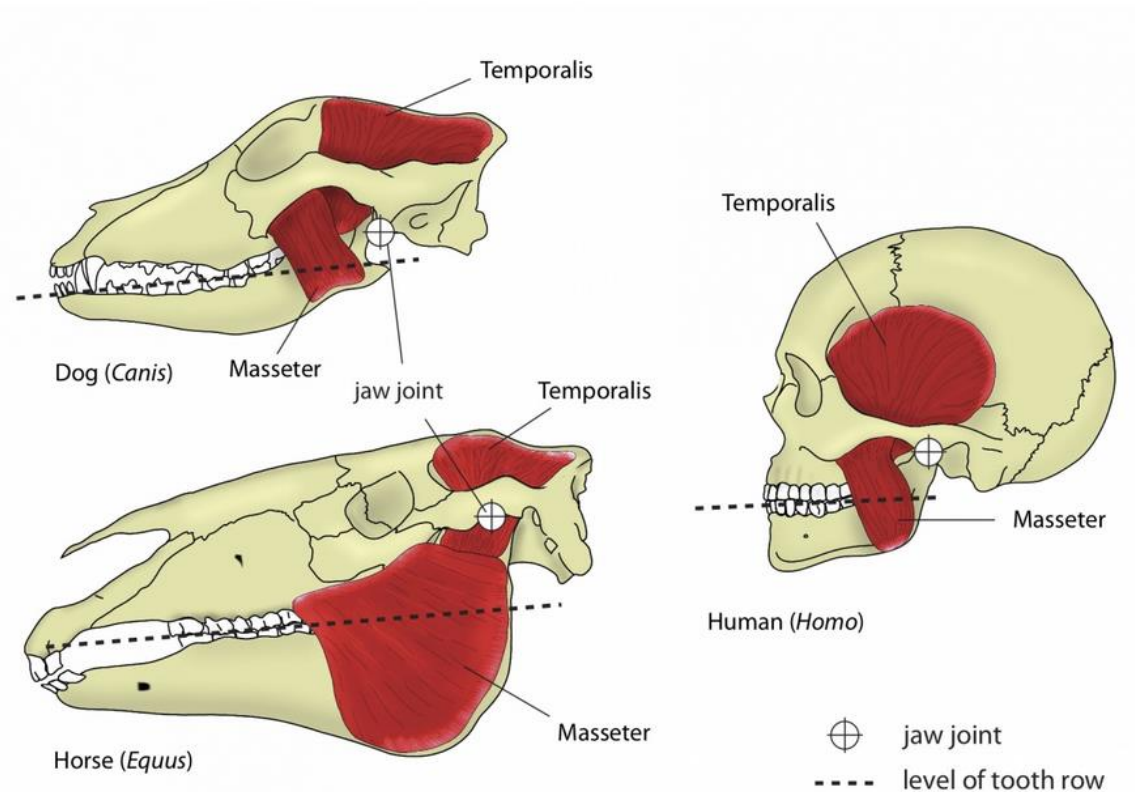
**Figure 1.2 The jaw adductors, the major muscles of mastication on a range of mammals. Showing regions of masseter and temporalis (in red) on a dog, horse, and human to show muscle area. Note how the muscles in the three species vary in their relative size, position and orientation relative to the jaw joint and tooth row.** *Image source: Feldhammer et al., 2007.*

## 1.2.3 Teeth

Teeth are a key part of the masticatory system, being the component with direct contact to the food, gripping and breaking down food objects. The basic mammalian dental form consists of an enamel crown, a dentine foundation and at least one dentine root, as well as an interior pulp cavity filled with living tissue (Lucas, 2004; Ungar, 2010). Dentine is found underneath the crown and forms the roots of the teeth (Lucas, 2004). This substance is less heavily mineralized than enamel, and is less hard and more elastic than enamel (Lucas, 2004). Enamel is the most heavily mineralized tissue and is both the hardest and most brittle dental tissue (Lucas et al., 2008). This material makes up the crown of the tooth, which may feature one or more cusps, elevations on the dental crown in a variety of shapes (Lucas, 2004).

Most mammals, including primates, have heterodont dentition, showing a range of dental forms along the dental row which perform different functions (Swindler, 2002; Lucas, 2004). The dental row is often divided between anterior and posterior dentition. Anterior dentition comprises the incisors and canines, which are used in food acquisition, grip, and preparation (Lucas, 2004; Ungar, 2010). Additionally, anterior dentition can perform paramasticatory functions including grooming as in the toothcomb of lemurs; fighting, as in the canines of gorillas; or digging, as in the incisors of burrowing rodents (Ungar, 2010). Incisors may also be used to prepare foods by removing inedible outer casings on fruits, scrape off adherent material, or even attempt to puncture seed casings (Daegling et al., 2011; McGraw et al., 2011). Posterior dentition refers to the premolars and molars, processes food, reducing food particle size by grinding, crushing, slicing, or shearing, (Kay, 1975; Ungar, 2010, 2015). Unlike the typically unicuspid anterior dentition, cusps in posterior dentition may be numerous and variable (Lucas, 2004; Ungar, 2010). Molar teeth can be used for powerful isometric bites (Daegling et al., 2011; McGraw et al., 2011), repetitive chewing of tough foods (Venkataraman et al., 2014), or puncture-crush softer foods (Hiiemae and Kay, 1972).

Dental form shows immense variation in different mammalian species (Fig 1.3a). Variation includes the relative size of each tooth, changes in internal properties such as enamel thickness, and cusp shape, size, and position (Ungar, 2015). These different forms have been linked with dietary groupings as they affect food processing (Lucas, 2004). In example, herbivorous species such as camels and horses often have high-crowned teeth with numerous long but low enamel ridges, while insectivorous bats have sharp and long shearing crests (Fig. 1.3a, Ungar, 2015). A still different form, as seen in the otter which cracks hard shells has broad and relatively flat teeth with crushing basins ( Fig. 1.3a, Ungar, 2015). These different dental forms are thought to be advantageous for the different material properties of the commonly eaten foods in the diets of these species (see 1.3.2; Lucas, 2004; Ungar, 2015). Another key region of variation in dentition is the number of teeth in different mammals, including primates (Fig. 1.3b). The number of teeth a mammal has may be increased or decreased relative to the predicted original 12-13 teeth per quadrant in ancestral mammals (Lucas, 2004).
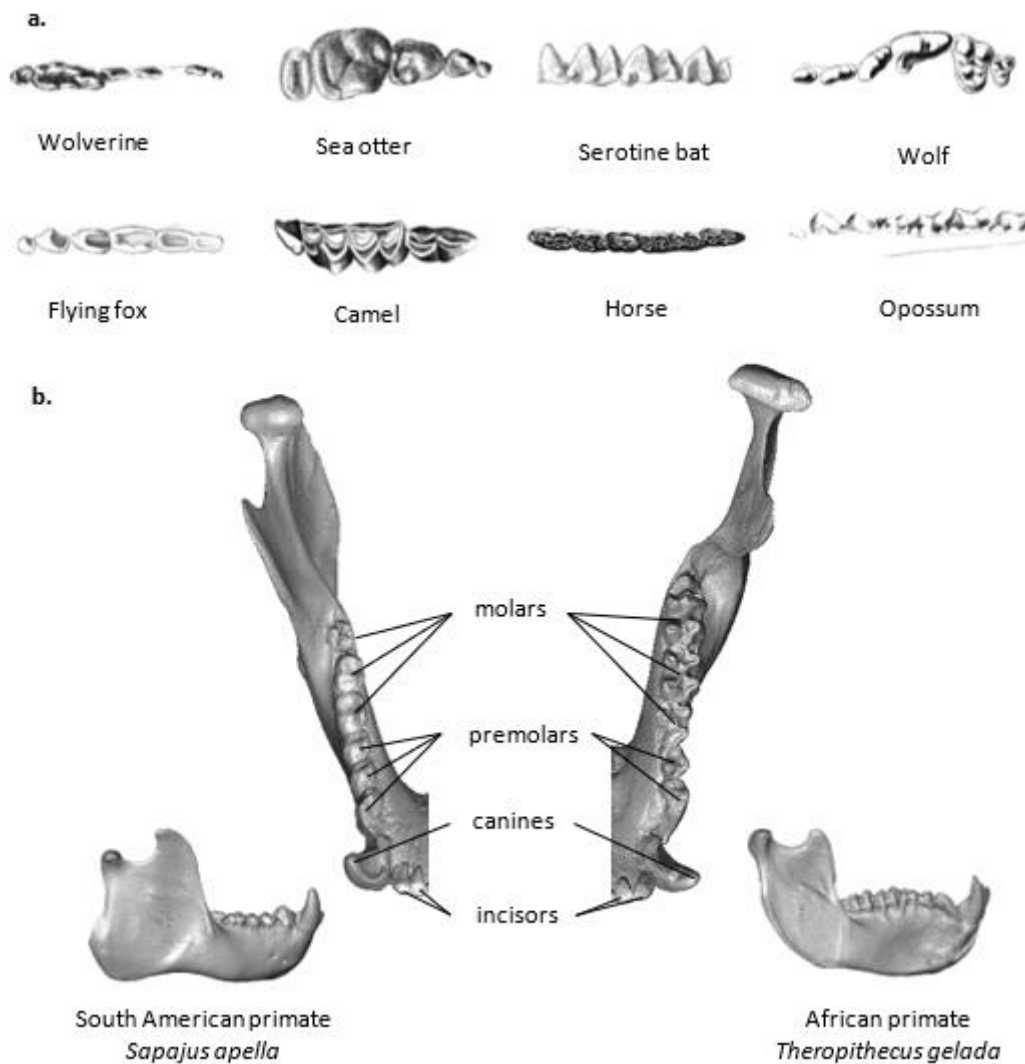
**Figure 1.3 Examples of mammalian teeth, highlighting diversity in dental form and number of teeth. Showing a. selection of mammalian teeth from the posterior dental row in lateral and occlusal view showing a wide range of dental forms, and b. comparison of mandibular dental rows in primates, showing a South American primate, left, and an African primate, right. Primates have a reduced number of teeth in each quadrant, with 2 incisors, 1 canine, 2-3 premolars, and 3 molars for a total of 8-9 teeth per quadrant (Swindler, 2002). The variation in premolar number is a key difference between African/Asian primates and South/Central American primates (Fig.3b, Swindler, 2002). Not to scale.** *Image source: adapted from Ungar, 2015.*

## 1.2.4 Feeding mechanism and bite cycle

Not all mammals masticate their food. Some ripe fruits are swallowed whole by spider monkeys (Dew, 2005) and carnivores often swallow large quantities of minimally processed meat (Hiiemae and Crompton, 1985). In most cases however animals masticate foods, reducing particle size with their teeth to the point that a bolus can be formed and then

23

swallowed (Hiiemae and Crompton, 1985; Lucas, 2004; Chen, 2009). Masticating food creates a greater surface area which increases and speeds metabolic digestion, allowing efficient energy intake (Kay, 1975).

The motions in which bites are performed can be referred to as a bite cycle or chewing cycle and consists of three phases: opening, closing, and the power stroke (Lucas, 2004; Hylander, 2006; Ungar, 2015). The opening phase sees the jaw rotate to the appropriate degree for the food being eaten, while closing is up to the point of tooth-food-tooth contact followed by the power stroke which sees force being exerted upon the food (Hylander, 2006). The type of bite carried out, the length of each phase, and the position of the food on the teeth during the power stroke depend on the size and shape of both the feeding animal and the food being eaten (Hylander, 2006). The tongue also plays an important role in bolus formation, moving the food around against the palate while the salivary glands provide necessary lubrication (Hiiemae and Crompton, 1985; Lucas, 2004; Chen, 2009).

## 1.3 Variability in diets and food properties

Mammalian diets vary and not all foods are equal. From grasses and leaves to meat or shellfish, foods have different material properties, structural defences, shapes, and sizes (Strait, 1997; Lucas, 2004). Some species are considered specialists, focussing their diet on particular types of foods on which they focus intensively, including primate seed predators such as *Cacajao calvus* or the exudate-extracting *Callithrix jacchus* (Eng et al., 2009; Norconk and Veres, 2011). Other species are described as generalists, eating a broad range of foods, such as *Papio anubis* which eats everything from fruits, seeds, and leaves to both small and large vertebrates, garbage, and farm crops (Harding, 1973; Okecha and Newton-Fisher, 2006). Within dietary categories and groups there is also seasonal variation due to the changing availability of foods (Marshall and Wrangham, 2007).

## 1.3.1 Dietary categories

Despite this variability diets can still in many cases be summarised by major dietary categories. Primate diets are often generalised into three major broad dietary categories: folivory, a diet consisting primarily of leaves and shoots, as observed in colobine monkeys and mountain gorillas; frugivory, a diet consisting primarily of fruits, as observed in spider monkeys and the common chimpanzee, and insectivory, a diet consisting primarily of

insects, as observed to the greatest degree in very small primates such as tarsiers and lorises (Fleagle, 2013; Thiery et al., 2017). In addition to these major dietary categories, smaller categories can be defined to refer to specialists, including graminivory, a diet of grasses and in primates truly characterised only by geladas; exudativory, which is feeding on exudates such as saps and gums, seen in many of the Callitrichidae family (Fleagle, 2013). Some primates are also unified by a diet with a high proportion of seeds which are masticated, destroying the seed embryo (see 1.5; Norconk et al., 2013). These seeds are often hard and/or encased in protective casing (pericarp) with pose a significant challenge to the masticatory apparatus.

## 1.3.2 Material properties in food

In mammals, most foods are masticated prior to swallowing. This increases food surface area, enabling more efficient digestion which in turn increases the energy available from foods (Lucas, 2004). However, foods vary in the challenges they present in mastication: foods have a wide range of material properties which determine their break-down (Fig. 1.4a).

A useful way to consider these differences is through the concepts of force and displacement. As an organism closes its jaw, teeth displace into the food and the muscles contract, providing force which loads the food item. Depending on the properties of the food, a tooth of the same shape may displace a considerable distance into the food at low force, a short displacement at a high force, or any other combination of these two variables (Lucas, 2004). The force and displacement (work) required to propagate a crack through a food item varies depending on the properties of the food itself, meaning that foods also vary in the energy required to access them. Energy is therefore not only gained by the organism from digesting food, but also must be expended to masticate food. As the food is broken down the forces applied during feeding act as stresses which provide energy to the food item, which can be stored within the food to be released into a crack, initiating fracture (Lucas, 2004).

One important mechanical property which describes how all materials, including the various foods eaten, deform under loading is Young's modulus, also known as the elastic modulus. Young's modulus provides a measurement of how a material resists deformation, indicating

its stiffness (Lucas, 2004). Measuring this value for an item involves stress, the force per unit area, measured by dividing the force applied uniformly to an object divided by cross-sectional area over which it acts, and strain, the deformation of the object from its original position, measured by dividing the length of the deformed object by the length of the original object (Ennos, 2012). The value of Young's modulus itself is the initial slope of the plotted stress-strain graph of an item during loading. This initial slope is typically linear up to point where a material reaches its yield strength: this is the point up to which an object can be deformed and then return to its original dimensions, should the loading be halted (Lucas, 2004; Fig. 1.4b). Up to this point deformation of the material is in the elastic region and is reversible. After reaching its yield strength, if the material continues to be loaded it will begin to deform plastically. In this region the object will undergo permanent deformation, and eventually, if loading continues, it will fail (Lucas, 2004; Fig. 1.4b). The behaviour of the object in the plastic region is variable: some objects are more ductile than others and can undergo considerable plastic deformation after reaching their yield strength before fracture occurs. In contrast to this, brittle objects fail suddenly after reaching their yield strength, with minimal or no plastic deformation (Lucas, 2004).

Another key property which will determine how a food fractures during feeding is toughness (Lucas et al., 2004). Once a crack is initiated in an item, it does not always take the same amount of work to spread the crack further due to varying toughness. Toughness measures the ability of an object to resist crack growth (Lucas et al., 2004; Lucas, 2004). More work is required to expose new surfaces on foods which are tougher, meaning more energy is required to propagate cracks in tough foods (Lucas et al., 2004; Lucas, 2004). In these cases, displacement may be of particular concern, as a very tough food may require more displacement than the feeding organism can achieve in a given bite in order to propagate a crack.

It is possible to frame this property with reference to the defensive structures of food, which are often described as 'stress-limited' or 'displacement-limited' (Lucas, 2004). These terms describe properties of foods which may provide barriers to access. Although all foods will need some level of stress and displacement in order to fail, a food which can be described as 'stress-limited' fractures at a very high stress, not necessarily at a high displacement. The primary challenge with these foods is generating enough stress to initiate

a crack (Lucas, 2004). Foods which are described as 'displacement-limited' fail after very lengthy displacement, but not necessarily at high stress. In these foods the access challenge is in propagating the crack (Lucas, 2004).

Displacement-limited foods are sometimes simply described as 'tough', and stress-limited foods as 'hard' (Lucas, 2004; Ledogar et al., 2013; Berthaume, 2016; Thiery et al., 2017). Hardness is a complex term, as although this is another important descriptor, it is not an actual physical property (Strait, 1997; Lucas, 2004; Berthaume, 2016). A simple definition of a hard object is that it resists deformation under indentation (Lucas, 2004). If two objects are pressed into each other the harder of the two will indent the softer (Lucas, 2004; Berthaume, 2016). While feeding, if all else remains equal the harder of two objects is the one that will require a higher bite force to initiate fracture. Measurements which quantify hardness also vary, and can be taken as puncture resistance, or in indentation tests of various types (Lucas et al., 1994; Pampush et al., 2011; Berthaume, 2016; Thiery et al., 2017). Such 'hard' food are included in the diets of some primates in the form of hard-shelled seeds and fruits (Norconk et al., 2013). These foods are thought to require high forces to break them down and access nutrients, providing a challenge for feeding (Ledogar et al., 2018). This is the 'stress-limited' nature of very hard foods, as the stress required to initiate fracture on a very hard food may be beyond the bite force an animal can produce.
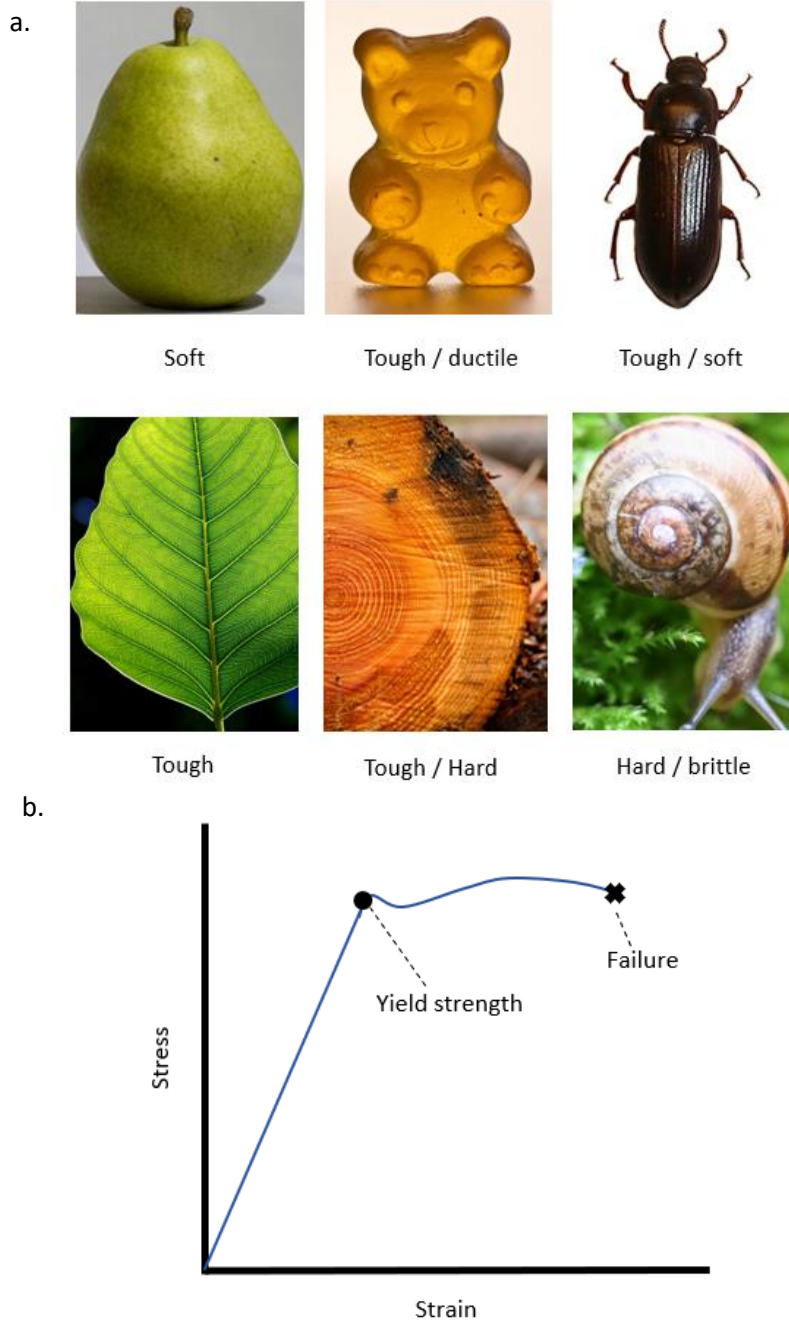
Figure 1.4 Material properties relating to foods, showing a. Series of everyday objects and their basic material properties. From top left: A soft ripe pear, tough and ductile gummy, tough and soft insect cuticle and body, a tough leaf, hard and tough wood, and hard and brittle snail shell; and b. Theoretical stress-strain curve, showing yield strength and failure. *After Lucas, 2004 Image sources, from top left: Rhododenrites, under a CC-BY-SA 4.0 license (https://commons.wikimedia.org/wiki/File:D%27anjou_pear.jpg); Hutter, for public domain; Evison et al., 2017; Sullivan, for public domain (https://commons.wikimedia.org/wiki/File:Leaf_1_web.jpg); van der Wel, under a CC BY-SA 2.0 license (https://commons.wikimedia.org/wiki/File:(417-365)_Tree_(6589657393).jpg); Dunn, under a CC BY-SA 2.0 license (https://commons.wikimedia.org/wiki/File:Capaea_hortensis_02.jpg).*

Most food objects do not have a single isolated mechanical property, falling within a range of properties (Strait, 1997). What is more, different parts of the same food may have different properties. Many biological materials are anisotropic and heterogenous, having different material properties when loaded in different directions, in contrast with isotropic materials, which have the same material properties when loaded in any direction (Lucas, 2004; Ennos, 2012; Berthaume, 2016). Another factor is that many objects consist of several elements with different material properties, such as the fruit skin, flesh and seeds, or insect chitin and insect organs. In result, the properties of certain types of whole food items may be challenging to quantify (Coiner-Collier et al., 2016). This also poses a challenge for the masticatory apparatus, with the jaws needing to be capable of processing varying properties.

### 1.3.3 Food size

Another challenge for the masticatory apparatus is that foods do not only vary in their material properties but also externally in their shape and size. Foods eaten vary in size, as do the individuals eating the foods. For example, mid-sized bearded saki monkeys process fruits with up to 22cm breadth, while large-bodied gelada baboon feeds on thin grass blades (Dunbar and Dunbar, 1974; Norconk et al., 2009). Each animal has to be able to achieve a suitable degree of jaw opening to fit a given food item between the teeth. For a given degree of gape, jaw opening at the anterior dentition will be larger than the posterior dentition, important due to the negative correlation between degree of mouth opening and bite force (see section 1.6.4; Dumont and Herrel, 2003; Berthaume, 2016). However, some species eat foods which are both hard and large relative to their body size, using either their anterior dentition as seen in *Cacajao* species or their posterior dentition as seen in the robust capuchin and the sooty mangabey (Norconk et al., 2013).

### 1.4 A mechanically challenging diet: Hard object feeding

Past studies suggest the material properties of a diet are more closely associated with masticatory morphology than overall dietary category: these properties reflect the true demands of diets in a way that broad food types do not (Santana et al., 2012; Coiner-Collier et al., 2016). This is both because broad dietary categories do not adequately capture the diet of an individual, which is generally far more broad than a grouping such as 'folivory' or

'frugivory', but also because even within these food categories a range of material properties is possible (Coiner-Collier et al., 2016). For example, not all leaves are equal in their material properties as young leaves are typically softer and less tough than mature leaves (Strait, 1997; Coiner-Collier et al., 2016).

One property of foods which can be used to group species is hardness. Hard-object feeding is an extreme feeding behaviour characterised by the consumption of mechanically highly resistant foods (Norconk and Veres, 2011; Santana et al., 2012). Past studies examining hard-object feeders have especially focussed on marine species as there are many extant and extinct marine species which feed by cracking the hard shells of molluscs and similar prey (Fig. 1.5; Crofts and Summers, 2014; Crofts et al., 2016). Hyenas are an impressive mammalian example, capable of cracking relatively large bones as part of their regular diet (Fig. 1.5; Tanner et al., 2008). Other organisms which feed on hard objects include a range of primate species. There are numerous primates which include large proportions of hard-shelled seeds and hard unripe fruits in their diets, collectively referred to as primate seed predators (Fig. 1.5; Norconk et al., 2013).
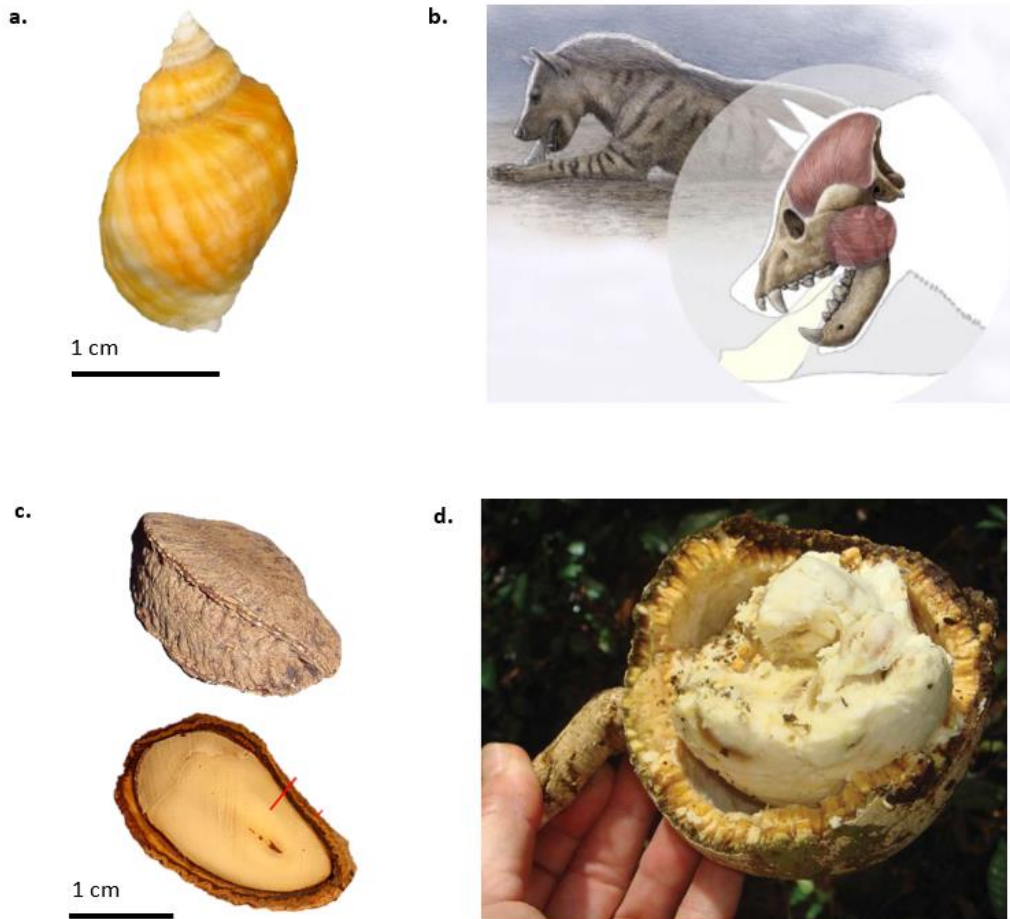
**Figure 1.5 Hard seeds, fruits, snails, and bones. Showing a. snail shell of *Nucella ostrina* which is fed upon by hard-object feeding marine species; b. reconstruction drawing of a bone-cracking giant hyena; c. Brazil nut as is consumed by the primate *Cacajao calvus,* showing external seed casing and opened casing to reveal nut within, and d. *Strychnos* fruit and seed, fed upon by the primate *Chiropotes*. Image sources: Armstrong, 2005; Norconk and Veres, 2011; Palmqvist et al., 2011; Tyler et al., 2014.**

## 1.5 Seeds and primate seed predators

Seed predation is considered a dietary category in its own right by some, due to the unifying and special challenges posted by this diet (Norconk and Veres, 2011; Norconk et al., 2013; Barnett et al., 2016; Thiery et al., 2017). This diet is defined by the consumption of seeds, either in combination with eating the fruit in which the seed is found or exclusively eating the seed (Norconk et al., 2013). A range of primate species incorporate seeds into their diet seasonally or as a major part of their annual diet (Norconk et al., 2013). It is thought that other sympatric species are not capable of eating these foods due to the mechanical challenges they present, creating new specialised niches for some primates (Kinzey and

Norconk, 1990, 1993; Norconk and Veres, 2011). This diet is sometimes referred to as 'extractive' or 'embedded' foraging, names which highlight the special challenge of seed predation (Norconk and Veres, 2011; Tamura, 2020). The challenge is that the animal must first get through an external layer in the form of a seed shell, husk, or fruit pericarp in order to access the nut and its nutrients within.

## 1.5.1 Anatomy of seeds

Seeds contain plant embryos but also the necessary nutrients for the embryo to grow and develop (Williamson and Lucas, 1995). Fruits have a symbiotic relationship with those species which do not destroy the seed during feeding (Strait, 1997; Dew, 2005). The soft outer layers on many fruits are typically preferred by primates, leaving the seed itself intact to be dropped or defecated if swallowed, facilitating dispersal (Dew, 2005; Ledogar et al., 2018). Primate seed predators consume the seed itself, destroying the plant embryo. Seeds do not want to be eaten and have evolved a series of defences to prevent ingestion. However, the need to germinate has resulted in a situation where seeds "need to open but not be opened" (Lucas, 2004:94). The mechanical defences of seeds are variable: the outer layers of a fruit, can be defended by a hard, brittle or tough, and potentially thick husk, or the internal seed casing itself can be hard and dense (Fig. 1.6; Lucas et al., 1991; Norconk et al., 2013; Ledogar et al., 2018). These defences protect the seed itself from destruction through feeding and can pose a considerable challenge to access.
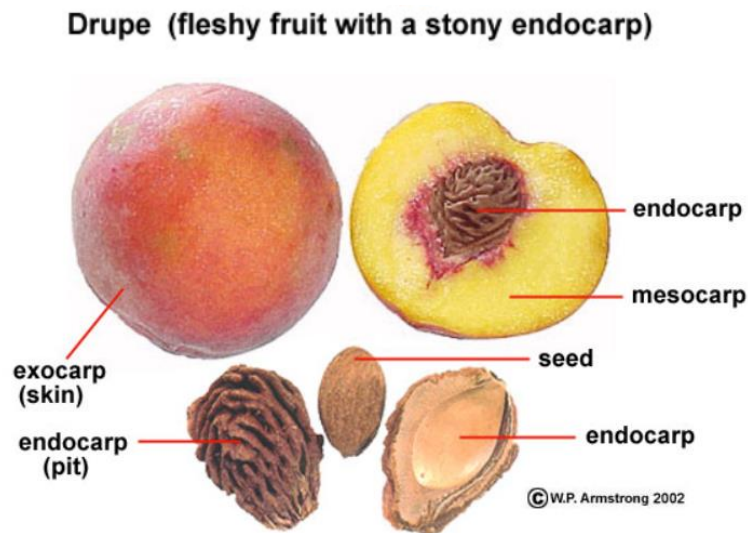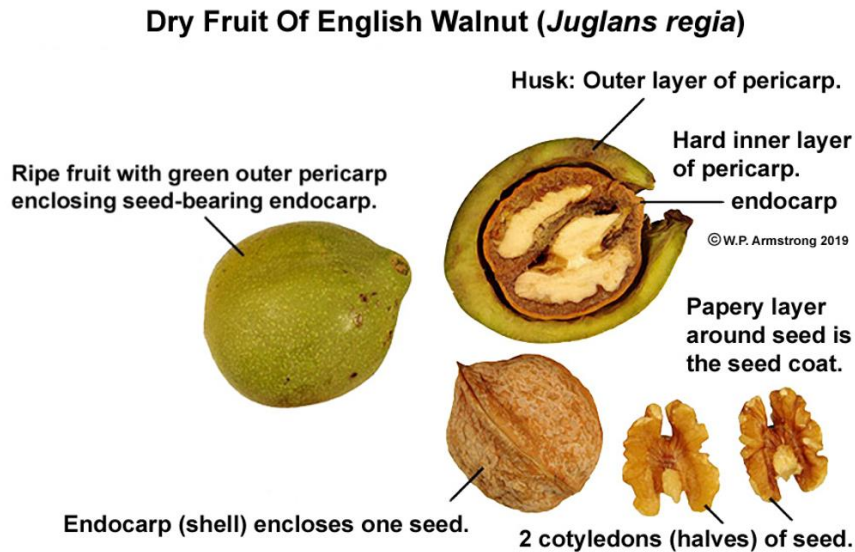
**Figure 1.6 Seed anatomy, showing fruit layers and different fruit morphologies. The seed is surrounded by the pericarp (exocarp, mesocarp, and endocarp) which can take different forms as seen in the walnut (top) and peach (bottom). The outermost layer of the pericarp can have a hard husk. The outer pericarp can be hard to defend the seed, the inner endocarp can be hard, or both may provide protection.** *Image sources: Armstrong, 2002, 2009.*

## 1.5.2 Seeds eaten by primates

Seeds eaten by primate seed predators can be found in a wide range of fruit and seed casing morphologies (Fig. 1.7; Lucas et al., 1991; Barnett et al., 2015; Geissler et al., 2020). There is variation in both internal and external morphology as well as procurement and processing methods. The size of both the seeds and the structures in which they are embedded varies widely. Very large hard-husked fruits, which may be up to 22cm in breadth, are foraged from trees and processed by pitheciine primates *Cacajao, Chiropotes,* and *Pithecia* to access

large seeds within ( Fig. 1.7 and Fig. 1.8; Norconk et al., 2009). The exocarp and mesocarp of these fruits protecting the seed can be very thick, up to 15cm of thickness protecting the seed (Norconk et al., 2009). A different approach is seen in the hard *Sacoglottis gabonensis* seed casings processed by *Cercocebus atys* (Fig 1.7) which are foraged on the forest floor (McGraw et al., 2011). This leaves only the hard seed casing, not the outer fruit layers, but the seed casing has been found to remain intact, not decomposing for many months in this environment (McGraw et al., 2011). The seed casing surrounds a honeycomb of pods where the seeds themselves are found, creating a network of dense woody fibres which reinforce the hard seed shell ( Fig. 1.7; Daegling et al., 2011).

These different seed types pose significant challenges for processing. In all cases the need for seed propagation is in contradiction with the need for seed defence from being eaten, which may result in weak areas of the seed structure. The anatomy of the seed has also been shown to impact how the seed fractures, in example *Mezzetia* seeds typically break along either side of the area from which the seed would eventually germinate if undamaged (Lucas et al., 1991). Different stages of seed and fruit maturity also present different nutritional and mechanical profiles. In example, unripe fruits processed for seeds eaten by *Chiropotes* species have higher nutritional and water content with lower tannin content than the seeds of softer ripe fruit, but the increased hardness poses a greater mechanical challenge to eat (Kinzey and Norconk, 1990). For those who are able to access seeds they are a rich source of nutrients, high in lipids and proteins. Consuming seeds can therefore allow seed predators to avoid the competition for softer ripe fruit (Kinzey, 1992; Norconk and Veres, 2011; Norconk et al., 2013).
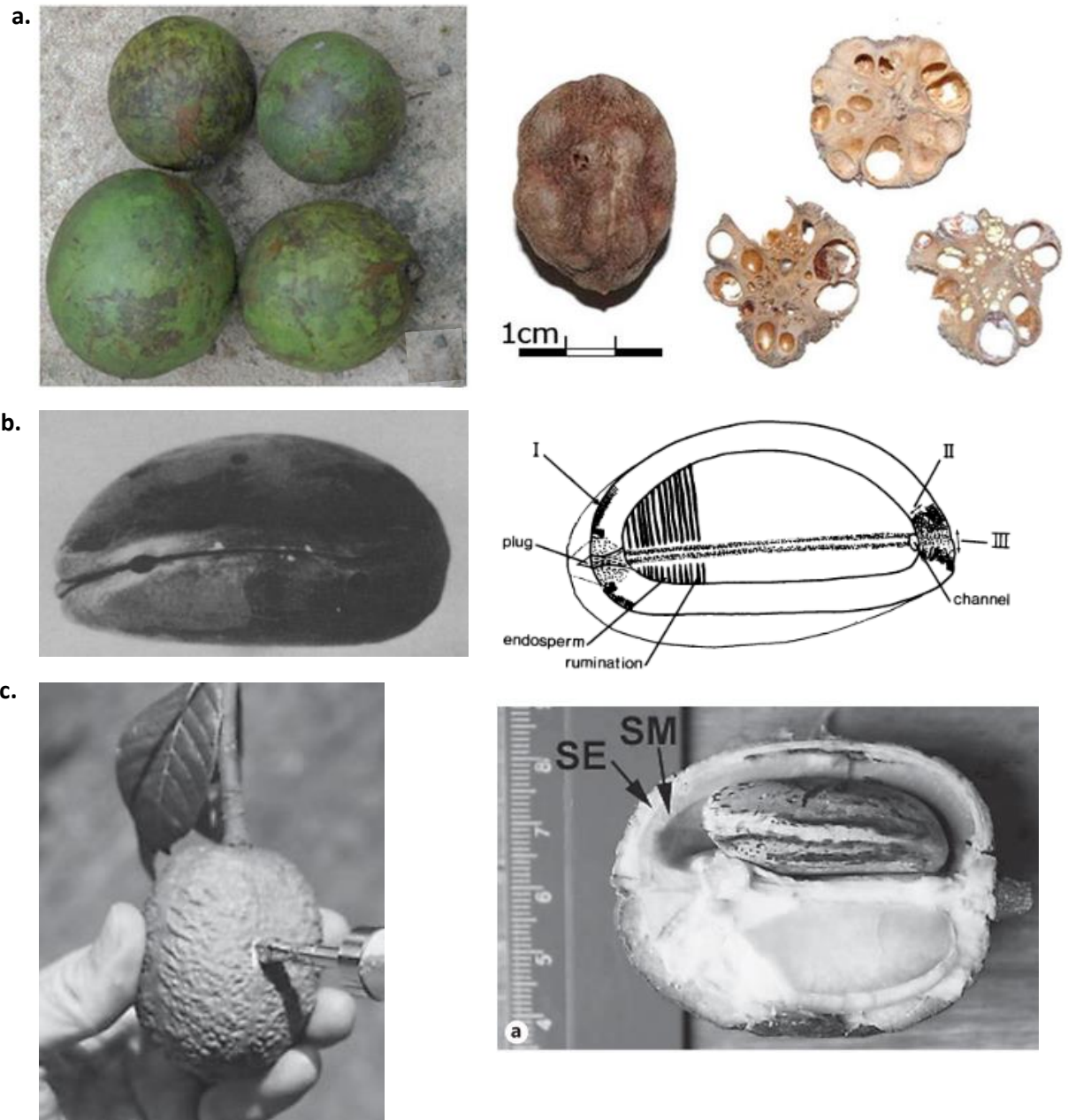
**Figure 1.7 Examples of seeds eaten by primate seeds predators with different internal and external fruit morphologies. Showing a. *Sacoglottis gabonensis* fruit (left) and seed with a its hard endocarp (centre) and a cross-section of the seed. Note the chambers within the seed casing which house the oil-rich seeds themselves which are eaten by *Cercocebus atys* (Daegling et al., 2011; Geissler et al., 2020); and b. *Mezzetia leptopoda* seed casing (left) with cross-sectional diagram (right), showing seed components and regions which correspond to different material properties. This seed is eaten occasionally by *Pongo pygmeaus* (Lucas et al., 1991); and c. *Hevea spruceana* whole fruit having its hardness measured (left) and internal morphology with seed pods (right). This fruit has a very hardened mesocarp (SM for sclerotised mesocarp) underlying a spongy exocarp (SE), protecting seeds on the interior which are eaten by *Cacajao calvus* (Barnett et al., 2015). *Image sources: Geissler et al., 2020; Lucas et al., 1991; Barnett et al., 2015.*

### 1.5.3 Types of primate seed predators

Primate seed predators vary both in the intensity of their seed predating behaviour and by the manner in which they process these foods. Some species focus very intensively on embedded seeds, which make up a very high proportion of their annual diet (Norconk et al., 2013; W. Scott McGraw et al., 2014; Barnett et al., 2016). Amongst catarrhine primates this includes several *Cercocebus* mangabey species, of which *Cercocebus atys* is especially noteworthy because a single seed type (*Sacoglottis,* see Fig. 1.7) makes up nearly 50% of its annual diet (Wieczkowski, 2009; McGraw et al., 2011; W.S. McGraw et al., 2014). Some colobine primates also feed on seeds very intensely, notably *Colobus angolensis* extracts a high proportion of seeds from very tough and hard casings (Koyabu and Endo, 2009; Norconk et al., 2013). In platyrrhine primates the pitheciines (*Cacajao, Chiropotes,* and *Pithecia*) stand out, accessing seeds embedded within large, hard-shelled fruits (Kinzey and Norconk, 1990; Kinzey, 1992; Norconk and Veres, 2011; Barnett et al., 2016). Other primates feed on seeds only seasonally or occasionally, often linked with times of low fruit availability (Izawa and Mizuno, 1977; Terborgh, 1984). For these primates, seeds make up a lower proportion of the annual diet but are essential at these times of the year (Norconk et al., 2013). Notable catarrhine examples include mandrills, and *Mandrillus sphinx* is thought to seasonally rely on a significant proportion of seeds (Hoshino, 1985; Lahm, 1986). Numerous colobine species also rely seasonally on seeds (Koyabu and Endo, 2009, 2010; Norconk et al., 2013). Amongst platyrrhine primates the robust capuchins stand out in this regard, and *Sapajus apella* seasonally consumes hard palm seeds (Izawa and Mizuno, 1977; Terborgh, 1984). Taken together, past work has identified 31 primate species which regularly incorporate seeds in their diet to varying degrees, highlighting that although this diet presents challenges, many disparate species are able to access this resource (Norconk et al., 2013).

Within these different primates there is variation in the manner of seed processing. Some primates primarily use their anterior dentition (incisors and canines) to gain access to seeds, while others use their post-canine dentition (premolars and molars) (Fig. 1.8; Kinzey and Norconk, 1993; McGraw et al., 2011; Norconk and Veres, 2011; Barnett et al., 2016). In primates these different feeding positions also relate to different methods of seed extraction. Past work has split primate seed predators into two categories: sclerocarpy and

durophagy (Fig. 1.8; Norconk et al., 2013). Sclerocarpy is extractive foraging which involves processing fruits with a hard pericarp, as seen in the pitheciine seed predators *Cacajao, Chiropotes,* and *Pithecia* (Kinzey, 1992). First this hard pericarp must be removed, accomplished with the anterior dentition in these primates, then the relatively soft seed can be masticated using the posterior dentition (Kinzey, 1992; Norconk et al., 2013). Durophagy in primates uses a crushing bite on the posterior dentition, and while the incisors may be used to prepare foods the main bite is on the posterior teeth (Norconk et al., 2013). This method is seen in mangabeys and robust capuchins to access seeds from within hard seed casings (Terborgh, 1984; McGraw et al., 2011). Hard-object feeding is a term used to describe all primate seed predators, but objections have been raised against this term because it focusses on the material properties of the objects without reference to processing methods (Norconk et al., 2013). However, the term 'hard-object feeding' is still regularly used as a useful term because the hardness of these seeds is thought to be a major barrier for accessing these foods (e.g. Lucas et al., 2008; Vinyard et al., 2011; W.S. McGraw et al., 2014).



**Figure 1.8 Primate seed predators with different feeding approaches. Showing (left) the sclerocarpic *Cacajao* using its anterior dentition to feed on a large, hard fruit, (right) the durophagous *Cercocebus* using its posterior dentition to feed on a *Sacoglottis*. *Image sources: Ingo Arndt, Nature PL; McGraw et al., 2011.***

## 1.6 How to be a hard object feeder - Masticatory form and function

Feeding on a mechanically challenging diet is predicted to require special adaptations (Strait, 1997). Seed predation is one example of a challenging diet, requiring seeds which are both large and hard to be processed. Seed predators are therefore predicted to require both wide gape and bite force in order to gain access to nutrients (Koyabu and Endo, 2009, 2010; Norconk et al., 2013; Ledogar et al., 2018; Taylor et al., 2018).

## 1.6.1 Bite force

Bite force is a performance metric which has a close relationship with vertebrate ecology (Anderson et al., 2008; Santana, 2016). It is the quantity of force which can be generated on a bite point at a given degree of mouth opening (Spencer and Demes, 1993; Santana, 2016). As such, it is a key indicator of feeding performance: the bite force of an individual poses a limit on which food objects they can eat. If a food requires a higher force to comminute than a species can generate, then it will not be able to process the food (Anderson et al., 2008; Santana and Dumont, 2009; Habegger et al., 2012) unless they circumvent this constraint by using tools (Verderane et al., 2013). However, many primate seed predators rely on their masticatory capabilities alone to consume their challenging diet.

Bite force can be measured *in vivo* or estimated using a range of modelling methods (Davis et al., 2010). *In vivo* bite force measurements are thought to provide the most accurate results but are generally very challenging to collect (Davis et al., 2010). Various species (i.e. bats) willingly bite on a transducer when presented with one, providing accurate readings (Dumont and Herrel, 2003; Anderson et al., 2008). Bite force data has been collected *in vivo* for several primate species although this is typically done with invasive methods (Dechow and Carlson, 1990; Wall et al., 2006; Ross et al., 2007). Maximum bite force was measured on anesthetised *Macaca mulatta* individuals and found to scale with positive allometry in an ontogenetic series, from 70.3N in juveniles to 139.9N in adults for bites on incisor (Dechow and Carlson, 1990). However, few studies work with maximum *in vivo* primate bite force, instead measuring other aspects of feeding biomechanics such as tracking how bite force changes during chewing (e.g. Wall et al., 2006; Ross et al., 2007). An example on *Papio anubis* examined biting forces at different stages of chewing activity using jaw-tracking devices and EMG recording, finding that the generation of jaw adductor muscle force varies

between the stages of a typical bite (Wall et al., 2006). Overall *in vivo* bite force studies are relatively rare as not all species are compliant, available, or suitable for bite force testing with transducers, and the invasive nature of past primate bite force experiments raises serious ethical concerns.

As an alternative, bite force can be estimated using photographs or 3D scans (e.g. Thomason, 1991; Anderson and Westneat, 2007; Ledogar *et al.*, 2018). Various methods have been applied to estimate bite force in a wide range of extinct and extant species, although non-hominin primate studies are relatively rare. These methods include 2D measurements using basic lever models from photographs or physical specimens as measured for numerous fossil hominins (Demes and Creel, 1988), Neanderthals and isolated modern human populations (Spencer and Demes, 1993), a broad range of carnivores (Thomason, 1991), and otters (Campbell and Santana, 2017). More complex 3D modelling methods can also be used. These methods include making finite element models, an approach which has been applied to pitheciine primates (Ledogar et al., 2018) and numerous hominins (Strait et al., 2009; Godinho et al., 2018). Another approach is to use multi-body dynamic models as made for macaques (Curtis et al., 2008; Shi et al., 2012), and *Tyrannosaurus rex* (Bates and Falkingham, 2012). Alternate computer-based simulations have been used to estimate bite force in placoderm fish (Anderson and Westneat, 2007) and bats (Davis et al., 2010; Santana et al., 2012).

These studies have found links between diet and bite force. The highest estimated value for a terrestrial animal has been predicted for the extreme predator *Tyrannosaurus rex,* modelled to be capable of 35 000 – 57 000N bite force (Bates and Falkingham, 2012). Another extreme predator, the extinct placoderm fish *Dunkleosteus terrelli,* was estimated to be capable of bite forces of up to approximately 5 300N (Anderson and Westneat, 2007). While these bites are extraordinarily powerful, species with lower bite forces yet with a high proportion of hard foods have also been shown to have high bite forces relative to species with softer diets (Aguirre et al., 2003; Santana et al., 2010, 2012). This has been observed in bats, for which increased dietary hardness was associated with increased estimated bite force and *in vivo* measurements of bite force (Aguirre et al., 2003; Santana et al., 2010, 2012). Durophagous marine species have also been found to have relatively high bite force, as seen in the horn shark, which feeds on molluscs and other hard foods (Huber et al.,

2005). The horn shark did not have the absolute highest bite force relative to a range of comparative vertebrates, but still was found to have a relatively large bite force (128N on anterior bites to 338N on posterior bites) for its body mass (Huber et al., 2005). As these sharks do not have an especially high bite force, other aspects of their morphology are thought to assist in facilitating their diet, including their dental morphology, jaw robusticity and feeding process (Huber et al., 2005). The association between hard diets and bite force in primates has not previously been directly tested except in a comparison within pitheciine seed predators (*Cacajao, Chiropotes,* and *Pithecia*) and their close relative *Callicebus,* which consumes a softer diet than the seed predator group (Ledogar et al., 2018). The seed predators varied, with the highest bite force estimated for *Cacajao* (148.67 – 171.56N on anterior bites and 263.11 – 285.03N on posterior bites) and the lowest for *Pithecia* (63.03-77.19N on anterior bites and 108.78 – 131.54N on posterior bites) (Ledogar et al., 2018). However all seed predators were estimated to have an absolutely higher bite force than *Callicebus* (38.41 – 44.44N on anterior bites and 69.37 – 77.73N for posterior bites) and produced this force more efficiently due to having higher mechanical advantage (Ledogar et al., 2018). How this performance compares to a broader range of seed predators and primates with other diets is unknown, as is how this performance varies at different gapes. Bite force has been estimated or measured for only a small number of other primates with any diet type (Dechow and Carlson, 1990; Wall et al., 2006; Ross et al., 2007). The high force to fracture measured for the seeds consumed by some primates produces an intriguing scenario as the components of the masticatory system which facilitate this diet in these species are not yet understood. Species with hard diets have been found to have relatively high bite forces, but a full understanding of which aspects of their morphology enable them to process this diet does not yet exist.

## 1.6.1.1 Mechanical advantage

One of the biomechanical parameters which affects bite force is mechanical advantage. Mechanical advantage is a measure of the efficiency of a system and is calculated as a ratio of in-lever to out-lever lengths (Fig. 1.9; Norconk et al., 2009). As previously discussed, the mandible is generally modelled as a third-class lever (Fig 1.9; Hylander, 2006). Mechanical advantage of the jaw adductors can be increased either by having a longer in-lever, a shorter out-lever, or both. In-lever length is increased through more anteriorly positioned

muscles relative to the TMJ, which moves the muscle further from the joint and thereby increases the length of its lever arm (Dechow and Carlson, 1990; Norconk et al., 2009; Taylor et al., 2018). Out-lever length is decreased by having a shorter dental row, bringing the teeth closer to the TMJ to shorten the length of the lever arm (Dechow and Carlson, 1990; Norconk et al., 2009; Taylor et al., 2018). The in-levers for jaw adductors are typically measured as the perpendicular distance from a measurement of muscle length to the centre of the jaw condyle, and the out-lever is the distance from the centre of the jaw condyle to a given bite point (Anapol and Lee, 1994; Wright, 2005; Norconk et al., 2009; Dickinson et al., 2018).
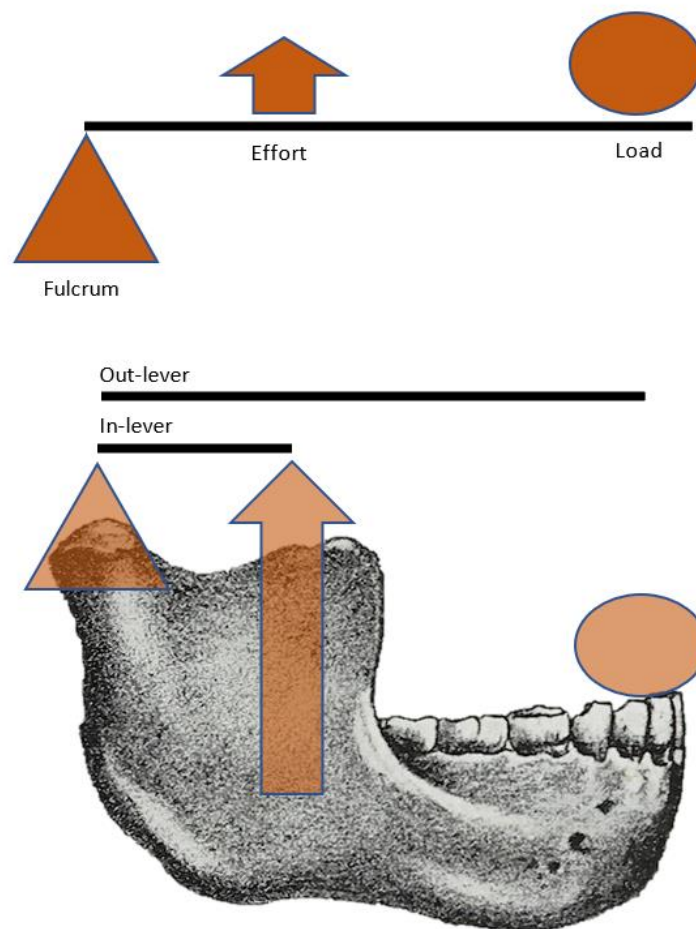


**Figure 1.9 Simplified diagram of mechanical advantage in the mandible, showing a basic third-class lever and how this lever works to measure mechanical advantage. The mandibular condyle is the fulcrum, effort is through the masticatory muscles. A bite point, shown here on the incisors, is the load. The distance from the fulcrum to the muscle line of action is the in-lever, the distance from the fulcrum to the bite point is the out-lever.** *Image source (mandible drawing): Braus, 1921.*

In-lever and out-lever distances can be measured using different methods. Measurements can be made on 2D photographs of the cranium on dry bone using exclusively the cranium (i.e. Spencer and Demes, 1993; Wright, 2005; Koyabu and Endo, 2010), or on mandible and cranium in occlusion, either using measurements made on cadaveric material (Taylor et al., 2018), 3D surfaces (Dickinson et al., 2018; Godinho et al., 2018), or digitised landmarks on mandible and cranium (O'Connor et al., 2005). If the mandible and cranium are in occlusion then origin and insertion sites can be used to reflect muscle line of action (Dickinson et al., 2018; Ledogar et al., 2018). This 3D method retains a greater amount of detail about the anatomy of the specimen than 2D methods or methods with the mandible or cranium in isolation but requires more data. In all cases these measurements use single points to represent muscle lengths or origin and insertion sites which does not capture the full range of a muscle. However, this method has been used in the past as a proxy for understanding the biomechanical function of a wide range of species and is widely seen as providing an adequate approximation of function (O'Connor et al., 2005; Norconk et al., 2009; Dickinson et al., 2018; Godinho et al., 2018; Taylor et al., 2018).

A higher mechanical advantage in the masticatory muscles will reduce the required muscular input effort to generate a given bite force. Alternatively, it will increase bite force if all other variables are left the same (Spencer and Demes, 1993; Taylor et al., 2018). As such, species with more mechanically challenging diets have been predicted to have a higher mechanical advantage than those which feed on less mechanically challenging foods (Wright, 2005; Santana et al., 2012; Ledogar et al., 2018; Taylor et al., 2018). These predictions have been partially met (Anapol and Lee, 1994; Wright, 2005; Koyabu and Endo, 2009, 2010; Santana et al., 2012; Ledogar et al., 2018; Püschel et al., 2018). This pattern has been identified in bats, and bat species with harder diets have been found to generate bite force more efficiently due to higher mechanical advantage (Santana et al., 2012). In primates the Cebidae, some of which feed on very hard objects seasonally, have been found to have high leverage relative to other platyrrhine primates, particularly on the temporalis (Anapol and Lee, 1994; Wright, 2005). Both Asian and African colobine seed predators were found to have higher mechanical advantage than colobines with less hard diets (Koyabu and Endo, 2009, 2010). Pitheciine seed predators are also thought to have high mechanical advantage, although studies have reported conflicting results comparing *Pithecia* to

*Callicebus* in terms of mechanical advantage with one study reporting low values for seed predator *Pithecia* (Ledogar et al., 2018; Püschel et al., 2018). These differences may be due to the type of measurement used or the role of gape as one study worked with a jaw rotated open and the other worked exclusively with the mandible (Ledogar et al., 2018; Püschel et al., 2018). Conflicting results have also been found for the seed predator *Cercocebus atys,* which failed to meet predictions of high mechanical advantage by comparison with close relatives with less challenging diets (Taylor et al., 2018). A complete, comparative understanding of how primate seed predator mechanical advantage varies relative to primates with less challenging diets is missing.

## 1.6.1.2 Muscle Force

As muscles contract, force is generated, although numerous factors impact on how much force is generated. For one, muscle recruitment varies within an individual depending on the activity being carried out. In the context of feeding, muscle activation varies between the different muscles of mastication and during the different stages of a bite (Vinyard et al., 2008). The measurement of muscle recruitment during feeding is a complex process which is not yet fully understood in all primates, but which will affect the ability of an individual to produce bite force (Ross and Iriarte-Diaz, 2019). The ability to produce force also varies with the length of the muscle. As muscles contract, more cross-bridges between myofilaments exist, which increases force up until a certain point of contraction, after which the number of cross-bridges decreases again and muscle force decreases (Fig. 1.10; Herzog, 2007; Ross and Iriarte-Diaz, 2019). A general pattern for skeletal muscle length-tension curves is upheld in a wide range of species, but the ranges of active force production vary between both muscles and species (Herzog, 2007; Eng et al., 2009). It has been suggested that this is linked with optimising properties for different muscle functions (Herzog, 2007). In feeding, this relationship is particularly relevant to gape as increased mouth opening also increases muscle stretch, potentially affecting the muscle force for biting which can be recruited (Eng et al., 2009). This relationship has been tested in bats with in vivo measurements confirming a lower bite force at higher gapes, although there is intraspecific variation in the extent of the decrease (Dumont and Herrel, 2003; Santana, 2016).
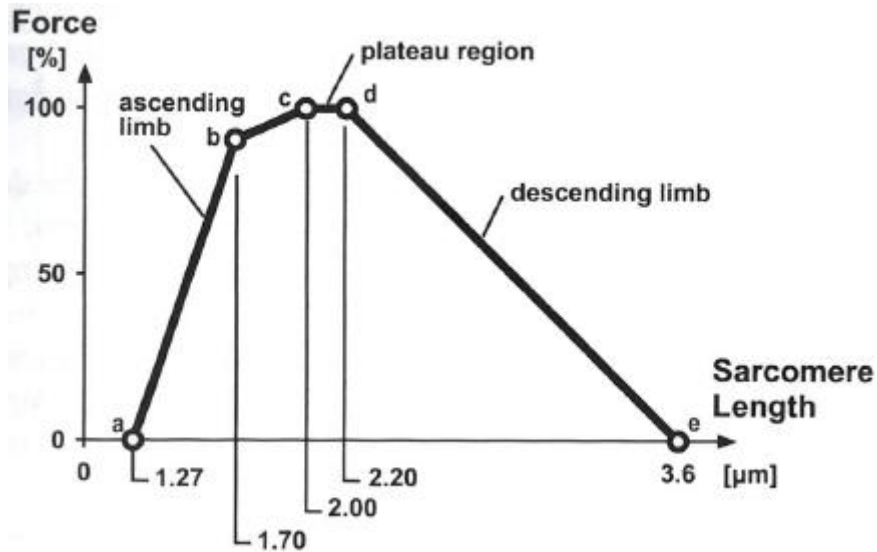
**Figure 1.10 Example of a length-tension curve for muscle fibres, showing the increase of force with greater sarcomere length (ascending limb) up to a certain point (plateau region), followed by a decrease in force after a certain stretch point is reached (descending limb). The possible force generated and associated sarcomere lengths vary by species and muscle.** *Image source*: *Herzog, 2007.*

Muscle force production is also strongly affected by muscle mass: increased muscle mass relates to increased muscle force production (O'Connor et al., 2005; Anderson et al., 2008; Santana et al., 2012; Toro-Ibacache et al., 2016), and all other things staying constant, will increase the bite force. Muscle mass is measured as the sum of the physiological cross-sectional areas (PCSA) of the masticatory adductors, the cross-sectional area of all muscle fibres (Toro-Ibacache et al., 2015). To calculate muscle force, muscle PCSA is multiplied by the intrinsic strength of the muscle being measured (Toro-Ibacache *et al.*, 2015). However, to measure PCSA either dissection or novel imaging techniques which use contrast enhancement to facilitate clear muscle visibility are necessary (Toro-Ibacache et al., 2015; Dickinson et al., 2018). Instead, PCSA is often estimated using muscle cross-sectional areas (CSA), which can be estimated using dry bone (Thomason, 1991; Christiansen and Adolfssen, 2005; Wroe et al., 2005b; Christiansen and Wroe, 2007; Campbell and Santana, 2017). PCSA more accurately reflects muscle mass, having been shown to directly relate to the force that muscle can produce because it captures muscle pennation angle, density, and fibre length, all of which can vary to affect muscle force (Maughan et al., 1983; Taylor and Vinyard, 2009, 2013; Dickinson et al., 2018). CSA as measured on dry bone can provide a reasonably reliable estimate of bite force, although it is important to note that the lack of information on fibre length and pennation angle affects measurements (Davis et al., 2010; Hartstone-

44

Rose et al., 2015; Toro-Ibacache et al., 2015; Dickinson et al., 2018). Past studies on bats have shown that dry bone measurements of CSA overestimate the PCSA of the masseter-medial pterygoid complex and underestimate the temporalis PCSA (Davis et al., 2010). While PCSA measurements are more accurate than CSA, these measurements are time-consuming to calculate, and the wealth of information required for calculations is often not available (Davis et al., 2010; Dickinson et al., 2018). As such, CSA from dry bone is often used as a proxy measurement in order to calculate bite force, requiring only skeletal material, and can be used when other options are not available (Thomason, 1991; Christiansen and Adolfssen, 2005; Wroe et al., 2005b; Christiansen and Wroe, 2007; Davis et al., 2010; Campbell and Santana, 2017).

Muscle CSA and PCSA have been measured on a wide range of vertebrates including otters, a range of felids and canids, various primates, and numerous marsupials (Thomason, 1991; Christiansen and Adolfssen, 2005; Wroe et al., 2005a; Christiansen and Wroe, 2007; Perry and Hartstone-Rose, 2011; Taylor et al., 2015; Campbell and Santana, 2017). Some general trends have been identified. For one, muscle mass is strongly correlated with body size (Anderson et al., 2008; Hartstone-Rose et al., 2018). However, scaling relationships show that this relationship is not always straightforward as muscle mass scales with negative allometry in some primate species, and isometry or positive allometry in others (Anapol et al., 2008; Perry and Wall, 2008; Perry and Hartstone-Rose, 2011; Taylor et al., 2015; Dickinson et al., 2018; Hartstone-Rose et al., 2018). Scaling relationships vary both between and within primate species. Within macaques, muscle PCSA has been shown to scale isometrically with body mass, but with positive allometry to facial size, indicating a link between prognathism and relatively larger PCSA (Anton, 1999). Comparisons between species have found some links between scaling relationships and broad dietary categories, finding the masticatory muscles of frugivorous and insectivorous strepsirrhine primates to scale with isometry but with positive allometry in folivores (Perry and Hartstone-Rose, 2011). Across platyrrhine primates PCSA has been shown to scale with negative allometry, but with positive allometry or isometry in hominoids and catarrhine primates (Taylor et al., 2015; Taylor and Vinyard, 2013; Anapol et al., 2008; Taylor et al., 2013). Broader comparisons of scaling with relation to dietary trends in other primates have at times found conflicting trends, with methodological debates in the method of muscle PCSA affecting

results (Taylor et al., 2015; Hartstone-Rose et al., 2018; Taylor et al., 2019). As such, while muscle force typically increases with body size this relationship is not necessarily straightforward or fully understood in primates.

This study will not measure muscle internal architecture, but as these structures have well-known consequences for muscle force it is important to consider the potential impacts that these variables could have on measurements made. This is particularly because the internal muscle architecture of primate seed predators is generally not known. *Cercocebus atys*, a very intensive seed predator, is an exception to this (Taylor, 2018). Male *C. atys* has long muscle fibre lengths which would contribute to maintaining high bite force at wide gapes, although it does not have large muscle PCSA when compared to other papionin primates with less extreme diets (Taylor et al., 2018). Given this surprising finding, further investigation of the masticatory morphology of this primate, particularly one which considers the role of dental form in seed fracture, is of special interest.

## 1.6.2 Dental form

Dental form is another important factor of masticatory form and function. The range of observed dental forms has been linked with the fracture behaviour of food, as different objects may be more easily fractured by different shapes, meaning that a more efficient tooth can reduce the work needed by the individual to induce fracture (Evans and Sanson, 2003; Lucas, 2004; Ungar, 2004; Anderson and Labarbera, 2008; Anderson, 2009; Anderson and Rayfield, 2012). Mammalian dental crowns in particular are quite complex, and mammalian post-canine teeth have increased in complexity over evolutionary time (Constantino et al., 2016).

Modelling has found that some mammalian teeth have optimised forms for the types of foods fractured, notably for carnivoran teeth (Evans and Sanson, 2003). Associations of dental form and function have been broadly applied to dietary groupings and indicate that folivorous primates have relatively large teeth with shearing crests, while frugivorous species have smaller teeth with less developed shearing features (Kay, 1975; Norconk et al., 2013; Allen et al., 2015; Terhune, Cooke, et al., 2015). Some frugivorous primates have a spatulate incisor form, associated with 'peeling' the fruit (Ang et al., 2006). The canines are used in feeding actions in some species such are carnivorous felids for piercing flesh, or in a

small number of primates for piercing fruit pericarp (Kinzey and Norconk, 1990; Christiansen and Adolfssen, 2005). However, canines may also be used for non-feeding purposes, as sexual display or aggression and fighting in primates (i.e. Delgado and Galbany, 2015).

Internal dental morphology has great potential for variability, showing differences in enamel thickness and microstructure (Lucas et al., 2008; Lawn et al., 2009). Enamel distribution on the occlusal surface of the tooth can also vary widely between species, ranging from an even distribution over the tooth surface to being considerably thicker in some regions, such as over cusp tips (Lucas et al., 2008). Thicker enamel has been shown to protect against cracking from feeding on hard foods, protecting the tooth from failure even when there are high stress concentrations (Lucas et al., 2008; Constantino et al., 2016). Another benefit of thicker enamel is slowing the wear process from abrasive or acidic foods (Ungar, 2015). It has been suggested that enamel thickness is an evolutionarily very plastic, such that relatively rapid adaptation is possible if there is selective pressure to do so (Pampush et al., 2013). The microstructure of enamel can also assist with resisting tooth failure, as enamel rods can be arranged in many different ways. Enamel rods may be decussated, shifting their path periodically to form a wave-like shape (Lucas, 2004; Lucas et al., 2008; Ungar, 2015). Such arrangements result in enamel rods that are not arranged entirely in a straight line, providing protection from crack propagation through the enamel (Lucas, 2004; Lucas et al., 2008; Ungar, 2015).

The surface of a given tooth will not remain the same throughout the entire lifespan of an individual due to dental wear (Ungar, 2015). Such changes can occur gradually, as the enamel surface is worn down by grit and phytoliths in the diet or can take the form of large cracks causing sudden, catastrophic failure caused by stresses too high for the tooth surface to withstand (Lucas et al., 2008; Ungar, 2015; Constantino et al., 2016). In some cases such gradual dental wear is advantageous, with teeth wearing to a beneficial secondary morphology as is seen in various graminivorous species, including the primate *Theropithecus gelada* (Koenigswald, 2011; Venkataraman et al., 2014). In other species and when dental wear is seriously advanced it can severely impact the ability of an individual to function and dental senescence can result in starvation (King et al., 2012). Some seed predators, notably *Cercocebus atys,* are noted for their rapid and extensive dental wear, but it is unknown

whether this wear may produce an advantageous morphology as is the case in *Theropithecus gelada*.

The most advantageous dental morphology for a hard-object feeder is currently unknown. Both tooth safety and the optimal shape for reducing the force required to access the seed are relevant. Large and hard foods such as the seeds eaten by some primates present a particular challenge, as with increasing food size and forces required to access the nutrients the risk of fracture increases (Lucas et al., 2008). The high forces involved in accessing such large, hard foods could result in the fracture of the whole tooth (Lawn and Lee, 2009; Lawn et al., 2009). In contrast, small hard foods are more likely to cause the enamel directly in contact with the food to yield, or potentially causing pitting on the tooth surface (Lawn and Lee, 2009; Lawn et al., 2009). This relationship highlights the potential links between dental morphology and diet. Predictions for the optimal tooth for a primate feeding on large, hard foods can be made based on overall tooth shape and size, internal morphology, and cusp morphology – although so many variables create potential for great complexity when examining dental form and function across species. In any case, the teeth have to be able to withstand the regular high forces without failing (Lucas et al., 2008).

Past work has modelled the relationships between tooth size, enamel thickness, and food size with particular reference to hard-object feeders (Lucas et al., 2008; Lawn and Lee, 2009; Lawn et al., 2009). Thicker enamel is expected to be able to withstand higher loads before failure (Lawn and Lee, 2009; Lawn et al., 2009). Indeed, diets of both heavily dental wearing foods and durophagy were found to be associated with thick enamel (Pampush et al., 2013). Orangutans, for example, have thick enamel and feed on nuts encased in large, hard shells (Lucas et al., 1994; Lawn et al., 2009). While feeding on these foods may cause damage in the form of radial cracks, arising from enamel base and radiating to the surface of the tooth, the damage is not necessarily catastrophic (Lawn et al., 2009). Thick enamel with uneven distribution over the occlusal surface is predicted to be optimal for diets which include large, hard foods (Lucas et al., 2008). Tooth size also plays a role here. If enamel thickness is constant, teeth of different sizes are also prone to different failure modes: larger teeth are more likely to show radial cracking, whereas smaller teeth are more likely to have cracks emerge at the dentin-enamel junction (Lawn and Lee, 2009).

The size, shape, arrangement and number of dental cusps affects the contact of the tooth with the food being eaten (Lucas, 2004; Berthaume et al., 2013; Berthaume, 2014). Some patterns between cusp shape and food material properties have been proposed. A narrow and sharp cusp will concentrate stress in a small area, so this could be predicted to be advantageous in a brittle and hard food (Fig. 1.11; Strait, 1997). However, a very sharp cusp will supress cracking, resulting in plastic deformation instead of cracking because the stress is applied to too small an area (Lucas, 2004). Instead, a blunter cusp spreads the stress more widely, which can better promote crack propagation (Lucas, 2004). Given this relationship it would be of great interest to know if seed predators have a dental morphology which facilitates more advantageous food fracture, requiring less work to feed on hard foods. The safety concern of sharp cusps is also important, and while the most advantageous form may fracture single items with low force it may also have poor durability when repeatedly feeding on challenging objects (Strait, 1997; Chai et al., 2009; Crofts and Summers, 2014).



**Figure 1.11 Pressure is concentrated in a sharp cusp (a.) and distributed in a blunt cusp (b.).** *Image source: Strait, 1997*

A range of forms have been observed in non-primate hard object feeders, ranging from low, rounded cusps in otters to domes, flat plates, or convex shapes in marine species (Constantino et al., 2011; Crofts and Summers, 2014). Past work has proposed that a 'complex' arrangement of cusps would be optimal for primate hard-object feeders, combining sharp and dull cusps to both transfer high stress and stabilise food (Berthaume et al., 2013, 2020; Berthaume, 2014). This is not the form identified on primate seed predator molars, which feature low crowns and bulbous cusps in some species (Constantino et al.,

2011; Berthaume et al., 2020). The contact surface area of the tooth with hard foods has not been quantified for seed predator primates, nor has the relationship between these teeth and the fracture mechanics of the food. What is more, not all seed predators feed using their molars, instead primates such as *Cacajao* sp. use their anterior dentition (Barnett et al., 2016). Past studies have examined the relationship between dental form and fracture mechanics in isolated teeth or with hypothetical dental models by using physical testing of foods with real or replica food objects (Lucas et al., 1994; Anderson and Labarbera, 2008; Anderson, 2009; Berthaume et al., 2010; Crofts and Summers, 2014; Barnett et al., 2016; Swan, 2016). Given the challenges faced by primate seed predators it would be of interest to know how the contact between hard foods and these teeth impacts on fracture performance, and if seed predators have dental adaptations which facilitate advantageous fracture performance when feeding on hard objects.

## 1.6.3 Bony adaptations to load

In addition to producing adequate bite forces and gapes for feeding, both the mandible and cranium are subjected to loading during feeding (Ross et al., 2011, 2016). Bone remodels when it is loaded (Pearson and Lieberman, 2004). In the case of the masticatory apparatus bones need to be strong enough to resist structural failure whist also allowing forces to be transmitted. How primate craniofacial and masticatory forms are influenced by mechanical loads has been a rapidly developing field over the last ten years (Strait et al., 2009; Dumont et al., 2011; O'Higgins et al., 2011; Ross et al., 2011; Rowland et al., 2015; Marcé-Nogué et al., 2017; Godinho et al., 2018). Several studies have recorded reduced stress or strain in species with extreme diets, from the tree gouging *Callithrix jacchus* (Dumont et al., 2011), to primate species with a tougher or harder diet (Marcé-Nogué et al., 2017), and fossil hominins (Strait et al., 2009; Smith et al., 2015). Two recent studies have focused on primate seed predators (Ledogar et al., 2018; Püschel et al., 2018). Sclerocarpic feeders appear to have increased craniofacial or mandibular strength compared to the other species, but differences within the group of sclerocarpic feeders did not correlate to dietary hardness, notably in the case of *Cacajao* (Ledogar et al., 2018; Püschel et al., 2018). These unexpected findings could, as proposed by the authors, be due to inaccuracies in known food material property data for the diets of these species. Simplifications in modelling may also be the cause. The contact surface area of the tooth should play a major role in how

efficiently an object will breakdown. The specialised dentition of these species may facilitate more efficient food breakdown (Barnett et al., 2016) which would cause the mandible and cranium to experience less stress and strain. Understanding the role of the teeth in food breakdown is therefore of particular need to further our understanding of how craniofacial and mandibular morphology adapts in response to diet.

## 1.6.4 Gape, muscle stretch, and bite force trade-off

The mouth opens during feeding to a wide enough angle for the food being eaten to be placed between the teeth, referred to as gape (Santana, 2016). The gape required to feed on a specific food varies as widely as the size of the foods eaten, relative to the size of the individuals eating them. The food may also be placed in different positions in the mouth. The same food placed on the posterior teeth instead of the anterior will require a greater degree of mouth opening to process. Some mammals consistently produce very wide gapes in feeding, such as carnivores (Herring and Herring, 1974), primates feeding on large fruits (Norconk et al., 2009) or tree-gouging behaviours (Eng et al., 2009). Others consistently feed with low gapes, especially in herbivorous animals which perform grinding actions in feeding (Herring and Herring, 1974). As with the other components of the masticatory system gape is also affected by non-feeding behaviours such as canine display (Hylander, 2013; Fricano and Perry, 2018). Especially in African papionin primates there is a strong relationship between canine display and wide gape (Hylander, 2013). Males with such large canines must open their mouths to quite a wide degree in order to gain canine clearance, so wide gape is essential (Fricano and Perry, 2018).

When feeding on large, hard objects at wide gapes, as is done by some seed predators (Norconk and Veres, 2011), species must have both high bite force and a large degree of mouth opening at the same time. However, there is a trade-off between high bite force and wide gapes, as increasing gape is known to lower bite force (Herring and Herring, 1974; Dumont and Herrel, 2003; Santana, 2016). The reasons for this are to do with muscle stretch, architecture and position, as well as mandibular morphology (Terhune, Hylander, et al., 2015; Santana, 2016). The length-tension curve of a muscle shows this relationship (section 1.6.1.2; Fig. 1.10), as muscle force changes with muscle length and decreases significantly after a certain degree of muscle stretching (Hylander, 2006; Herzog, 2007).

By virtue of the effect of excessive muscle stretch during wide gapes, relative muscle position will have an effect on this trade-off. More anteriorly positioned muscles will experience a greater degree of stretch, reducing muscle force, so more posteriorly positioned muscles would be expected for species which generate wide gapes (Herring and Herring, 1974; Terhune, Hylander, et al., 2015; Fricano and Perry, 2018). Masseter is predicted to be especially strongly affected by wide gape bites due to the shape and position of this muscle, as it will stretch to a very high degree at wide mouth opening (Herring and Herring, 1974). Because of this it could be predicted that species that need to feed on large hard objects will encounter difficulties. However, mechanical advantage also increases with a more anterior muscle position, so adaptations for generating high bite force with wide gape are in conflict. This adds to the interest as to how such dietary specialists have adapted their morphology.

These negative effects of gape and muscle stretch may be mitigated by variations in muscle architecture as increasing muscle fibre length and decreased pennation can reduce stretch to facilitate wide gapes, but this adaptation comes at the loss of muscle PCSA, lowering bite force if PCSA is not increased (Taylor and Vinyard, 2004, 2009; Terhune, Hylander, et al., 2015; Perry, 2018). A skeletal adaptation correlated with gape is mandible length, as a longer mandible will allow for a greater gape (Terhune, Hylander, et al., 2015). However, an increase in mandible length typically moves bite points further from the TMJ, especially on the anterior dentition, thereby increasing the out-lever length and thereby lowering mechanical advantage (Terhune, Cooke, et al., 2015). As a result, species generating high bite force at wide gapes face conflicting demands and may have different morphological solutions to this dilemma.

Other skeletal features associated with maximising gape may also contribute to reducing muscle stretch, in example low condyles are predicted to reduce masseter muscle stretch and would therefore be an advantageous configuration for wide gape bites (Vinyard et al., 2003; Fricano and Perry, 2018). Anterior translation of the mandible is also thought to reduce the stretch on masseter (Carlson, 1977; Hylander, 2006; Terhune, 2011). Internal muscular architecture can also alter the degree of muscle stretch, as long muscle fibres will reduce the stretch of the muscle (Taylor and Vinyard, 2004; Eng et al., 2009; Iriarte-Diaz et al., 2017). Such a configuration can retain high bite force at a relatively higher gape (Taylor

and Vinyard, 2004; Eng et al., 2009; Iriarte-Diaz et al., 2017). These adaptations present a range of configurations which may help primate seed predators meet the challenges of their high bite force and wide gape diets. Whether or not these primates produce significantly less muscle stretch, or relatively wider gapes than primates with less extreme diets has not yet been investigated.

## 1.7 Do all seed predators possess the same anatomical adaptations? Convergence and many-to-one mapping.

It is clear that the diet of seed predators is mechanically challenging, and that the form of the masticatory apparatus impacts biting force and gape. Whether all seed predators have evolved the same anatomical forms to tackle this challenge is currently unknown. The acquisition of the same biological traits is a relatively common outcome when different species exist in similar environments (Stayton, 2008; Losos, 2011). This process, known as convergence, can be broadly defined as the emergence of similar phenotypes across multiple lineages which have evolved independently of each other (Stayton, 2015a). This is a route by which different species may attain the same function by converging on forms which are both morphologically highly similar and functionally equivalent. Examples of convergence have been documented in a broad range of species and functions (Moen et al., 2013; Aristide et al., 2016; Botton-Divet et al., 2017). Convergence has been observed in the masticatory system, for example in the striking degree of convergence in the masticatory morphology of the primate *Daubentonia madagascariensis* and multiple sciurid species, linked with their shared biomechanical demands from intensive and regular incisor gnawing during feeding (Morris et al., 2018). *Daubentonia madagascariensis* presents an example of a specialist diet, accessing larval burrows underneath tree bark using this unusual dentition (Morris et al., 2018). It has been found that specialists, who are often under tight constraints, are particularly likely to converge in forms (Herrel et al., 2008; Morris et al., 2018; Sherratt et al., 2018). For example, natricine snakes with similar prey-striking behaviour have been shown to converge on a similar head shape (Herrel et al., 2008). Given the extremity and common constraints in the diets of primate seed predators, it is possible that these species have converged both morphologically and functionally.

Alternatively, multiple morphologies may perform the same function. The concept referred to as "many-to-one mapping" has previously been observed in the masticatory system of labrid fish jaws, which possess numerous different 4-bar configurations yet remain functionally equivalent (Alfaro et al., 2005; Wainwright et al., 2005). Similarly, diverse morphology but similar biomechanical function in shrew species which feed on similar foods has been observed (Young et al., 2007). It has been proposed that many-to-one mapping may be a very widespread and common feature of functional morphology (Wainwright et al., 2005; Martinez and Sparks, 2017). This is especially the case in systems with numerous components, as morphological diversity is possible without necessarily altering the biomechanics of the system (Anderson et al., 2014). Many-to-one mapping may allow organisms to occupy the same functional space without occupying the same morphospace (Herrel et al., 2008) and has been reported in hard-object feeders, in example durophagous rays, which vary in many aspects of their masticatory morphology yet are still capable of crushing very hard prey (Kolmann et al., 2015).

Many-to-one mapping presents opportunities for different yet functionally equivalent configurations. Different combinations of in-lever and out-lever lengths achieved through different musculoskeletal forms can result in an equivalent ratio (Alfaro et al., 2005; Wainwright et al., 2005). Different configurations of musculoskeletal form may have the same resulting bite force with both higher mechanical advantage or larger muscles contribute to bite force, while optimised dental form may additionally contribute to reducing force to fracture in feeding (Alfaro et al., 2005; Santana et al., 2012; Evans and Pineda-Munoz, 2018). This functional redundancy allows morphological diversity while maintaining equivalent function, contributing to diversity (Wainwright et al., 2005; Anderson et al., 2014).

Which configurations seed predators possess is unknown. By exploring the different components of the primate seed predator masticatory system it may be possible to determine if primate seed predators show functional equivalence but occupy different morphospaces, or if some of these primates are convergent in their masticatory form, with similar morphologies and function – or indeed, if seed predators vary in both their morphology and their masticatory function, being neither convergent nor functionally equivalent.

## 1.8 Study aims and objectives

Within primates a number of distantly related species face the similar mechanically challenging diet of hard seeds (Norconk et al., 2013). This grouping presents an excellent opportunity to investigate how different species face similar challenges: do primate seed predators show similar solutions to the mechanical challenges presented by their diet in order to retain functional equivalence, or do seed predators vary widely in both form and function? To investigate this, first the masticatory shape of primate seed predators will be quantified and examined for convergence (chapter 2). If these primates are convergent it would suggest that they have evolved the same solution to the challenges presented by their diet. If they are not convergent then the differences in their masticatory configurations must be explored. In either case, to better understand primate seed predator masticatory morphology biomechanical performance indicators (such as mechanical advantage, muscle cross-sectional area, and gape) will be quantified (chapter 3) and the functional capability of seed predators compared, both against each other and wite non-hard object feeding primates. Given their stress-resistant diets of large foods, primate seed feeders should possess more advantageous functional capabilities for both wide gapes and bite forces compared to other primate species. Finally, the ability of primate seed predator's dentition to breakdown hard seeds will be investigated with physical testing and compared against non-seed predators (chapter 4). Understanding the role of teeth in food breakdown using this novel combined approach should add to our understanding of masticatory configurations in primates. Together, these studies aim to examine the question: are there many ways to be a primate nutcracker?

# Chapter 2 - Seed predation: Testing for convergence in masticatory anatomy

## 2.1 Introduction

Stress-resistant feeding offers a great opportunity to understand the evolution of primate skulls in relation to diet. This dietary niche poses particular demands, potentially leading to the evolution of specialist morphologies able to process such a challenging diet (Herrel et al., 2008). Within primates, distantly related taxa have been observed feeding on large, stress-resistant seeds which other sympatric species appear unable to access orally (Norconk and Veres, 2011; Norconk et al., 2013). While past work has described the masticatory morphologies of some of these species (Anapol and Lee, 1994; Wright, 2005; Daegling et al., 2011; Makedonska et al., 2012; Terhune, 2013; Taylor et al., 2018) this has generally focussed on small groups of closely related species. None have carried out a broad comparison of masticatory form in distantly related primates which feed on large stress-resistant foods such as hard seeds and hard-husked unripe fruits. Furthermore, both males and females of these species are known to consume this mechanically challenging diet (Bowler and Bodmer, 2011; McGraw et al., 2011). Given the sexual dimorphism that exists within some primates, especially in relation to body size and canine size, how the sexes have evolved to specialise on this diet is of interest.

To consume large, hard food objects it can be expected that primate seed predators need to attain a high bite force at wide gape (Norconk et al., 2013; Ledogar et al., 2018). However, as reviewed in chapter 1 (section 1.6.4) these performance indicators are often conflicting; features which increase gape can often lead to a reduction in biting force. How these different primate groups have adapted to meet these challenges is unknown. One option is that primates have evolved multiple ways to achieve the same mechanical goal (many-to-one mapping). Another route by which different species may attain the same function is by converging on forms which are both morphologically highly similar and functionally equivalent. Convergence, often seen in nature, produces similar phenotypes across multiple lineages which have evolved independently of each other (Stayton, 2015a). The extreme mechanical demands of requiring both high bite force and gape to consume large, hard seeds may result in convergent masticatory morphology amongst primates which specialise

on these foods. However, given both the potential for many-to-one mapping in the masticatory system and the known broad range of feeding behaviours, morphologies, and body sizes in primates it is also possible that seed predators have different forms which meet the same need.

By combining the tools of geometric morphometric with testing for convergence this study will compare the masticatory morphology of seed predators against each other and against sympatric and closely related species who do not consume such a stress resistant diet. If these primates have converged in their form, it would suggest that they have the same morphological solution to the challenges presented by their diet. If these primates are not convergent, an understanding of the manner in which they vary should offer insights into the range of adaptive variation in the primate masticatory apparatus.

### 2.1.1 Morphologies for increasing bite force and gape

Bite force is a critical measure of potential feeding performance: it is the force generated at a bite point at a given degree of mouth opening. Without additional adjustments by the feeding organism, the maximum attainable bite force poses a limit on which food objects are accessible (Habegger et al., 2012; Santana, 2016). Numerous morphological adaptations in primates have been associated with increased bite force (see chapter 1 review, section 1.6), but two key features include possessing larger muscles and an increased mechanical advantage. Bony proxies have links with muscle size, indicating the size of muscle attachment sites, which would be expected to be relatively large for an organism generating a relatively high bite force (Koyabu and Endo, 2009; Singleton, 2015). A higher mechanical advantage can be achieved by having relatively more anteriorly positioned muscles, for a longer in-lever, or a reduced distance between the joint and the bite point, thereby reducing the length of the out-lever, or a combination of both (Spencer and Demes, 1993; Norconk et al., 2009). As such, increasing muscle size, and/or altering muscle configuration relative to the dental row could improve an individual's performance for stress resistant feeding.

The masticatory configuration most advantageous for wide gape is different. Some proposed gape-increasing morphologies do not necessarily impact bite force, such as an antero-posteriorly longer glenoid (Terhune, 2011), or a low temporo-mandibular joint relative to the occlusal plane (Herring, 1972; Vinyard et al., 2003). Other modifications

directly relate to mechanical advantage: for wide gape, increased prognathism as seen in increased rostrum length permits wider jaw opening, particularly essential for canine clearance in primates with large canines (Hylander, 2013). Anteriorly positioned muscles which increase mechanical advantage, may be disadvantageous in this context, as they may become stretched beyond their optimal length at wide gapes (Herring and Herring, 1974; Fricano and Perry, 2018). As such, the need to produce a wide gape is at odds with some of the major adaptations for high bite force. This is of particular relevance for one primate dietary group; the seed predators who consume food items requiring adaptations for both wide jaw opening and stress resistant feeding.

## 2.1.2 Examining differences and similarities between primate seed predators

Seed predation (as reviewed in chapter 1, section 1.5) is a mechanically challenging dietary specialisation. Primates that consume such a diet are often known for their diet of hard and large seeds and unripe fruits. Given the nutritional value of seeds, the ability to access such a resource would be highly beneficial, however sympatric or closely-related species are excluded, leading to assumptions that seed predator primates possess anatomical adaptations for seed access and crushing (Kinzey, 1992; Daegling and W Scott McGraw, 2007; Koyabu and Endo, 2010; Daegling et al., 2011; Taylor et al., 2018). The feeding position used to consume these seeds varies. One group uses sclerocarpic foraging, in which the anterior dentition is used to extract seeds from their shells, as seen in the pitheciine primates (uakaris, bearded saki, and saki monkeys) (Kinzey, 1992). Another approach is durophagy, which is mastication or crushing of hard seeds using the posterior dentition, as is seen in mangabeys, mandrills, and sometimes in robust capuchins (Norconk et al., 2013). A key difference amongst these groups is the importance of hard seeds in the diets of different primates. For intensive seed predators this resource comprises a high proportion (>50%) of the annual diet, while for other species seeds serve as a fallback resource. For this second group of primates, seeds make up a smaller, but seasonally essential component of the diet (Norconk et al., 2013). However, the intensity of the diet does not necessarily affect the material properties of the seed in question, and seasonal seed predators must still overcome the challenges of this diet, albeit with less repetition.

## 2.1.2.1 Intensive seed predators

Intensive seed predators are found in both South America and Africa. The pitheciine seed predators (*Cacajao,* uakari monkeys; *Chiropotes,* the bearded saki, and *Pithecia*, saki monkeys) are medium-sized South American primates which use their procumbent incisors and robust, laterally splayed canines to gain access to nuts through hard seed casings and hard fruit husks (Fig. 2.1; Kinzey, 1992; Norconk and Veres, 2011; Barnett et al., 2015). The objects eaten by these primates can be extremely large, up to 22 cm in breadth (Norconk et al., 2009), and puncture tests on some of these foods have confirmed their hardness, showing a maximal puncture resistance of 37.8kg/mm2 for *Chiropotes* and 30kg/mm2 for *Pithecia* (Norconk and Veres, 2011). The importance of seeds in the diets of these primates does vary seasonally, but annually seeds make up a very high proportion of the diet of each genus. Reported values are particularly high for *Cacajao calvus* and *Cacajao melanocephalus,* making up 66.9% and 71.2% of the diet respectively (Ayres, 1989; Boubli, 1999). Similar intensities are reported for various *Chiropotes* species (Norconk et al., 2013). Values for *Pithecia* are generally slightly lower, with the proportion of seeds in the diet of *Pithecia pithecia* reported to be 53.3% (Norconk et al., 2013).

The difference in seed quantities eaten and varying robustness of morphology in the pitheciines has caused some researchers to predict an adaptive 'morphocline' in these species (Kinzey, 1992). This morphocline ranges from the most extreme morphology, characterised by the most robust canines and muscle markings as seen in *Cacajao* species, with *Chiropotes* intermediate and *Pithecia* the most gracile (Kinzey, 1992). This relationship is also reflected in body size: *Pithecia* is the smallest-bodied of these three genera with a male mean body mass of 1.94 kg, as compared with 2.9 kg in *Chiropotes* and 3.45 kg in *Cacajao* (Smith and Jungers, 1997). Recent work has found that this may not be an entirely straightforward relationship, as studying bone strain in canine feeding in this group found that *Pithecia* may most efficiently dissipate stresses in feeding (Ledogar et al., 2018).

A very different morphology is seen in the African seed predator *Cercocebus atys* (Fig. 2.1). *Cercocebus atys*, sooty mangabeys, terrestrial primates which are residents of West African forests (Daegling et al., 2011). In contrast to the pitheciine primates this cercopithecid primate is relatively prognathic, with a comparatively long rostrum and long, slender

canines especially in males (Singleton, 2005). *Cercocebus* species are also larger-bodied than the pitheciines primates, with mean body mass ranging from 6.2 kg in females to 11 kg in males (Smith and Jungers, 1997). Sooty mangabeys feed on multiple seed types but the very hard seed *Sacoglottis gabonensis* is an exceptionally large component of their total diet, accounting annually for 49% of the total diet in adult females and an even greater proportion in males (McGraw et al., 2014). The seed is approximately 2.5 cm in breadth and can require up to 3000N in compression testing to initiate fracture (Daegling et al., 2011). *C. atys* consumes these hard seeds with a crushing bite on its posterior dentition, and has greatly enlarged premolars which are presumed to facilitate this diet (McGraw et al., 2011).

The extreme diet of *C. atys* has garnered much interest, which has led to this primate being used as a potential model in hominin evolution, as well as in research exploring the functional morphology of this species (Daegling et al., 2011; Taylor et al., 2018). Especially the enlarged post-canine dentition and posterior feeding position of this primate have been used as a predictive model for *Australopithecus* diet (Daegling et al., 2011). Given this morphology it is surprising that a recent investigation of the morphology of *C. atys* found that it did not have an exceptional mechanical advantage (Taylor et al., 2018). This study did not work with wild-caught specimens, and made comparisons within a narrow phylogeny (Taylor et al., 2018). Other studies have noted interesting features, including facial and palatal shortening relative to other papionins, potentially improving mechanical advantage on the masseter (Singleton, 2005). Further investigation is needed to better understand how this primate is capable of feeding on such an extreme diet.
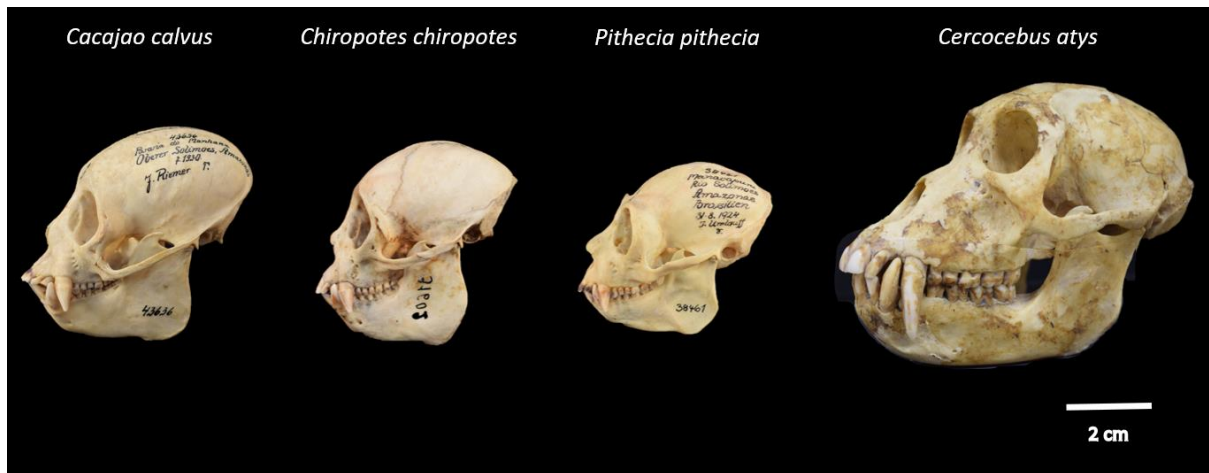
**Figure 2.1 Intensive seed predators (*Cacajao, Chiropotes, Pithecia, Cercocebus*), showing variations in skull morphology. All specimens are male. The pithecines (*Cacajao*, *Chiropotes* and *Pithecia*) have procumbent incisors and splayed canines, as well as prominent muscle markings and deep gonial angle. *Cercocebus* (a cercopithecine) is prognathic, possess longer canines and expanded premolars (not visible on image).**

## 2.1.2.2 Seasonal seed predators

Seasonal seed predators, for whom seeds are thought to serve an essential part of the diet only at specific times of the year, have representatives in both South American and Africa. *Sapajus apella,* the tufted capuchin, is a robust, platyrrhine primate (Fig. 2.2) with a large habitat range and a mean body mass of 3.65 kg in males (Smith and Jungers, 1997). It has a broad diet, often described as omnivorous, which includes hard palm seeds fed upon both by using post-canine bites and, in some populations, by using tools (Izawa and Mizuno, 1977; Izawa, 1979; Terborgh, 1984; Port-Carvalho et al., 2003; Spencer, 2003; Sampaio, 2005). Seed consumption varies seasonally and is only truly important at times when fruit is not abundant, however at times of fruit scarcity seed eating constitutes approximately 25% of feeding bouts or feeding time (Terborgh, 1984; Galetti et al., 1994). These palm seeds (*Astrocaryum* sp.,) are 2-4 cm in diameter and can require up to 6000N of compressive force to fracture (Terborgh, 1984; Visalberghi et al., 2008). Notably, hard seeds are not the only challenging food consumed by *S. apella*, as this primate also feeds on very tough foods positioned on both anterior and posterior dentition (Wright, 2005).

By contrast, the feeding behaviour of *Mandrillus sphinx,* the mandrill (Fig. 2.2), is lesser known due to the reclusive nature and inaccessible habitats of this primate (Hoshino, 1985; Lahm, 1986; Astaras, 2009). This large-bodied African primate has a mean body mass of 31.6

kg in males, with a considerably lower body mass in females, 12.9 kg (Smith and Jungers). Mandrills are described as an opportunistic omnivore, or even generalist, although fruits and seeds are especially important (Hoshino, 1985; Butynski and Koster, 1994; Hongo et al., 2017). Seeds retain some moderate importance year-round, but are very important when fruit is scarce (Astaras, 2009; Hongo et al., 2017). While there is a bulk of evidence to support the claim that mandrills crush and eat hard seeds, this information has been obtained from faecal samples (Hoshino, 1985; Lahm, 1986; Astaras, 2009). As such it is not possible to know the precise contribution of seeds to the mandrill diet, nor have the seeds consumed been measured to test their material properties or their size (Hoshino, 1985; Lahm, 1986; Astaras, 2009). In fruit scarce seasons seeds may account for up to 50% of the mandrill diet, with this value dropping considerably when fruits are plentiful (Hongo et al., 2017). The manner in which mandrills feed on seeds has not been observed, but the use of crushing bites on the posterior dentition is predicted due to the greatly expanded premolars in mandrills (Fleagle and McGraw, 2002). This morphology is also similar to that of their close relative *C. atys*, and as such a similar feeding behaviour is predicted (Fleagle and McGraw, 2002). Given the large body size and highly prognathic morphology of this primate associated with its extremely large canines in males, it serves as an interesting comparison to its close relative *Cercocebus*, but the masticatory form of *Mandrillus* has yet to be examined.
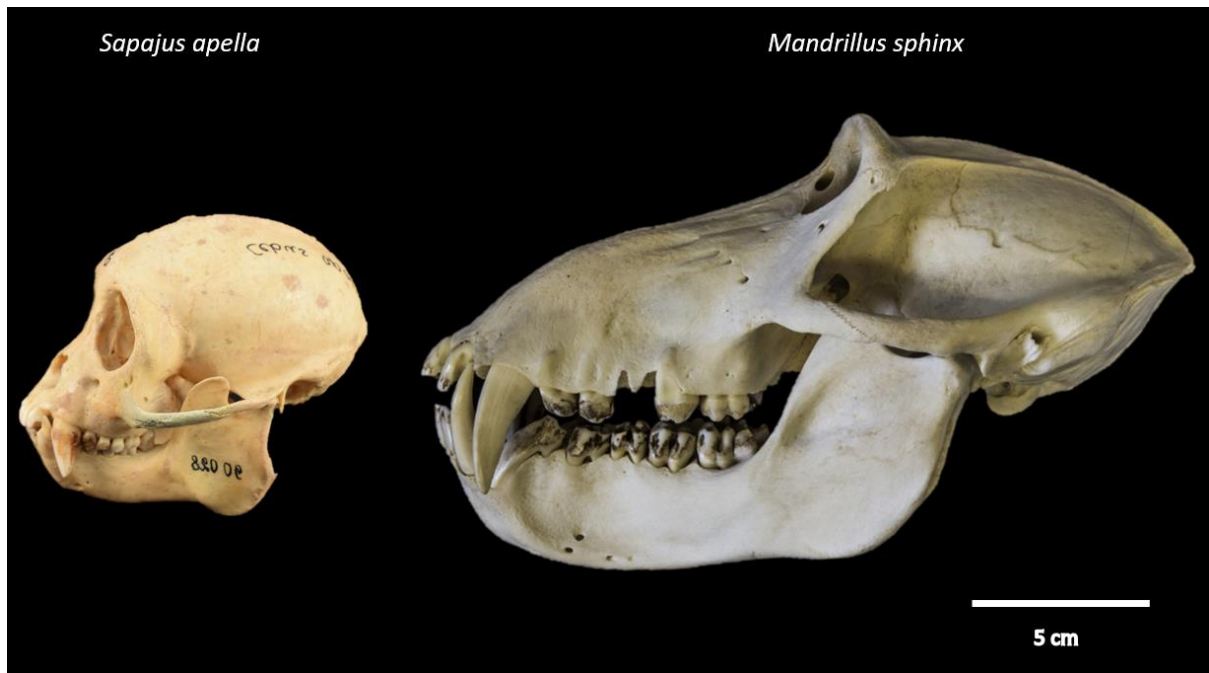
**Figure 2.2 Seasonal seeds predators (*Sapajus* and *Mandrillus*), showing variations in skull morphology. *Image source (Mandrillus): Dirks et al., 2020.***

### 2.1.3 Different forms for different needs?

Taken together, primate seed predators span a broad range which encompasses different approaches to eating hard seeds and hard-husked fruits. The challenges of generating high bite force at wide gape are shared, and these behaviours are to the exclusion of sympatric primates or close relatives with different dietary niches. Whether the masticatory morphology of primate seed predators has advantageous adaptations to increase bite force and mechanical advantage while maintaining gape is not universally known, nor is the pathway taken by different groups. The items eaten by posterior-feeding seed predators are absolutely smaller than those eaten by the anterior-feeding seed predators (see 2.1.2), but as posterior-feeders must place foods further back in the mouth both must attain wide gapes. Anterior-feeding places the food in a location which may decrease mechanical advantage as this position has a longer out-lever than the posterior (Dechow and Carlson, 1990). Particularly given the relatively small body size of anterior-feeding pitheciines this may increase the selective pressure for more extreme forms, but this has yet to be investigated.

Work on predicting the diet of extinct species highlights the importance of achieving an understanding of the link between masticatory form and function. The robust australopiths,

with their large sagittal crests and anteriorly placed zygomatic arches, were long thought to have similar masticatory form due to a diet with comparable mechanical challenges (Rak, 1983; Lee-Thorp, 2011). Indeed, *Paranthropus boisei* was referred to as a "nutcracker" due to their enlarged dentition and skeletal features (Ungar and Sponheimer, 2011). Isotope and microwear data, however, suggests that instead of nuts, tough grasses were the major component of their diet (Ungar and Sponheimer, 2011). The morphologically similar *A. robustus* was consuming a generalist diet which may have included mechanically challenging fall-back foods (Wood and Strait, 2004). Using masticatory morphology to infer dietary specialisations is common in hominin palaeontology (e.g. Strait et al., 2009; Daegling et al., 2011; Smith et al., 2015) but far from accurate. One reason for this complexity is that there could be many ways to make a species mechanically capable of consuming the same diet.

## 2.1.4 Constraints on masticatory form

Part of the complexity underpinning the wide range of feeding behaviours observed even amongst primates with extreme diets can be linked to the wide range of constraints which affect masticatory form. These include non-dietary needs such as usage of teeth for aggression or sexual display (Ross and Iriarte-diaz, 2014). Some primates, such as male mandrills, have exceptionally large canines which are linked to rank, sexual competition and fighting (Setchell et al., 2001; Leigh et al., 2005). Phylogeny and geography can also affect masticatory form: the phylogenetic history of a species can constrain masticatory variability (Ross and Iriarte-Diaz, 2014; Bjarnason et al., 2015), and geography has been found to affect cranial size and shape (Cardini and Elton, 2009).

Another important aspect is body size. Primate seed predators vary widely in body mass, ranging from the pitheciine primates with a body mass of 1.5 – 3.5 kg body to the very large-bodied mandrill, with males having a body mass of approximately 31 kg (Smith and Jungers, 1997). Body mass in some primates (*Cercocebus galeritus,* pitheciine species, and *Ateles paniscus*) have been shown not to correlate with puncture resistance of foods in the diet (Norconk and Veres, 2011). By contrast, muscle mass – a key predictor of bite force – is strongly correlated with body size (Anderson et al., 2008; Hartstone-Rose et al., 2018). It is therefore likely that smaller-bodied primates face constraints in their masticatory form and

are therefore more likely to show adaptations which increase bite force and gape relative to larger-bodied primates with similar dietary needs.

Related to body size, another component to consider with regard to feeding biomechanics and possible convergence is sexual dimorphism. Some primate species show extreme sexual dimorphism, expressed in body size as well as in other traits such as canine size (Fig. 2.3; Hylander, 2013). Males typically have a larger body size than females, which without any other changes in morphology would increase bite force through increased muscle size (Koyabu and Endo, 2009). An especially extreme example of this is seen in *Mandrillus*, where males have more than twice the body mass of females at an average of 31.6 kg compared with 12.9 kg for females (Smith and Jungers, 1997). However, males are also more likely to have increased canine size, associated with greater prognathism (Singleton, 2005; Hylander, 2013). This may affect their mechanical advantage and could result in functional equivalence between males and females despite differing morphologies. Both female and male seed predators feed on similar diets, meaning they must overcome similar dietary challenges. As such, they must each have features which enable this diet, although whether the same adaptations can be seen in both sexes has yet to be examined.
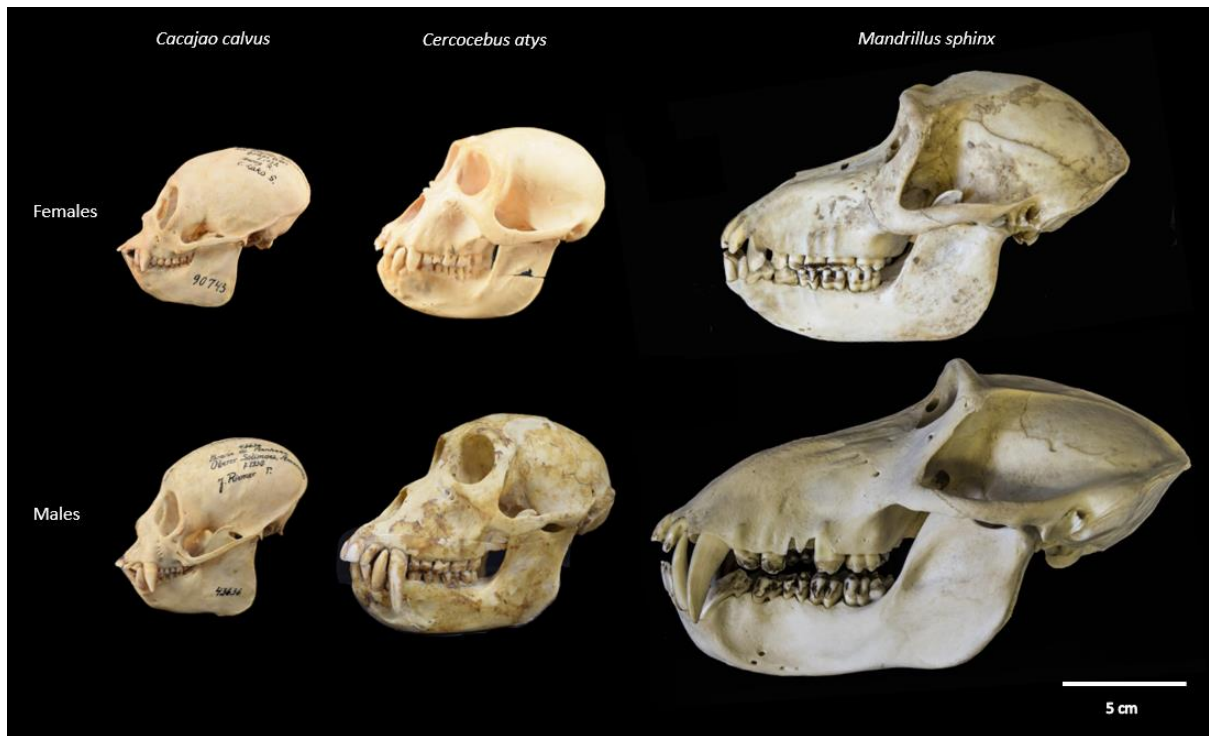
**Figure 2.3 Examples of differing degrees of sexual dimorphism within the skulls of some primate seed predators. Note how *Cacajao calvus* males and females are very similar in overall skull morphology compared to the highly sexually dimorphic *Mandrillus sphinx*. *Image sources (Mandrillus female and male)*: *Dirks et al., 2020.***

## 2.1.5 Convergence and many-to-one mapping in the masticatory system

The many constraints which affect masticatory form in combination with the known variation in primate seed predators suggest that there may be more than one advantageous morphology for seed predation, rather than convergence on one optimal adaptation. Convergence and many-to-one mapping are not mutually exclusive and serve to highlight pathways by which organisms may attain functional equivalence. By many-to-one-mapping different organisms can inhabit the same area of 'functional space' without occupying the same morphological space (Herrel et al., 2008). However, systems with a high chance of many-to-one-mapping have a decreased likelihood for convergence as there are multiple possible forms which can achieve equivalent function (Thompson et al., 2017). The masticatory system is a classic example of many-to-one mapping as different configurations can result in the same bite force. Many-to-one mapping has been repeatedly observed in the masticatory system and is especially well-observed in labrid fish (Ch.1, 1.7; Alfaro et al., 2005; Wainwright et al., 2005)

This is not to say that convergence has never been observed in the masticatory system. Although convergence in masticatory form has never been tested for in primate seed predators, dietary extremists are often clearly distinguished from other groups when examining masticatory forms, as the challenges of their diet are thought to constrain their masticatory form (Metzger and Herrel, 2005; Herrel et al., 2008; Santana et al., 2010). The striking convergence in the masticatory morphology of aye-ayes (*Daubentonia madagascariensis*) and two sciurids is one recent example of convergence linked with the functional morphology of feeding (Morris et al., 2018). These groups both face extreme specialist demands from intensive and regular incisor gnawing during feeding (Morris et al., 2018). A further example can be seen in different river dolphin genera which converge in their skull morphology, with features linked to predictions on feeding biomechanics (Page and Cooper, 2017). The role of the strong selective pressures imposed by specialist diets is highlighted by the example of convergent evolution in sea snakes, as those sea snakes which are specialist predators of burrowing eels were found to converge in their morphotype, while species with a different diet did not converge (Sherratt et al., 2018). In these species, either by chance or by the specific constraints imposed by their dietary needs they have found similar solutions to meeting the needs of their diet.

For morphological convergence to occur it is thought that species need to be faced with a narrow set of morphological options to meet their functional needs, as otherwise many-to-one mapping is more likely (Herrel et al., 2008). Convergence can arise for multiple reasons, which may be random and not necessarily related to trait functionality, or indeed non-convergent adaptations can occur despite similar pressures (Stayton, 2008; Losos, 2011). In any case it is important to evaluate the functional consequences of traits examined (Stayton, 2008; Losos, 2011). It is not known whether the morphological options to meet functional needs of primate seed predators are narrow enough to result in convergent masticatory form. Primate seed predators do face some similar challenges in their diet, but they appear to face these challenges with different approaches: it may be that there is more than one approach for accessing seeds (Fig. 2.4). Whether the systems are more similar than they appear and converge, many-to-one mapping is present, or neither is present in primate seed predators is unknown.

**Figure 2.4 Many tools with the same out-come – variation in mechanical nutcrackers.** *Image sources, from top left: Allorge, distributed under a CC-BY-SA-3.0 licence (https://commons.wikimedia.org/wiki /File:Bol_casse-noix.jpg); Avery, distributed under a CC-BY-SA-4.0 licence (https://commons.wikimedia.org/ wiki/File:Heatmaster_Crackerjack_nutcracker_2.JPG); Spears, distributed under CC-BY-SA-3.0 (https://commons.wikimedia.org/wiki/File:Common_nutcracker.jpg); public domain (https://commons. wikimedia.org /wiki/ File:Nutcracker_1.jpg).*

## 2.1.6 Testing for convergence, or a lack thereof.

Past studies investigating the relationships between extreme diet and morphology within closely-related primate groups have not always met predictions. While no study has examined a broad group of seed predators, past work has sought to quantify the masticatory form of these primates individually or within closely related groups using various methods. One such approach is taking and comparing linear measurements of skeletal features (e.g. Anapol and Lee, 1994; Wright, 2005; Koyabu and Endo, 2010; Daegling et al., 2011). Measurements taken in this manner can be used to calculate biomechanical variables including mechanical advantage, as well as estimating the size of skeletal and muscular traits relating to feeding and resistance to loading. While informative, these measurements omit potentially significant anatomical information which could be captured

in much greater detail by using 3D measurements (Terhune, 2013). 3D coordinate data can also be used for geometric morphometric (GMM) analysis. GMM methods can be used for statistical testing as well as for visualising shape changes between different species or specimens (e.g. Makedonska et al., 2012; Terhune, 2013; Delgado and Galbany, 2015). A key strength of GMM is the ability to visualise shape variation, often by using deformation grids and surface warps to show how morphology varies between specimens (Mitteroecker and Gunz, 2009). This can provide an understanding of complex shape changes between groups. By statistically testing the degree to which complex shapes exhibit similarities in form it is possible to use this data to measure the degree of convergence between individuals (Stayton, 2015a; Aristide et al., 2016; Morris et al., 2018). A recently developed method incorporating both morphological similarity and distance to last common ancestor can quantify the degree of convergence between two specimens (Stayton, 2015a). This method can establish whether two organisms have evolved to be more similar to one another than would be expected under a Brownian motion model of evolution (Stayton, 2015a). This can be applied to the study of species with known different morphologies which are predicted to face similar challenges in their diet, such as primate seed predators.

## 2.1.7 Comparison species

Not all primates feed on hard seeds, instead feeding on softer foods or foods with different challenges, such as tough grasses. If primate seed predators have adaptations which facilitate accessing stress-resistant diets, it would be expected that relatives and sympatric species have a different masticatory form. A notable example is *Ateles paniscus,* the red-faced spider monkey (Fig. 2.5), which is sympatric with *Chiropotes satanas* and *Pithecia pithecia* in Guyana and yet has been shown to consistently feed on softer fruits despite its larger body size (Norconk and Veres, 2011). This mid-sized primate feeds on ripe fruit intensively, in some cases swallowing fruits whole, with the seed intact (Dew, 2005). Interestingly through defecating undamaged seeds the spider monkey has become a very important seed disperser in its habitats (Dew, 2005). There is overlap between especially the saki and spider monkey diet, but the fruits eaten by *Ateles* have lower puncture resistance and are smaller, approximately 5cm in breadth (Norconk et al., 2009; Norconk and Veres, 2011).

Other interesting comparisons can be made within the Cebidae. Until recently all capuchins were classed in one genus, *Cebus,* but recent work has divided them into the robust *Sapajus* and more gracile *Cebus* genera (Alfaro et al., 2012). Past studies of *Sapajus apella* have often compared it with its close relatives, gracile *Cebus* capuchins (Fig. 2.5). Gracile capuchins are omnivorous but consume a high proportion of fruit and their diet is less hard and tough diet than their close relatives (de Ruiter, 1986; Dorothy M Fragaszy and Boinski, 1995; Alfaro et al., 2012). For example, they are not known to feed on undamaged hard palm seeds (Terborgh, 1984). An even higher proportion of soft fruits is eaten by another cebid, the squirrel monkey *Saimiri* (Fig. 2.5). This small-bodied primate occupies a different feeding niche, turning to invertebrates when fruits are rare (Rosenberger, 1992; Lima and Ferrari, 2003). The common squirrel monkey, *Saimiri sciureus,* is sympatric with numerous seed predators in north-eastern South America (Norconk et al., 2003). Their diet varies seasonally, swinging between 20% plant and 80% animal in a fruit-scarce season, and reversed in seasons when fruits are plentiful (Lima and Ferrari, 2003). They are considered a relatively gracile primate (Anapol and Lee, 1994) but the likely function of their masticatory form has yet to be thoroughly investigated.

An intriguing African example can be made with the western chimpanzee *Pan troglodytes verus,* which is sympatric with *Cercocebus atys* (Fig. 2.5; Boesch, C. and Boesch, 1982). Fruit features heavily in the diet of this large-bodied primate, and they are variously referred to as ripe fruit specialists or as omnivorous due to their opportunistic feeding on a wide range of food types (Sugiyama, 1987; Doran, 1997). Numerous species of nuts are processed by these chimpanzees using natural tools in several different populations, including *Coula edulis* and *Sacoglottis gabonensis* (Boesch and Boesch, 1982; Koops et al., 2013). Notably these seeds are eaten by *Cercocebus atys* without the aid of tools, using only their teeth (Daegling et al., 2011; McGraw et al., 2011; McGraw et al., 2014). Although chimpanzees are not typically referred to as seed predators (Norconk et al., 2013), there are some reports of chimpanzees feeding on extremely hard seeds even without stone tools, crushing very hard seeds directly on their teeth (Yamakoshi, 1998; Norconk and Veres, 2011). It is noteworthy however that tools are considered essential to nut-cracking behaviours, and while teeth may be used occasionally this is not a regular behaviour (Yamakoshi, 1998). Whether this is

because chimpanzees cannot repeatedly feed on such challenging foods or because tools are more efficient is unclear.

By contrast, there is one large-bodied papionin which feeds on an extremely unusual diet for primates. *Theropithecus gelada,* the gelada baboon, feeds on a very tough diet consisting almost entirely of grasses and grass parts (Fig. 2.5; Dunbar and Dunbar, 1974; Iwamoto et al., 1996). This unusual primate occupies a very different feeding niche to seed predators or frugivorous primates, requiring small gape for its diet and very repetitive chewing of tough, but not hard foods. It likely has very different masticatory needs in comparison to most other primates and it would be interesting to explore this variation.
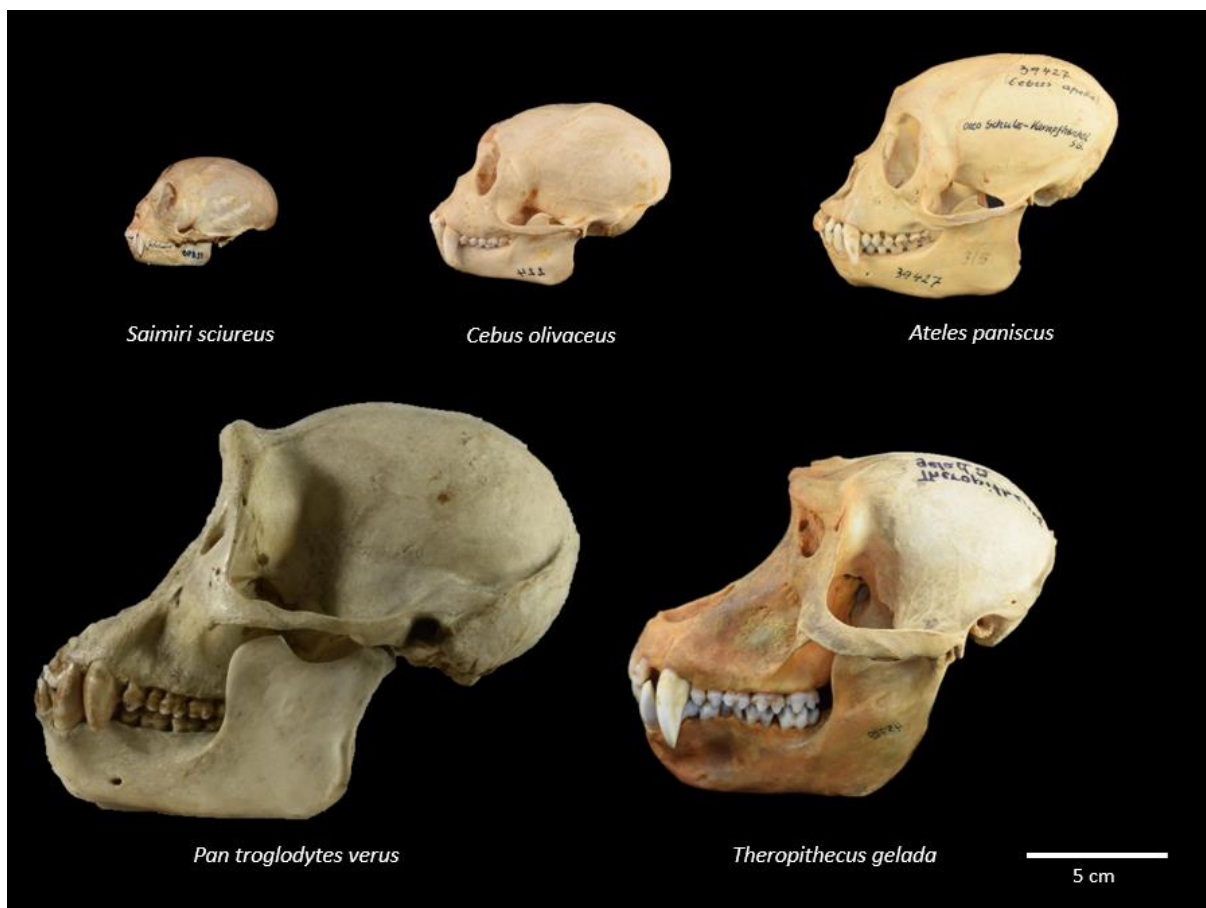


**Figure 2.5 Comparison species (*Saimiri, Cebus, Ateles, Pan,* and *Theropithecus*), showing variations in skull morphology. *Image source (P. t. verus): Hungarian Natural History Museum.***

## 2.2 Aims and hypotheses

The aim of this study is to determine whether different primate seed predators have found different solutions to meet the demands of their challenging diet, despite their unifying need of high bite force and wide gape during feeding. To meet this aim the masticatory shape of seed predators will be examined. Due to differences in body size and processing methods these primates are not expected to converge in their masticatory form. Notably, the smaller-bodied anterior-feeding primates are predicted to show the most extreme adaptations to overcome the additional challenges presented by feeding in this position (longer out-lever). Posterior-feeding primates must feed at a wide gape, and as such adaptations for high bite force are still expected. Another important source of variation is predicted to be sex, as female primates are typically smaller in body size than males yet feed on similarly challenging foods in seed predator species. To surmount this challenge despite their likely smaller muscle mass females can be expected to show even more extreme morphologies than males. These predictions will be tested using GMM methods with a carefully selected set of landmarks with clear links to function, an approach which has been shown to identify complex shape differences between groups (Terhune, 2013). Convergence will be tested using Stayton's $C_1$ (Stayton, 2015a) and plotted as a phylomorphospace. If convergence is found it will indicate that primate seed predators meet the challenges of their diet in a similar manner, but it is expected that primate seed predators have different morphologies.

The following hypotheses will be tested:

**H1:** There will be no convergence in masticatory shape between seed predators.

**H2:** All seed predators will show masticatory shapes which relate to high bite force at wide gape.

**H3:** Females seed predators will be morphologically distinct from males; shapes associated with maximising biting force are expected to be even more extreme in females.

## 2.3 Materials and methods

### 2.3.1 Sample selection

The sample used comprises mandible and crania of 11 primate species from 5 families. The sample was sourced from numerous collections: The Berlin Natural History Museum, the Senckenberg Institute, the Hull York Medical School collection, Museum of Zoology of the University of São Paulo, and numerous institutions via the online repository Morphosource (for specimen database see Appendix 1). Species were selected from a range of dietary groupings in order to represent a range of seed predators and sympatric or closely related primates which are not seed predators (Table 2.1, Fig. 2.6). Platyrrhine and catarrhine species are both represented to showcase a broad phylogeny. Comparison species are primarily those sympatric with seed predators but with a different diet were selected.

Seed predators include both regular, intensive seed predating primates which consume seeds year-round (*Cercocebus, Cacajao, Pithecia,* and *Chiropotes*), as well as primates which seasonally feed on seeds (*Mandrillus, Sapajus*) (Norconk et al., 2013). Comparison species include primates who are typically described as primarily frugivorous (*Ateles, Cebus, Pan*) as well as a primate with mixed frugivory-insectivory (*Saimiri*), and a graminivorous primate with a consistently very tough diet (*Theropithecus*) (Dunbar and Dunbar, 1974; van Roosmalen, 1985; McGrew et al., 1997; Lima and Ferrari, 2003).

Both female and male primates were included in the sample as both sexes feed on similar diets, albeit to different degrees of extremity in some cases (Bowler and Bodmer, 2011; McGraw et al., 2011; Geissler et al., 2020). Data collection attempted to equally represent females and males, but the higher numbers of males found in the collections used resulted in a better representation of males in the sample (Table 2.1). Furthermore, *Cebus olivaceus* was poorly represented in collections and only a very small sample of males was included. All specimens are wild-caught with exceptions only for *Theropithecus,* for which it was impossible to gain access to sufficient wild-caught specimens (Appendix 1 for details). The sample was collected with the aim of including one species per genus, but this was not attainable in all cases. This was especially the case for *Cacajao* as it was not possible to gain access to sufficient individuals of one species, although the individuals collected still span overall a relatively small range and have very comparable diets (de Sousa, 2009).

**Table 2.1 Genus and species of specimens in the sample, showing majority diet and the number of males and females composing the sample. Intensive seed predators are listed first, followed by seasonal seed predators, then comparison species. Feeding position is only commented on for seed predators. Additional details for each specimen can be found in Appendix 1.** *Body mass data: Smith and Jungers, 1997.*

| Genus | Species | Dietary category* | Feeding position | Female body mass (kg) | Male body mass (kg) | *n* Male | *n* Female | *n* Unknown sex |
|---|---|---|---|---|---|---|---|---|
| *Cacajao* | *Cacajao calvus; C. c. rubicundus; C. melanocephalus* | Seed predator (intensive) | Anterior | 2.88 | 3.45 | 8 | 3 | 0 |
| *Chiropotes* | *Chiropotes chiropotes; C. sagulatus* | Seed predator (intensive) | Anterior | 2.58 | 2.9 | 5 | 5 | 1 |
| *Pithecia* | *Pithecia pithecia* | Seed predator (intensive) | Anterior | 1.58 | 1.94 | 5 | 3 | 2 |
| *Cercocebus* | *Cercocebus atys* | Seed predator (intensive) | Posterior | 6.2 | 11 | 6 | 2 | 0 |
| *Mandrillus* | *Mandrillus sphinx* | Seed predator (seasonal) | Posterior | 12.9 | 31.6 | 6 | 5 | 0 |
| *Sapajus* | *Sapajus apella* | Seed predator (seasonal) | Posterior | 2.52 | 3.65 | 5 | 6 | 0 |
| *Ateles* | *Ateles paniscus* | Non-seed predator (soft fruit) | | 8.44 | 9.11 | 6 | 5 | 0 |
| *Cebus* | *Cebus olivaceus* | Non-seed predator (fruit and invertebrates) | | 2.52 | 3.29 | 2 | 0 | 0 |
| *Pan* | *Pan troglodytes verus* | Non-seed predator (fruit) | | 41.6 | 46.3 | 4 | 4 | 0 |
| *Saimiri* | *Saimiri sciureus* | Non-seed predator (fruit and invertebrates) | | 0.662 | 0.779 | 4 | 5 | 0 |
| *Theropithecus* | *Theropithecus gelada* | Non-seed predator (grasses) | | 11.7 | 19 | 5 | 4 | 0 |
| **Total count of sample:** | | | | | | **56** | **42** | **3** |
| | | | | | | | | **Grand total: 101** |

* (Dunbar and Dunbar, 1974; Izawa and Mizuno, 1977; Izawa, 1979; Boesch and Boesch, 1982; Terborgh, 1984; Hoshino, 1985; van Roosmalen, 1985; Lahm, 1986; Sugiyama, 1987; Mcgrew et al., 1988; Ayres, 1989; Peres, 1991, 1993; Kinzey, 1992; Kinzey and Norconk, 1993; Galetti et al., 1994; Dorothy M Fragaszy and Boinski, 1995; Lima and Ferrari, 2003; Wieczkowski, 2003; Dew, 2005; Astaras, 2009; Norconk and Veres, 2011; Bowler and Bodmer, 2011; Daegling et al., 2011; Alfaro et al., 2012; W.S. McGraw et al., 2014; Barnett et al., 2016)

**a. Geographic distribution of platyrrhine species included in the sample.**



**Intensive seed predators**

Cacajao sp. (*Cacajao calvus, Cacajao calvus rubicundus, Cacajao melanocephalus*)

*Chiropotes* sp. (*Chiropotes chiropotes, Chiropotes sagulatus*)

*Pithecia pithecia*

**Seasonal seed predator**

*Sapajus apella*

**Comparison species**

*Ateles paniscus*

*Cebus olivaceus*

*Saimiri sciureus*

Region where all species, with the exclusion of *Cacajao* sp., are sympatric.
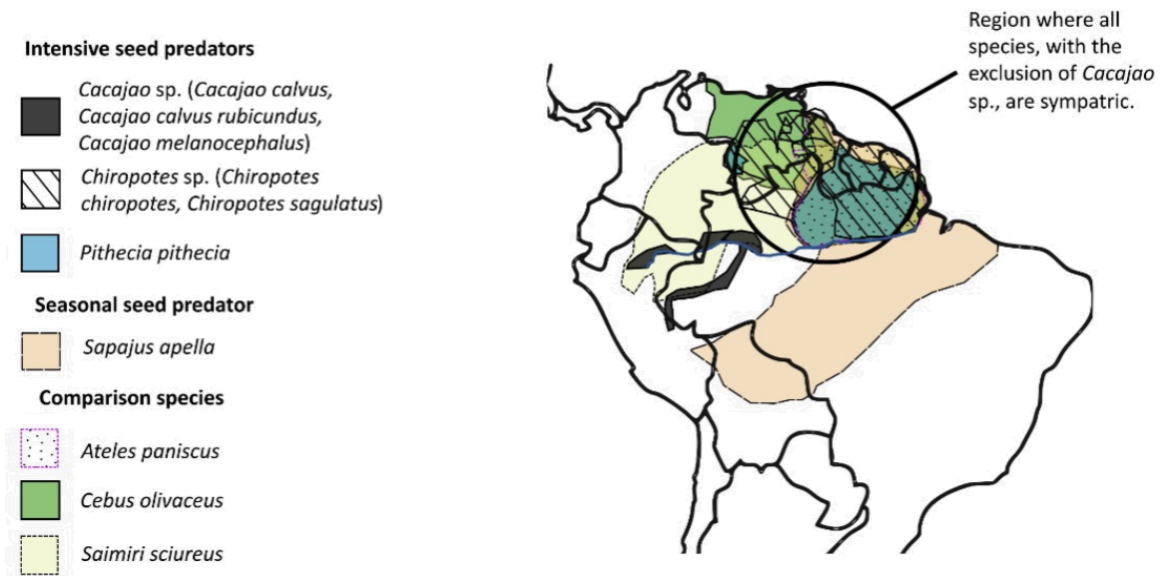
**b. Geographic distribution of catarrhine species included in the sample.**



**Intensive seed predator**

*Cercocebus atys*

**Seasonal seed predator**

*Mandrillus sphinx*

**Comparison species**

*Pan troglodytes verus*

*Theropithecus gelada*
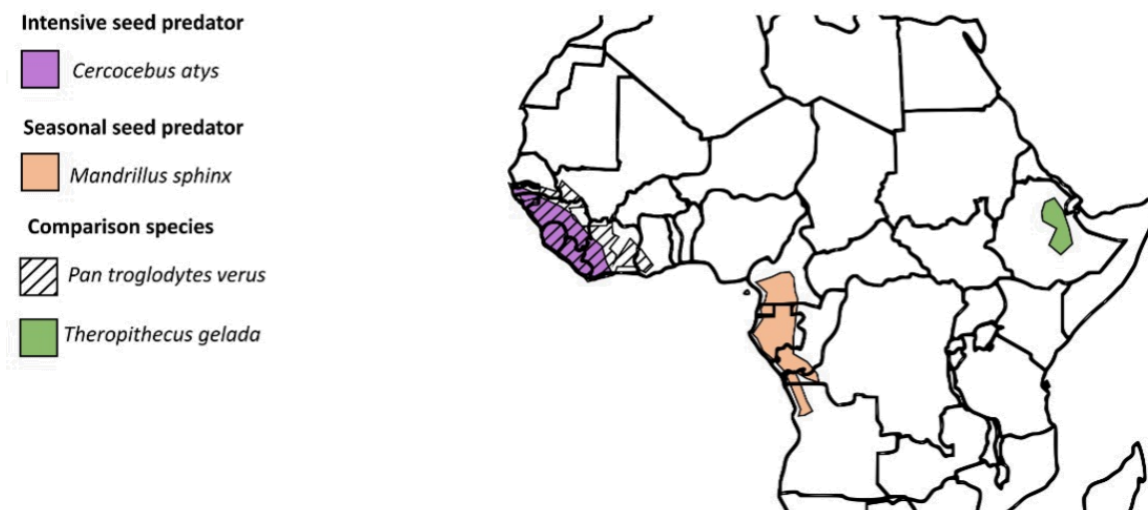
**Figure 2.6 Maps showing distributions of species in the sample. Showing sample distribution in a. South America (platyrrhine) and b. Africa (catarrhine).** *Distribution data sources:* **Boinski and Cropp, 1999; Telfer, 2003; de Sousa, 2009; Gippoliti, 2010; Clee et al., 2015; Morales-jimenez et al., 2015; Martins-junior et al., 2018; Ferreira da Silva et al., 2020.**

## 2.3.2 Data acquisition

3D models of the sample were used in this study, using both mandible and crania. As a first step the specimens had to be digitised. Scans were sourced from the collections of numerous institutions (see specimen database in Appendix 1 for full details). A large number of scans spanning many species were accessed digitally via MorphoSource.org (scans used uploaded by Harvard University Museum, Smithsonian Institution, American Museum of Natural History). Permission was also obtained from the Berlin Natural History Museum (Naturkundemuseum Berlin) to collect a large number of samples representing many species. Specimens from the Naturkundemuseum Berlin were scanned directly for this study. Three further collections which had been previously scanned also contributed to the sample: Hull York Medical School (*Cercocebus*), the Senckenberg Institute collection (*Pan*) and the Museum of Zoology at the University of São Paulo (*Cacajao*).

## 2.3.2.1 Imaging

Four imaging modalities were used to digitise the sample: medical CT, microCT, structured-light surface scans, and photogrammetry (Table 2.2). Both medical and microCT scans offer internal and external anatomy. Photogrammetry and surface scans can only capture external anatomy but are portable and more cost-effective methods of data collection. For this study, medical and microCT scans were accessed via numerous repositories (Table 2.2; full details in Appendix 1). Surface scans and photogrammetry were collected at the Berlin Natural History Museum. A Breuckmann Smartscan 3D (www.aicon.com) was used for surface scanning, mounted with optical lenses (diagonal scope of 250mm and average spatial precision of 18 μm). After scanning, surface scans were aligned and merged to a full model in the Breuckmann scanner's own software, Optocat (Breuckmann, 2014). Photogrammetry models were made from photographs taken with a 24.3 mega-pixel digital single-lens reflex (DSLR) Nikon D5300 camera mounted with a Nikon AF-P 18-55 mm f/5.6 lens. Photographs were processed to create 3D surfaces using Agisoft (PhotoScan Professional, Agisoft LLC). Additionally, to aid in alignment to occlusion, a series of 'composite' photogrammetry models - scans of the skull in occlusion - were made for each specimen collected as surface scan or photogrammetry scan. A protocol was set up for each modality following pilot testing to ensure quality and repeatability (Appendix 2, A2.1).

**Table 2.2 Number of specimens processed with each imaging modality.**

| Imaging modality | Number of specimens | Source |
|---|---|---|
|  |  |  |
| Medical CT | 16 | Hull York Medical School collection, Senckenberg Institute |
| MicroCT | 44 | Museum of Zoology of the University of São Paulo; Collections accessed through Morphosource (see Appendix 1) |
| Surface scan | 20 | Natural History Museum, Berlin |
| Photogrammetry | 21 | Natural History Museum, Berlin |
|  | **Total: 101** |  |

## 2.3.3.2 Sensitivity: samples sourced from multiple imaging modalities

The reliability of combining data from multiple types of imaging modalities was evaluated to determine if this could be a potential source of error. Use of scanned data from multiple imaging modalities is a necessary and common procedure as it is often not possible to source a sufficiently large sample using only one modality (Robinson and Terhune, 2017). Previous studies which used data collected with surface scans, microCT scans, and 3D digitisers found that while combining multiple observers and data sources can increase error, there was greater variance between observers than between methods (Robinson and Terhune, 2017). A similar result was found when comparing photogrammetry and surface scans, where the two surfaces were found to have very low degrees of deviation from one another (Katz and Friess, 2014; Evin et al., 2016), or when surface scan, photogrammetry and MicroCT were compared (Giacomini et al., 2019). Photogrammetry and MicroCT have also been found to produce comparable results (Buzi et al., 2018). Photogrammetry is a relatively new method for digitising skeletal material which has been shown to result in a very close match between physical measurements and resulting models (Morgan et al., 2019). Taken together, past work indicates that while mixing modalities introduces the potential for some errors, this is relatively small and does not affect the interpretation of results, especially when considering a broad sample (Robinson and Terhune, 2017; Giacomini et al., 2019).

In order to test for a potential impact on this study a sensitivity study was carried out (Appendix 2, A2.2). A mandible (*Cercocebus atys* #C13.21) had previously been scanned by

both medical and Micro CT. This same mandible was imaged again using both photogrammetry and surface scanning. A landmark set of 33 landmarks were placed repeatedly on each modality type, 5 days in a row, using Avizo (v9.2, FEI, Thermo Fischer Scientific). Finally, four additional *Cercocebus* individuals (medical CT scans) were landmarked once each. Geometric morphometric methods were then used to assess variance between modalities. While some differences between modality groupings were found, all results on all days for the repeated specimen clustered very tightly when other *Cercocebus* individuals were included (Appendix 2, A2.2). As other studies have also shown, there are some inevitable effects when combining data from multiple modalities, but the differences are minor even when comparing individuals of the same species, which are clearly distinguishable.

## 2.3.3 Sample preparation

## 2.3.3.1 Scan processing

Models required additional processing after digitisation to prepare them for landmark placement. Medical and Micro-CT scans were processed using threshold-based segmentation in Avizo. In order to allow for processing some scans had to be down-sampled due to their large size (for voxel sizes see specimen database, Appendix 1). This was done to the least possible degree to preserve scan integrity and avoid loss of information (Veneziano et al., 2018). Extraneous material was removed and, where necessary, mandible and cranium were separated to form two distinct surfaces. No smoothing was applied to final surfaces as smoothing has been found to modify or simplify models (Veneziano et al., 2018). Less processing was required for surface and photogrammetry scans. Extraneous material was removed in the dedicated software used to create each scan type. Mesh integrity issues such as flipped vertices were repaired using Geomagic (Geomagic Studio, 3D Systems).

## 2.3.3.2 Alignment to occlusion

Scans were aligned to occlusion for this study in order to include the entire masticatory form. The majority of past shape analyses have either examined the cranium or mandible in isolation (e.g. Singleton, 2002; Taylor, 2002; Makedonska et al., 2012; Galland and Friess, 2016), or compared measurements taken separately on the mandible and cranium, without

aligning them to be in occlusion (e.g. Anapol and Lee, 1994). Correctly aligning mandible and cranium to be in occlusion is challenging, as a small error in alignment will affect the total shape. However, analysing mandibles and crania in occlusion presents great advantages in considering the full shape, size, and relative position of the masticatory muscles.

To guide alignment to occlusion, photogrammetry models of the articulated mandible and cranium ('composite' models) were made in addition to surface scans and photogrammetry models of separated mandibles and crania (Fig 2.7) for each species recorded with these modalities. These models were used to create a highly accurate model of the specimen in occlusion by aligning separated mandible and cranium to the composite model. At least one such model in occlusion was made for each species and sex. Data collected in the Natural History Museum of Berlin included a photogrammetry model of each individual in occlusion. If no scan representing a species was made at the Natural History Museum of Berlin then a model of both a male and female specimen was 3D printed (Zprint 350) and a photogrammetry model was made of the specimen in occlusion to use as a guide. These could be used to align nearly half of the sample (n = 47, Appendix 1 for list) to occlusion using rigid landmark warping in Avizo.
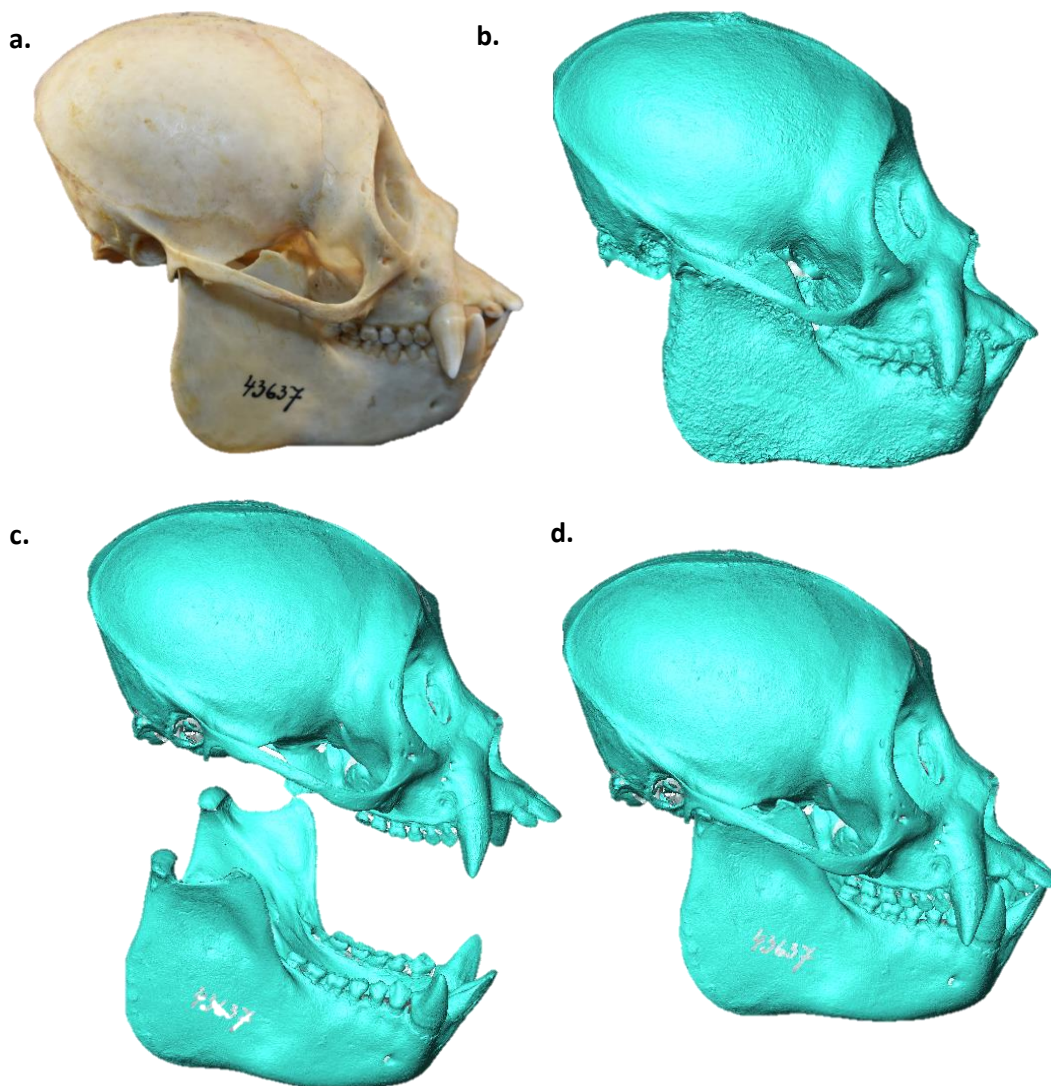
**Figure 2.7 Alignment to occlusion with composite model. Demonstrating process with *Cacajao* specimen #43637 showing: a. photograph of the original specimen set in occlusion, as used in the creation of the photogrammetry model itself; b. quick composite model of the same specimen collected via photogrammetry; c. separately made high resolution unaligned surface scan models of the mandible and cranium; and d. surface scans of the mandible and cranium aligned to occlusion using the photogrammetry composite model (b.) as a guide.**

Specimens aligned using a composite model (Fig. 2.7) were then used to create reference guides of occlusion. This reference guided landmark placement so that the remainder of the sample could be rigidly warped to occlusion. A sensitivity study was carried out to ensure that models could be accurately and repeatedly aligned to occlusion using this method. This sensitivity study tested multiple alignment techniques to determine firstly whether it is

80

possible to accurately align models to occlusion without using a composite model, and secondly to assess which of several methods for occluding models most closely matches the model warped to the composite scan.

To examine this a specimen was selected to use in testing (*Cacajao* specimen #45251) and was warped to the exact position of the composite model (landmark-based rigid warp in Avizo). This was taken as the most accurate alignment and used as the basis for comparison in other alignment attempts. It was also used to create a template of accurate occlusion to serve as a reference. Next, the warped-to-composite model was landmarked to provide a basis for comparison after a series of rigid landmark-based warps (Table 2.3). Five different attempts were made to re-align the mandible to the cranium using different techniques (Table 2.3). A "master set" of landmarks which did not move were used to compare with each alignment attempt. The landmark set used matches that used for the main study (please see section 2.3.4 below, Table 2.4). After landmarking, the mandible was manually translated to a recorded value by a second researcher to re-separate it from the cranium. The master set of landmarks was translated by the same value by the second researcher so that the set could be warped with the mandible and serve as the basis for comparison.

**Table 2.3 The different methods used for each of the five attempts to re-align the mandible and cranium.**

| Alignment method | Method |
|---|---|
| V1 | Rigid landmark warp using few condylar landmarks (n = 1) and numerous dental landmarks (n = 11) on each side. |
| V2 | Rigid landmark warp using numerous condylar landmarks (n = 3) and a decreased number of dental landmarks (n = 6) on each side. |
| V3 | Rigid landmark warp using numerous condylar landmarks (n = 3) and numerous dental landmarks (n = 11) on each side. |
| V4 | Bookstein warp, in which it was attempted to see if an aligned model of a closely related individual could be used as a template for alignment. The aligned photogrammetry model of a second specimen, *Cacajao* #43636, was selected. The cranium of the aligned specimen and the cranium of specimen #45251 were landmarked. A "bookstein warp", which translates a surface and deforms it to most closely match the landmarks placed, was carried out, warping the composite model to the cranium of the specimen to be aligned. The aligned and deformed model #43636 was then used to align the mandible of specimen #45251 to the cranium of #45251. |
| V5 | Manual re-alignment, in which the mandible was manually translated by a known amount to a position of occlusion. |

The reference guide made from the alignment to occlusion with the composite model was used as a template. The same method used to re-align the mandible was then used to move the landmark set with it by exactly the same degree. This meant that there is no concern for the role of intraobserver error, as the landmarks were only ever placed once, then moved with the mandible as it was separated from then re-aligned to the cranium.

To test how much the re-aligned mandible had moved relative to its original position in the optimally aligned model, the mandibular landmarks were isolated from the cranial landmarks for each re-aligned model. This was done as only the mandible had shifted its position relative to the cranium. To broaden the comparison and to gauge the relative distance of the landmark sets from one another, two further landmark sets were created. First the same specimen, *Cacajao* #45251, was landmarked again, with the same full landmark set placed a second time at a considerably later date than the original master set. This was to assess whether intraobservor error or alignment attempts produced greater error. Secondly, an additional *Cacajao* individual, #43636, was landmarked with the same landmark set, to compare the differences between alignment attempts, intraobservor error, and the difference between two closely related individuals. The landmarks were analysed by principal component analysis in RStudio with the packages Arothron (Profico et al., 2019), Morpho (Schlager, 2017), and geomorph (Adams et al., 2020).

Examining exclusively the original landmarked specimen and the 5 different alignment attempts found that all three rigid-landmark warp alignment attempts (V1-V3) clustered relatively closely to the original landmark set, suggesting that all three landmark-based warps came very close to an identical alignment to the original (Fig. 2.8). Of these three, the second (V2), which had an intermediate total landmark number (n = 18 landmarks in total, 9 on each side), is the closest to the original. The manual alignment, v4, and the Bookstein warp alignment, V5 are distinct both from each other and from the group including the original and the three landmarked versions (V1-V3) along both the first and second principal component.
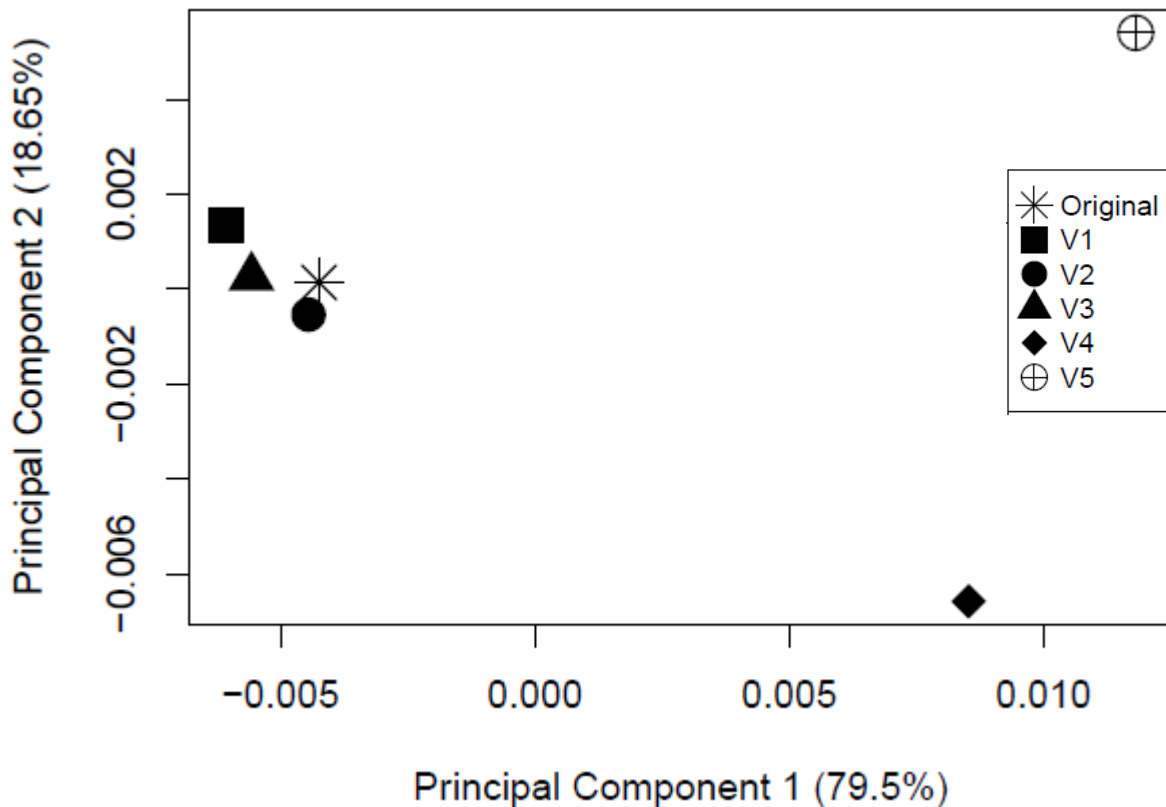
**Figure 2.8 Principal components plot for comparison of alignment to occlusion methods (PC1 and PC2).** Showing PC1 (79.5% of variance) and PC2 (18.6% of variance) for the 5 different re-alignment attempts, labelled v1-v5, and the original landmark set placed on the model warped directly to the composite.

The close clustering of the three rigid landmark warps (V1-V3) is emphasised when the re-landmarked original and comparison specimen are included (Fig. 2.9). The three rigid landmark alignment methods (V1-V3) group tightly with the original, to a greater degree than the re-landmarked original. This would suggest that the effect of rigid landmark warps to occlusion is less than the effect of intraobserver error. The manual alignment (V4) and the Bookstein warp alignment (V5) again show quite a clear separation from the original. The closely related second individual is distinctly separated along the first principal component from all other points.
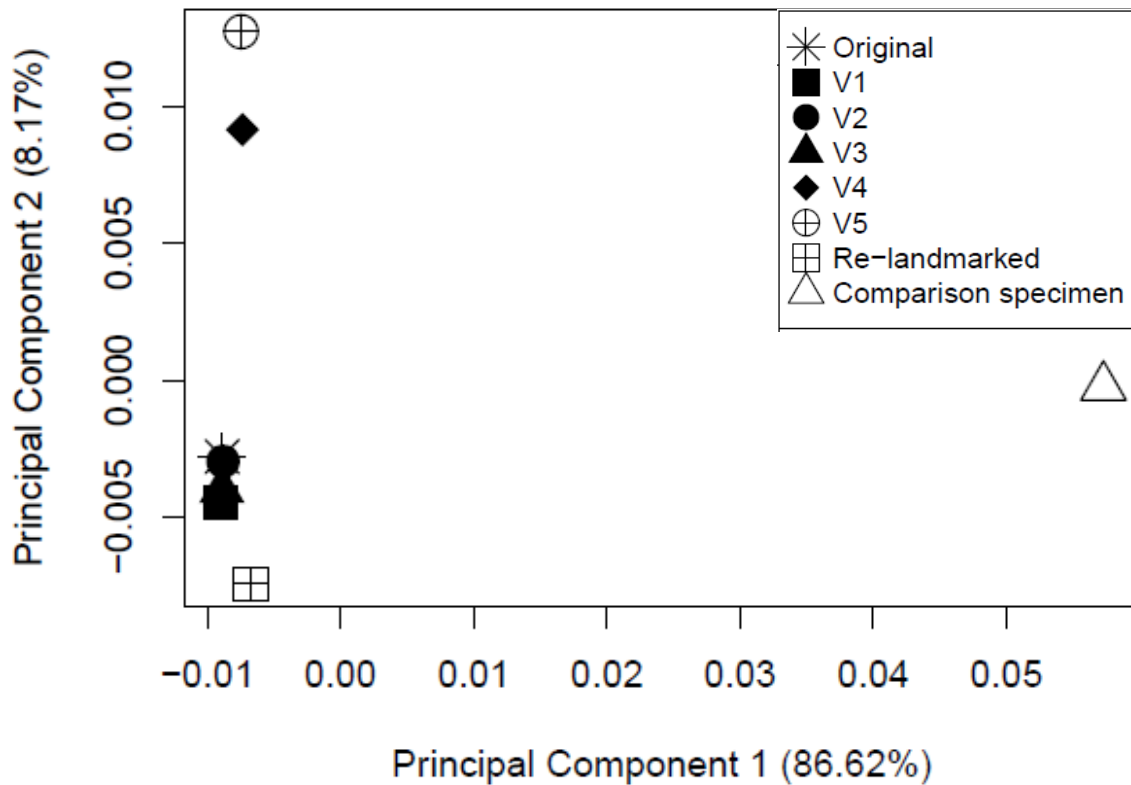
**Figure 2.9 Principal components plot for comparison of alignment to occlusion methods (PC1 and PC2), including comparison specimens. Plot shows PC1 (86.62% of variance) and PC2 (8.17% of variance) for the 5 different re-alignment attempts, labelled V1-V5 and the original set of landmarks, as well as this same specimen re-landmarked and a second individual for comparison.**

Taken together, this sensitivity analysis shows that the rigid landmark warp for alignment to occlusion is very reliable, producing less difference than intraobserver error when comparing results of alignment to composite model and alignment using rigid landmarks based on the template . This approach was used to align all specimens to occlusion which did not have a 'composite' photogrammetry model to use as guide (details of alignment type for each specimen, see Appendix 1).

## 2.3.4 Landmark set and placement

A set of 3D landmark coordinates encompassing masticatory muscle origin and insertion sites, joint morphology, and relative dental position was selected to reflect masticatory function (Terhune, Cooke, et al., 2015). Landmarks were placed on each specimen in the software Avizo. The selected landmarks comprised a set of 90 points (51 cranial, 39 mandibular) per specimen (Table 2.4 and Fig. 2.10), placed bilaterally. Landmarks were either of Type I or II, with the exception of two bilateral semi-landmarks (centre of

temporalis and masseter origin sites). To place semi-landmarks, a surface path was drawn along the site of muscle origin in Avizo using the geodesic surface path tool. This surface path was exported, then it was imported into RStudio (v1.1.383, RStudio Team, 2015), where the packages Arothron (Profico et al., 2019) and bezier (Olsen, 2018) were used to calculate the midpoint along the surface path and export it as a landmark. For referencing all R package material an additional package named bibtex was used (Francois, 2020).

**Table 2.4 Landmarks employed in this study, including both cranial and mandibular landmarks. The landmarks represent the origin and insertion sites of muscles of mastication, the relative position of dentition, and joint morphology**.

| Subset | # | Functional significance | Landmark placement |
|---|---|---|---|
| **Cranium** | 1,2 | Superficial masseter origin | Most anterior and medial point on cranial masseteric scar |
| | 3,4 | Superficial masseter origin | Most anterior and lateral point on cranial masseteric scar |
| | 5,6 | Superficial masseter origin | Most anterior and central point on cranial masseteric scar between medial and lateral attachment points |
| | 7,8 | Deep masseter origin | Most inferior point on articular tubercle |
| | 9,10 | Deep masseter origin | Most posterior point on margin of temporal fossa |
| | 11,12 | Temporalis origin | Most anterior and superior point along temporal line |
| | 13,14 | Temporalis origin | Most posterior and superior point along temporal line |
| | 15,16 | Medial Pterygoid origin | Most inferior point on lateral pterygoid plate |
| | 17,18 | Medial Pterygoid origin | Anterior-most point on lateral pterygoid plate |
| | 19,20 | Medial Pterygoid origin | Posterior-most point on lateral pterygoid plate |
| | 21,22 | Dental position | Point posterior to the alveolus of the last maxillary molar |
| | 23,24 | Dental position | Centre of last molar |
| | 25,26 | Dental position | Centre of first molar |
| | 27,28 | Dental position | Paracone of first premolar |
| | 29,30 | Dental | Canine cusp tip |
| | 31:34 | Dental | Centre of incisor edge for first and second incisor |
| | 35 | Dental | Prosthion |
| | 36,37 | Dental | Mesial centre-point on the alveolus at the base of the canine |
| | 38,39 | Dental | Distal centre-point on the alveolus at the base of the second incisor |
| | 40,41 | Joint morphology | Deepest point in the mandibular fossa |
| | 42,43 | Joint | Most inferior point on the postglenoid process |
| | 44,45 | Joint | Most inferior point on the entoglenoid process |

| | | | |
|---|---|---|---|
| | 46,47 | Joint | Most anterior point on the articular surface of the glenoid fossa T |
| | 48,49 | Superficial masseter origin | Semi-landmark: Centre of inferior zygomatic arch, midpoint between landmarks 1,3 and 2,4 |
| | 50,51 | Temporalis origin | Semi-landmark: Centre of temporal line, midpoint between landmarks 9,11 and 10, 12 |
| **Mandible** | 52,53 | Masseter & Medial Pterygoid insertion | Gonion |
| | 54,55 | Superficial masseter insertion | Anterior inferior point of masseteric scar on mandibular body |
| | 56,57 | Superficial masseter insertion | Superior posterior post of masseteric scar on mandibular ramus |
| | 58,59 | Temporalis insertion | Most superior point on coronoid process |
| | 60,61 | Temporalis insertion | Most posterior and inferior point of the coronoid process |
| | 62,63 | Temporalis insertion | Point where mandibular ramus meets alveolus laterally |
| | 64,65 | Dental | Point posterior to the alveolus of the last maxillary molar |
| | 66,67 | Dental | Centre of last molar |
| | 68,69 | Dental | Centre of first molar |
| | 70,71 | Dental | Protocone of first premolar |
| | 72,73 | Dental | Canine cusp tip |
| | 74:77 | Dental | Centre of incisor edge for first and second incisor |
| | 78 | Dental | Infradentale |
| | 79,80 | Dental | Point between second incisor and canine on the alveolar bone |
| | 81,82 | Joint | Most lateral point on the articular surface of the mandibular condyle |
| | 83,84 | Joint | Most medial point on the articular surface of the mandibular condyle |
| | 85,86 | Joint | Most posterior point on the articular surface of the mandibular condyle |
| | 87,88 | Joint | Most anterior point on the articular surface of the mandibular condyle |
| | 89,90 | Joint | Fulcrum of the condyle, taken as the point through which a line between 81,83 (L), 82,84 (R) and 85, 87 (L), 86,88 (R) pass. |
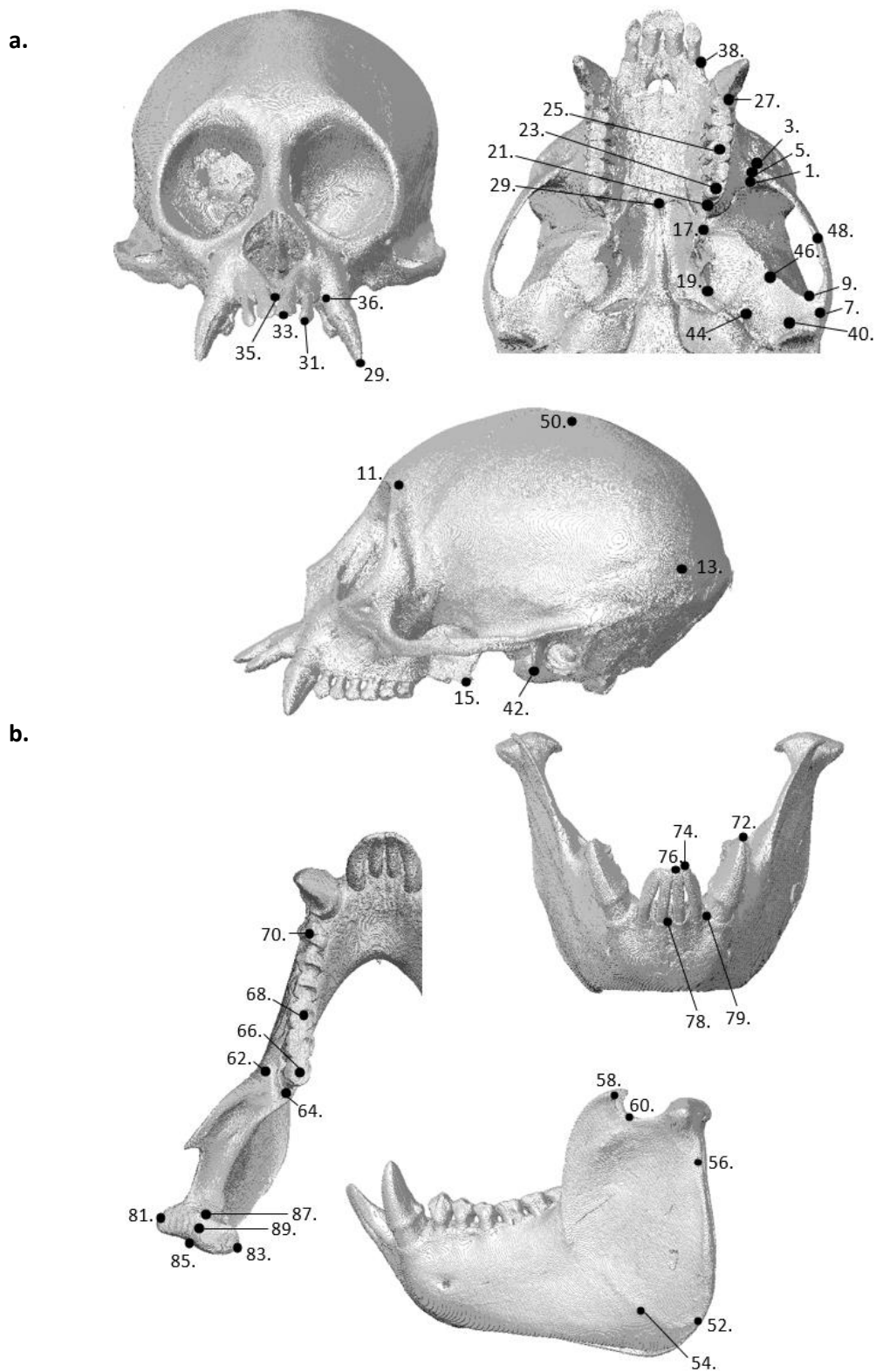
**Figure 2.10 Landmark set used in study. Demonstrated on *Chiropotes* (left side), showing a. cranial landmarks displayed in frontal, inferior, and lateral view and b. mandibular landmarks, showing frontal, superior, and lateral view.**

## 2.3.4.1 Missing data repair

Accommodation for missing data is unfortunately a common issue in GMM studies as it is often impossible to acquire a sufficiently large sample of specimens in perfect condition (Arbour and Brown, 2014). For this study, although the most complete specimens possible were selected for analysis, some have damage to relevant areas. To resolve this issue landmarks can be repaired in some manner, or missing data can be removed. Past studies have advised that it is better to estimate data than to work with missing data, and that estimation methods, if sensibly chosen, can produce very reliable results (Arbour and Brown, 2014). The best method of dealing with missing data depends on the sample at hand. Method includes estimating landmarks using bilateral symmetry, thin plate spline interpolation, mean substitution, and regression-based methods (Mitteroecker and Gunz, 2009; Neeser et al., 2009; Couette and White, 2010; Arbour and Brown, 2014). The most appropriate and accurate method to use should be chosen based on both the size of the sample at hand and the type of damage (Neeser et al., 2009). In example, with very large samples, regression-based methods have been found to produce highly accurate results, but this is not the case for relatively small samples, where thin plate spline (TPS) warping was found to produce more accurate results (Neeser et al., 2009). Another method of repairing is restoring bilateral symmetry where damage is unilateral, a simple yet highly effective method to repair data (Mitteroecker and Gunz, 2009). Past studies using bilateral symmetry to estimate missing landmarks found very low error (Couette and White, 2010) and this 'mirroring' method has been used in past studies examining primate cranio-facial landmarks (Galland and Friess, 2016).

Specimens for this study were evaluated ahead of data collection to assess damage. Due to the rarity of some species in accessible collections, damaged specimens had to be included. However, certain types of damage were excluded from the sample: if bilateral dental or zygomatic damage was present, or bilateral damage affecting the temporal line the specimen was excluded based on the fact that these are key regions for analysis and full estimation of landmark position may have too large an effect on the results. As a result of careful specimen selection, the sample has a relatively small total number of missing landmarks. A total of 3.03% of landmarks are missing, spread over a large number of individuals: 90 / 101 individuals have some form of damage, but 3 or fewer landmarks are

affected in 77 / 101 individuals (2.7% damage or less). Following the past examples (Couette and White, 2010; Galland and Friess, 2016), all specimens have <20% missing landmarks, with the exception of two *Cercocebus* individuals, both of whom have exactly 20% of landmarks missing. It was not possible to access *Cercocebus* specimens with less damage. (percentage missing landmarks for each specimen detailed in Appendix 1).

The most suitable repairs given this sample are to first use bilateral symmetry where possible and using TPS warping where necessary due to bilateral damage, following the example of Galland and Friess (2016). RStudio with packages Arothron (Profico et al., 2019) and Morpho (Schlager, 2017) was used to read the data and carry out the landmark repairs. Landmarks were mirrored if a bilateral counterpart was present, which restored the majority of specimens to a complete state. For each species, these complete landmark sets were returned to the pool of specimens, which by result was now large enough for use with the TPS warping repair. Four complete specimens within a single species were used as a reference for the TPS warp, which estimates the position of the new landmark based on the position of the landmarks in the comparison sample. No TPS repairs were needed for *Cebus*, which had a <4 specimen sample size. The unrepaired and repaired landmark sets were superimposed and examined in a 3D grid as an initial check of the success of the repair, before being exported individually for a final check against the original scan in Avizo (Fig 2.11).
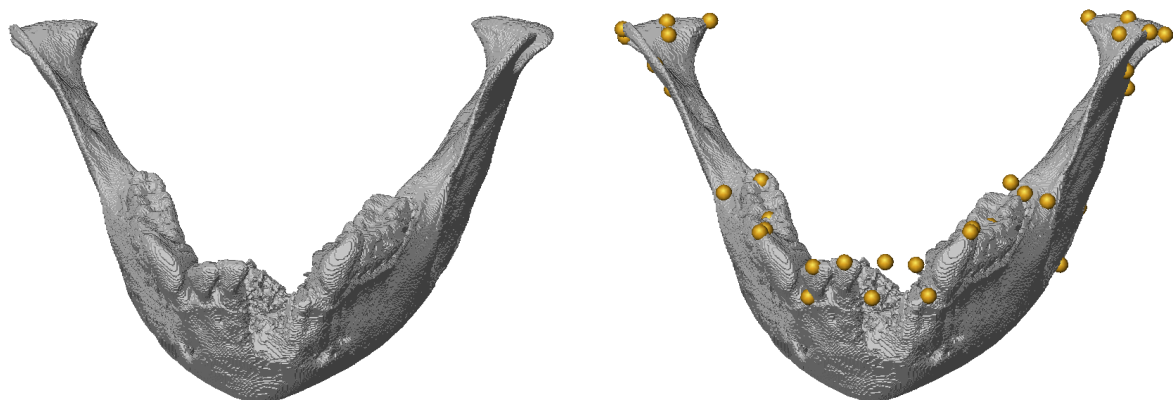


**Figure 2.11 Repairing missing landmarks. Showing damaged *Saimiri* (#30568) mandible, missing both left incisors, left M3, and damaged alveolar bone in region of infradentale. Dental landmarks could be repaired using bilateral symmetry, a TPS-based estimation is used to estimate infradentale.**

## 2.3.4.2 Intraobserver error

In order to confirm the reliability of placing the landmarks a study of intraobserver error was carried out on all Type I and II landmarks. Testing for the role of intraobserver error is standard practice in landmark-based shape analysis studies (Singleton, 2002; Terhune, Cooke, et al., 2015; Robinson and Terhune, 2017). A specimen with no damage to landmarked areas was selected (*Pithecia pithecia* specimen #38461, surface scan) and landmarks were placed for 5 consecutive days then compared using GMM methods to two other specimens (*Ateles* 39432 and *Pan* 383) landmarked once each. A Procrustes Anova showed that the repeated landmark sets on *Pithecia* were not significantly different, and the repeats clustered tightly when the comparison specimens were included in a principal component analysis (Appendix 2, A2.4). Overall results indicate that landmarking is very accurate and repeatable. To further increase accuracy for final data collection a reference guide including all landmarks was created and used to guide placement.

## 2.3.5 Data analysis

## 2.3.5.1 Geometric morphometric analysis

A geometric morphometric (GMM) analysis was carried out to examine the masticatory shapes of the primates in the sample (H2 and H3). The shape of an object is defined as its geometrical properties which are unaffected by scaling, rotation, and translation, whereas form examines the properties of an object which are affected by scale but not by rotation and translation (O'Higgins, 2000; Mitteroecker and Gunz, 2009). To register the landmark set (Table 2.4) in shape-space, a Generalised Procrustes Analysis (GPA) was carried out in which the sum of squared distances between equivalent landmarks is minimised by translating, rotating, and scaling to centroid size (O'Higgins, 2000; Slice, 2007). The resulting sets of shape coordinates were then analysed using Principal Components Analysis (PCA), plotting the scores of both the shape and shape-size datasets and examining all components representing >5% of variance. Centroid size was also plotted against the two components with the highest variance. Thin plate splines (TPS) and 3D surface deformations were computed in order to visualise the changes in shape associated with the principal components (O'Higgins, 2000; Mitteroecker and Gunz, 2009). A specimen from the centre of the distribution (*Cercocebus* 25626) was selected for these deformations and was warped to

the most positive and negative PC (principal component) scores. RStudio was used for all analyses and visualisations, using the packages Arothron (Profico et al., 2019), Morpho (Schlager, 2017), geomorph (Adams et al., 2020), and rgl (Adler and Murdoch, 2020).

A small number of individuals with unknown sex (n = 3) are included in two species (*Chiropotes, Pithecia*) to increase sample size. Species were also classified by dietary categories in order to visualise their diet when examining their shape (Table 2.1). Intensive and occasional seed predators both feed on similar foods, but to very different degrees, so are considered distinct categories. Comparison species were collectively grouped as 'non-hard' to facilitate the comparison, although it is noted that the comparison species in this study feed on a range of diets.

## 2.3.5.2 Analysis: Convergence

The degree of convergence between primate seed predators was determined using Stayton's $C_1$ (Stayton, 2015a) in order to test H1. Convergence is broadly defined as the emergence of similar phenotypes across multiple lineages which have evolved independently of each other, but it can be defined, measured, and tested for in many different manners (Stayton, 2008, 2015a). For this study, pattern-based convergence was tested for in primate seed predators. This is a definition of convergence which refers to cases where two organisms have evolved to have a greater degree of similarity to one another than was present in their ancestors, and accepts independently evolved similarity without reference to a specific process or mechanism (Stayton, 2008, 2015b, 2015a). The similarity between the two taxa of interest can be quantified using Stayton's $C_1$, (Stayton, 2015a), which takes both morphological similarity and distance to last common ancestor into account, and is calculated as:

$$C_1 = 1 - (D_{tip} / D_{max}),$$

where morphological similarity is referred to as $D_{tip}$ and is measured as the distance between the two individuals of interest in phenotypic space (using, i.e. Procrustes distance), and $D_{max}$ accounts for the distance to the last common ancestor by measuring the maximum distance between individuals of interest (Stayton, 2015a). The resulting value indicates whether the two specimens tested are closer in the morphospace than would be expected under a model of Brownian Motion (Sherratt et al., 2018). A $C_1$ value is given between 0 and

1, where 0 would show absolutely no convergence and 1 would show two lineages which have converged to the point of being indistinguishable (Stayton, 2015a). Tests of significance can also be carried out on these values, using simulations of evolution under a Brownian motion model as comparison values to assess the significance of the convergence (Stayton, 2015a; Morris et al., 2018; Sherratt et al., 2018). Results are visualised by plotting the phylomorphospace, which projects the sample phylogeny onto a multivariate trait space, in this case a principal component plot constructed using GMM methods (Stayton, 2015a; Morris et al., 2018).

For this study, intensive and seasonal seed predators from different primate families were tested to calculate the degree of convergence between their masticatory shapes. The phylogeny of the sample (Fig 2.12) was constructed using the online resource 10k Trees (Arnold et al., 2010), which constructs phylogenies using Bayesian inference. The sample spans five families: Atelidae, Cebidae, Pitheciidae, Cercopithecidae and Hominidae. A representative specimen was selected for each species and sex from each family (Appendix 1). The representative specimen was selected from the centre of the distribution in a principal component analysis of all specimens in shape space, separated by sex, calculated in RStudio using the packages Morpho (Schlager, 2017) and Arothron (Profico et al., 2019). If multiple specimens were similarly centred in the morphospace then the individual with the lower number of repaired landmarks was selected. No photogrammetry models were used as representatives, emphasising surface scans and MicroCT where possible and MedCT where necessary, following the results of the sensitivity study and past research best practice advice (Appendix 2, A2.3).

To carry out these tests, the previously described landmark dataset (Table 2.3) was used in conjunction with the sample phylogeny data to construct a phylomorphospace in RStudio with the package phytools (Revell, 2012). Females and males are considered separately as the sexes are predicted to present morphological differences. A Generalised Procrustes Analysis (GPA) was carried out to calculate the principal component scores of the sample. These scores were then used to calculate a measure of convergence using the package convevol (Stayton, 2018). The significance of the convergence was assessed using 1000 simulations (Stayton, 2015a; Morris et al., 2018; Sherratt et al., 2018). The statistical significance criterion was set to a p-value of <0.05.
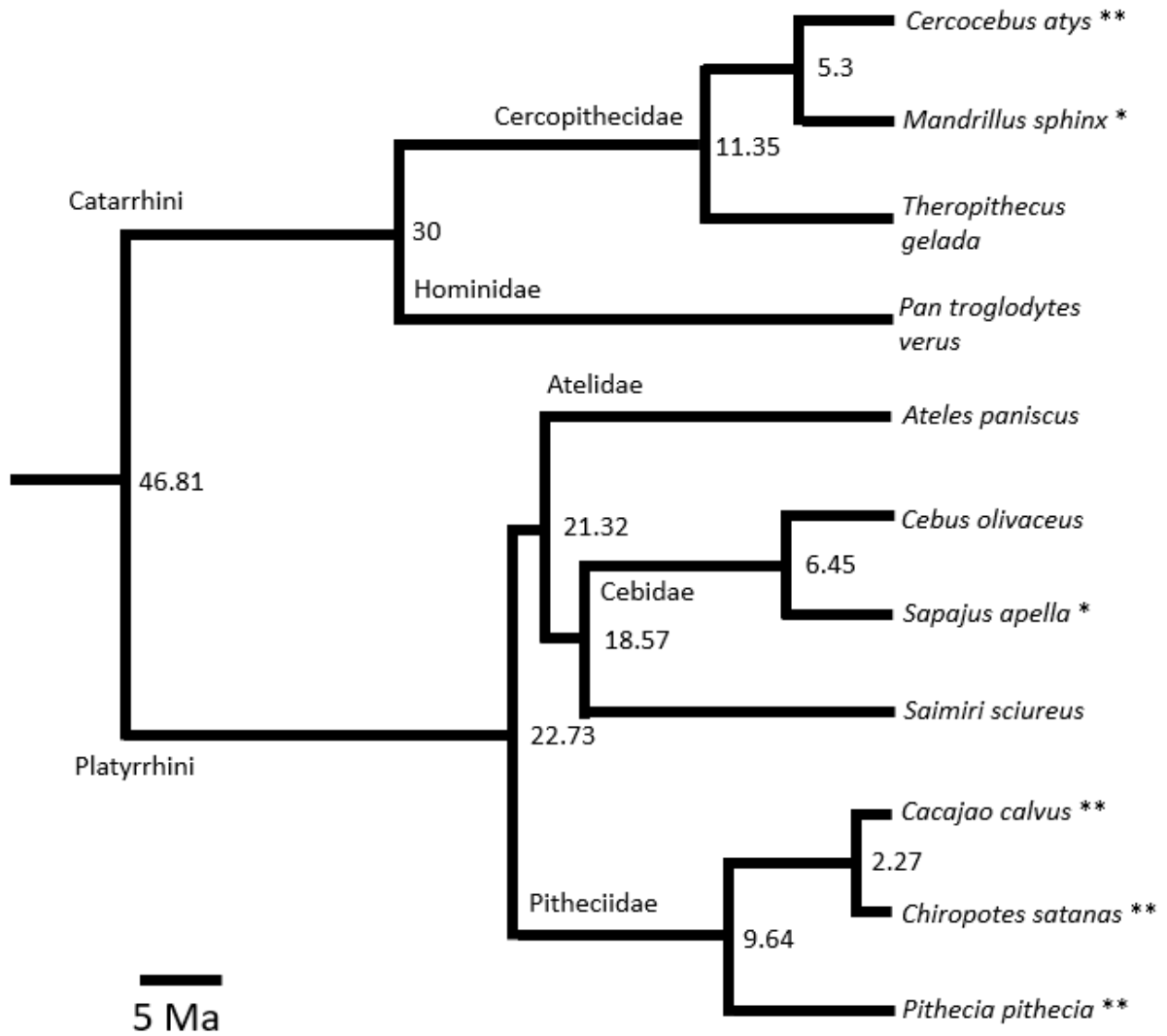
**Figure 2.12 Phylogeny of the sample with species included and family name. Tree generated using data from 10k trees (Arnold et al., 2010) and FigTree (v1.4.4, Rambaut, 2007) and shows divergence dates in millions of years with scale bar = 5 million years. Intensive seed predators are indicated with **, seasonal seed predators with *.**

## 2.4 Results

### 2.4.1 GMM results: Shape space, PC1 and PC2

A principal component analysis of the full sample (Fig. 2.13) shows relatively clear separation between species. PC1 (42.3% of variation) is characterised by a split between African and South American primates. Shape change along this principal component is strongly linked with prognathism. Species at the most positive PC1 (*Mandrillus* and *Theropithecus*) show a relatively high degree of prognathism, with a long dental row and rostrum paired with a small, low and posterior cranial vault and high zygomatic arch relative to the dental row. The gonial angle is also more anterior and the oblique line is strongly posteriorly slanted and both lower and more posterior relative to the dental row. These features are reversed on the most negative PC1 (*Saimiri* and *Chiropotes* are most extreme, along with *Sapajus*), where prognathism is greatly reduced, resulting in a relatively shorter dental row, the cranial vault is higher and more anteriorly positioned relative to the dental row, and the zygomatic is lower relative to the dental row. The zygomatic arches are also more expanded at negative PC1. However, there is variation in the extremity of these features in female and male primates of different species. The sexes are separated along PC1 in some species but not in all: Papionin primates (*Mandrillus, Theropithecus,* and *Cercocebus*) show a prominent split along PC1, with females at the more negative end, suggesting a lesser degree of prognathism. The remaining species do not show a clear sex-based split along PC1.

Examining dietary categories shows that the most intensive seed predators all fall out at the more negative end of PC1, with the exception of *Cercocebus. Cercocebus* occupies a middling position on PC1 and overlaps with highly frugivorous *Ateles.* Phylogeny is also clearly reflected in this axis, as African primates (*Cercocebus, Mandrillus, Theropithecus, Pan*) fall out more positively on PC1, particularly males. Of this group *Pan* and female *Cercocebus* fall out most negatively, indicating less prognathism. *Ateles* is the only South American primate to overlap on PC1 with African primates. While intensive seed predators do occupy the most negative space on PC1, they also share this space with non-seed predators, notably *Saimiri* at the most negative of PC1. Additionally, seasonal seed predator

*Mandrillus* is at the extreme positive of PC1, indicating that the relationship between seed predators and PC1 is not universal or exclusive.

PC2 (18.2%) shows a split less clearly linked to phylogeny (Fig. 2.13). The most negative end is characterised, relative to the most positive PC2, by an elongated and broad posterior cranium, a longer and more posterior cranial vault relative to the dental row, a lower, less broad, and more posterior zygomatic arch relative to the dental row, and a lower and more posterior coronoid process relative to dental row. In relation to mechanical performance these features could reduce mechanical advantage, reduce muscle attachment size, and increase relative gape. Interestingly, all intensive seed predators occupy a more positive space on PC2, although *Cercocebus* is more negative than the pitheciines. Occasional seed predator *Sapajus* falls out with the pitheciines, but *Mandrillus* does not and is at the extreme negative of PC2. Additionally, as with PC1, this grouping is not exclusive to seed predators, as both *Pan* and *Theropithecus* occupy very positive positions on PC2 alongside the seed predators. As such, while some particularly frugivorous primates do occupy a more negative space and the seed predators do group together, especially when PC1 and PC2 are taken together, this is not entirely to the exclusion of non-seed predators.

PC2 also shows a relatively clear split between females and males. In most species, males occupy the more positive end of PC2. This is the case in all seed predators, both seasonal and intensive. The separation is particularly clear in *Chiropotes* and *Cacajao,* while *Pithecia* shows a more mixed pattern and there is one *Sapajus* outlier to this trend. Only *Saimiri* and *Pan* show no obvious separation between sexes along this PC.
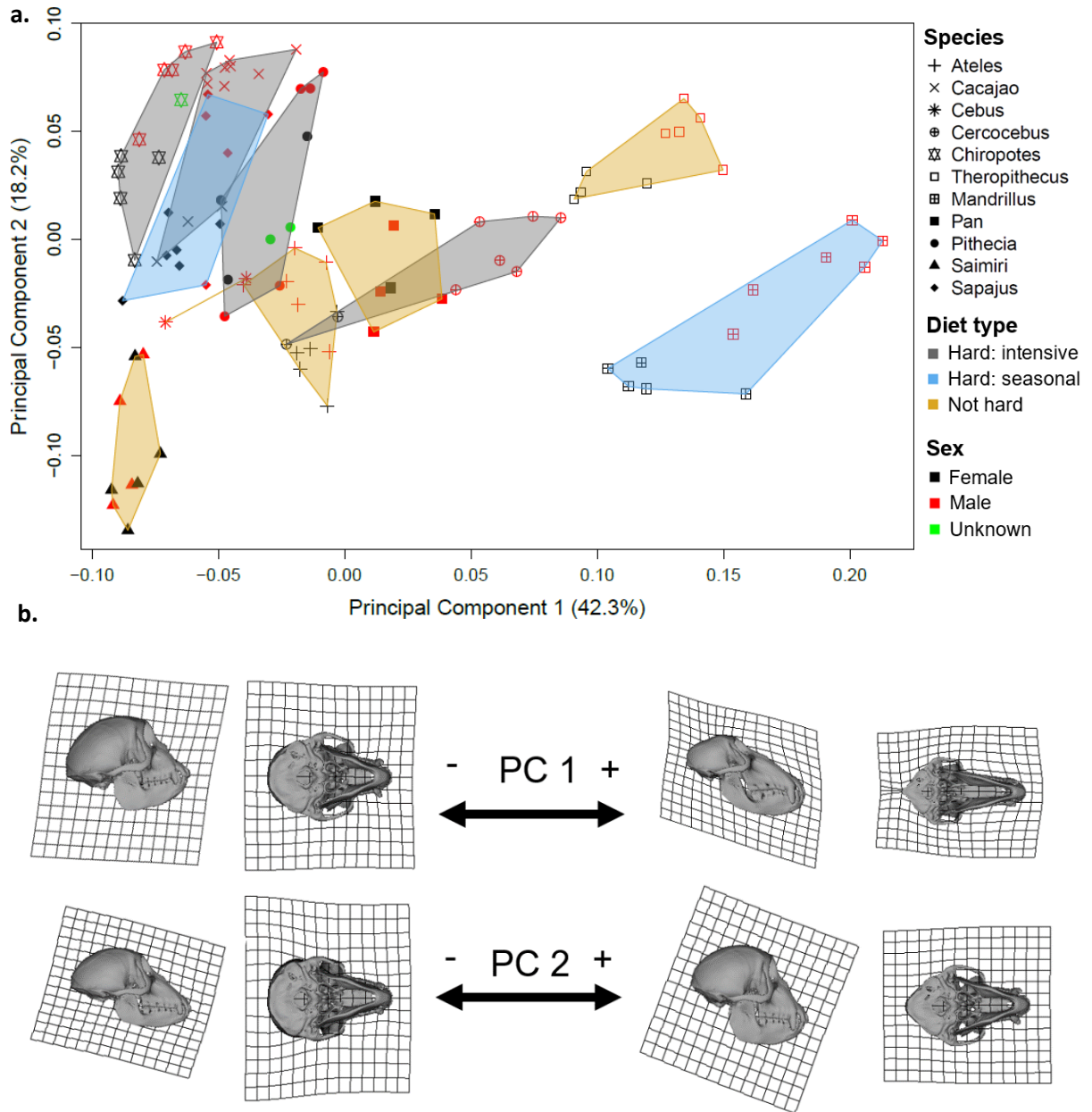
**Figure 2.13 Results of PCA for both sexes, PC1 and PC2. Showing a. PC1 (42.3% of variance) and PC2 (18.2% of variance), denoting species by symbol, dietary grouping by shading, and sex by symbol colour; and b. thin plate spline warps with surface deformation along PC1 and PC2, warping along each axis to show the most negative (left) and most positive (right) deformations.**

## 2.4.2 GMM results: Shape space, PC3 and PC4

The third and fourth principal components (Fig. 2.14) each still reflect a considerable degree of variance (8.4% and 6.5%). The third principal component shows cranial flexion, with the negative end of the PC3 showing a greater degree of cranial flexion, associated most strongly with *Pan,* and with *Mandrillus* at the extreme of the positive end. Interestingly, all intensive seed predators group in the centre of this distribution. Other changes along PC3 include an elongated, relatively low and posteriorly less broad cranium and shorter ramus height. There is separation between the sexes in some, but not all species. In all seed predators, intensive and seasonal, there is a tendency for a more positive PC score in males, although this relationship is not entirely exclusive.

The fourth PC (Fig. 2.14) relates to incisor shape and cranial shape. At the positive end of PC4 the incisors are less protruding and the cranium is longer, more narrow, and more downward-oriented at the positive end. Seed predators which use their anterior dentition extensively group at the negative PC4, and share this space with *Mandrillus* and *Saimiri*. *Sapajus* is strongly at the positive end of PC4 and *Cercocebus* relatively positive, and in all cases there is overlap with the comparison species. There is no clear separation by sex on this PC.
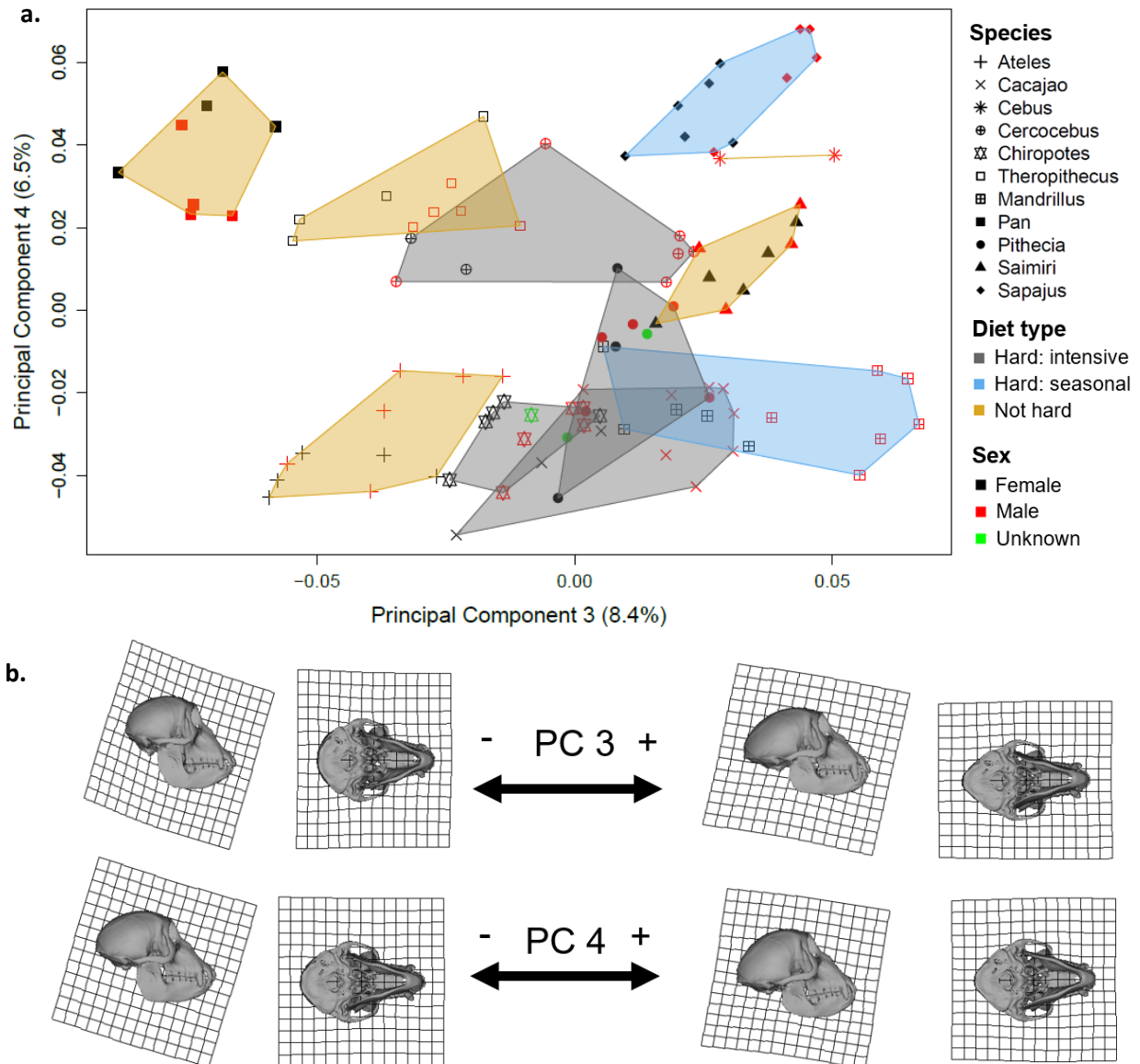
**Figure 2.14 Results of PCA for both sexes, PC3 and PC4. Showing a. PC3 (8.4% of variance) and PC4 (6.5% of variance), denoting species by symbol, dietary grouping by shading, and sex by symbol colour; and b. thin plate spline warps with surface deformation along PC1 and PC2, warping along each axis to show the most negative (left) and most positive (right) deformations.**

## 2.4.3 GMM results: Centroid size

Given the wide range of body sizes in the sample, the effect of size on PC scores was also explored by plotting centroid size against each PC. The first PC highlights the very strong relationship with size and phylogeny (Fig. 2.15). Male primates have the largest centroid size, with *Mandrillus* at the most extreme. There is a prominent split between females and males in the papionin primates (*Mandrillus, Theropithecus, Cercocebus*). A notable outlier is *Pan,* which was shown to be less prognathic given its size than the other African primates in the sample. A further outlier is *Pithecia,* which shows itself to be more positive on PC1 than other primates with a similar centroid size.

The second PC (18.2% variance) does not show a clear size relationship (Fig. 2.16). Although the platyrrhine primates (*Ateles, Cacajao, Cebus, Chiropotes, Pithecia, Saimiri,* and *Sapajus*) all show a broad spread along PC2, particularly separated by sex, they are clustered tightly in terms of centroid size. The African primates (*Cercocebus, Mandrillus, Theropithecus, Pan*) show a spread of centroid sizes as well as a spread along PC2.
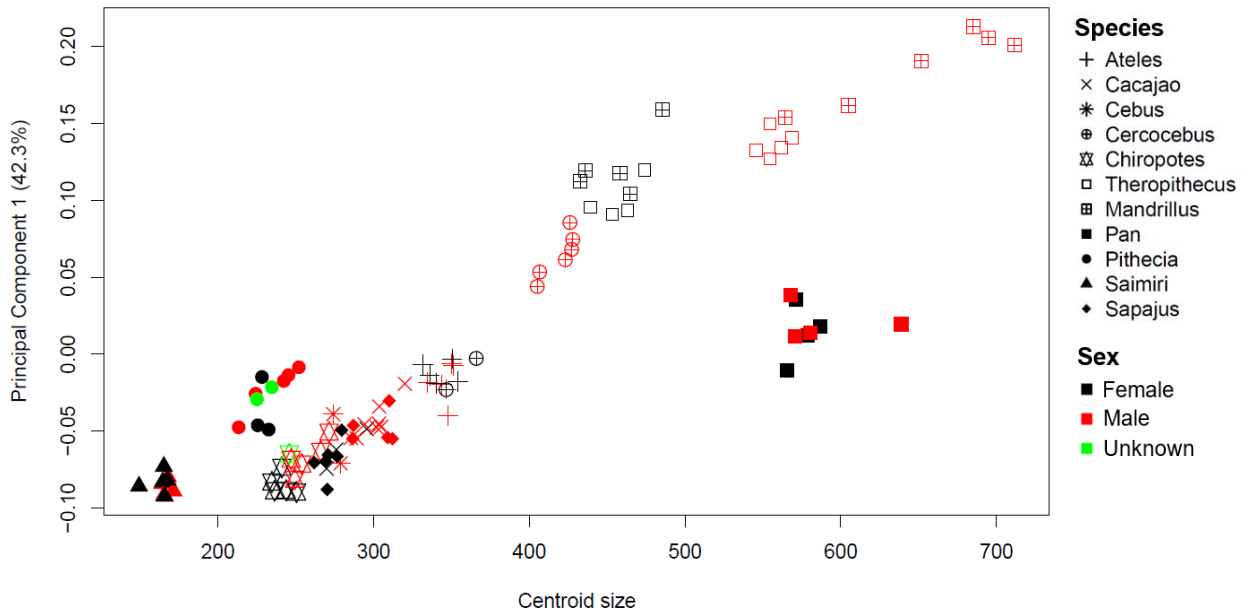


**Figure 2.15 Plot showing PC1 (42.3% variance) against centroid size. Species are denoted by symbol shape and sex by symbol colour**
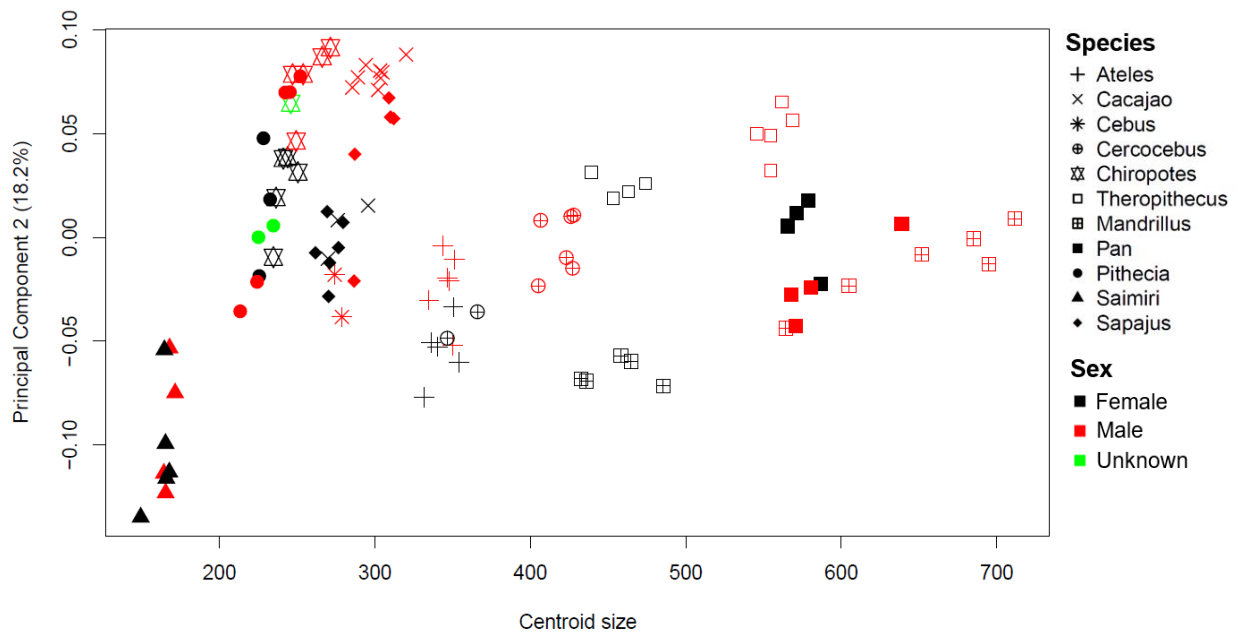
**Figure 2.16 Plot showing PC2 (18.2% variance) against centroid size. Species are denoted by symbol shape and sex by symbol colour**

## 2.4.4 Convergence results: Phylomorphospace

The phylomorphospace for the females in the sample (Fig. 2.17) highlights patterns observed in the PC analysis. The first PC is characterised by a relatively clear split between African and South American primates, although seed predating *Cercocebus* moves negatively along the first PC, away from closely related and seasonal seed predator *Mandrillus*, relatively close to highly frugivorous *Ateles*. Intensive seed-predator *Cacajao* and more distantly related seasonal seed predator *Sapajus* nearly overlap along PC1 and have moved toward each other along the second. *Chiropotes* on the other hand moves away from the pitheciine group along both principal components.
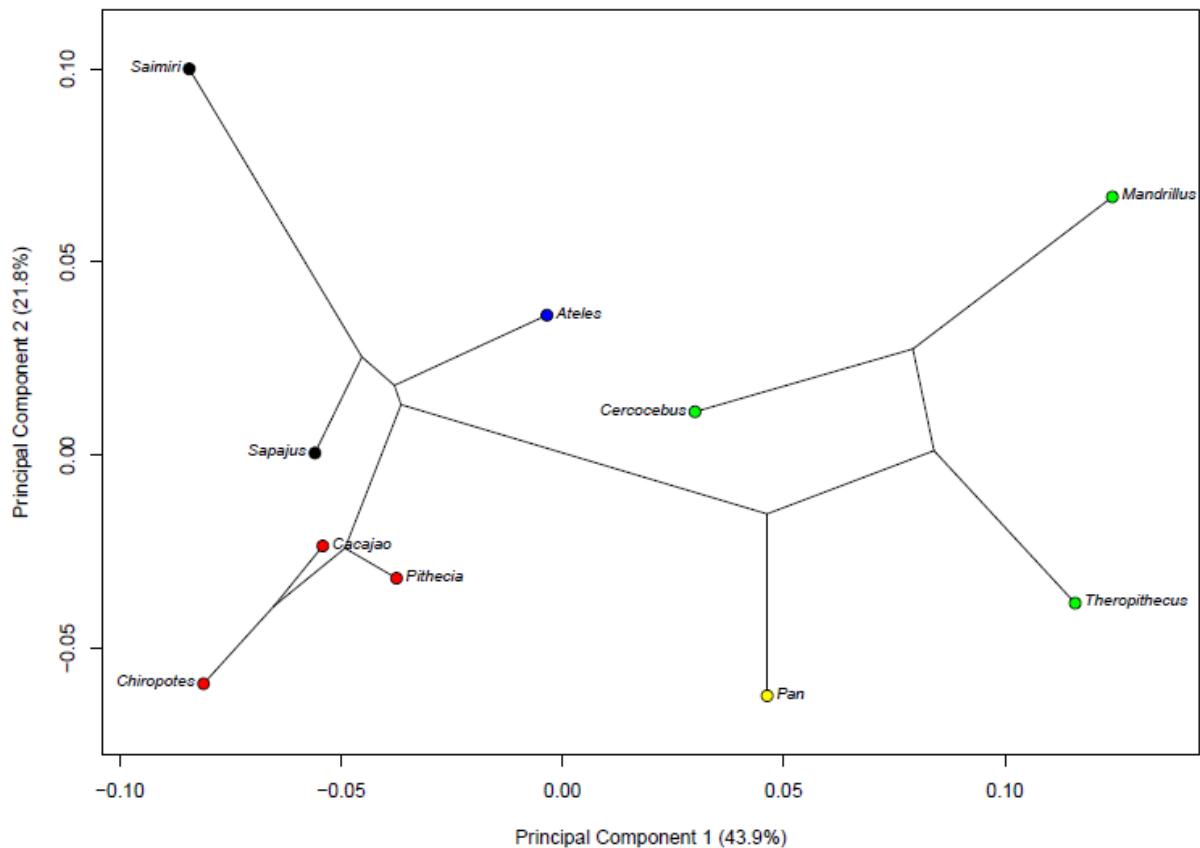
**Figure 2.17 Phylomorphospace showing the first two principal components of variation for female masticatory morphology. Species name plotted, coloured by family, key: Blue: Atelidae (*Ateles*); Black: Cebidae (*Sapajus* and *Saimiri*); Yellow: Hominidae (*Pan*); Red: Pitheciidae (*Cacajao, Chiropotes, Pithecia*); Green: Cercopithecidae (*Cercocebus, Mandrillus, Theropithecus*).**

The male phylomorphospace again highlights the exaggerated trends of shape variation in males (Fig. 2.18). Notably, *Cercocebus* still moves prominently away from *Mandrillus* along the first principal component, toward the pitheciine and *Sapajus* group. This distance in males is shorter than that seen in the females. Seasonal seed predator *Sapajus*, on the other hand, is prominently separated from its close relative *Cebus* along PC2. Instead *Sapajus* moves directly toward to the centre of the pitheciine group. The inclusion of *Cebus* in the male sample highlights this separation. Finally, the position of *Pan* is reversed, as female *Pan* fell out very negatively on PC2, whereas for males *Pan* is strongly positive on PC1.
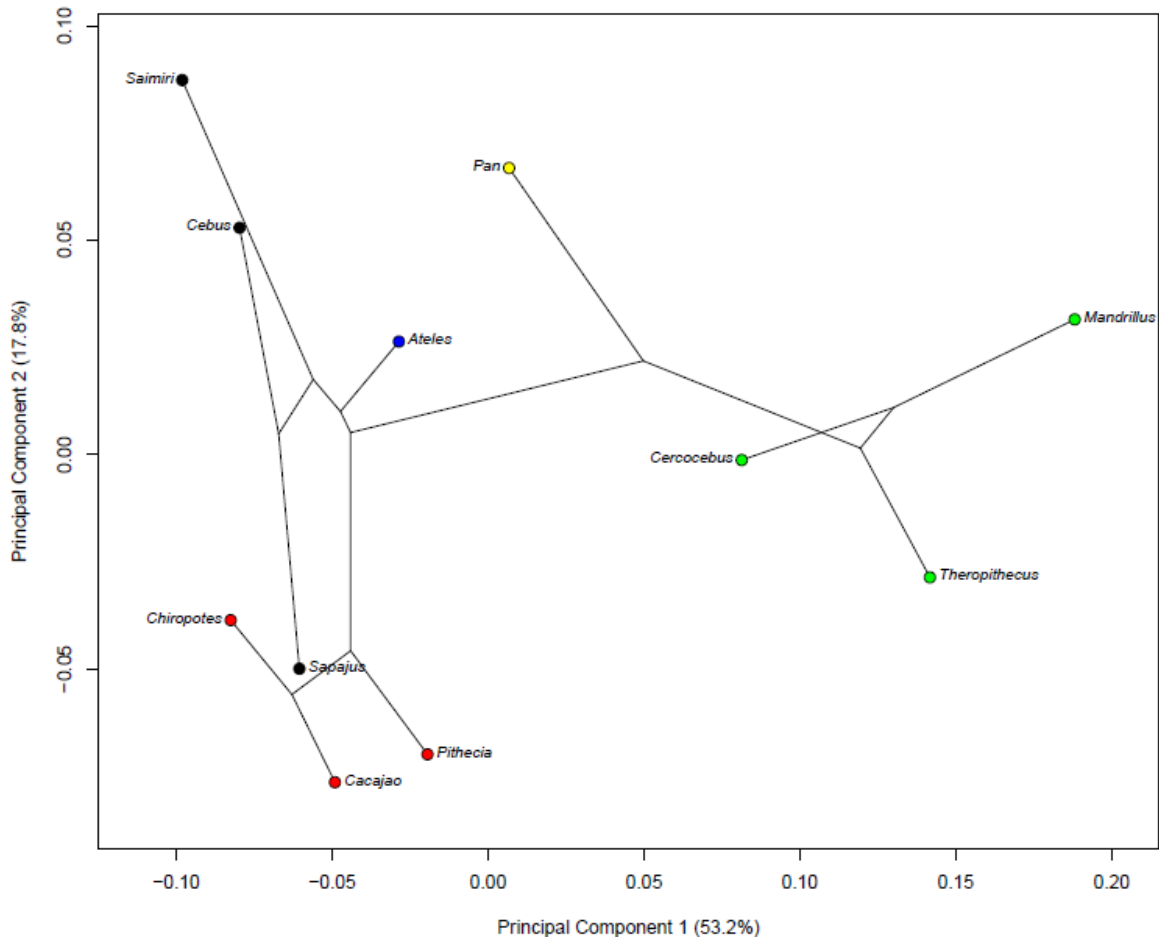
**Figure 2.18 Phylomorphospace showing the first two principal components of variation for male masticatory morphology. Species name plotted, coloured by family, key: Blue: Atelidae (*Ateles*); Black: Cebidae (*Sapajus, Cebus,* and *Saimiri*); Yellow: Hominidae (*Pan*); Red: Pitheciidae (*Cacajao, Chiropotes, Pithecia*); Green: Cercopithecidae (*Cercocebus, Mandrillus, Theropithecus*).**

## 2.4.5 Convergence: Statistical testing

Phylomorphospace results show partial support for the hypothesis that seed predators are not convergent. Not all seed predators are clearly grouped, but *Sapajus* and the pitheciine primates are more closely grouped than was predicted. Testing the statistical significance of these results provides more clarity, demonstrating convergence between some seed predators. In females, this is most prominent with the pitheciine group and *Sapajus*, which found highly significant convergence between *Cacajao* ($C_1$ = 0.51)*, Chiropotes* ($C_1$ = 0.43)*,* and *Pithecia* ($C_1$ = 0.56) with *Sapajus* ($p$ <0.002 in all three cases). *Cercocebus* shows some separation from other African primates along the first principal component in the

phylomorphospace. Comparisons between pitheciine primates and *Cercocebus* did not show significance. The highest $C_1$ value for these comparisons was between *Cacajao* and *Cercocebus* ($C_1$ = 0.21, *p* = 0.065). A comparison between *Cercocebus* and *Sapajus* on the other hand was significant ($C_1$ = 0.26, *p* = 0.043). Occasional seed predator *Mandrillus* showed no convergence in any comparisons with other seed predators.

The significance of convergence in males between the pitheciines and *Sapajus* increases in males relative to females, showing highly significant convergence for all three (*p* = <0.000 in each case). This is most prominent in *Cacajao* ($C_1$ = 0.61), but similarly strong in both *Pithecia* ($C_1$ = 0.59) and *Chiropotes* ($C_1$ = 0.58). Comparisons between both *Chiropotes* and *Cacajao* with *Cercocebus* are not significant, but there is significant convergence between *Pithecia* and *Cercocebus* ($C_1$ = 0.298, *p* = 0.044). Male *Sapajus* and *Cercocebus* also show significant convergence, to a greater degree than in females ($C_1$ = 0.36, *p* = 0.019). No convergence was found in any comparison with occasional seed predator *Mandrillus*.

## 2.5 Discussion

The objective of this study was to determine if primate seed predators would present with divergent solutions to problems inherent with the extreme masticatory demands of their diet. An additional aim was to test predictions that features related to maximising bite force are apparent in seed predators, and that these features would be particularly associated with females relative to males. All hypotheses found mixed support in the results of the analyses performed.

### 2.5.1 Convergence in seed predators

The prediction that there would be no convergence in seed predators (H1) was not met, as some seed predators displayed significant convergence. This was most prominent among seasonal seed predator *Sapajus* and the pitheciine group. Significant convergence was found between both male and females pitheciines and *Sapajus*, with the most prominent $C_1$ value found between male *Cacajao* and *Sapajus*. These results show that platyrrhine seed predators are more similar than would be expected under a Brownian motion model of evolution. Interestingly, this occurs despite the different manner of seed processing utilised by *Cacajao* and *Sapajus* (Wright, 2005; Norconk et al., 2013; Barnett et al., 2016). *Cacajao* practices sclerocarpic foraging while *Sapajus* practices durophagy (Norconk et al., 2013). Their common need for high bite force at wide gape, in addition to their similar body size may have a stronger effect than the variation in feeding behaviour observed in these primates. Other objects in the diet of *Sapajus* may have also produced this effect, as previous studies predicted convergence between *Chiropotes* and *Sapajus* due to similar canine usage in accessing hard or tough foods (Wright, 2005). Although palm seed processing by *Sapajus* is thought to take place on the molars, *Sapajus* also processes exceptionally tough food on its anterior dentition (Wright, 2005). There is variation in the material properties of the hard foods eaten by *Cacajao,* variously categorised as hard and tough and as hard and brittle (Bowler and Bodmer, 2011; Barnett et al., 2015, 2016). It is possible that tough and hard feeding require similar adaptations, or that the overall adaptations for anterior and posterior seed predation are similar in these primates.

Another intriguing relationship is the prominent separation between closely related gracile capuchin *Cebus* and robust capuchin *Sapajus* in the phylomorphospace (Fig. 2.18). Gracile

capuchins are noted for their less robust cranial morphology, and also have diets which consist of a greater proportion of soft fruits and less tough and hard foods than more robust capuchins (Alfaro et al., 2012). Past observations found that sympatric robust and gracile capuchins process hard palm seeds differently: *S. apella* is able to crack open palm seeds to access the nut with a single bite, while sympatric gracile capuchins can only consume seeds which have been weakened by insects, therefore requiring much longer to forage for each nut (Terborgh, 1984). The convergence results presented here highlight the divergence in masticatory morphology between these two closely related primates.

By contrast, African seed predators are, in most cases, not convergent with South American seed predators, indicating that these groups have differences in their masticatory form. Seasonal seed predator *Mandrillus* did not show any convergence with other seed predating primates. The very large body size of this primate likely contributed to this result. The intensive seed predator *Cercocebus* was convergent with other seed predators, although to a relatively low degree. In males this includes convergence between *Cercocebus* and *Pithecia*. Interestingly, *Pithecia* is typically characterised as the least extreme of the three pitheciine seed predators, with the smallest body size and a softer diet and the least specialised dental morphology of this group (Kinzey, 1992; Ledogar et al., 2018). *Pithecia* occupies a more positive position on the first PC (Fig. 2.13) than the other pitheciines and may therefore exhibit a greater degree of prognathism than other pitheciines. *Cercocebus* also is convergent with seasonal seed predator *Sapajus* in both sexes, to a greater degree in males. It would be of great interest to further investigate the source of these similarities in anatomy by quantifying biomechanical variables related directly to function (Ch. 3).

Taken together, this suggests there may be some shared masticatory traits between *Cercocebus* and some seed predators, but the group as a whole does not converge on one form. Overall results therefore do not show one exclusive masticatory form in seed predators, although some traits are shared.

## 2.5.2 Masticatory shape

GMM results give the shape-space context for the observed convergence results. Taken together, results indicate a range of morphologies in primate seed predators exist (as discussed above, 2.5.1), and it is not clear that all seed predators show masticatory shapes

which relate to high bite force at wide gape (H2). The most extreme change along the first PC is prognathism, highlighting the high degree of prognathism in papionin primates. A prognathic morphology is expected to result in a wide gape, which in papionins is linked with large canine size and the need for canine clearance (Ravosa, 1990; Hylander, 2013). However, by lengthening the potential distance of the dental row from the jaw joint increased prognathism is likely to reduce mechanical advantage. Size and scaling have an important effect here. Canine size, and by result prognathism are known to scale with positive allometry in Cercopithecines (Ravosa, 1990). *Mandrillus*, the most prognathic primate in the sample, is categorised as seasonal, not intensive seed predator, but was separated entirely in the morphospace from the other seed predators and showed no convergence. Mandrills have a very large body mass, with males approximately three times the body mass of the next largest seed predator in the sample, *Cercocebus* (Smith and Jungers, 1997). The centroid size plots (Figs. 2.15 and 2.16) highlight both the pronounced separation between sexes in *Mandrillus* but also the exceptional prognathism for body size relative to *Pan. Pan* has previously been noted to have high mechanical advantage relative to other apes, contrary to predictions made for their relatively frugivorous diet (Taylor, 2002). The very large male mandrill canines for sexual display may place competing demands on their masticatory form (Hylander, 2013). Estimating the dietary grouping of this species is a challenge as feeding observations are very limited, however it is known to eat a considerable volume of hard-shelled seeds at least occasionally (Hoshino, 1985; Lahm, 1986; McGrew et al., 1997). The large body size of this primate may be the solution for having both wide gape and high bite force.

This is especially intriguing given that of the seed predating primates *Mandrillus* not only falls out most positively on PC1 but also falls out the most negatively on PC2. The second PC relates to shapes which may affect mechanical advantage, and positive PC2 shows anteriorly positioned muscles relative to the dental row for a long in-lever, as well as relatively enlarged areas associated with muscle size. Seed predators were predicted to group in the shape-space corresponding with these forms. This prediction was met for the anterior feeding pitheciines (*Cacajao, Chiropotes,* and *Pithecia*) and posterior feeding seasonal seed predator *Sapajus*, highlighting the shared masticatory shape in these groups. How this group attains wide gape requires further investigation, as results suggest that pitheciines improve

their mechanical advantage with features that would reduce gape. It has been suggested that the laterally splayed pitheciine canines may serve to increase gape without adjusting mandible length (Ledogar et al., 2018), allowing for feeding on larger foods with less mouth opening than primates with more upright canines.

While further quantification of these trends is needed, the grouping of small-bodied seed predators at negative PC1 and positive PC2 suggests possible adaptations for high mechanical advantage and expanded muscle sizes. *S. apella* has previously been observed to have a high mechanical advantage relative to other platyrrhine species including *Ateles paniscus* and *Cebus olivaceus*, and a similar mechanical advantage to *Pithecia pithecia* and *Chiropotes satanas* (Wright, 2005; Norconk et al., 2009). This study suggests that this relationship may remain valid when compared to catarrhine primates as well. A relatively high mechanical advantage would provide an advantage to these primates in feeding and set them apart from primates with other diets. The context of body size is important here as well, as the three pitheciine primates and *Sapajus* are all of relatively small body size. Purely by virtue of its size, a primate like *Mandrillus* is expected to have a higher bite force than a much smaller-bodied primate such as *Cacajao* due to the relationship between muscle PCSA and body mass (Herrel et al., 2008). This may explain why the smaller-bodied intensive and occasional seed predators show convergence and group in the area of the morphospace relating to features which increase bite force, but larger-bodied seed predators do not. It is possible that no morphological specialisations are needed for primates of a certain body size, as they are able to generate sufficient bite force by virtue of their body size alone without additional adaptations (Taylor et al., 2018).

*Cercocebus* on the other hand shows a mixed picture. This mid-sized intensive seed predator does not occupy the space matching predictions for seed predator morphology. However, *Cercocebus* does show reduced prognathism relative to *Mandrillus*, which may produce a higher mechanical advantage. Additionally, there was some convergence with seed predators in *Cercocebus*, notably between male *Cercocebus* and *Pithecia*. The relatively increased prognathism seen in *Pithecia* may underpin this link, although the same connection cannot be made for *Sapajus* and *Cercocebus*. Other biomechanical factors may contribute: *Cercocebus* has been previously predicted to exhibit features for greater mechanical advantage than *Mandrillus* (Singleton, 2005). Sooty mangabeys were found to

exhibit facial and palatal shortening relative to other papionins, resulting in a more posterior dentition, although their overall small body size indicates an absolutely lower bite force and, especially due to facial shortening, a smaller gape than other species such as *Mandrillus* (Singleton, 2005). This relationship may show an example of functional compensation, although further quantification of biomechanical variables is needed to confirm this. Notably, other studies have found relatively low mechanical advantage in *Cercocebus* (Taylor et al., 2018). While the usage of zoo specimens may have affected results in this study (Taylor et al., 2018), the position of *Cercocebus* relative to the other seed predators in the results of this study suggests that *Cercocebus* does not meet the predicted specialised masticatory forms to facilitate their challenging diets. *Cercocebus* is a mid-sized primate, with considerably lower body weight than *Mandrillus,* but larger than the pitheciine group (Smith and Jungers, 1997). Body size very likely contributes to the ability of this primate to feed on hard seeds, suggesting again that increasing size is one pathway to seed predation, while increasing relative muscle size and mechanical advantage is another. *Cercocebus* may show a mixture of these patterns.

Some surprising results were also observed in the comparative sample. *Theropithecus* shows prominent overlap with seed predators and separation from other comparison species along the second PC, especially clear in males. *Theropithecus* is also relatively prognathic, with large canines, yet unlike the other papionins in the sample occupies a very positive space on PC2, overlapping with intensive platyrrhine seed predators. Given the intensely tough grass diet of *Theropithecus* (Dunbar and Dunbar, 1974), it is possible that there are overlapping dietary constraints amongst primates with tough diets. *Sapajus*, with whom *Theropithecus* overlaps, is also known to process very tough foods (Wright, 2005). The possibility that the convergence between *Sapajus* and the pitheciines is related to tough-food processing on the anterior dentition has already been noted. Toughness and hardness both present dietary challenges, and these results indicate that the demands of processing a tough diet may overlap with those of processing a hard diet.

### 2.5.3 Female and male seed predators

Female and male seed predators were predicted to be morphologically distinct. While this prediction (H3) was met, the prediction that females would show more extreme features

relating to maximising bite force was met for some, but not all species. African seed predators (*Cercocebus, Mandrillus*) show prominent spread linked with prognathism (Fig. 2.13), with males showing a higher degree of prognathism than females. Such a result could suggest that female *Cercocebus* and *Mandrillus* have improved mechanical advantage relative to males of the same species, although such an observation requires quantification. Past studies have found contrary results for *Cercocebus*, finding males and females to show similar mechanical advantage (Taylor et al., 2018). Results of this study suggest that female *Cercocebus* may show a greater degree of adaptations for seed predation than males in this regard but these values must be further quantified to verify this observation. Both male and female *Cercocebus* feed on the very hard *Sacoglottis* seed intensively, but the seed constitutes an even greater percentage of the male diet, at 61.8% of their observed dietary profile as compared with 49.2% in females (McGraw et al., 2011). It was recently found that male *Cercocebus* feed on even harder seeds than females, with females more likely to reject harder seeds (Geissler et al., 2020). The larger body size of male *Cercocebus* may result in higher bite force, but if indeed females have improved mechanical advantage this may result in some degree of functional equivalence.

Although a similar level of detail is not known for the mandrill diet, the considerable reduction in prognathism in the females and relatively much larger body size in males can be predicted to result in a similar effect to that observed in sooty mangabeys. It is surprising that females in this highly sexually dimorphic species do not show a higher PC2 score, but instead a lower one (Fig. 2.13). However, past observations of *Mandrillus* have however indicated that the more arboreal females may feed on a different diet to the males, with more soft fruits in their diet (Stammbach, 1986). This could account for the female *Mandrillus* falling out more closely to the most frugivorous primates (*Ateles*) on PC2 than to the other seed predators (Fig 2.13). Further quantification of these relationships is needed to investigate these trends.

Female and male South American seed predators also show distinct morphologies, however contrary to predictions in these primates it is the males which show shapes associated with maximising bite force. In contrast to the African seed predators the variability here is along the second PC, with males falling out more positively. The shape changes along this principal component could suggest that South American male seed predators have masticatory

shapes which increase their bite force, but direct measurements are needed to quantify this. Few studies have compared female and male platyrrhine diets, although one study has found that male *Cacajao* feed more intensively on a harder diet than females (Bowler and Bodmer, 2011). The different sexes may occupy slightly different feeding niches, and as seen documented in *Cercocebus* it is possible that males of many species feed on harder foods than females.

Taken together, these results show there are some differences between female and male seed predators relating to masticatory form. This is particularly interesting in the context of extreme diets, as both sexes are thought to feed on similarly challenging foods, albeit to a greater or lesser degree. It is intriguing that these relationships hold even when examining functional landmarks in primates with presumed extreme needs, as their diet would be expected to be a strong constraint. While differences may be due to the generally lower proportion of hard foods in female diets (Bowler and Bodmer, 2011; McGraw et al., 2011) it is also possible that this study has not captured the full picture, and that further work quantifying these observations is needed. Paramasticatory functions likely also play a role. It has been observed that canine tooth size has an influence on facial shape (Cardini and Elton, 2008), and that the male seed predators in this sample do have larger canines than the females. Further measurements are needed to examine these differences in more detail.

## 2.5.4 Conclusions: Many-to-one mapping?

Primates with hard diets do share some morphological characteristics, expressed both in convergence statistics and in the shape space, but they do not form a group in the morphospace to the exclusion of non-hard object feeders. The closely related pitheciines do group with *Sapajus* and show shapes meeting biomechanical predictors for high bite force, but *Cercocebus* is a prominent outlier. *Cercocebus* feeds intensively on an exceptionally hard diet, with numerous field observations recorded over multiple sightings confirming this behaviour (McGraw et al., 2011; W.S. McGraw et al., 2014). The results of this study highlight that *Cercocebus* also does not match predictions for an intensive seed predator when considering a broader phylogeny, although it may show some advantages by comparison with close relatives. Dental form may also play a role, for example enlarged and relatively flat premolars in *Cercocebus* may facilitate feeding on hard seeds (Swan, 2016).

Finally, the range of gapes and food sizes encountered by seed predators during feeding may also necessitate different adaptations.

The combination of body size and the many ways in which the masticatory system can be altered to increase bite force may have resulted in different solutions to the same problem. It has previously been predicted that convergence will occur in cases where there are very limited numbers of morphological solutions to the same functional problem (Herrel et al., 2008). The results of this study match this prediction. While convergence was observed in the smaller primates, it was not universally observed in the larger seed predators. To further understand these patterns quantification of mechanically relevant measurements is needed. GMM is a powerful tool for describing complex shape variation between groups, but for a full understanding of masticatory form and function it is also necessary to quantify biomechanical variables with direct relationship to bite force (Ross and Iriarte-Diaz, 2019). The next chapter will quantify mechanical advantage at a range of gapes and estimate bite force in primate seed predators and comparison species with alternate diets in order to further explore these relationships.

# Chapter 3 - Gape, mechanical advantage, and muscle size – pathways for functional equivalence in primate seed predators?

## 3.1 Introduction

All primate seed predators face similar challenges in generating a high bite force at a wide gape (Daegling et al., 2011; McGraw et al., 2011; Norconk and Veres, 2011). This is particularly difficult to achieve given the contradictory demands posed by bite force and gape (see Ch. 1 section 1.6.4; Dumont and Herrel, 2003; Taylor and Vinyard, 2004; Santana, 2016). How the masticatory apparatus of primate seed predators is adapted to this biomechanical challenge is not fully known. It has been shown that the shape of the masticatory apparatus, and thereby the relative positions of the joints, musculoskeletal anatomy and dental form vary between primate species which specialise on stress-resistant food items (Ch. 2). Such changes should alter the basic lever arm mechanics of the masticatory apparatus, but to understand these changes and their potential impacts on performance these measurements must be quantified.

In chapter 2 convergence in masticatory shape was identified between some, but not all, primate seed predators. Morphological differences between females and males were also identified which could have functional implications. While GMM and associated statistical tests are excellent tools for examining complex shape variation they do not directly inform on biomechanical variables (Ross and Iriarte-Diaz, 2019). By quantifying functionally relevant variables which underpin maximum bite force and gape capability, it may be possible to further our understanding of how a diverse group of dietary specialists (including both females and males) functionally converge.

Using 3D mathematical modelling this chapter will measure muscle in-lever arm lengths and load arm lengths along the dental row at a range of gapes in order to examine variation in mechanical advantage for a range of stress-resistant and non-stress resistant feeders. Other functionally relevant parameters which contribute to bite force (muscle cross-sectional area) and the ability to generate a wide gape (muscle line of action length increase at wide gape as well as bony measurements relating to gape, condyle height and length of the glenoid) will also be quantified. By examining these individual anatomical components this study investigates how primate seed predators maintain high bite force at wide gape in

order to process hard seeds. This aims to answer the question of whether primate seed predators present an example of many-to-one-mapping, evolving different morphological solutions to the same challenges – or if primate seed predators present examples of both variable morphology and variable masticatory function.

### 3.1.1 Morphologies which increase bite force and gape

Bite force, the amount of force an individual can generate on a given bite point, is a key dietary predictor and imposes a limit on the foods an organism can access (see Ch.1, 1.6.1; Spencer and Demes, 1993; Santana, 2016). Mechanical advantage (MA) is one of the metrics which affects bite force capability (see Ch. 1, 1.6.1.1; Fig. 3.1). A higher MA will reduce the muscular input effort required to generate a given bite force or increases bite force if all other variables are left the same (Spencer and Demes, 1993; Taylor et al., 2018). MA of the jaw adductors can be increased by having a longer in-lever, a shorter out-lever, or both. More anteriorly positioned muscles relative to the temporomandibular joint (TMJ) increase the length of the muscle in-lever arm (Dechow and Carlson, 1990; Norconk et al., 2009; Taylor et al., 2018). Having a shorter dental row brings the teeth closer to the TMJ, reducing the length of the out-lever arm (Dechow and Carlson, 1990; Norconk et al., 2009; Taylor et al., 2018).

Another way to increase bite force is to increase the force production capabilities of the masticatory adductor muscles (see Ch. 1, 1.6.1.2). Maximum muscle force is a function of muscle cross-sectional area, and assuming similarly arranged internal architecture, muscle mass can be a good proxy for muscle force capabilities (O'Connor et al., 2005; Anderson et al., 2008; Santana et al., 2012; Toro-Ibacache et al., 2016). Larger muscles will generally have more bundles of muscle fibres, and as such it is generally expected that larger animals will have larger muscle forces (O'Connor et al., 2005; Anderson et al., 2008; Santana et al., 2012; Toro-Ibacache et al., 2016). The impact of increased body mass on primate masticatory force production has been investigated by researchers interested in allometry, and several scaling relationships have been suggested (Anton, 1999, 2000; Anapol et al., 2008; Perry and Wall, 2008; Taylor and Vinyard, 2013; Andrea B Taylor et al., 2015; Dickinson et al., 2018). In order to quantify muscle mass it must be measured, but approaches to do so vary. One approach is measuring muscle physiological cross-sectional

area (PCSA) which takes both muscle mass and fibre architecture (orientation and length) into account. Studies have shown that catarrhine primates PCSA scales with isometry or positive allometry (Anton, 1999, 2000; Anapol et al., 2008; Taylor and Vinyard, 2013), while in platyrrhines PCSA scales with negative allometry (Taylor et al., 2015). However, although this scaling relationship affects relative muscle PCSA, with smaller-bodied platyrrhines having a relatively larger muscle PCSA than larger-bodied platyrrhines, there is still an increase in PCSA mass with greater body mass. Larger platyrrhines, and other primates, have absolutely larger muscle PCSA, which may be capable of producing higher bite force as a simple consequence of their size (Taylor et al., 2015).

The gape of an individual is the degree to which their mandible is opened (Santana, 2016), and is important both for feeding and non-feeding behaviours. The gape height, the distance between the respective tooth rows, varies according to absolute size of the individual and gape/mandibular rotation. In feeding, a wider gape is required in diets which feature objects that are large relative to the feeding animal (Eng et al., 2009; Santana, 2016) but ultimately it is the maximum gape height of a species that will constrain the maximum food size an individual can process intra-orally (Fricano and Perry, 2018). Even within individuals, for a given degree of jaw rotation, the distance between teeth varies along the dental row; with larger distances measured anteriorly compared to posteriorly. In general, placing foods on the posterior dentition (a position with higher MA and therefore higher bite force) also requires a relatively wider gape than feeding on the anterior dentition for objects of the same size.  However, this assumes a consistent tooth row, and in many African primates there is a strong relationship between canine size and wide gape in males to allow canine clearance used in threat displays (Fig. 3.1; Hylander, 1979, 2013; Lucas, 1982; Ravosa, 1990).

A wide range of anatomical features can affect gape, including internal muscle architecture, muscle configuration, and skeletal shape (Herring and Herring, 1974; Carlson, 1977; Taylor and Vinyard, 2004; Hylander, 2013; Fricano and Perry, 2018; Ross and Iriarte-Diaz, 2019). Morphologies which reduce muscle stretch are considered key to facilitating wide gape, as excessive muscle stretch will reduce the active force a muscle can generate (Ch.1, 1.6.4; Herring and Herring, 1974; Taylor and Vinyard, 2004) and increase passive tensions as the muscle reaches its excursion limits (Anapol and Herring, 1989). Some changes to muscle

internal architecture can facilitate wider gapes by reducing stretch, such as increased muscle fibre length and decreased pennation angles (Taylor and Vinyard, 2004, 2009). Changes to skeletal morphology and muscle position are also thought to affect gape potential. A lower temporo-mandibular joint relative to the occlusal plane is predicted to permit a greater linear height of gape per degree of mandibular rotation, thereby reducing muscle stretch at equivalent gape heights (Herring, 1972; Vinyard et al., 2003). The opposite morphology, of a high TMJ relative to the occlusal plane, is strongly associated with highly folivorous diets (Anapol and Lee, 1994), a dietary category with low gape requirements. The masseter muscle has a shape and position which is predicted to be especially strongly affected by stretching at wide degrees of wide mouth opening (Herring and Herring, 1974; Fricano and Perry, 2018). In primates as the mandible rotates it also anteriorly translates (Carlson, 1977; Iriarte-Diaz et al., 2017). Anterior translation of the mandible is predicted to reduce muscle stretch, especially on the masseter, which may help with maintaining high force at wide gape (Herring and Herring, 1974; Carlson, 1977; Eng et al., 2009). A longer antero-posterior length of the glenoid is predicted to facilitate wider gapes and anterior feeding (Vinyard et al., 2003; Terhune, 2011). Such a morphology could increase the amount of anterior translation of the mandible and consequently reduce muscle stretch (Carlson, 1977; Hylander, 2006; Terhune, 2011). Finally, a greater mandible length (out-lever length) can facilitate wide gapes by creating a wider distance between the teeth at a lower degree of jaw rotation, as seen in primates with a high degree of prognathism (Fig. 3.1; Ravosa, 1990; Hylander, 2013). As such, with an increase in overall mandible length due to increasing body mass, gape size would increase as with each degree of mandibular rotation a greater distance would exist between the teeth. In some papionin primates there is positive allometry of facial length with body size, resulting in a high degree of prognathism at large body size – and therefore also a relatively very wide gape (Ravosa, 1990; Singleton, 2002; Frost et al., 2003; Hylander, 2013). A range of features can therefore affect the attainable gape in an individual, but many of these include a potential trade-off with bite force.

Maximum mammalian gape has been proposed to be approximately 60 – 70 degrees of rotation of the mandible, but some species may surpass this extreme value (Herring and Herring, 1974; Hylander, 2013). However, the maximum gape height and maximum

functional gape are two different values because of muscle stretch (see Ch. 1, 1.6.1.2). Determining the point when the length-tension curve enters its descending limb is challenging (Eng et al., 2009). Humans are predicted to have optimum jaw adductor function between 5-14 degrees of gape (Koolstra and van Eijden, 1997). One of few non-human primate studies measuring jaw adductor operating range compared tree-gouging *Callithrix* with non-tree gouging *Saguinus* (Eng et al., 2009). Tree-gouging requires a wide gape, and *Callithrix* was found to have muscle architecture which enables a longer operating range, meaning it retains good muscle function at higher degrees of gape angle than *Saguinus* (Eng et al., 2009). In tree-gouging *Callithrix* the predicted optimum operating range is between 37 and >55 degrees of gape rotation, whereas in *Saguinus* this range is between 28 and 30 degrees, in both cases varying by muscle (Eng et al., 2009). These measurements highlight some of the complexities in modelling this range as there is variation between different muscles, between individuals of the same species, and between species (Eng et al., 2009; Taylor et al., 2019). Recent research has also examined length-tension curves in macaques, finding that these primates have wider sarcomere operating ranges than many other mammals, presumed to maintain high bite force at wider degrees of gape (Taylor et al., 2019). As these primates are highly prognathic this muscular architecture is hypothesized to contribute to their ability to produce very wide gapes, as in canine display behaviour (Taylor et al., 2019).
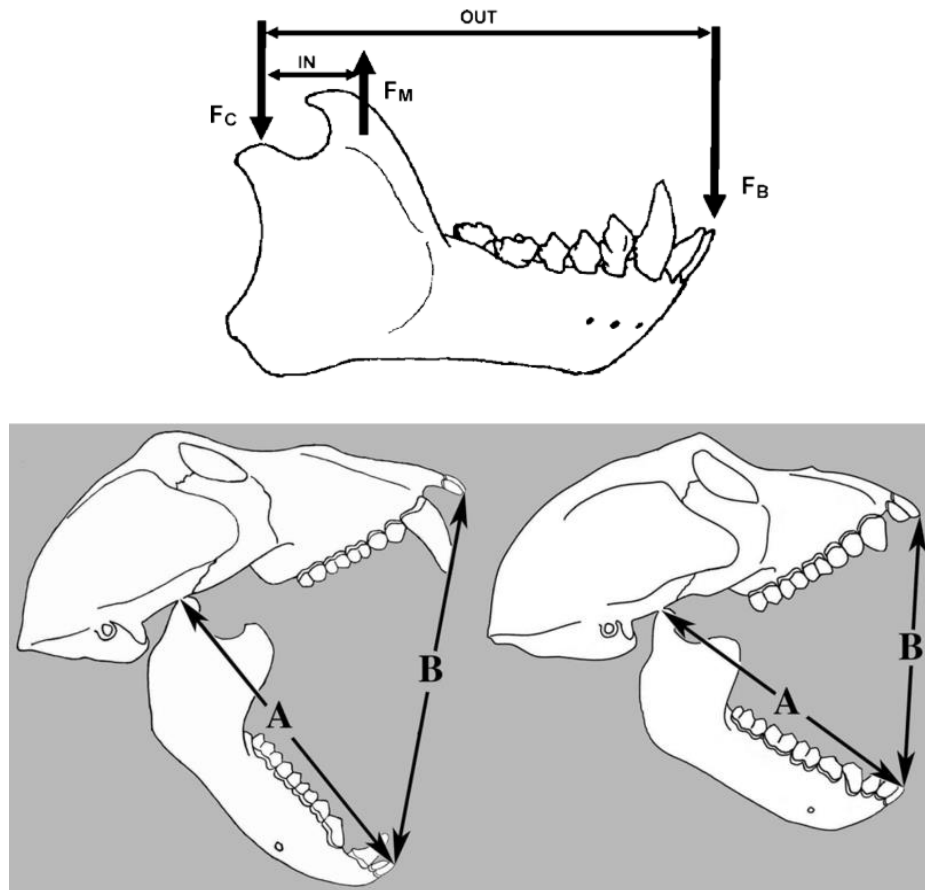
**Figure 3.1 Gape and lever arms. Showing (top) measurement of levers for calculation of MA (in-lever / out-lever) and (below) the relationship between mandible length and gape. The left skull is more prognathic than the right with a longer rostrum and out-lever. Line A shows the distance from the fulcrum to the incisor bite point (out-lever) and Line B the linear gape measured at the incisors. Note that when the out-lever increases gape is wider but MA reduces, when the out-lever reduces gape is smaller but MA increases.** *Image sources Norconk et al., 2009; Hylander, 2017*

A trade-off exists between bite force and gape. Bites on posterior teeth have advantageous MA but require a greater degree of mouth opening than the anterior teeth for an object of the same size (Greaves, 1978; Ravosa, 1990). The opposite is the case for anterior bites, which require lower gape to consume foods of equivalent size but also have a lower MA. The length of the mandible is also closely related to this trade-off (Fig 3.1). While a longer mandible will allow for a wider gape, it will also typically result in bite points further from the temporomandibular joint (fulcrum), especially on anterior bites, lowering MA (Ravosa, 1990; Terhune, Hylander, et al., 2015). A more anterior muscle position could increase MA, especially on anterior bites, but this can result in increased muscle stretch at equivalent gape (Herring and Herring, 1974). Adjustments to internal muscle architecture can mitigate

for this, increasing muscle fibre length and decreasing pennation to facilitate large gapes (Taylor and Vinyard, 2004, 2009). However, this adaptation comes at the loss of muscle PCSA, lowering bite force if PCSA is not increased correspondingly (Taylor and Vinyard, 2004, 2009; Terhune, Hylander, et al., 2015; Perry, 2018). Other internal adjustments are also possible, and some species have been found to have adjustments to their masticatory adductor length-tension curves to facilitate maintaining high forces at relatively higher degrees of stretch (Taylor and Vinyard, 2004; Eng et al., 2009; Taylor et al., 2018). Taken together, a wide range of features affect the relationship between bite force and gape.

It is clear that species generating high bite force at large gapes face conflicting demands and may have different morphological solutions to this dilemma. Species with mechanically challenging diets are often predicted to have a higher MA than those which feed on less mechanically challenging foods, but gape is rarely considered in this equation (Wright, 2005; Ledogar et al., 2018; Taylor et al., 2018). So, what are the anatomical solutions for primates who have both a hard and large diet?

## 3.1.2 Primate seed predators

Primate seed predators feed on large and hard seeds which require both high bite force and relatively large gapes to process (see Ch.2, 2.1.2 for review; Koyabu and Endo, 2009, 2010; Daegling et al., 2011; McGraw et al., 2011, 2014; Norconk et al., 2013). Seed predation is typically thought of as an extreme and niche diet, one that other species are not able to process due to the mechanical challenges it poses (Norconk et al., 2013). Primates which feed on seeds vary in their processing methods, the proportion of their diet made up by seeds, and their overall body mass. Some species, such as the pitheciine primates (*Cacajao, Chiropotes,* and *Pithecia*), process very large hard-shelled fruits and seeds on their anterior dentition while others, such as mid-sized primate *Cercocebus atys* process large hard seeds on their posterior dentition (Fig. 3.2; Kinzey, 1992; McGraw et al., 2014). These mid-sized primates feed on seed diets very intensively, making up over 50% of the total annual diet in most dietary reports, and up to nearly 100% of the diet in some months (McGraw et al., 2011; Norconk and Veres, 2011; Norconk et al., 2013; McGraw et al., 2014). Other primates such as large-bodied *Mandrillus sphinx* and mid-sized *Sapajus apella* also feed on hard seeds using their posterior dentition, but seeds are thought to only be of great importance to

these primates in certain seasons (Terborgh, 1984; Lahm, 1986; Norconk et al., 2013; Hongo et al., 2017). The mandrill diet is not well-documented, but in seasons of fruit scarcity seeds are thought to be an important resource in their diet, accounting for up to 50% of dietary volume (Hongo et al., 2017). For *Sapajus* seeds can account for up to 64% of feeding observations in months where other resources are scarce (Terborgh, 1984). Interestingly some *Sapajus* populations feed directly on hard palm seeds, while others process seeds with manual dexterity and tools instead of performing a crushing bite (Izawa and Mizuno, 1977; Izawa, 1979; Terborgh, 1984; Port-Carvalho et al., 2003; Spencer, 2003; Sampaio, 2005; Laird et al., 2020). It is also noteworthy that *Sapajus apella* additionally feeds on exceptionally tough foods such as the bases of palm leaves and woody legume pods (Wright, 2005). *S. apella* frequently uses its anterior dentition to process these tough foods (Wright, 2005). In all cases these primate seed predators are able to feed on hard seeds. Whether they do so throughout the year or not they must be capable of sufficient bite force to fracture the seed casing and access the nutrients within.

The gape required to process these seeds is also considerable. The largest seed breadth currently measured for seed predators is 22cm, as fed upon by *Chiropotes satanas* (Norconk et al., 2009). Similarly, large seeds are eaten by *Pithecia pithecia*. Notably these relatively small-bodied primates cannot fit this entire seed in its mouth, instead it uses its procumbent incisors and splayed canines to prise the seed open (Fig. 3.2; Norconk et al., 2013). Other hard seeds eaten by *Chiropotes* and other pitheciines are smaller, including the Brazil nut (c. 2 cm breadth) which is eaten by *Cacajao* (Fig. 3.2; Norconk et al., 2009, 2013; Barnett et al., 2015, 2016). This is a similar size to the hard *Sacoglottis* (c. 2.5 cm) which makes up a very large proportion of the *Cercocebus atys* diet is approximately 2.5 cm wide (Norconk et al., 2009; Daegling et al., 2011). Although the seed size is smaller for *Cercocebus atys*, the posterior placement of the seed means the required gape would still be substantial relative to body size. This is also the case for *Sapajus*, which places palm seeds of 2-4 cm diameter on its posterior dentition (Terborgh, 1984; Visalberghi et al., 2008). The size of seeds eaten by *Mandrillus* is not known, although the prognathic facial morphology of this large-bodied species, which enables tremendous gape, paired with its expanded second premolar has led to the suggestion that it feeds on posterior dentition (Fleagle and McGraw, 2002).

**Figure 3.2 Primate seed predators with wide jaw openings. a.** *Cacajao* **feeding on a large fruit using its canines, b.** *Cercocebus atys* **feeding on** *Sacoglottis* **using its post-canine teeth, c.** *Pithecia* **feeding on a large fruit using its incisors, and d.** *Mandrillus* **engaging in wide gape canine display.** *Image sources (from top left): Norconk et al., 2013; Geissler et al., 2020; M. Norconk; Leigh et al., 2008*

Previous studies have investigated some of the features which underpin bite force and gape performance in primate seed predators. MA at occlusion has been calculated for a wide range of primates, including extinct and extant species (e.g. Spencer and Demes, 1993; Anapol and Lee, 1994; O'Connor et al., 2005; Wright, 2005; Norconk et al., 2009; Dickinson et al., 2018; Godinho et al., 2018; Perry, 2018; Taylor et al., 2018). High MA has been found in some platyrrhine species with challenging diets. For example, the Cebidae have repeatedly been found to have high MA relative to other platyrrhine primates, particularly on their very anteriorly positioned temporalis muscle (Anapol and Lee, 1994; Wright, 2005). This feature has been linked with their regular and intensive incisor feeding (Anapol and

Lee, 1994; Wright, 2005). The robust capuchin *Sapajus apella* shows the most exaggerated pattern of this adaptation, which has been associated with its especially intensively tough and hard diet (Wright, 2005). Intensive seed predating pitheciines have also met predictions of relatively high MA when compared against other platyrrhine primates, to a greater degree in *Chiropotes* and *Cacajao* than in *Pithecia* (Anapol and Lee, 1994; Wright, 2005; Ledogar et al., 2018; Püschel et al., 2018). High MA has also been observed in some catarrhine primates; both African and Asian colobine seed predators have met predictions for a high mechanical advantage compared to closely related colobines which do not feed on seeds (Koyabu and Endo, 2009, 2010).

Other seed predators have not met predictions linking diet and mechanical advantage. Given its extremely hard diet of intensive seed predation, *Cercocebus atys* was predicted to show a greater MA than non-hard object feeding *Papio anubis* and two *Macaca* species (Taylor et al., 2018). However, the prediction was only partially met, and while *Cercocebus* did show slightly increased MA in some positions, this was not the case on all bite points (Taylor et al., 2018). How *Cercocebus* compares relative to a broader sample is unknown, although from past GMM studies it has been predicted that *Cercocebus* has high MA relative to at least some other papionins (Singleton, 2002, 2005). Although MA has not been measured in mandrills, their extreme prognathism is predicted to result in low MA (Singleton, 2002, 2005). Notably none of these past studies have investigated the effect of gape on MA, typically measuring MA in occlusion. This effect is important, as MA is one of the masticatory parameters affected by gape. As no study has previously examined the MA of a broad grouping of seed predators, especially taking both 3D measurements and gape into account, such an investigation could greatly further understanding of seed predator feeding performance.

Examining how primates achieve wide gape is relatively rare, especially for primate seed predators. Length-tension curves have not been measured for the jaw adductors of primate seed predators yet. However, other aspects of internal muscle architecture have been measured in *Sapajus apella*, finding that this primate has increased muscle fibre length and PCSA to maintain high force at wide gape (Taylor and Vinyard, 2009). This suggests that some primates do have adaptations for high force at wide gape, although they have only been measured in a small number of species.

Measuring these values is challenging and requires access to material for dissection which is not always available. In rare cases where material is available, custom devices can be designed to rotate the mandible in specimens with intact joint capsules, pairing measurements with dissection data - although the challenges of this approach necessitate a small sample size (Eng et al., 2009). Other methods of understanding gape include modelling bony gape using skeletal material to manually rotate the jaw open on a custom frame (Fricano and Perry, 2018). Fricano and Perry (2018) predicted the seed predator *Pithecia pithecia* to be capable of high linear gape relative to body size, but the features enabling such wide gapes were not elucidated. A longer glenoid (anterior-posterior length) may permit a greater degree of anterior translation, facilitating gape, although past GMM analysis of platyrrhine primates only found some wide gape feeders to meet this prediction (Terhune, 2011). Low condyle height is another potentially relevant morphology and has been observed in some callithrichids (Vinyard et al., 2003). These primates are not seed predators but use tree-gouging at wide gapes to access exudates (Vinyard et al., 2003). Tree-gouging callithrichids also were found to have relatively low condyle height above the occlusal plane when compared against callithrichids which feed at lower gapes (Vinyard et al., 2003). A low condyle height has also been observed in *Mandrillus*, especially in comparison with graminivorous *Theropithecus* (Ravosa, 1990; Ravosa et al., 2000; Vinyard et al., 2003). Combining these variables with MA measurements may highlight how different seed predators are able to feed on their challenging diet.

Underpinning these measurements is the ability to produce sufficient bite force to feed on hard, large foods. Measurements comparing PCSA in different primates have found relatively large PCSA in *Sapajus apella* by comparison to more gracile capuchins (Taylor and Vinyard, 2009). As this primate has also been observed to have very high MA, it is predicted that *Sapajus apella* has a relatively high bite force (Anapol and Lee, 1994; Wright, 2005; Taylor and Vinyard, 2009). This is not the case for *Cercocebus atys,* which does not have enlarged PCSA or especially advantageous MA when compared to macaque species and *Papio anubis*, suggesting it does not have an especially high bite force (Taylor et al., 2018). However, by not examining a range of gapes and including other skeletal variables these studies have not yet put together the full picture of how primate seed predators access large, hard foods.

### 3.1.3 Sex differences in seed predators

Sexual dimorphism affects primates in a range of ways. In primates, due to socioecological factors, males typically have larger bodies and larger canines than females (see Fig. 3.1; Fleagle, 2013; Hylander, 2013). Without any other changes to muscle architecture and configuration this larger body size will increase bite force in male primates (Anton, 1999; Taylor and Vinyard, 2013; Dickinson et al., 2018). However, the increased canine size in males and associated prognathism, especially in African primates, may affect lever-arm lengths which reduce MA in males (Singleton, 2002, 2005; Hylander, 2013). If females are less prognathic, their shortened out-lever may increase MA and provide some degree of functional equivalence.

This is especially interesting in primates with mechanically challenging diets, as both sexes of seed predators feed on similarly hard foods (Bowler and Bodmer, 2011; McGraw et al., 2011). Only a small number of studies have quantified both dietary differences and associated variations in material properties in female and male primate seed predators (Bowler and Bodmer, 2011; McGraw et al., 2011). These studies have found that although both sexes do feed on hard objects, males appear to process a higher degree of hard foods in *Cercocebus atys* (McGraw et al., 2011). In one *Cacajao calvus* population although both sexes rely on seeds, the seeds eaten by males were found to be harder than those eaten by females, although seeds eaten by both sexes are still very hard (Bowler and Bodmer, 2011). Another study has indicated that there are sex-related differences in the manner of fracture employed to open hard walnut seeds by *Macaca fuscata* (Tamura, 2020). Whether these relationships hold for all seed predators, and whether related differences in morphology exist, is unknown. Given that both males and females feed on a similarly challenging diet but show some differences in size and shape (Ch. 2), it is important to examine the functional morphology of both sexes.

### 3.1.4 How to measure and quantify differences in functional performance

A range of methods have previously been used to quantify the parameters which influence bite force and gape, as well as estimating bite force itself. Multibody dynamic analysis (MDA) is a computational method that simulates 3D rigid body movements and the muscle forces that drive them (O'Higgins et al., 2012; Shi et al., 2012; Curtis et al., 2014). This

modelling approach has been used to investigate numerous structure-function relationships within the masticatory apparatus. Past work has examined the role of muscle tension (Peck et al., 2000), jaw joint morphologies (Koolstra and Van Eijden, 1995) and optimal fibre length (Langenbach and Hannam, 1999) in maximum jaw opening, as well as predicting muscle activation patterns during various bite scenarios (Koolstra and van Eijden, 1992; Shi et al., 2012). This masticatory system modelling approach however has been limited to humans (Koolstra and van Eijden, 1992; Koolstra and Van Eijden, 1995; Langenbach and Hannam, 1999; Peck et al., 2000; Sellers and Crompton, 2004), reptiles (Moazen et al., 2008; Curtis et al., 2009); a rabbit (Watson et al., 2014) and in non-human primates *Macaca fascicularis* (Curtis et al., 2008; Shi et al., 2012). In all cases the sample size was one, and a high level of *in vivo* experimental data was required to run the simulations.

The required data for such modelling (kinematics, muscle properties, bite force) are not available for the majority of primate species, many of which are endangered. Simplifying the modelling approach is therefore necessary. The main mechanical and anatomical parameters which are likely to impact bite force and gape capability (muscle in-lever lengths, out-lever lengths at different biting points, muscle stretch, anteroposterior length of the glenoid, height of the condyle above the occlusal plane, and estimated muscle cross-sectional area) are however fairly easy to model and measure in a simplified mathematical model.

Mechanical advantage has previously been measured for a range of primates (e.g. Spencer and Demes, 1993; Anapol and Lee, 1994; O'Connor et al., 2005; Wright, 2005; Norconk et al., 2009; Dickinson et al., 2018; Godinho et al., 2018; Perry, 2018; Taylor et al., 2018). Past research varies widely in the methodologies used to collect lever arm measurements for the calculation of MA. These measurements can be taken on the cranium exclusively, using 2D photographs (e.g. Spencer and Demes, 1993), callipers (e.g. Anapol and Lee, 1994; Wright, 2005) or a 3D digitiser (e.g. Koyabu and Endo, 2009, 2010). Studies which only work with cranial material cannot use muscle origin and insertion sites to determine the muscle line of action, and instead often use a line passing through the left and right postglenoids to set an axis on the cranium (e.g. Anapol and Lee, 1994; Wright, 2005). Other studies have used both mandible and cranium in occlusion, sometimes using a combination of dissection and 3D modelling to estimate MA on 3D surfaces (Dickinson et al., 2018) or measuring directly on

the physical specimen (Taylor et al., 2018). Working with a 3D model in occlusion has advantages over measuring MA using 2D distances as this retains greater detail of the specimen anatomy than 2D measurements.

Another advantage to working with specimens in occlusion is the ability to simulate gape. Past work has estimated bony gape using physical primate specimens, rotating the mandible open and measuring the gape (Fricano and Perry, 2018). This study found links between gape height and diet, as maximum gape and maximum recorded food size eaten were correlated (Fricano and Perry, 2018). This past research did not quantify biomechanical variables which underpin these relationships however, which are key to understanding how wide gape relative to body size is achieved via skeletal changes and macro-level muscle variations. Other studies have included gape in their models by taking measurements on a model rotated to a specific gape (Ledogar et al., 2018). These studies have not combined measurements of variables such as lever arm lengths with changing gapes.

Muscle mass, whether for comparison on its own or for calculating bite force, has been measured using a similarly broad range of methods. *In vivo* estimates of bite force are considered the most accurate, but are extremely challenging to collect (Davis et al., 2010). Either muscle CSA or PCSA is used as a measurement of muscle mass in order to estimate muscle force. Although PCSA is considered more accurate it requires dissection material which is often not available. Muscle CSA can been calculated using 2D measurements on photographs of dry bone (Thomason, 1991). This approach has been used to calculate CSA for a wide range of vertebrates, including otters, a range of felids and canids, and numerous marsupials (Thomason, 1991; Christiansen and Adolfssen, 2005; Wroe et al., 2005b; Christiansen and Wroe, 2007; Campbell and Santana, 2017). Studies comparing methods have found that certain dry-bone methods of estimating bite force with CSA are reasonably accurate and can be used when other options are not available, taking potential issues into account when interpreting the results (Davis et al., 2010).

These biomechanically relevant parameters can also be investigated together in a measure of total masticatory performance by estimating bite force. Two key parameters must be measured to estimate bite force: mechanical advantage and a measure of muscle force of the masticatory adductors, calculated using muscle CSA or PCSA and estimated muscle tension (Raadsheer et al., 1999). The role of gape in the context of bite force has only rarely

been investigated (e.g. Eng, 2009; Santana, 2016), and due to the complexity of estimating gape (Fricano and Perry, 2018) a wide range of parameters must be considered to predict gape capabilities.

Bite force has rarely been estimated in non-human primates, however both simplified and highly complex estimations have been made for a wide variety of organisms (see Ch. 1, 1.6.1; e.g. Thomason et al., 1991; Christansen and Wroe, 2007). These modelling or measurement approaches are a common solution for estimating bite force given the challenges of in vivo data collection (Thomason, 1991; Christiansen and Adolfssen, 2005; Wroe et al., 2005b; Christiansen and Wroe, 2007; Davis et al., 2010; Campbell and Santana, 2017). Complex modelling approaches combining 3D anatomy with dissection data have been found to give accurate results, closely matching *in vivo* data, but dissection data is not always available and this approach is extremely time-consuming (Davis et al., 2010). Studies which do estimate primate bite force have often focussed on closely related species (e.g. Ledogar et al., 2018). 3D models were used to estimate the possible ranges of bite forces in the pitheciines *Cacajao, Chiropotes,* and *Pithecia* (Ledogar et al., 2018). Results found higher bite force in the pitheciines relative to comparison species *Callicebus* which feeds on a less mechanically challenging diet (Ledogar et al., 2018). Broader comparisons of bite force have yet to be carried out for primates, likely due to the complexity of estimating bite force with dissection data or 3D modelling. In other mammals simplified estimates using 2D measurements are often used when *in vivo* measurements or dissection data are not available (e.g. Thomason, 1991; Davis et al., 2010). Although these measures are unlikely to represent the true bite force of measured specimens, they can provide estimates which are particularly useful in a comparative sample.

## 3.2 Aims and objectives

The shape of the masticatory apparatus varies in primate seed predators (Ch. 2; 2.1.2) but the details of how functional components vary between different seed predators is unknown. The complexity of the masticatory system may permit a degree of functional equivalence, as there are so many options for changing output, but this this has yet to be quantified for a group of primate seed predators.

The aim of this study is to investigate whether primate seed predators (both males and females) have advantageous masticatory morphologies for producing high biting forces at wide gapes when compared to other primate species.

Objectives:

1)  Develop a 3D musculoskeletal mathematical model of primate jaw opening capable of measuring mechanically relevant parameters.

2)  Collect mechanically relevant parameters (linear gape at a series of positions along the dental row, muscle in-lever lengths, out-lever lengths at different biting points, muscle stretch, anteroposterior length of the glenoid, height of the condyle above the occlusal plane, estimated muscle cross-sectional area at a series of jaw opening positions, and estimated bite force at a series of jaw opening positions) for a range of primate species.

3)  Compare the results of mechanically relevant parameter measurements in seeds predators to non-seed specialist primate species to ascertain if seed predators are indeed mechanically exceptional.

4)  Compare the results of the mechanically relevant parameter measurements within seed predators to ascertain if performance is equivalent and if seed predators have the same anatomical configuration.

5)  Evaluate any differences between the sexes within the seed predator groups.

The following hypotheses will be tested in conjunction with these objectives:

**H1 - Primate seed predators (males and females) will have features which will enable them to achieve a high bite force at a large gape relative to non-seed predator primates.**

No single advantageous morphology is predicted because there are multiple functional parameters of the masticatory system which can be altered to increase bite force and to maintain high bite force even at large gapes (section 3.1.1). The measurements collected (objective 2) will be evaluated for seed predators. Seed predators (both sexes) are predicted to display a mosaic of the following features: High MA (either via relatively short out-lever, long in-lever, or both), large muscle CSA, low muscle stretch at wide gape (estimated via increase in muscle length), high estimated bite force, anteroposteriorly long glenoid surface, and low condyle height above the occlusal plane. Absolute and relative linear gape heights at maximum gape will also be measured to evaluate the maximum gape potential in the sample.

**H2. Females and males will differ in the features which will enable them to achieve a high bite force at a large gape within the same species.**

This is due to sexual dimorphism between the sexes in primates, including changes in body mass and shape, including canine size. These differences may provide different constraints between sexes. However, seed predators of both sexes are still expected to show similar performance relative to the other primates of the sample, as both sexes are known to feed on large, hard foods.

## 3.2 Materials and Methods

In order to address hypotheses of this study it was first necessary to develop a mathematical musculoskeletal model capable of simulating jaw opening. The model needed to be capable of outputting a number of mechanically relevant values at different stages of jaw opening in order to compare performance in a range of primate species.

### 3.2.1 Objective 1: Develop a 3D musculoskeletal mathematical model of primate jaw opening capable of measuring mechanically relevant parameters.

Complex 3D musculoskeletal models of the primate masticatory apparatus, capable of predicting mechanical advantage during changes in gape, have previously been created using methods such as MDA (Sellers and Crompton, 2004; Shi et al., 2012; Curtis et al., 2014). However, due to model complexity only a few individuals are evaluated by such models. To address the aims of this study it was necessary to carry out a comparative study using a large range of primate species for which soft tissue anatomy was unavailable. A more simplified modelling approach was therefore necessary. Previous studies have shown that even with significant modelling assumptions and simplifications estimates of the functional parameters for masticatory function can be measured (e.g. Herring and Herring, 1974; Weijs et al., 1989; Koolstra and van Eijden, 1997; O'Connor et al., 2005; Davis et al., 2010).

To model the jaw as a third-class lever (Maynard Smith and Savage, 1957; Hylander, 1975) a 3D mathematical model was created which contains landmark points representing the jaw joint as the fulcrum. Landmarks also represent the origin and insertions of the jaw adductors and biting points on the teeth. Rotations and translations of the jaw were calculated to simulate basic jaw kinematics and measure key functional parameters at different gapes.

Three functions were written to run this model and calculate the measurements using RStudio (v1.1.463, RStudio Team, 2018). Using 3D landmark coordinate data taken on mandibles and crania in occlusion it measures mechanically relevant parameters (muscle in-lever lengths, out-lever, MA at different biting points, muscle stretch, glenoid length, height of the condyle above the occlusal plane, estimated muscle cross-sectional area) at a series of jaw opening positions. Measurements were collected for a range of primate species

(objective 2). 3D surfaces of the mandible and cranium had previously been processed and prepared for 3D digitising (see Ch. 2, 2.3.1 for specimen summary; see Ch. 2, 2.3.2 and 2.3.3 for data acquisition and preparation, Appendix 1 for full specimen database, and Appendix 2, A2.2 and A.2.3 for further details on specimen preparation).

## 3.2.1.1 Model design and input parameters

*Raw data:* 3D landmark coordinates are the main raw input data for the model. Before collecting landmark data it was necessary to register surface files of a primate cranium and mandible to a standard position within the global coordinate system. This registration was carried out using a rigid warp in Avizo v9.2 (FEI, Thermo Fischer Scientific). In order for the model to rotate around a biomechanically meaningful axis the right condyle was fixed as the origin (0,0,0) and fulcrum. The x-axis passed through the left condyle point, and the centre point between the mandibular incisors was rotated to lie on the XY plane (see Fig. 3.3). The same transformation was applied to both mandible and cranium so their correct alignment relative to each other was maintained.
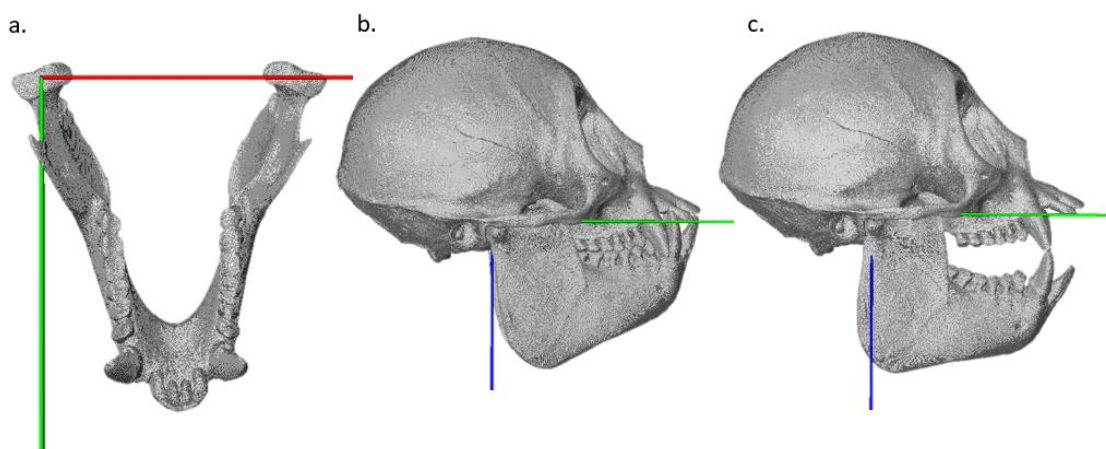


**Figure 3.3 The centre of rotation used in this study. Showing a. X-axis passing through both mandibular condyles, with the right condyle the centre of rotation, b. specimen in occlusion and c. specimen with jaw rotated open along the x-axis with the mandibular condyle centre of rotation.**

*Landmark data:* 3D landmark co-ordinates were collected from the aligned virtual skulls in occlusion using Avizo. Landmarks (see Table 3.1 and Fig. 3.4) were placed unilaterally, with the exception of the mandibular condyles, upon which landmarks were place bilaterally to facilitate jaw rotation. The right side was chosen except for those specimens with missing

landmarks on their right side, in which case the left was used (side used listed in specimen database, Appendix 1).
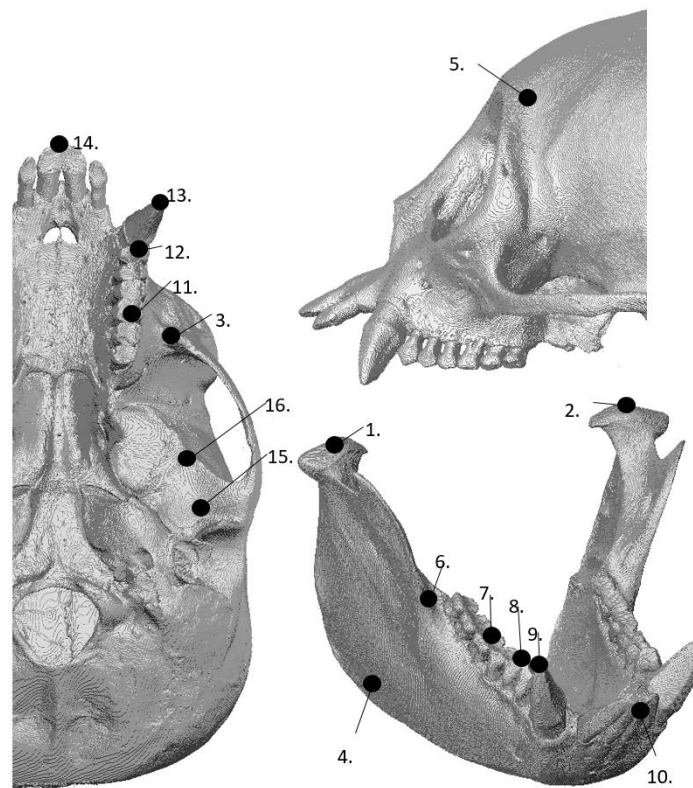


**Figure 3.4 Landmarks required for 3D mathematical model input. Demonstrated on a *Chiropotes chiropotes* specimen. See Table 3.1 for list of landmark descriptors.**

These landmarks included the main jaw adductor muscle origin and insertions (superficial masseter and anterior temporalis), four bite points, centre of the TMJ and the most anterior and posterior limits of the joint. See Table 3.1 for a full description of these landmarks and their roles within the model. Muscle landmark placement was guided by bony anatomy and previous anatomical reviews (Schumacher, 1961; Swindler and Wood, 1973; Madeira and De Oliveira, 1979; Ross, 1995; Anton, 1999; Diogo and Wood, 2012; Ledogar et al., 2018). It is noted that catarrhine and platyrrhine primates differ in their number of premolar teeth (as reviewed in Ch. 1, 1.2.3). For consistency, the first premolar in all species will henceforth be referred to as PM1.

**Table 3.1 Landmarks used in the 3D mathematical model. Note different landmarks calculate different parameters within the model.**

| Landmark number | Anatomical feature | Landmark placement | Roles in model |
|---|---|---|---|
| 1,2 | Centre point of the mandibular condyle | Point at the meeting of the lines between the antero-posterior most points on the condyle and most medial and most lateral points on the condyle, left and right sides | Fulcrum – used to define the axis of rotation and used to calculate the lever arm lengths |
| 3 | Superficial anterior masseter origin | Centre of the cranial masseteric scar | Muscle origins and insertions. Used to calculate the muscle line of action and in-lever lengths |
| 4 | Superficial anterior masseter insertion | Anterior inferior point of masseteric scar on mandibular body | |
| 5 | Anterior temporalis origin | Most anterior and superior point along temporal line | |
| 6 | Anterior temporalis insertion | Medial surface of ascending ramus on muscle scar | |
| 7 | Molar bite point | Centre of first molar, mandible | Mandibular bite point. Used to calculate the out-lever lengths, and the bite height |
| 8 | Premolar bite point | Protocone of first premolar, mandible | |
| 9 | Canine bite point | Canine cusp tip, mandible | |
| 10 | Incisor bite point | Centre of incisor edge between left and right first incisors, mandible | |
| 11 | Molar bite point | Centre of first molar, cranium | Maxillary bite point. Used to calculate the bite height |
| 12 | Premolar bite point | Protocone of first premolar, cranium | |
| 13 | Canine bite point | Canine cusp tip, cranium | |
| 14 | Incisor bite point | Centre of incisor edge between left and right first incisors, cranium | |
| 15 | Most posterior aspect of upper articular joint surface | Most inferior point on the postglenoid process | Maximum articular surface length and subsequent maximum translation capability of the model |
| 16 | Most anterior aspect of upper articular joint surface | Most anterior point on the articular surface of the glenoid fossa. | |

*Jaw kinematics:* To simulate jaw opening and vary gape within the model a centre of rotation had to be set. In reality, the centre of rotation is thought to be located inferior and posterior to the mandibular condyles within the areas of masseter and medial pterygoid in humans, rabbits, and several non-human primates (Weijs et al., 1989; Hylander, 2006; Terhune et al., 2011; Ross et al., 2012, 2017; Iriarte-Diaz et al., 2017). This position is known to vary between primates (Iriarte-Diaz et al., 2017) and calculating this position requires *in vivo* data (Terhune et al., 2011; Iriarte-Diaz et al., 2017). Given that this data was unobtainable and given the diverse range of species in this study a more simplified approach was taken. Two landmarks representing the mandibular condyles were chosen as a simplified axis of rotation (Landmarks 1,2 in Table 3.1; axis demonstrated in Fig. 3.3). This approach is highly repeatable and standardised across all species and follows the approach used in other studies (Iriarte-Diaz et al., 2017).

An upper limit of rotation had to be set for the model, which would represent maximum gape. Comparisons of maximum gape between species are measured as a degree of jaw opening (jaw rotation) (Wall, 1999; Eng et al., 2009; Terhune, Hylander, et al., 2015) at which point the distance between respective upper and lower dentition (linear gape) can be measured. Although absolute maximum gape in mammals may be up to 70 degrees of mandibular rotation, due to muscle stretch, the maximum functional gape may be considerably lower (Herring and Herring, 1974; Eng et al., 2009; Hylander, 2013). Optimal sarcomere operating range is predicted to end at as low as 28 degrees for some species and muscles, but >55 degrees in others (Eng et al., 2009). Taking this into account, 40 degrees of rotation was chosen as the maximal gape angle for this study. This value captures a wide range of bite heights that have a realistic chance of being within all or most species functional, non-damaging range.

Translation was also included in the model. The purpose of including translation was to address the shortcomings of using a rotational centre which results in pure rotation instead of rotation with translation as is the case in the true helical axis of the jaw (Hylander, 2006; Iriarte-Diaz et al., 2017). Additionally, this enabled an evaluation of the role of translation in muscle stretch during jaw opening. The anteroposterior length of the upper articular joint surface was measured to reflect the maximum possible anterior translation of the mandible in jaw opening. This distance was then applied to the mandibular landmarks after rotating

to 40 degrees. Measurements and calculations could then be made for both translated and untranslated models in order to provide a comparison of possible impact (see Fig. 3.5).

A rotation matrix and translation component were applied to the original mandibular landmarks within the model code. Rotations were carried out in increments of one degree up to the pre-determined maximum of 40 degrees.

a.                                              b.
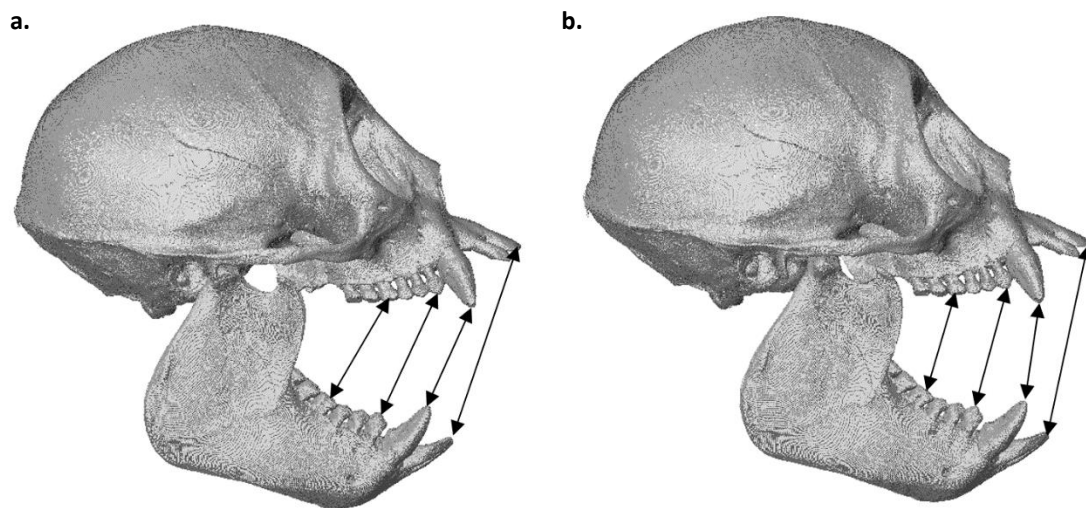


**Figure 3.5 Example of the effect of mandibular translation on the relative position of the upper and lower jaw in *Chiropotes* and a measure of linear gape, showing a. mandible rotated to maximum gape 40 degrees with no translation and b. specimen rotated to 40 degrees and after applying anterior translation equivalent to the length of the glenoid. Notice the differences in the alignment of the upper and lower teeth.**

## 3.2.1.2 Model calculations: Linear gape

The model calculated linear gape at each degree of rotation. Linear gape is defined as the absolute distance between the corresponding upper and lower dentition (using bite point landmarks, landmarks 7 – 14 in Table 3.1; see Fig. 3.5). The model was designed to calculate this value at four bite points M1, PM1, canine, and central incisor at every degree of jaw rotation. When linear gape reached a pre-determined value (eg. 20mm on the incisors) mechanically relevant parameters were automatically exported. Measurements could be exported up to the pre-selected maximum gape of 40 degrees. As the mandible rotates 1 degree at a time, a small amount of tolerance was built into the model for extracting linear gape height, as most specimens would never reach precise linear gape measurements without rounding. The script automatically located the closest value to pre-set bite heights.

The canine bite height required an additional calculation, as canine clearance is required before foods could be placed between them so bite height could not be measured from the first degree of rotation. Measurements were set to detect when the distance between canine tips first reached 0 (initial canine clearance), and to measure linear gape only from that point onwards, although retaining total gape angle to represent total degree of mouth opening.

## 3.2.1.3 Model calculations: Mechanical advantage (MA)

Methods for measuring lever arm lengths for the calculation of mechanical advantage vary (Fig. 3.6). In cases where 3D data is available, in-levers for jaw adductors are typically measured as the perpendicular distance from a measurement of a muscles line of action to the centre of the jaw joint (e.g. O'Connor et al., 2005; Dickinson et al., 2018; Godinho et al., 2018). The out-lever is generally measured as the distance from the centre of the jaw joint to a given bite point (e.g. Anapol and Lee, 1994; Wright, 2005; Norconk et al., 2009; Dickinson et al., 2018).
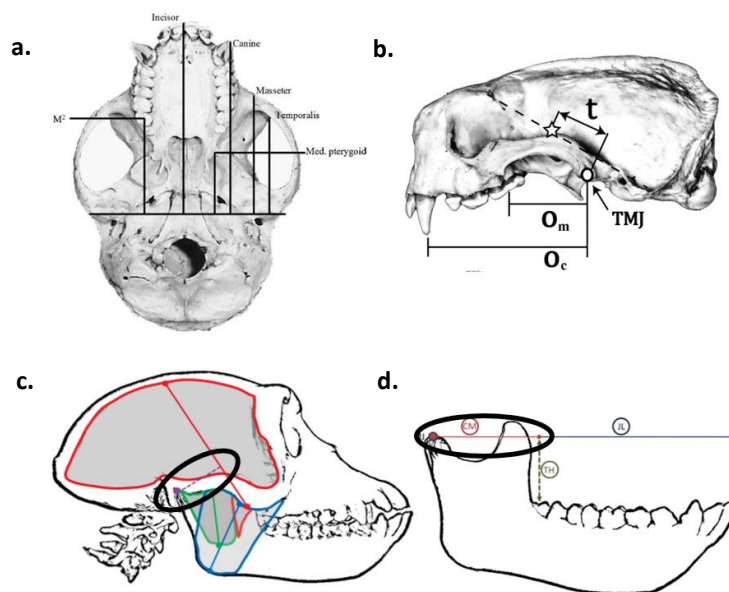


**Figure 3.6 Examples of different methods for measuring in-levers and out-levers for the calculation of mechanical advantage. a. 3D method on dry bone, cranium in isolation (Wright, 2005), b. 2D method using photographs using distance from muscle centroid to TMJ as in-lever (t) (Campbell and Santana, 2017), c. schematic showing 3D in-lever calculation method on mandible and cranium in occlusion, in-lever for temporalis circled (Dickinson et al., 2018) and d. schematic demonstrating 3D out-lever measurement (Dickinson et al., 2018).**

For the purpose of this study muscle in-levers were measured within the model for two key jaw adductors: anterior temporalis and superficial anterior masseter. Muscle origin and insertion sites visible on the bone were used to mark the muscle lines of action (Landmarks 3:6, Fig. 3.4 and Table 3.1). The in-lever was calculated as perpendicular distance from the muscle line of muscle to the fulcrum, taken as the centre of the mandibular condyle (Fig. 3.7; following Dickinson et al., 2018; Godinho et al., 2018).
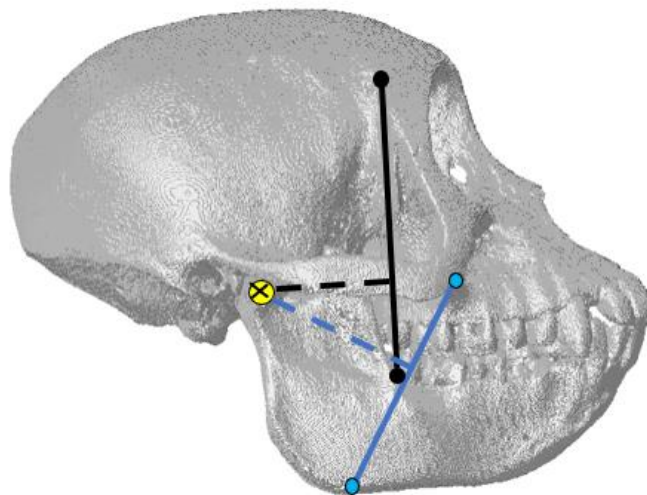


**Figure 3.7 Images showing muscle lines of action used to estimate in-lever length on specimen (*Cercocebus*). Image shows fulcrum (condyle) as yellow circle with cross. Muscle line of action in solid line and in-lever in dashed line.**

The out-lever for the masticatory system was measured for four bite points: incisors, canines, premolars and molars (Landmarks 7 – 10, Fig. 3.4 and Table 3.1). The out-lever length was measured using a plane parallel to the occlusal plane projected vertically to the height of the condyle (Fig. 3.8; O'Connor et al., 2005; Dickinson et al., 2018; Godinho et al., 2018). To establish this plane the 3D models were aligned to an occlusal plane using rigid warping in Avizo. This plane was determined by three points: the last molar bilaterally and the second premolar unilaterally. The distance from the TMJ to the vertical component from each bite point intersecting this plane was measured as the out-lever (Fig. 3.8). The occlusal plane selected for alignment was chosen with the intention of standardising between specimens with highly variable anterior dentition. A sensitivity study found that in primates with very procumbent anterior dentition or a high curvature of Spee there was a prominent

effect to MA if the occlusal plane was aligned using anterior dentition. To understand the potential effect of this, a sensitivity study examined the impact of using different occlusal planes (see Appendix 3 for additional details). The effect of calculating out-levers using different occlusal planes was found to be extremely minimal in species with very flat dental rows (i.e. *Mandrillus*), but very prominent in those with procumbent anterior dentition (i.e. *Cacajao*) (Appendix 3, Fig. A3.1). A posterior occlusal plane (M3 – PM2) was found to be the most conservative plane, removing the prominent effect of orienting using anterior dentition which varies highly between species. The posterior occlusal plane was used for the calculation of out-lever in all specimens.
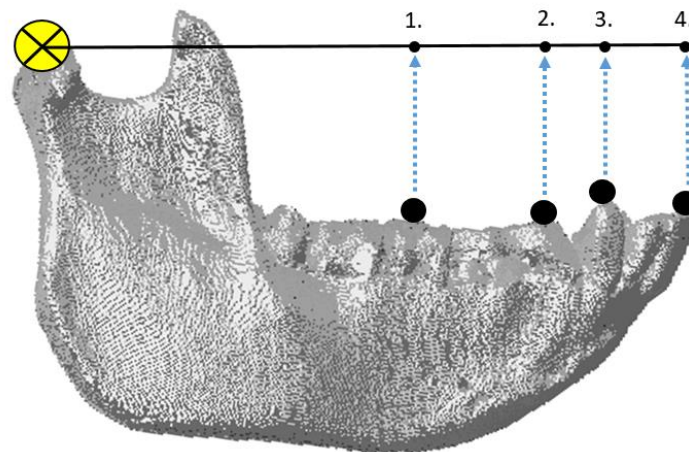


**Figure 3.8 Example of out-lever calculation for four bite points. The out-lever length for each tooth (black line) is measured as the perpendicular distance between the fulcrum (yellow cross) and a vector (dotted arrow) representing the vertical component of the bite (1. M1, 2. PM1, 3. Canine, 4. Centre point of incisors).**

After measuring in-lever and out-lever length mechanical advantage (MA) was calculated using the following formula:

$$MA = Length_{IN} / Length_{OUT},$$

Where $Length_{IN}$ is the length of the in-lever and $Length_{OUT}$ the length of the out-lever. Measurements were made repeatedly for each bite-point (out-lever length) and during jaw opening to account for changes in the in-lever length.

## 3.2.1.4 Model calculations: Muscle cross sectional area

Muscle PCSA contains information regarding the internal architecture of a muscle, pennation angle and fibre length (Taylor et al., 2009; Davis et al., 2010; Dickinson et al., 2018). While having such data is desirable as it increases accuracy in measurements relating to predicting muscle force, such data was available for this study as the sample consists of a wide range of endangered and previously wild shot specimens. As such, CSA from dry was used as a proxy measurement as this requires only skeletal material (Thomason, 1991; Christiansen and Adolfssen, 2005; Christiansen and Wroe, 2007; Campbell and Santana, 2017).

The Thomason (1991) approach for measuring CSA was used here. This method estimates CSA of the temporalis and of the masseter-medial pterygoid complex using the area of the infratemporal fossa. Without dissection data it is not possible to predict masseter CSA in isolation, and the masseter-medial pterygoid complex is more reflective of true total jaw adductor mass.

To make these measurements, cranial surfaces were aligned to the condyle-incisor plane and muscle boundaries selected (Fig. 3.9). Using Avizo the masseter-medial pterygoid CSA was segmented in the most inferior slice where a complete zygomatic arch outline was visible. In this slice, the lateral boundary was the lateral edge of the zygomatic arch, the medial boundary was the lateral border of the lateral pterygoid bone, the anterior boundary was the anterior masseter attachment on the zygomatic arch, and the posterior boundary was the post-glenoid process. For temporalis the most superior slice with a complete zygomatic arch outline visible was located. The lateral boundary was the medial edge of the zygomatic arch, the anterior boundary was the most anterior extent of the zygomatic arch, and the posterior boundary was the most posterior extent of the zygomatic arch. The medial muscle boundary required additional segmentation: the most protuberant point on the infratemporal crest was identified by locating it on the model surface file, then segmenting a line along this crest. This line was then used as the medial boundary. Measurements of muscle CSA were exported for analysis.
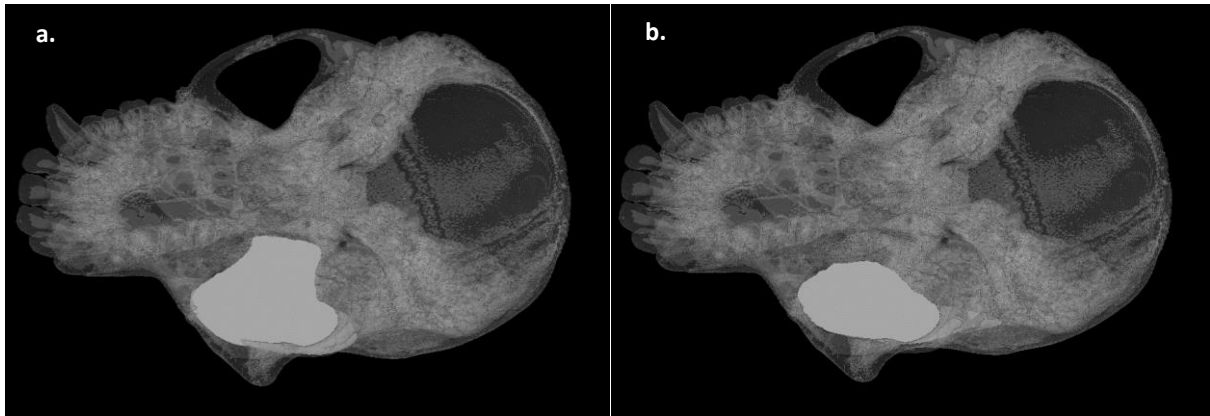
**Figure 3.9 Cross sectional areas measured for the masseter-medial pterygoid (a) and temporalis (b).**

## 3.2.1.5 Model calculations: Condyle height, glenoid length, muscle stretch

Three additional values were calculated within the model in order to investigate aspects of masticatory form which may contribute to an increased gape.

*Condyle height*: Condyle height above the occlusal plane was measured as a potential indicator of gape performance.  This height does not change with jaw opening or translation, so it was only calculated once. The value was measured as the vertical distance between a landmark on the centre of M3 and the same landmark project along the vertical component to the height of the TMJ, taken in a posterior occlusal plane (Fig. 3.10).
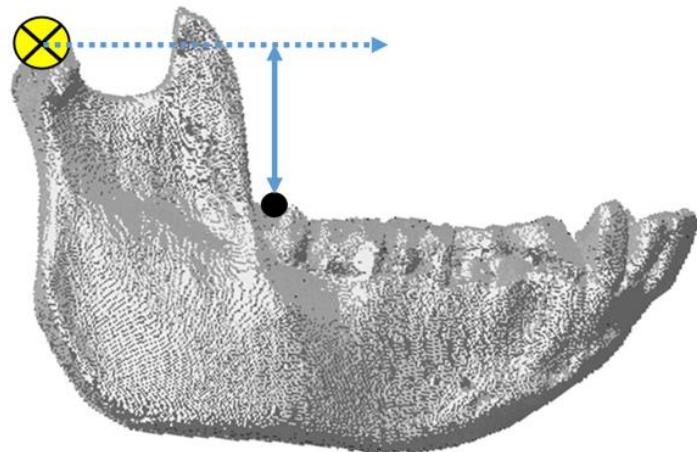


**Figure 3.10 Measuring the height of the condyle above the occlusal plane as the vertical component from the centre M3 to the height of the TMJ.**

*Muscle stretch*: The length of each muscles (distance from origin to insertion) was measured during jaw opening at each bite height. By comparing the original length at occlusion to the lengths at stages of jaw opening an estimate of the percentage increase in muscle length could be calculated and used as a simplified estimate of muscle stretch in jaw opening. This value was also examined with and without translation.

*Glenoid length:* The 3D distance of the anteroposterior length of the glenoid was measured to be applied as an estimate of translation jaw opening while the mandible was rotated open. This distance was calculated using two landmarks (Landmarks 15,16 in Table 3.1), one at the most posterior and inferior glenoid at the base of the postglenoid process and one at the most anterior glenoid surface. This value was also extracted from the model for comparative purposes.

## 3.2.1.6 Model calculations: Bite force estimates

The values calculated at each stage of model building (linear gape height, lever arm lengths, muscle CSA) were used to produce an estimate of bite force at increasing gape height across the sample.

As a first step, muscle force was calculated. To calculate muscle force, CSA was multiplied by a value selected for muscle tension. In keeping with numerous past studies including many based on primates, $0.03 / mm^2$ was selected (Close, 1972; Thomason, 1991; Ledogar et al., 2018; Perry, 2018).

After all measurements were taken bite force was calculated using the following formula (Thomason, 1991):

$$B_f = \frac{M_f \times m_{in} + T_f \times t_{in}}{out}$$

Where $M_f$ and $T_f$ are masseter/medial pterygoid and temporalis muscle force, and $m_{in}$ and $t_{in}$ are masseter and temporalis in-levers. Out represents the out-lever length.

In-lever length changes with increasing linear gape. Bite was calculated using the corresponding in-lever length at each increasing linear gape height (ranging from occlusion to 40mm linear gape).

Bite force estimates were calculated with 100% muscle activation assumed. Bite force was calculated unilaterally and results were not multiplied as the primary aim was to compare estimates of bite force between specimens. As is the case in past studies (i.e. Demes and Creel, 1988; Wroe et al., 2005; Dumont et al., 2009) it is important to note that the methods used produce bite force estimates which are useful for their comparative value within the sample, but which cannot be taken as absolute bite force values.

## 3.2.1.7 Scaling

The additional step of scaling was taken for data which were affected by scale as the sample spans a wide range of body sizes. This included length measurements (condyle height and length of glenoid) and linear gape (bite height) at set degrees of rotation. To scale data, the body mass values for primates in the sample were sourced (Smith and Jungers, 1997). Body mass (Table 3.2) was chosen because of the strong link between dietary grouping and mandibular shape expected for this sample (Perry and Hartstone-Rose, 2011). The measures were then regressed against the cube root of body weight in RStudio, then the residuals were extracted to be used as the scaled value.

## 3.2.1.8 Code design for model and exporting values

Three functions were written to run this model and calculate the measurements using RStudio with the packages Arothron (Profico et al., 2019), linkR (Olsen, 2016), MALDIquant (Gibb and Strimmer, 2012), and stringr (Wickham, 2019). The first function extracted and combined the landmark coordinates from Avizo files. The second function calculated the out-lever length to produce single values for each examined tooth. Finally, the third function carried out the rotation of the coordinates and all other measurements and calculations. Here, a 3D rotation matrix function (Olsen, 2016) was applied to rotate the mandible coordinates, then the model calculations were made. A top-level script ran the three functions then exported the raw data for each specimen. All data was paired with the relevant tooth, muscle, specimen, its sex and side of the mandible and cranium measured. Raw code for all three functions is presented in Appendix 4. Raw data was exported directly to Excel, then used in RStudio to carry out analyses and make plots using the packages ggplot2 (Wickham, 2016) and ggrepel (Slowikowski, 2020).

### 3.2.2 Objective 2: Collect mechanically relevant parameters at a series of jaw opening positions for a range of primate species

In order to address the main aim of this study a sample of primates was selected. The sample includes stress-resistant feeders and non-stress resistant feeders. Mechanically relevant parameters were collected using the above model.

### 3.2.2.1 Sample

Eleven species from five families were included in this study, comprising intensive seed predators (*Cercocebus atys, Cacajao calvus, Cacajao rubicundus, Cacajao melanocephalus, Pithecia pithecia, Chiropotes chiropotes and Chiropotes sagulatus*), seasonal (occasional) seed predators (*Mandrillus sphinx* and *Sapajus apella*), and comparison species which span a range of diets and are either closely related or sympatric species to the seed predator sample. Diets represented by the comparison species are broadly classified as frugivory (*Ateles paniscus, Cebus olivaceus, Pan troglodytes verus*), mixed frugivory-insectivory (*Saimiri sciureus*) and graminivory, a very tough diet (*Theropithecus gelada*). A further split divides the seed predators between those which feed primarily using their anterior dentition (*Cacajao, Chiropotes, Pithecia*) and those which primarily use their posterior dentition (*Cercocebus, Mandrillus, Sapajus*).

The specimens included in this study were the same as the previous chapter 2 (Table 3.2; see 2.3.1 for further details). Both females and males are included in the sample, and all species were wild-caught with the exception of some *Theropithecus* specimens (listed in specimen database Appendix 1). Full specimen details are available in Appendix 1 (specimen database).

3D surface files for each specimen had previously been collected and processed by aligning to occlusion and landmarking (see chapter 2, 2.3.2 - 2.3.4 and Appendix 2). In order to scale the relevant mechanical parameters body mass estimates were collected for both sexes for each species (Table 3.2).

**Table 3.2 List of species and number of specimens included in the study, including an average estimated body mass in kilos (Smith and Jungers, 1997).**

| Species | Number of specimens in sample | Body mass in kg | | % difference | Dietary category* |
|---|---|---|---|---|---|
| | | Female | Male | | |
| *Ateles* | Females 5; Males 6 | 8.44 | 9.11 | 7.64% | Non-seed predator (soft fruit) |
| *Cacajao* | Females 3; Males 8 | 2.88 | 3.45 | 18.01% | Seed predator (intensive) |
| *Chiropotes* | Females 5; Males 5 | 2.58 | 2.9 | 11.68% | Seed predator (intensive) |
| *Pithecia* | Females 3; Males 5 | 1.58 | 1.94 | 20.45% | Seed predator (intensive) |
| *Cebus* | Females 0; Males 2 | 2.52 | 3.29 | 26.51% | Non-seed predator (fruit and invertebrates) |
| *Sapajus* | Females 6; Males 5 | 2.52 | 3.65 | 36.63% | Seed predator (seasonal) |
| *Saimiri* | Females 4; Males 5 | 0.662 | 0.779 | 16.24% | Non-seed predator (fruit and invertebrates) |
| *Cercocebus* | Females 2; Males 6 | 6.2 | 11 | 55.81% | Seed predator (intensive) |
| *Mandrillus* | Females5; Males 6 | 12.9 | 31.6 | 84.04% | Seed predator (seasonal) |
| *Theropithecus* | Females 4; Males 5 | 11.7 | 19 | 47.56% | Non-seed predator (grasses) |
| *Pan* | Females 4; Males 4 | 41.6 | 46.3 | 10.69% | Non-seed predator (fruit) |

* (Dunbar and Dunbar, 1974; Izawa and Mizuno, 1977; Izawa, 1979; Boesch and Boesch, 1982; Terborgh, 1984; Hoshino, 1985; van Roosmalen, 1985; Lahm, 1986; Sugiyama, 1987; Mcgrew et al., 1988; Ayres, 1989; Peres, 1991, 1993; Kinzey, 1992; Kinzey and Norconk, 1993; Galetti et al., 1994; Dorothy M Fragaszy and Boinski, 1995; Lima and Ferrari, 2003; Wieczkowski, 2003; Dew, 2005; Astaras, 2009; Norconk and Veres, 2011; Bowler and Bodmer, 2011; Daegling et al., 2011; Alfaro et al., 2012; W.S. McGraw et al., 2014; Barnett et al., 2016)

## 3.2.2.2 Mechanically relevant parameters collected.

For each of the specimens the following data was collected (as per method described in 3.2.1): muscle in-lever lengths, out-lever lengths, mechanical advantage, muscle stretch, glenoid length, height of the condyle above the occlusal plane. Mean values for each species and sex were calculated and used for further analysis (raw value database in Appendix 5; tables of mean values in Appendix 6). In cases where one specimen within a sex and species group could attain a higher gape than the remaining sample this individual was removed as the final value no longer represented a mean. Estimated muscle CSA was collected for one female and one male representative of each species. The representative species was selected from the centre of the distribution in a principal component analysis of all specimens in shape space, separated by sex (see Ch. 2, 2.3.5.2).

Primates are known to feed on foods with a range of sizes, with a particular density of seeds in the c. 20 mm diameter range. This includes the *Sacoglottis* seed eaten by *Cercocebus* on their posterior dentition (diameter c. 20 – 25mm) and the Brazil nut (breadth c. 23 mm)

eaten by *Cacajao* on its anterior dentition (Norconk et al., 2009, 2013; Daegling et al., 2011; Barnett et al., 2015). The palm seeds processed by *Sapajus* are also within this size range with a breadth of 20 – 40mm (Terborgh, 1984; Visalberghi et al., 2008). Larger seeds are also eaten by *Chiropotes* (up to 220mm) on its anterior dentition, although it does not fit the entire seed in its mouth in this process (Norconk and Veres, 2011). The seed size eaten by *Mandrillus* has not been previously reported. Results from past studies (Lahm, 1986) indicate a range of sizes in the fruit and their seeds eaten, including the large fruit *Pentadesma butyreca* (c. 100 – 140 mm diameter) with its numerous seeds (c. 20 mm breadth), and fruits such as *Irvingia gabonensis* (c. 30mm fruit breadth with seeds c. 15mm breadth) (Awono et al., 2009; Ewédjè et al., 2012).

To model different seed feeding positions and sizes data was extracted for bite points at the central incisor, canine, PM1 and M1. Linear gape heights from 0 mm (occlusion) to 40 mm are examined, as well as maximum angular gape, gape at maximum rotation (40 degrees) with and without anterior translation. Translation is included in order to examine the impact of translation of the mandible at maximum jaw rotation. Each parameter measured is presented using bar plots, line graphs, scatterplots, or tables in order to fulfil objectives 3 -5 and test the hypotheses.

## 3.4 Results

## 3.4.1 Gape

To test predictions relating to seed predator performance at maximum gape three measurements are considered. First, the maximum linear gape height which could be attained is explored. Following this, muscle stretch and mechanical advantage at maximum gape are presented.

### 3.4.1.1 Maximum linear gape height

To determine the maximum attainable gape for each species the mandible was rotated to maximum angular gape (40 degrees) and the linear gape height was measured along the dental row. Results for the absolute (unscaled) linear gape recorded for females show a broad range of linear gape heights along the dental row (Table 3.3). For the incisors, the linear gape ranges from 83mm in *Pan* to 22mm in *Saimiri*, while for the M1 (most posterior measurement) linear gape heights measured range from 55mm in *Pan* to 13mm in *Saimiri*. Seasonal seed predator *Mandrillus* has amongst the highest linear gapes of the measured species on all teeth (70mm on incisor – 44mm on M1). The remaining seed predators have considerably smaller linear gape. This is especially notable for *Chiropotes* and *Pithecia* which have very similar values on all teeth and group with second smallest gape height of the sample (33-34mm on incisor – 20mm on M1). *Cacajao* has somewhat higher gape, especially on incisor (41mm), and has very similar values to *Sapajus* on the remaining teeth (24-26mm on canine, 23-24mm on M1). These values are still relatively low amongst the sample. *Cercocebus* has middling performance, and while it has a considerably smaller gape than *Mandrillus* and *Theropithecus* it still has a wide gape within the sample, particularly on the incisor (52mm, with 31mm on M1).

Male results for absolute (unscaled) linear gape (Table 3.4) show a similar pattern to females for most primates on all teeth, but gape is absolutely larger in the males except for on the canine. No comparison can be made for *Cebus* as there are no female *Cebus* specimens. One key difference within the male results is the fact that *Mandrillus,* rather than *Pan*, has the largest absolute gape on all bites except canine (104mm on incisor – 65mm on M1). The smallest gape of the sample remains in *Saimiri* (22mm on incisor –

14mm on M1). Seed predator gape height, with the exception of *Mandrillus*, remains middling to low. *Chiropotes* and *Pithecia* follow the pattern observed in females and group very closely in gape height. The exception to this pattern is incisor, on which *Chiropotes* has a slightly larger gape than *Pithecia* (37mm in *Chiropotes* and 34 mm in *Pithecia*). *Cacajao* has larger gape than both *Chiropotes* and *Pithecia* as in females, especially on incisor (45mm). On other teeth *Cacajao* and *Sapajus* have very similar gape heights (23-25mm on canine, 26-27mm on M1). Notably the linear gape on the canine is very similar between females and males seed predators *Cacajao, Chiropotes,* and *Pithecia* (difference c. 1 mm between sexes). Male *Cercocebus* has middling gape height within the sample, which is notably high on incisor (62mm, and 39mm on M1).

Scaling the results (Tables 3.3 and 3.4) show an increase in the relative gape capability of some of the intensive stress resistant feeders in both sexes. *Cacajao* and *Cercocebus* have a relatively larger gape compared to *Pan*, particularly on the incisor. In males, *Cacajao* has a relatively high linear gape on all teeth, especially on the canine. Following scaling, *Pithecia* has a larger linear gape height compared to *Sapajus* and *Cebus* on posterior bites in males and has a relatively very high gape on the canine. Female *Pithecia* follows similar patterns to a lesser degree and is not exceptional on the canine. Interestingly *Chiropotes* after scaling still has one of the smallest relative gapes in the sample. By contrast, *Mandrillus* in both sexes retains a high gape after scaling on the incisor and PM1. *Cercocebus* retains a middling to high scaled gape in both sexes on all teeth except M1, where it has a relatively small gape after scaling.

**Table 3.3 Absolute linear gape height (mm) and scaled linear gape height after jaw rotation to maximum gape (40 degrees rotation) in females. Table is ordered by diet type.**

| Species | Diet type | Measurement | Incisor | Canine | PM1 | M1 |
|---|---|---|---|---|---|---|
| *Cacajao* | Hard: intensive | Linear gape (mm) | 40.71 | 24.84 | 28.80 | 24.25 |
| | | Linear gape (scaled) | 10.63 | -5.24 | -1.28 | -5.83 |
| *Chiropotes* | Hard: intensive | Linear gape (mm) | 33.99 | 19.47 | 23.31 | 20.05 |
| | | Linear gape (scaled) | 4.98 | -9.55 | -5.70 | -8.97 |
| *Pithecia* | Hard: intensive | Linear gape (mm) | 32.85 | 19.78 | 23.45 | 20.15 |
| | | Linear gape (scaled) | 8.31 | -4.76 | -1.08 | -4.39 |
| *Cercocebus* | Hard: intensive | Linear gape (mm) | 51.24 | 39.81 | 38.64 | 31.35 |
| | | Linear gape (scaled) | 12.19 | 0.76 | -0.41 | -7.69 |
| *Mandrillus* | Hard: seasonal | Linear gape (mm) | 69.59 | 59.10 | 56.20 | 44.17 |

| Species | Diet type | Measurement | Incisor | Canine | PM1 | M1 |
|---|---|---|---|---|---|---|
| | | Linear gape (scaled) | 19.67 | 9.19 | 6.28 | -5.75 |
| *Sapajus* | Hard: seasonal | Linear gape (mm) | 37.23 | 26.89 | 28.02 | 22.64 |
| | | Linear gape (scaled) | 8.43 | -1.91 | -0.78 | -6.16 |
| *Ateles* | Not hard | Linear gape (mm) | 50.96 | 37.66 | 39.77 | 33.35 |
| | | Linear gape (scaled) | 7.65 | -5.65 | -3.54 | -9.96 |
| *Pan* | Not hard | Linear gape (mm) | 82.90 | 64.91 | 63.62 | 55.78 |
| | | Linear gape (scaled) | 9.31 | -8.68 | -9.97 | -17.81 |
| *Saimiri* | Not hard | Linear gape (mm) | 21.83 | 15.80 | 16.65 | 13.33 |
| | | Linear gape (scaled) | 3.48 | -2.55 | -1.70 | -5.02 |
| *Theropithecus* | Not hard | Linear gape (mm) | 67.44 | 55.93 | 55.84 | 47.17 |
| | | Linear gape (scaled) | 19.23 | 7.72 | 7.63 | -1.05 |

**Table 3.4 Table Absolute linear gape height (mm) and scaled linear gape height after jaw rotation to maximum gape (40 degrees rotation) in males. Table is ordered by diet type.**

| Species | Diet type | Measurement | Incisor | Canine | PM1 | M1 |
|---|---|---|---|---|---|---|
| *Cacajao* | Hard: intensive | Linear gape (mm) | 44.65 | 24.99 | 30.96 | 26.89 |
| | | Linear gape (scaled) | 14.94 | -4.72 | 1.24 | -2.82 |
| *Chiropotes* | Hard: intensive | Linear gape (mm) | 37.31 | 18.53 | 25.54 | 22.42 |
| | | Linear gape (scaled) | 9.38 | -9.39 | -2.38 | -5.50 |
| *Pithecia* | Hard: intensive | Linear gape (mm) | 33.82 | 20.21 | 24.79 | 21.34 |
| | | Linear gape (scaled) | 9.92 | -3.68 | 0.90 | -2.56 |
| *Cercocebus* | Hard: intensive | Linear gape (mm) | 62.21 | 34.72 | 45.31 | 38.95 |
| | | Linear gape (scaled) | 16.60 | -10.89 | -0.29 | -6.66 |
| *Mandrillus* | Hard: seasonal | Linear gape (mm) | 104.40 | 55.18 | 75.07 | 65.14 |
| | | Linear gape (scaled) | 37.75 | -11.47 | 8.42 | -1.51 |
| *Sapajus* | Hard: seasonal | Linear gape (mm) | 42.32 | 23.33 | 30.54 | 25.66 |
| | | Linear gape (scaled) | 11.93 | -7.05 | 0.16 | -4.72 |
| *Ateles* | Not hard | Linear gape (mm) | 50.78 | 30.15 | 38.58 | 32.56 |
| | | Linear gape (scaled) | 8.09 | -12.55 | -4.12 | -10.14 |
| *Cebus* | Not hard | Linear gape (mm) | 38.76 | 20.58 | 27.36 | 22.61 |
| | | Linear gape (scaled) | 9.49 | -8.69 | -1.91 | -6.65 |
| *Pan* | Not hard | Linear gape (mm) | 86.72 | 60.43 | 64.84 | 57.05 |
| | | Linear gape (scaled) | 10.45 | -15.85 | -11.44 | -19.23 |
| *Saimiri* | Not hard | Linear gape (mm) | 22.20 | 11.96 | 16.30 | 13.58 |
| | | Linear gape (scaled) | 5.69 | -4.55 | -0.20 | -2.92 |
| *Theropithecus* | Not hard | Linear gape (mm) | 83.51 | 45.94 | 64.61 | 55.59 |
| | | Linear gape (scaled) | 27.83 | -9.74 | 8.93 | -0.10 |

## 3.4.1.2 Muscle stretch at maximum gape, with and without anterior translation

The percentage increase in muscle length at maximum gape was examined in order to test the prediction that seed predators would have relatively low muscle stretch at high gapes. Muscle length increase was examined with and without translation at maximum gape rotation.

Results without translation (pure rotation) show a greater increase in muscle length of the masseter than for the temporalis for all species and on all bite positions (Figs. 3.11 – 3.12 Appendix 6, Table A6.1 – A6.2). At maximum gape seed predators do not have the lowest percentage increase in muscle length (either for the temporalis and masseter) of the sample in both sexes. For the masseter the lowest percentage increase in muscle length is *Theropithecus* in both sexes (46.61% and 46.49% increase muscle length in females and males, respectively). Some seed predators have relatively low muscle stretch for the masseter, notably *Chiropotes* has values very close to *Theropithecus* (48.12% and 47.86% increase in length in females and males). However, other seed predators have amongst the higher muscle stretch in the sample. Notably, the highest stretch in females is seen in *Cacajao* (59.43% increase muscle length) and in males it is seen in *Pithecia* (60.7% increase). High stretch is also seen in *Mandrillus* in both sexes.

 For the temporalis the muscle length increase is, across all species and both sexes, lower than for the masseter when examining the results from pure rotation (no translation). *Theropithecus* again has amongst the lowest increase in muscle length of the sample (26.09% in females, 25.9% in males), but this is no longer the lowest stretch in females, which is observed in *Mandrillus* (25.3% increase muscle length). In males it is notable that both *Cercocebus* and *Theropithecus* have very similarly low increases in muscle stretch (25.95% and 26.39%, respectively). Unlike for the masseter, the highest muscle stretch is not observed in seed predators for the temporalis. In females this is in *Ateles* (42.56% increase length) and in males in *Cebus* (39.64%) although as with other results *Cebus* was not included in the female sample.

In almost all species there was a reduction in muscle stretch after translation, for both muscles (Figs. 3.11 – 3.12, Appendix 6, Table A6.1 – A6.2). This effect is very pronounced

and consistent in the masseter but is not entirely consistent or very pronounced in the temporalis. None of the seed predators are most affected by translation, in either sex or for either muscle. In females *Saimiri* has the largest reduction in muscle length after translation for the masseter (reduction from 49.3% increase in length to 24.5% relative to length at occlusion). In males it is *Cebus* which has the largest reduction in length for the masseter (reduction from 50.9% to 27.5% relative to length at occlusion). The specimen with masseter length least affected by translation is *Theropithecus*, a non-seed predator, followed by *Mandrillus*. Notably *Theropithecus* had an especially low muscle stretch before translation was applied, after translation is considered *Theropithecus* has relatively high stretch within the sample, but not the highest.

Numerous species (male *Cercocebus,* both sexes of *Mandrillus, Theropithecus,* and *Pan*) show an increase in muscle length after translation in the temporalis. This effect is most pronounced on *Mandrillus* in both sexes. Female *Cercocebus* has an extremely small reduction in length after translation (from 27.23% to 27.05% increase in length relative to length at occlusion). Male *Cercocebus* has a small increase in length (from 25.9% to 27.2%). By contrast, all other species show a small reduction in muscle length after translation. In females this effect is most pronounced on seed predator *Chiropotes* (reduction from 32.2% to 30.4% relative to length at occlusion). In males this effect is most pronounced on seed predator *Cacajao* (reduction from 36.3% to 34%.4). However, it is noteworthy that the differences between all groups on temporalis are relatively small.
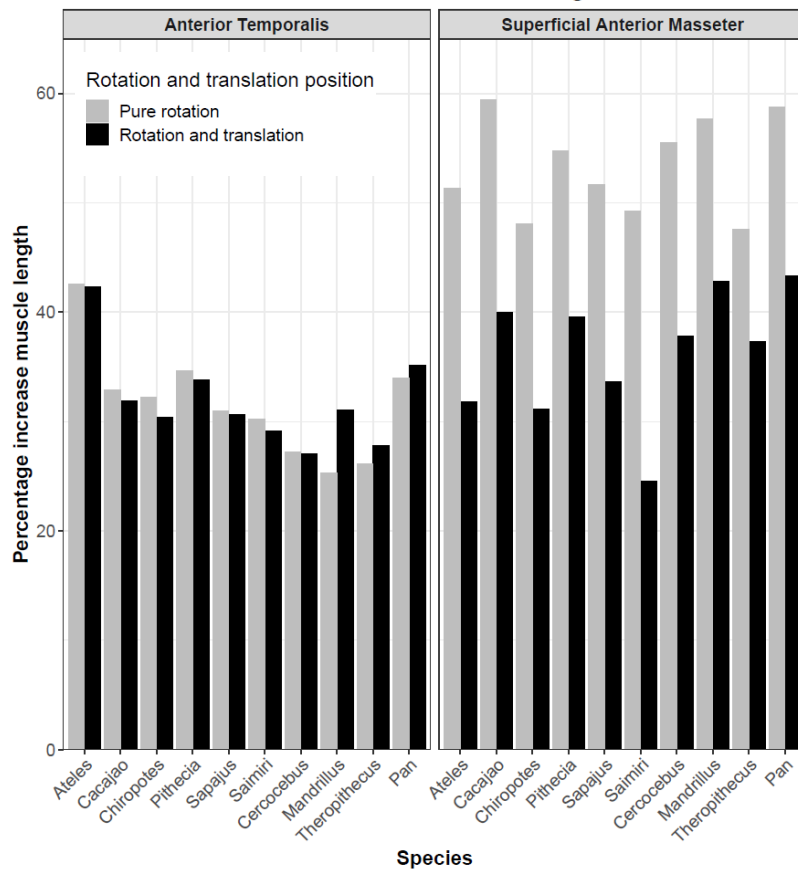
**Figure 3.11 Percentage increase in muscle length for females on incisor, showing the percentage increase for each muscle after rotation of the mandible by 40 degrees before and after anterior translation along the glenoid.**
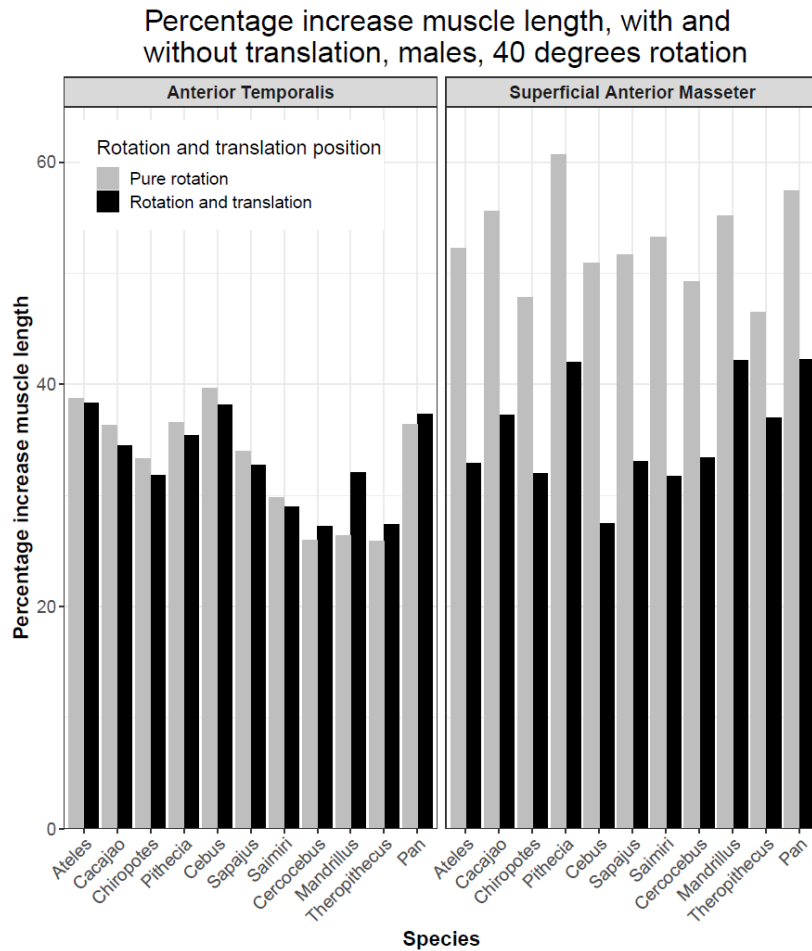
**Figure 3.12 Percentage increase in muscle length for males on incisor, showing the percentage increase for each muscle after rotation of the mandible by 40 degrees before and after anterior translation along the glenoid.**

## 3.4.1.3 Mechanical advantage (MA) at maximum gape, with and without anterior translation

One parameter which is predicted to change with gape is MA, as seed predators are predicted to retain high MA at high gape. MA is examined here first at maximum gape (Figs. 3.13 – 3.14, Appendix 6, Tables A6.3 – A6.4; See section 3.4.2 for MA values over changing linear gape heights). MA at maximum gape is measured both with and without the effect of anterior translation of the mandible. Results are presented for incisor (Appendix 6, Tables A6.3 – A6.4 for absolute values and additional teeth).

For results with no translation (pure rotation) some seed predators in both sexes meet predictions and have the highest MA of the sample, however this is not the case for all seed predators. For the masseter in the female sample (Fig. 3.13) the highest MA is seen in intensive seed predator *Cacajao,* closely matched by *Pithecia*. The next highest MA is seen in *Pan,* which is not a seed predator. Intensive seed predators *Cercocebus* and *Chiropotes* both also have relatively high MA, with very similar values to *Chiropotes.* The lowest value is seen in *Saimiri*, closely followed by seasonal seed predator *Mandrillus*. Applying translation reduces MA on the masseter considerably across the full sample. The distribution of results remains similar after translation is applied, however one major difference is that *Mandrillus* has a greater reduction in MA than *Saimiri,* and after translation is applied seasonal seed predator *Mandrillus* has the lowest MA for the masseter.

For the temporalis in females, results with no translation again find some, but not all seed predators to meet predictions of high MA when examining maximum gape. Seasonal seed predator *Sapajus* stands out with the highest MA, followed by non-seed predator *Ateles*. Intensive seed predators *Cacajao, Chiropotes,* and *Pithecia* have values close to, but less than those for *Ateles*. Non-seed predator *Pan* also stands out with high MA on the temporalis, while seed predators *Cercocebus* and *Mandrillus* have the lowest MA of the sample. Translation again reduces MA across the sample, and while the overall distribution of results mostly matches the untranslated values, some species are more affected than others. *Cacajao, Chiropotes,* and *Pithecia* have a slightly higher MA than *Ateles* after translation is applied and, along with *Sapajus*, have the highest MA of the sample.

In the male sample (Fig. 3.14) the highest MA for the masseter in pure rotation is seen in intensive seed predator *Cacajao*, with other seed predators *Chiropotes* and *Pithecia* having similarly high MA to *Cacajao*. Seasonal seed predator *Sapajus* also has high MA relative to the rest of the sample. In contrast, intensive seed predator *Cercocebus* has a middling value within the sample, and *Mandrillus* has the lowest MA of the sample. The distribution of results remains similar after translation is applied, although translation reduces MA on the masseter considerably across the full sample.

For the temporalis the highest MA without translation in males is seen in seasonal seed predator *Sapajus*, with a higher MA at maximum gape to the remaining sample by a considerable margin. The next highest MA is in intensive seed predator *Cacajao*, followed by

non-seed predator *Cebus*. Seed predators *Chiropotes* and *Pithecia* also have relatively high MA for the temporalis. By contrast, *Cercocebus* has amongst the lowest MA values for the temporalis, and seasonal seed predator *Mandrillus* has the lowest of the sample. As with the masseter in males, results follow a very similar distribution after translation is applied, although MA is reduced after translation across the full sample.
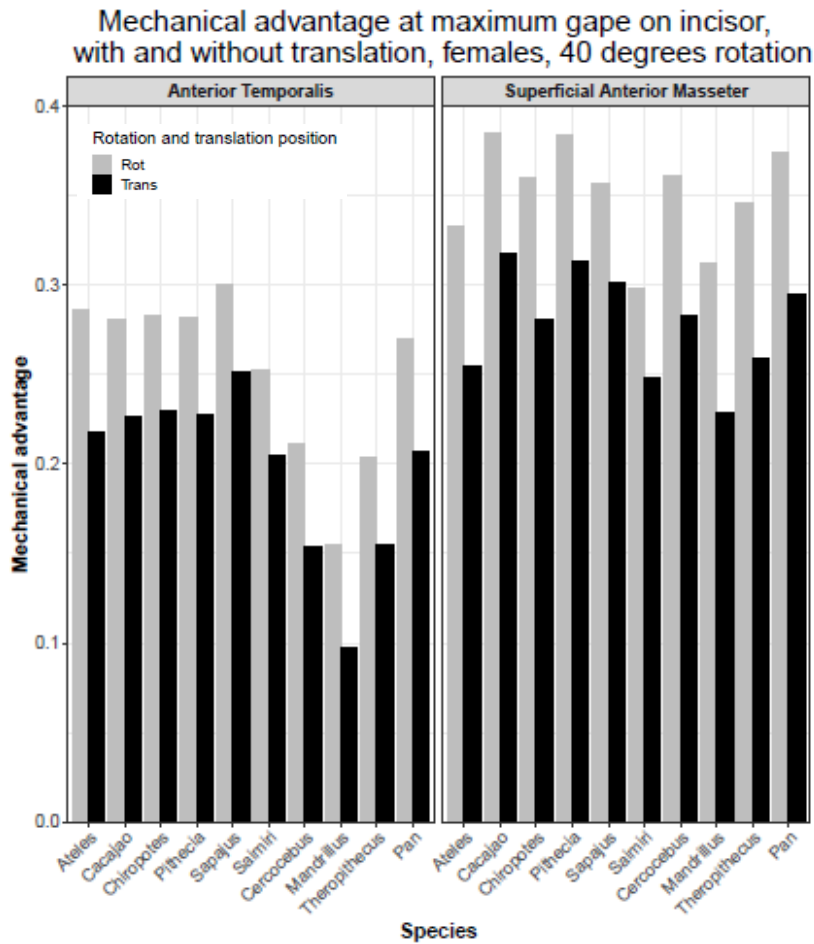


**Figure 3.13 MA on incisor in females with jaw rotated to maximum gape (40 degrees rotation), showing MA with and without anterior translation of the mandible.**

**Mechanical advantage at maximum gape on incisor, with and without translation, males, 40 degrees rotation**
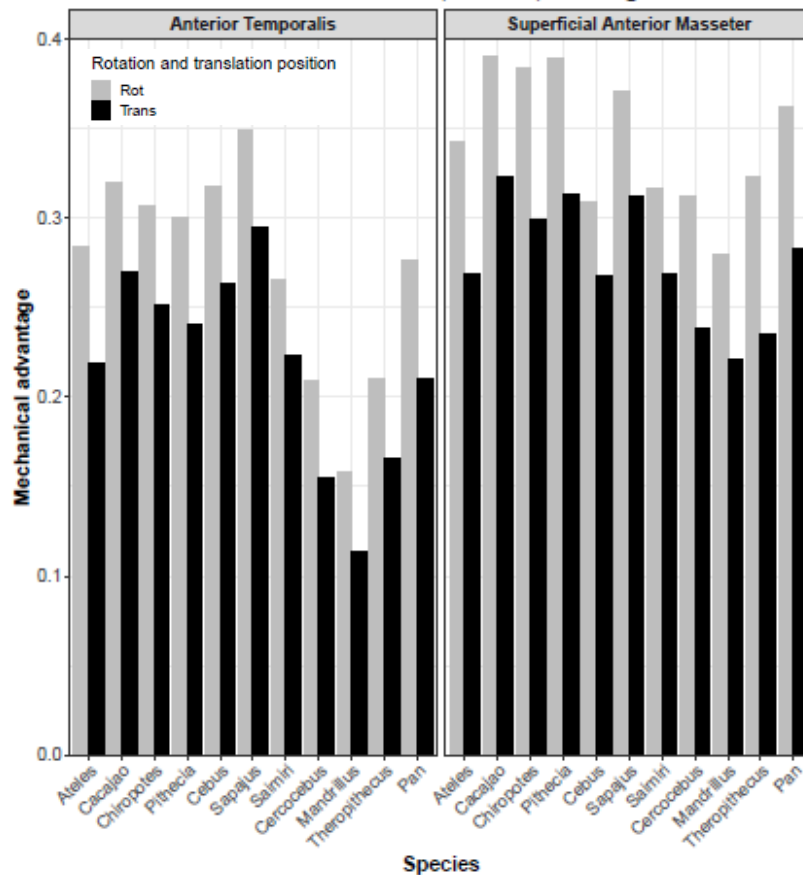
**Figure 3.14 MA on incisor in females with jaw rotated to maximum gape (40 degrees rotation), showing MA with and without anterior translation of the mandible.**

## 3.4.2 Mechanical advantage (MA)

MA was measured at a series of increasing linear gape heights (occlusion – 40mm linear gape height) simulating jaw opening. Jaw rotation was halted at maximum gape rotation (40 degrees), meaning that not all primates attained high linear gape heights: the ultimate value shown for each specimen is the highest linear gape attained at 40 degrees jaw rotation. Results show that some, but not all seed predators have exceptionally high MA on all gape positions and on all teeth (Figs. 3.15 – 3.16; Appendix 5 for absolute values; Appendix 6, Tables A6.5 – A6.8). MA varies by sex and is higher in some females relative to males (*Cercocebus, Mandrillus, Theropithecus,* for the masseter in *Pan*) and lower in other females relative to males (*Ateles, Cacajao, Chiropotes, Pithecia, Sapajus, Saimiri*).

In females (Fig. 3.15) at occlusion the highest MA on the masseter is seen in *Cacajao* on all teeth, while results for the temporalis are more variable. *Sapajus* has the highest MA at

occlusion on incisor for the temporalis, and clusters very tightly with *Cacajao* and *Chiropotes* on other teeth. The performance of other seed predators at occlusion is variable. *Pithecia* groups closely with *Cacajao* and *Chiropotes* to have high MA for the masseter and temporalis on incisor and canine and has slightly lower values on PM1 and M1. *Cercocebus* has relatively high MA on the masseter on all teeth, with values slightly lower than other seed predators but still higher than the majority of non-seed primates. This is not the case on the temporalis, where *Cercocebus* has amongst the lowest values of the sample. At occlusion the lowest MA of the sample on all positions and for both muscles is in *Mandrillus*, especially extreme on temporalis.

With increasing linear gape a changed pattern emerges for much of the female sample. At a gape of 20mm the primate with highest MA in females is *Pan* for all teeth and for measurements of the masseter and temporalis, although *Cacajao* has very similar values to *Pan* especially at PM1 and M1 for the masseter. *Cercocebus* retains relatively high performance especially on PM1 and M1 (masseter), and relatively low performance for the temporalis. Other seed predators *Pithecia*, *Chiropotes* and *Sapajus* have absolutely and relatively lower MA at high linear gape than at occlusion, especially on canine for both muscles. Their performance is still elevated compared to *Theropithecus* for the temporalis, but not at the incisor or canine for the masseter. Lowest MA of the sample at high gape is still seen in *Mandrillus*, with the exception of the incisor for the masseter, where the lowest MA is seen in *Saimiri*. It is notable that *Saimiri* experiences a very rapid and steep decrease in MA as linear gape increases, particularly relative to *Mandrillus,* which has a low MA overall but minimal decline in MA with increasing linear gape.

At linear gapes above 20mm in females there is a different picture, as much of the sample cannot attain such high gapes at maximum jaw rotation. This includes intensive seed predators *Cacajao, Chiropotes,* and *Pithecia,* with the exception of *Cacajao* for the incisor. Although *Cacajao* can attain this high linear gape it does not have a high MA at a 40mm bite on incisor, instead being middling amongst the sample for both the masseter and temporalis. Seasonal seed predator *Mandrillus* retains the lowest MA for the temporalis even at very high gapes but has very similar values to non-seed predator *Ateles* at high gapes for the masseter. The highest MA at high linear gape is seen in *Pan* for both the masseter and the temporalis.

Results for males (Fig. 3.16) broadly follow similar patterns to female results on all bite positions and all teeth with the exception of the canine. A key difference between sexes is the relatively lower MA of *Cercocebus* for both muscles on all teeth, with relatively low values within the sample. Other patterns are more consistent between sexes. At occlusion, for the masseter, male *Cacajao* matches females in having the highest MA for all bites, although male *Cacajao* groups closely with *Pithecia* on M1 and *Chiropotes* on other teeth. Male *Sapajus* has exceptionally high MA for the temporalis on all teeth, especially the incisor. This is in contrast to female results as female *Sapajus* and *Cacajao* have very similar MA on the temporalis. *Cebus* is included in the male sample and has relatively high values for the temporalis MA, especially on the incisor, but amongst the lowest values of the sample on all teeth for the masseter. *Mandrillus* males match females by having the lowest MA of the sample at occlusion in all positions and for all teeth.

After increasing linear gape to 20mm, male seed predators retain the highest MA of the sample on most bite positions. For the masseter, *Cacajao* has the highest MA with the exception of canine, on which *Pan* has the highest MA. Notably *Pan* retains high MA on all high gape bites and has higher MA than *Pithecia* and *Chiropotes* on all teeth. For the temporalis *Sapajus* has the highest MA on all teeth with the exception of canine, for which it groups very closely with *Pan* and *Cacajao*. The lowest performance at high gape is *Mandrillus* in many cases, for all teeth on the temporalis. For the masseter, *Mandrillus* and *Cebus* have near equivalent MA on all teeth except incisor, with the lowest values of the sample. *Saimiri* has the lowest MA at the incisor, notably *Saimiri* could not attain 20mm linear gape at more posterior positions so cannot be compared.

As with females, many male primates did not attain a linear gape of 40mm after jaw rotation to maximum gape, with the exception of incisor. For the masseter, non-seed predator *Pan* has the highest MA for high linear gapes on all teeth, although *Cacajao* retains a very high MA within the sample on the incisor. For the temporalis, *Sapajus* has exceptionally high MA on incisor even at very high linear gape. The lowest MA is variable between muscles. For the masseter, *Mandrillus* has the lowest MA at low linear gapes and for all gape heights on the canine, but at high linear gape it is intensive seed predator *Cercocebus* which has the lowest MA. For the temporalis it is consistently *Mandrillus* which has the lowest MA, although values for *Cercocebus* are similarly low at high linear gape.
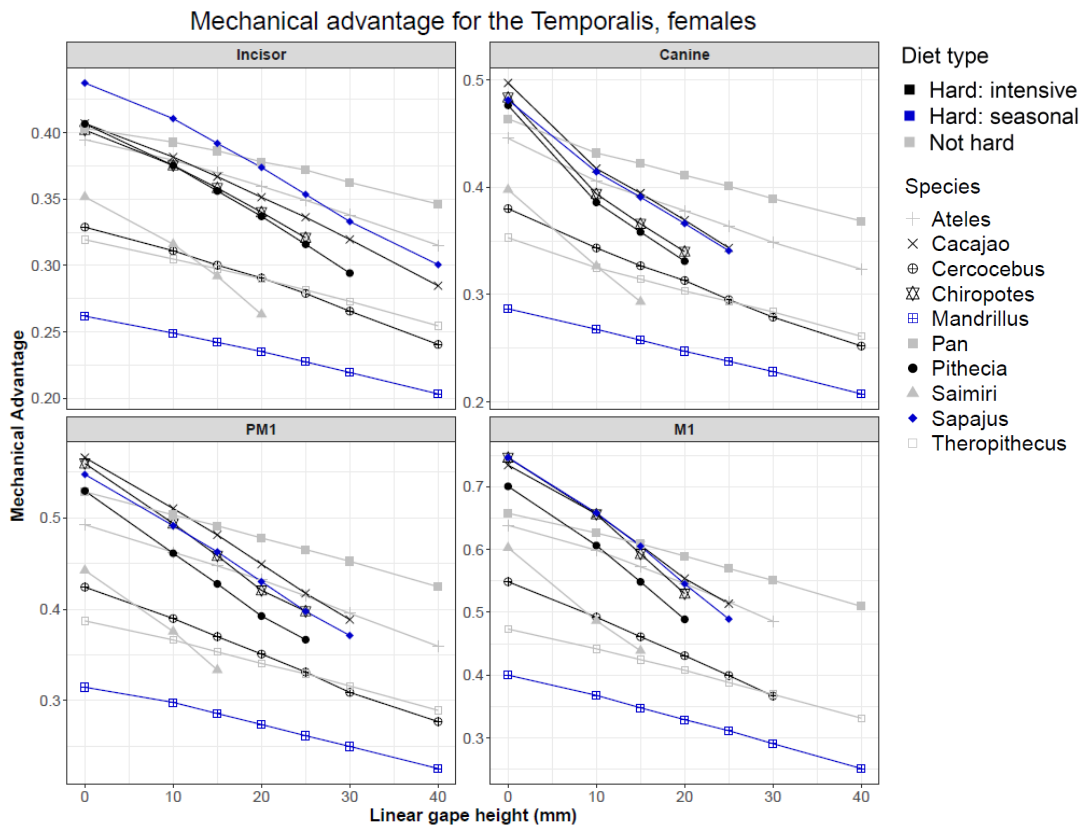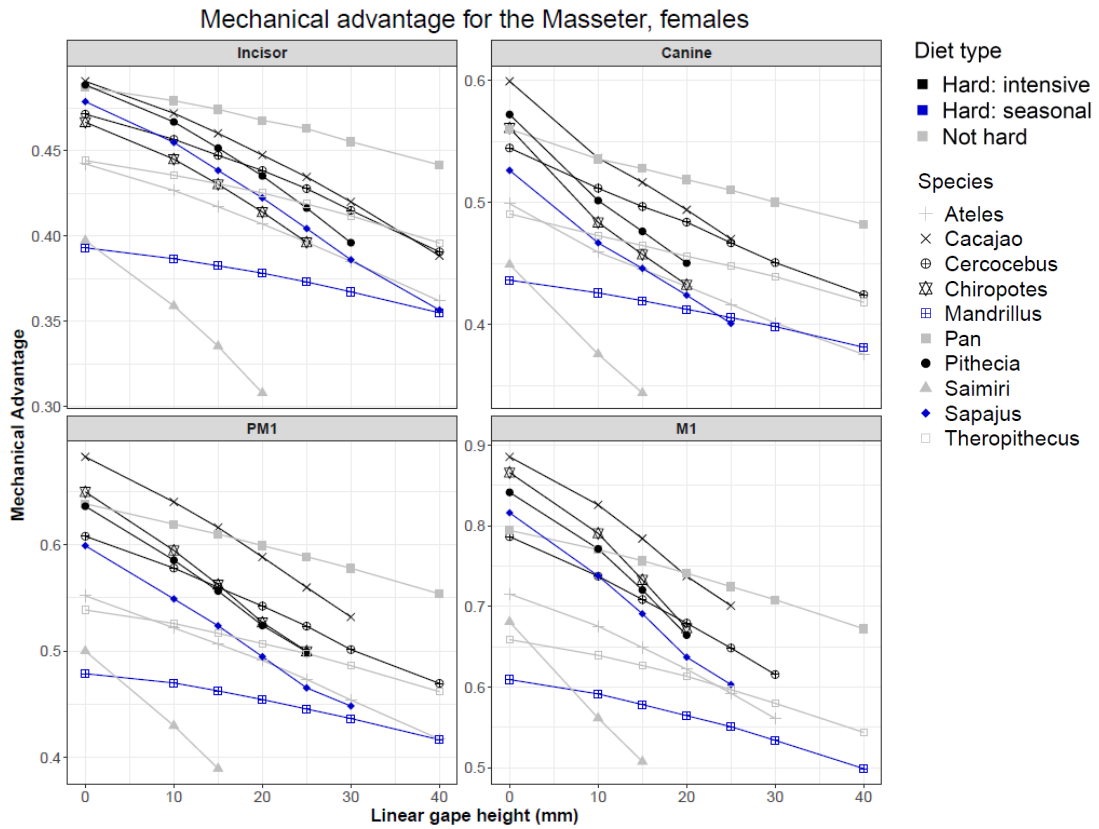
**Figure 3.15 MA along the dental row for females for the masseter (top) and temporalis (below). Showing MA at increasingly wide linear gape heights (mm) from occlusion (0 mm) through to a maximum of 40 mm. Species are noted by symbol type and dietary category by colour.**
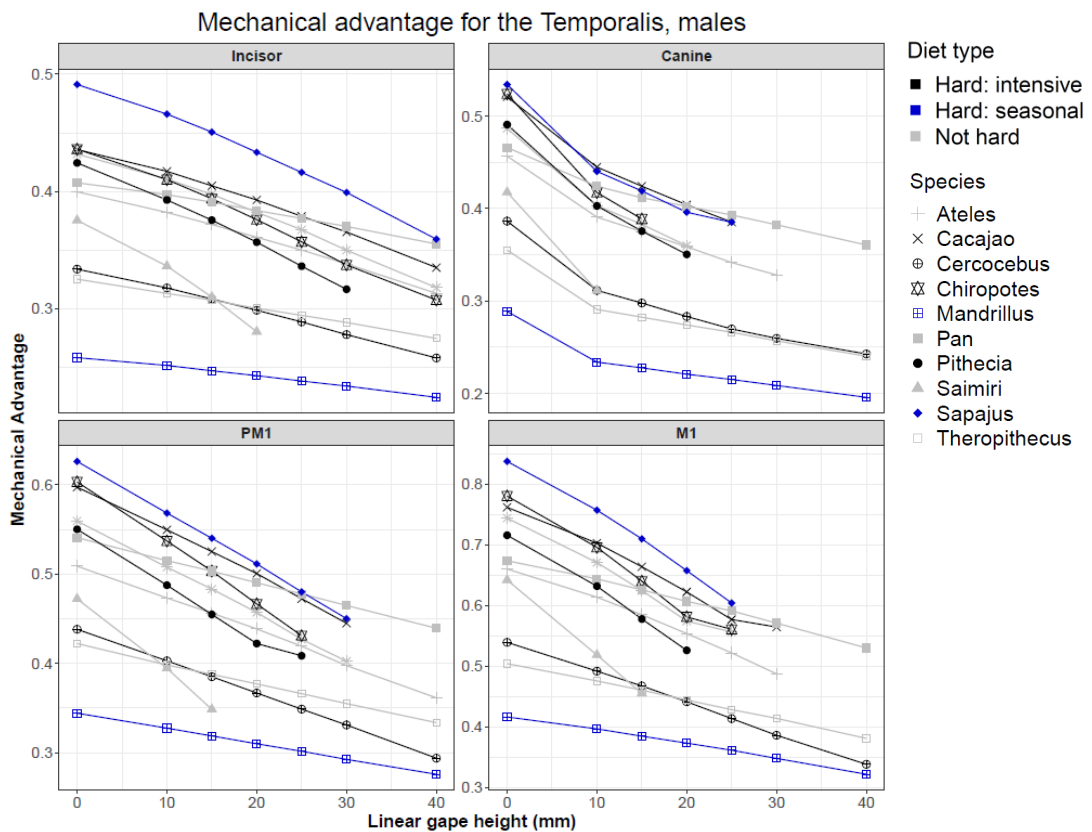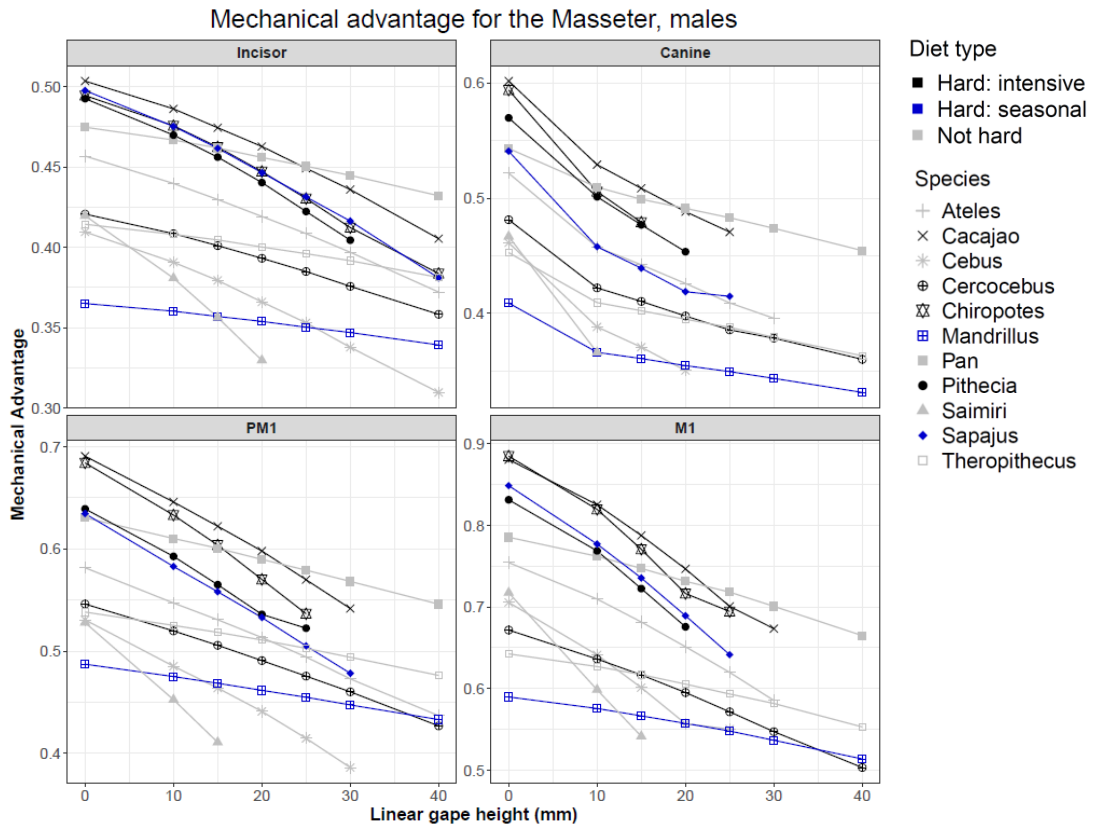
**Figure 3.16 MA along the dental row for males for the masseter (top) and temporalis (below). Showing MA at increasingly wide linear gape heights (mm) from occlusion (0 mm) through to a maximum of 40 mm. Species are noted by symbol type and dietary category by colour.**

### 3.4.2.1 Lever length comparisons

Plotting in-lever and out-lever lengths against each other highlights the lever length variation amongst the primates in the sample (Figs. 3.17 – 3.18, Appendix 6, A6.9). In both sexes this highlights the fact that *Mandrillus*, which is characterised overall by large gapes and low MA, has an especially long out-lever for all dental positions. The absolute length is greater in males but stands out in both sexes. Interestingly, in males, *Mandrillus* has a very similar absolute in-lever length to *Pan* but a much longer out-lever. *Cacajao* which has exceptionally high MA has a relatively long in-lever for both masseter and temporalis in both sexes. A contrast can be made between *Cacajao* and *Cercocebus* females on the temporalis, as both species have a near identical in-lever length but *Cercocebus* has a considerably longer out-lever length. This is also the case in males, but the out-lever length in male *Cercocebus* is considerably greater than in females. Also noteworthy is the particularly long in-lever length for *Sapajus* for the temporalis, underpinning the exceptionally high MA for *Sapajus* in this muscle. In both sexes lever lengths for *Sapajus* and *Cacajao* shows that *Cacajao* has a longer out-lever on the incisor but near equivalent on more posterior bites.

In-lever length and out-lever length, females
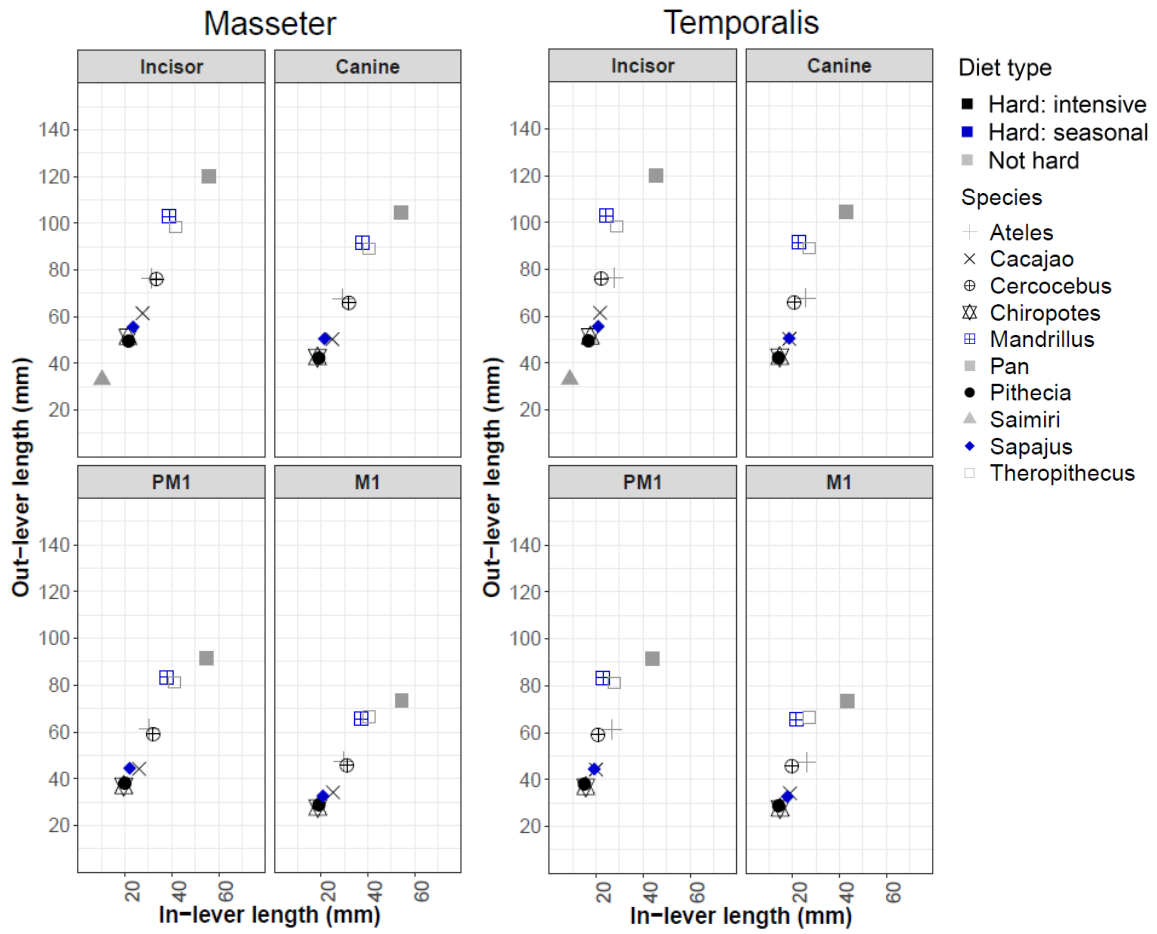


**Figure 3.17 In- vs out-lever lengths for female primates on the masseter and temporalis for bites at 20mm linear gape on all teeth. Species are noted by symbol type and dietary category by colour.**

In-lever length and out-lever length, males
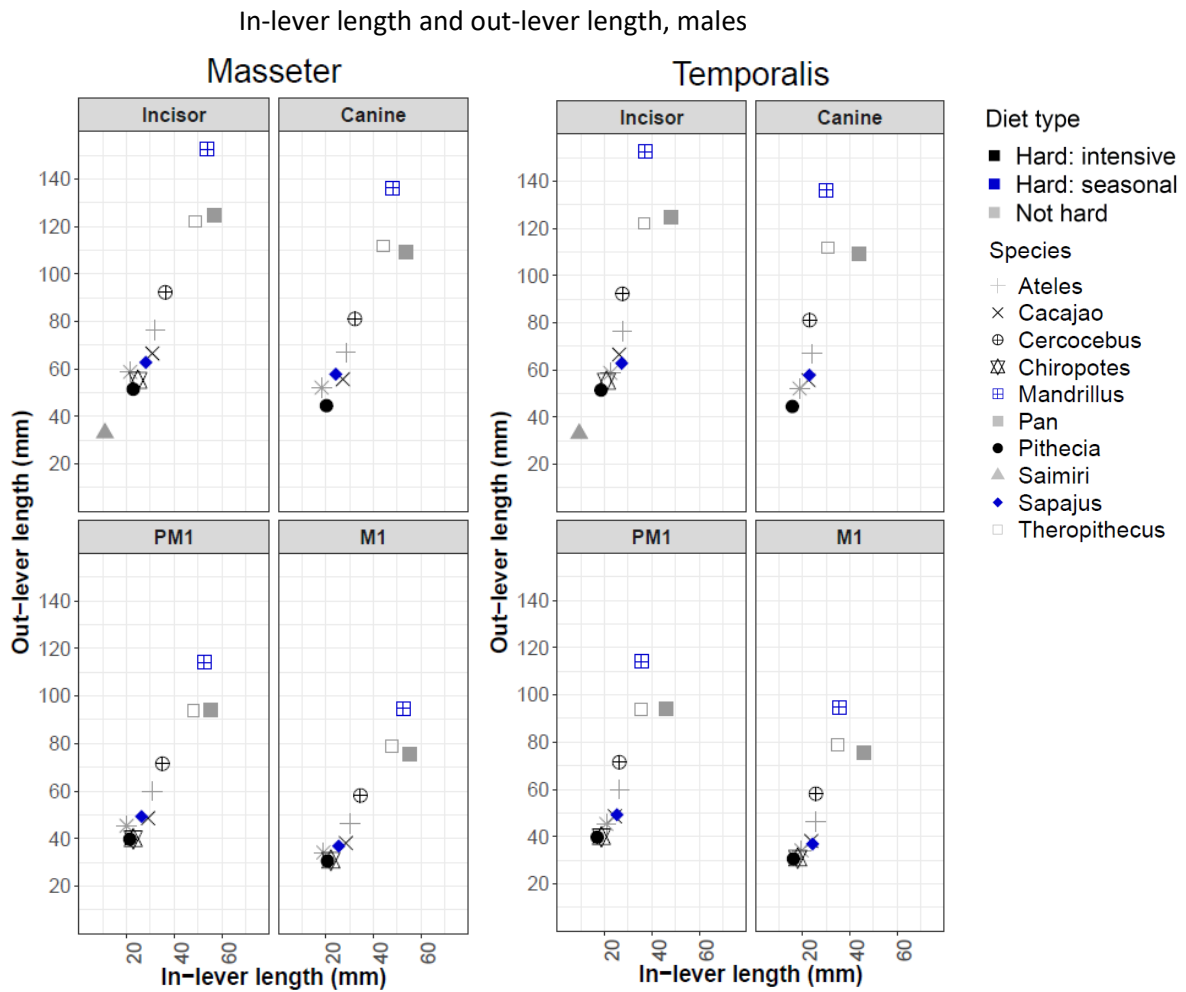
**Figure 3.18 In- vs out-lever lengths for female primates on the masseter and temporalis for bites at 20mm linear gape on all teeth. Species are noted by symbol type and dietary category by colour.**

## 3.4.3 Bony gape correlates: Anteroposterior glenoid length, condyle height above occlusal plane

An anteroposteriorly longer glenoid and higher condyle above the occlusal plane were predicted to facilitate wide gape. Results for the unscaled anteroposterior glenoid length in both sexes (Table 3.5) find the highest value in *Pan*, followed by *Mandrillus*. Most seed predators have short glenoids relative to other primates in the sample, but the shortest length is in *Saimiri* in both sexes. Scaled results for glenoid length cluster tightly in both sexes. Results do highlight that relative to body mass *Pan* has the shortest glenoid length of the sample, despite its absolutely long glenoid. In females seed predator *Cercocebus* has the highest relative length, followed by non-seed predator *Ateles*. In males, all of the seed predators, with the exception of *Mandrillus,* (i.e. *Cacajao, Chiropotes, Pithecia, Sapajus,*

*Cercocebus*) cluster tightly, but the highest result after scaling is found in *Theropithecus*. *Theropithecus* stands out prominently from the remaining sample in both sexes.

Condyle height results for females show a relatively broad spread in both raw and scaled values. In both sexes the absolutely highest condyle above the occlusal plane is found in *Pan* and the lowest in *Saimiri*. There is a prominent change after scaling, and the relatively highest condyle position is in *Theropithecus*, while the relatively lowest condyle is in *Mandrillus*. Other seed predators do not have the lowest condyle height in the sample in scaled or unscaled results. However, all seed predators with the exception of *Mandrillus* (*Cacajao, Chiropotes, Pithecia, Sapajus, Cercocebus*) cluster very tightly in the middle of the sample after scaling in females. In males, the platyrrhine seed predators (*Cacajao, Chiropotes, Pithecia, Sapajus*) still group in the middle of the sample, but *Cercocebus* males have a relatively low condyle height.

**Table 3.5 Absolute and relative anteroposterior glenoid length and condyle height in females and males. Absolute values in mm, scaled values scaled by body mass.**

| Species | Diet type | Glenoid length (mm) | Glenoid length scaled | Condyle height (mm) | Condyle height scaled |
|---|---|---|---|---|---|
| Sex: females | | | | | |
| *Cacajao* | Hard: intensive | 8.84 | 0.35 | 13.09 | 0.38 |
| *Chiropotes* | Hard: intensive | 7.93 | -0.31 | 11.37 | -0.61 |
| *Pithecia* | Hard: intensive | 6.60 | -0.56 | 9.34 | 0.45 |
| *Cercocebus* | Hard: intensive | 11.56 | 0.92 | 18.71 | -0.19 |
| *Mandrillus* | Hard: seasonal | 13.67 | 0.41 | 21.01 | -5.38 |
| *Sapajus* | Hard: seasonal | 7.90 | -0.29 | 11.91 | 0.08 |
| *Ateles* | Not hard | 12.25 | 0.58 | 17.07 | -4.76 |
| *Pan* | Not hard | 17.88 | -1.06 | 44.58 | 1.85 |
| *Saimiri* | Not hard | 5.04 | -0.64 | 6.49 | 1.87 |
| *Theropithecus* | Not hard | 13.45 | 0.60 | 31.54 | 6.32 |
| Sex: males | | | | | |
| *Cacajao* | Hard: intensive | 9.67 | 0.69 | 13.71 | 0.58 |
| *Chiropotes* | Hard: intensive | 8.75 | 0.18 | 12.95 | 0.84 |
| *Pithecia* | Hard: intensive | 7.67 | 0.01 | 10.52 | 0.71 |
| *Cercocebus* | Hard: intensive | 12.99 | 0.39 | 19.26 | -2.92 |
| *Mandrillus* | Hard: seasonal | 16.43 | -0.94 | 25.57 | -8.59 |
| *Sapajus* | Hard: seasonal | 9.58 | 0.44 | 15.17 | 1.66 |
| *Ateles* | Not hard | 12.00 | 0.07 | 17.31 | -3.21 |
| *Cebus* | Not hard | 8.62 | -0.25 | 8.66 | -4.21 |

| | | | | | |
|---|---|---|---|---|---|
| *Pan* | Not hard | 18.90 | -0.66 | 43.03 | 3.39 |
| *Saimiri* | Not hard | 4.54 | -1.44 | 7.01 | 1.40 |
| *Theropithecus* | Not hard | 16.41 | 1.52 | 38.24 | 10.33 |

## 3.4.4 Muscle mass: CSA

Absolute values for muscle CSA in females show a broad separation (Table 3.6). Seed predators do not have the highest CSA in females. The female highest value is held by *Pan* with a considerably margin, followed by *Theropithecus* and then *Mandrillus*. In males this is different, and seed predator *Mandrillus* has the highest CSA, followed by *Pan*. In both sexes *Cercocebus* has a middling CSA within the sample. Other seed predators (*Cacajao, Chiropotes, Pithecia, Sapajus*) group with relatively low CSA, although *Cacajao* has the highest CSA of this group in both sexes. *Saimiri* has the lowest CSA of the sample in both sexes.

After scaling, no female seed predators are outliers in terms of their CSA. Instead, *Theropithecus* has the relatively largest CSA. In males *Mandrillus* has the relatively highest CSA after scaling. Notably, after scaling, the values for *Cercocebus* and *Mandrillus* are very similar in females, but male *Cercocebus* has a relatively lower value than *Mandrillus.* Other seed predators (*Cacajao, Chiropotes, Pithecia, Sapajus*) have middling values, with *Cacajao* standing out within this group in both sexes. Results for *Cacajao* are particularly notably in males, as after scaling male *Cacajao* has amongst the highest values of the sample. The same cannot be said for *Pithecia* which in both sexes has one of the lowest values of the sample. The lowest value after scaling is *Ateles* in both sexes. Notably *Pan* also has a relatively small CSA after scaling, in contrast to its absolute values which is especially pronounced in males.

**Table 3.6 Absolute and scaled muscle cross-sectional area (CSA) in females and males, absolute values in cm²,
scaled values scaled by body mass.**

| Species | Diet type | Muscle CSA (cm²) | Muscle CSA scaled |
|---|---|---|---|
| Sex: females | | | |
| *Cacajao* | Hard: intensive | 6.86 | 0.20 |
| *Chiropotes* | Hard: intensive | 5.03 | -1.21 |
| *Pithecia* | Hard: intensive | 4.65 | 0.12 |
| *Cercocebus* | Hard: intensive | 10.88 | 0.78 |
| *Mandrillus* | Hard: seasonal | 14.95 | 0.67 |
| *Sapajus* | Hard: seasonal | 6.15 | -0.01 |
| *Ateles* | Not hard | 8.42 | -3.32 |
| *Pan* | Not hard | 22.43 | -0.95 |
| *Saimiri* | Not hard | 2.25 | 0.10 |
| *Theropithecus* | Not hard | 17.24 | 3.62 |
| Sex: males | | | |
| *Cacajao* | Hard: intensive | 10.91 | 2.22 |
| *Chiropotes* | Hard: intensive | 5.24 | -2.41 |
| *Pithecia* | Hard: intensive | 6.07 | 0.76 |
| *Cercocebus* | Hard: intensive | 16.62 | -1.29 |
| *Mandrillus* | Hard: seasonal | 36.71 | 6.60 |
| *Sapajus* | Hard: seasonal | 10.85 | 1.77 |
| *Ateles* | Not hard | 10.20 | -6.02 |
| *Cebus* | Not hard | 6.47 | -1.96 |
| *Pan* | Not hard | 30.59 | -5.10 |
| *Saimiri* | Not hard | 2.33 | 1.29 |
| *Theropithecus* | Not hard | 27.87 | 4.12 |

## 3.4.5 Bite force estimates

As with MA, bite force was estimated at a series of increasing linear gape heights (occlusion
– 40mm linear gape height) simulating jaw opening, halting jaw rotation at maximum gape
rotation (40 degrees). In consequence, not all primates attained high linear gape heights:
the ultimate value shown for each specimen is the highest linear gape attained at 40
degrees jaw rotation.

Estimated bite forces in both females and males across the sample shows the highest
estimated bite force to be at occlusion for all measured teeth (Fig. 3.19; Appendix 6, Tables

6.10 and 6.11). In both sexes no seed predator has the highest estimated bite force. Estimated bite force varies by sex and is higher in males relative to females across all species.

In females, the highest bite force with a considerable margin is estimated for *Pan* (ranging from 470N on M1 to 294N on the incisor, at occlusion). Although the lowest bite force of the sample is estimated for *Saimiri* (34N on M1 – 23N on incisor, at occlusion), the majority of the seed predators are estimated to have relatively low bite force within this sample. Of the seed predators, the highest bite force is estimated for *Mandrillus* (22N on the M1 - 145N on the incisor, at occlusion), notably this is very closely matched by *Cercocebus* (209N on the M1 -130N on the incisor, at occlusion).

Males follow a similar pattern, although across the sample the bite force is estimated to be higher. *Pan* is estimated to have the highest bite force (653N on the M1 – 401N on the incisor, at occlusion), and *Saimiri* the lowest (39N on the M1 – 25N on the incisor, at occlusion). As such, seed predators again are not predicted to have the highest bite force. One notable change in trend in males as compared to females is that male *Mandrillus* much more closely approaches *Pan* in its estimated bite force (537N on the M1 – 339N on the incisor, at occlusion), and that unlike in females this is much higher than estimates for *Cercocebus* (283N on the M1 – 182N on the incisor, at occlusion). Another difference to females is the improved performance of *Sapajus,* which closely matches *Cacajao* on all positions and gape heights.
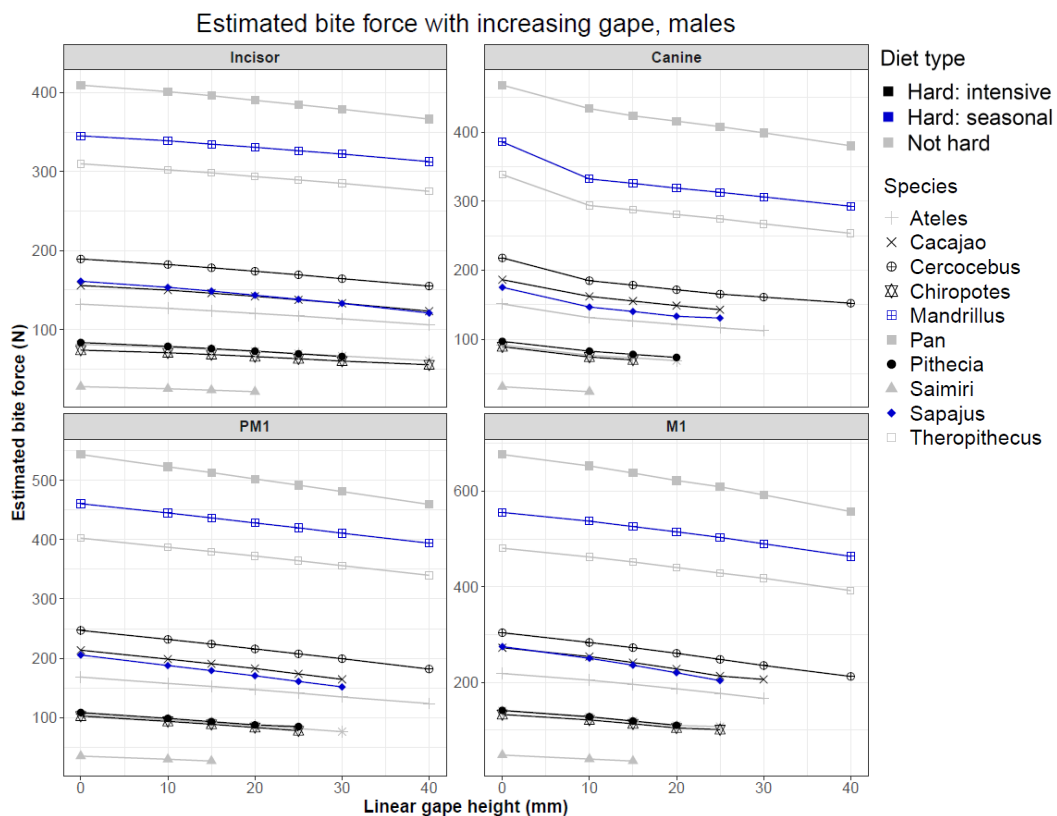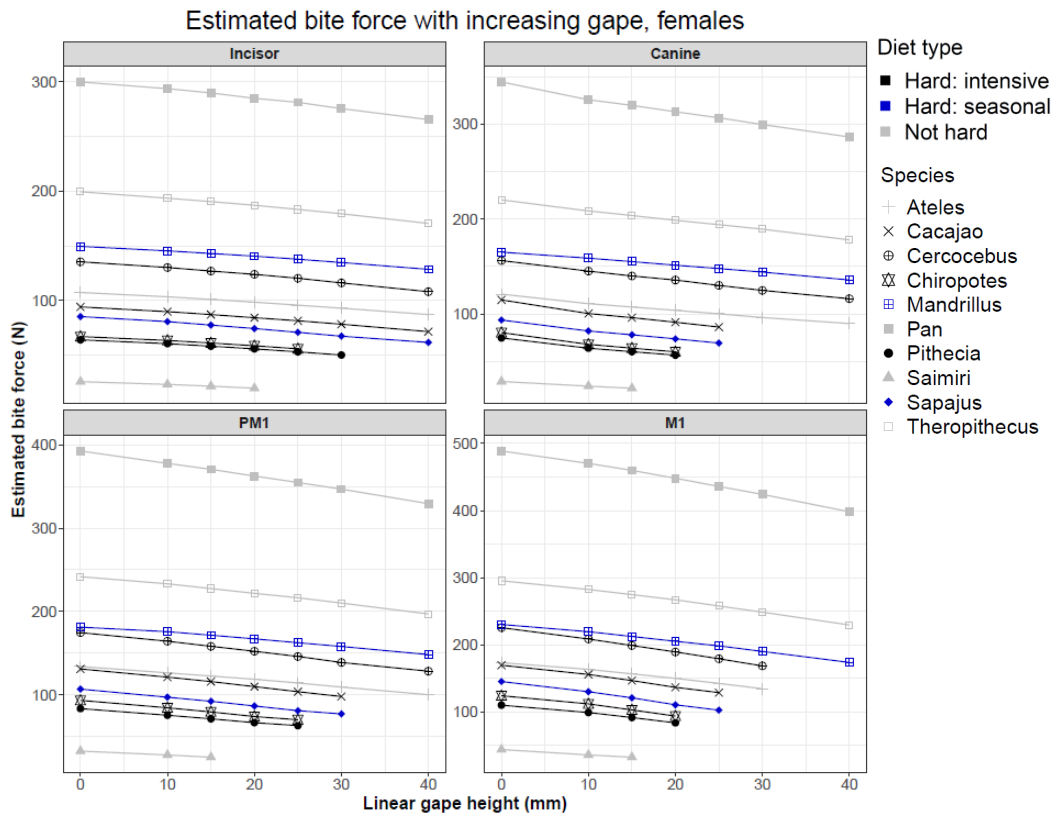
**Figure** 3.19 **Bite force estimates along the dental row for females (top) and males (below). Showing bite force at increasingly wide linear gape heights (mm) from occlusion (0 mm) through to a maximum of 40 mm. Species are noted by symbol type and dietary category by colour.**

## 3.5 Discussion

The aim of this study was to determine if primate seed predators have advantageous masticatory morphologies for producing high bite forces at wide gapes, relative to other primate species with less stress-resistant diets. A 3D mathematical model of the primate masticatory apparatus was designed (objective 1) and used to collect mechanically relevant parameters (objective 2) in order to address objectives 3-5. It was hypothesised that primate seed predators (males and females) will have features which enable a high bite force at a large gape. As it was predicted that multiple morphologies could be advantageous for such a diet no one suite of features was expected. It was also hypothesised that females and males within the same species will differ in the features enabling them to achieve a high bite force at a large gape. The results will be discussed within the context of relevant project objective by discussion male results first (Objectives 3 and 4) before considering both considering both sexes (Objective 5).

### 3.5.1 Objective 3: Compare the results of mechanically relevant parameter measurements in seeds predators to non-seed specialist primate species to ascertain if seed predators are indeed mechanically exceptional.

Seed predators have exceptionally high values for some, but not all parameters measured relative to primates with non-seed diets. Of the seed predators, *Cacajao* has exceptionally high results on a number of measurements (MA and scaled muscle CSA and linear gape). *Sapajus* has some very high MA results (anterior dentition for the temporalis), and both *Chiropotes* and *Pithecia* have high MA on some teeth for multiple gape positions. However, these seed predators share low unscaled linear gape height, high estimated muscle stretch, and low unscaled muscle CSA within the sample. In contrast, *Mandrillus* has very large muscle CSA and linear gape, and low estimated muscle stretch. Measurements on the majority of parameters for *Cercocebus* are middling, or in the case of MA relatively low. With the exception of *Mandrillus,* no seed predators are estimated to have high bite force within the sample. As such, not all seed predators had high values for the measured parameters. High values were also not necessarily exclusive to non-seed specialists.

These results highlight a consistent relationship which transcends diet. There is a prominent split in the results which can be linked to phylogeny and body mass. The larger-bodied

African primates in the sample (*Cercocebus, Mandrillus, Theropithecus,* and *Pan*) collectively have the highest CSA values, highest bite force estimates, largest linear gape, and lowest muscle stretch in the sample, and with the exception of *Pan* these primates also have the lowest MA values of the sample. These results are not surprising given the scaling relationships between body mass and facial shape (Ravosa, 1990; Singleton, 2002; Frost et al., 2003; Hylander, 2013). Across primate species there are different scaling relationships for the masses of the jaw adductor muscles (Anton, 1999; Anapol et al., 2008; Taylor and Vinyard, 2013; Terhune, Hylander, et al., 2015), but overall body mass increases result in increased muscle CSA (O'Connor et al., 2005; Anderson et al., 2008; Santana et al., 2012; Toro-Ibacache et al., 2016).

Papionins are known for prognathism, which is especially extreme in *Mandrillus* in association with the tremendous canine height in this species (Singleton, 2002; Leigh et al., 2005; Hylander, 2013). Past work has identified positive allometry between facial length and body size in papionins (Ravosa, 1990; Singleton, 2002; Frost et al., 2003; Hylander, 2013). This present study highlights that the low MA caused by this long out-lever is paired with similarly large muscle mass and wide gape in some primates which feed on seeds (*Mandrillus*) and those with very different, non-seed diets (*Theropithecus*). Notably gape height and muscle CSA, both absolutely and relatively, are greater in graminivorous *Theropithecus* than in seed predator *Cercocebus*, while muscle stretch is lower. *Cercocebus* also has relatively low MA, with nearly identical values to *Theropithecus* in the majority of measurements. Both the hardness of the *Sacoglottis* eaten by *Cercocebus* and the high proportion of their diet made up by this seed (McGraw et al., 2011; W.S. McGraw et al., 2014; Geissler et al., 2020) means this is surprising. However, recent work has found that *Cercocebus* does not have large PCSA or MA relative to macaques or *Papio anubis* (Taylor et al., 2018). Past work used zoo specimens (Taylor et al., 2018), which was thought to potentially impact results. It would appear that the wild-shot specimens of *Cercocebus* used in this study follow a similar pattern, and also does not meet predictions for intensive seed predation on other variables not previously measured.

In terms of exceptional performance on a range of variables *Pan* stands out despite not being a seed predator. *Pan* outperformed *Cacajao* for MA on high linear gape on some bite points and gape positions (Fig. 3.14). *Pan* has a considerably longer out-lever than *Cacajao*

(e.g. 125mm in *Pan* and 67mm in *Cacajao* for out-lever on incisor in males), and is therefore also capable of a higher linear gape at a much lower degree of rotation – although scaling highlights that gape in *Pan* is not high relative to body mass. It is interesting to note that the out-lever length in *Pan* is in fact relatively short by comparison with more prognathic large-bodied primates such as *Mandrillus* (152mm out-lever on incisor in males). This is key to facilitating the high MA in *Pan,* but also the fact that *Pan* has low gape relative to body mass. As an overall frugivore with some challenging objects in its diet (Boesch and Boesch, 1982; Sugiyama, 1987; Mcgrew et al., 1988), *Pan* was not predicted to fare especially well in terms of mechanical parameters relative to seed predators. *Pan* is generally thought to use tools when consuming seeds (Boesch and Boesch, 1982; Yamakoshi, 1998; Humle and Matsuzawa, 2004; Humle, 2011). It has previously been noted that *Pan* has high MA given its diet relative to other apes (Taylor, 2002), this study finds that *Pan* also has high MA relative to a broad sample of primates and at large gapes. *Pan* is estimated to have a very large bite force, achieved due to the combination of high MA and large muscle CSA relative to a broad primate sample. By having large body size *Pan* is also able to maintain a wide linear gape despite also having excellent MA.

Although some non-seed predators have exceptional performance across multiple variables, this was not the case in all comparisons. Notably *Ateles*, a primate with a strongly frugivorous diet (Dew, 2005; Russo et al., 2005), and *Saimiri,* a primate which fluctuates seasonally between insectivory and frugivory (Lima and Ferrari, 2003), have low performance on a range of values relative to seed predators. *Ateles* has amongst the lowest gape heights after scaling, average to low MA, high muscle stretch despite relatively large body mass, and very low CSA after scaling. This also translates to a middling bite force, and notably in males some seed predators, including *Cacajao* and *Sapajus*, have a higher estimated bite force than *Ateles,* despite having approximately one-third the body mass of *Ateles* (Figs. 3.19 – 3.20, Table 2.1). MA in *Saimiri* is especially poor at high linear gape, but CSA and linear gape height are average to low in this small-bodied primate scaling is applied. As such, although not all seed predators have exceptional performance across all variables, some comparison species highlight elevated measurements in seed predators.

The effect of translation at maximum gape in *Saimiri* does highlight interesting biomechanical relationships. Muscle stretch on the masseter was greatly reduced following

translation (Figs. 3.18 – 3.19) in all species, matching the predictions of past studies (Herring and Herring, 1974; Carlson, 1977). The stretch on the temporalis was less affected. However, even smaller-bodied seed predators were not most affected by translation. Instead, translation most strongly affected *Saimiri* and *Cebus* in reducing their muscle stretch. These species had an especially high degree of stretch before translation was applied, suggesting that translation may reduce variability in stretch between species. The effect of phylogeny is again very visible, as South American primates as a group experienced a greater reduction in stretch due to anterior translation than African primates. However, the lack of advantage in the form of overall reduced muscle stretch in platyrrhine large gape feeders leaves questions open which only studies of internal muscle architecture can answer.

An especially clear example of contrasting performance in seed predators and non-seed predators can be seen in *Sapajus* and *Cebus*. *Sapajus* feeds on a diet with a greater degree of toughness than *Cebus* and is known to seasonally crush hard palm seeds between its posterior dentition, while *Cebus* can only access structurally weakened seeds (Terborgh, 1984). *Sapajus* has very high MA, to an exceptional degree on the incisor when measured for the temporalis (Fig. 3.14). This is in keeping with past research which found *Sapajus* to have anteriorly positioned masticatory muscles for long in-lever lengths, and to have higher MA than gracile capuchins including *Cebus olivaceus* (Wright, 2005). *Sapajus* has also been found to have large muscle PCSA with fibre architecture suggesting internal muscle adaptations for wide gape (Taylor and Vinyard, 2004). Indeed, bite force estimates here match these past results, and suggest that *Sapajus* has considerably higher bite force than *Cebus* (Fig. 3.20). While *Sapajus* did not produce exceptionally wide gape at maximum rotation within the sample, and has relatively high muscle stretch, past work suggests that *Sapajus* has other adaptations to facilitate these behaviours which could not be measured in this study (Taylor and Vinyard, 2004). Notably this study highlights differences between these two capuchin species, in keeping with the results of Chapter 2 which found *Sapajus* to be convergent with pitheciine seed predators (*Cacajao, Chiropotes,* and *Pithecia*), in contrast to *Cebus* (see Chapter 2, Fig. 2.16 section 2.4.1.1). Results here show that *Sapajus* has higher MA, higher absolute and scaled linear gape and muscle CSA, and lower muscle stretch than *Cebus,* matched by estimates of higher bite force at higher gapes than *Cebus.*

While many measurements taken show some relationships to challenging diets, bony measures associated with gape do not give a clear picture for most of the sample. Glenoid length predictions were not met, with no clear trend between absolute or relative glenoid lengths and gape behaviours. However, although past studies have suggested this could be a possible adaptation in some species, clear links between glenoid length and gape have not been established in all platyrrhine primates (Terhune, 2011). Condyle height has been measured more frequently, and low condyle height was predicted for seed predators because of their association with wide gape in some species, notably *Callithrix* (Vinyard et al., 2003) and in *Mandrillus* relative to graminivorous *Theropithecus* (Ravosa, 1990; Ravosa et al., 2000). A lower condyle height is predicted to reduce stretch at each degree of rotation and affects the relative positions of the upper and lower dental row (Vinyard et al., 2003). *Mandrillus* in both sexes does indeed have exceptionally low condyle height after scaling is applied, conforming to the low condyle prediction (Fig. 3.20). This is in direct opposition to *Theropithecus* with its exceptionally high condyle in both sexes. Such a high condyle may aid this species in intensively feeding on grasses, with previous studies on folivorous diets with a lot of small chewing motions having been associated with high condyle height in other primate species (Anapol and Lee, 1994). However, not all primates can be clearly grouped by diet and condyle height, as highly frugivorous female *Ateles* also fell out with very low condyle height in females, and other seed predators grouped with middling condyle height. There have been recent findings which question the low condyle – gape relationship in primates (Fricano and Perry, 2018). There are multiple possible explanations for this. Tree-gouging callitrichids may be unusual in their morphology, and the need to retain specific dental alignment via low condyle height may be essential for exudate access (Vinyard et al., 2003; Fricano and Perry, 2018). The different dentition and varying feeding behaviours of seed predator primates may not face the same constraint. It has also been predicted that extremely low condyle height may reduce the effectiveness of the masseter and medial-pterygoid complex (Osborn, 1987). As such, it is possible that the middling condyle height seen in seed predators in this study may provide a compromise between these different constraints.

Taken together, some but not all seed predators display adaptations to increase bite force, particularly relative to body mass. However, with the exception of *Mandrillus* no seed

predators are estimated to have exceptionally high bite force within the comparative sample. These observations partially meet the predictions of H1, although not all species meet any predictions. The sources of these variations between seed predators will now be examined more closely (Objective 4).

## 3.5.2 Objective 4: Compare the results of the mechanically relevant parameter measurements within seed predators to ascertain if performance is equivalent and if seed predators have the same anatomical configuration.

As observed above, performance is not equivalent between different seed predators, nor do seed predators have the same anatomical configuration. Within the pitheciines (*Cacajao, Chiropotes, Pithecia*) the highest MA was consistently seen in *Cacajao* for all teeth and all gape positions. MA is similar in *Chiropotes* and *Pithecia* for the masseter, but higher for the temporalis in *Chiropotes. Cacajao* also has the highest linear gape of this group, both absolutely and relative to body mass. *Pithecia* has a smaller gape before scaling, but a higher gape after scaling than *Chiropotes*. A similar pattern is clear in muscle CSA, with absolutely and relatively highest measurements in *Cacajao*, but *Pithecia* has both absolutely and relatively larger muscle CSA than *Chiropotes* despite smaller body mass. These patterns are matched by bite force estimations in these three species. *Cacajao* is estimated to have the highest bite force within this group by a considerable margin, with lower but similar values observed in *Pithecia* and *Chiropotes*.

Although all three species intensively feed on large, hard seeds it has been observed that there are differences in their diets (Kinzey, 1992; Norconk and Veres, 2011). *Chiropotes* feeds on harder and larger fruits than *Pithecia,* and although the hard foods eaten by *Cacajao* have not been compared to the other pitheciines directly they are thought to be the hardest of this group due to the observed morphology of *Cacajao* (Kinzey, 1992; Bowler and Bodmer, 2011; Barnett et al., 2015, 2016; Ledogar et al., 2018; Püschel et al., 2018). This relationship has recently been questioned, finding minimal differences in bone strain during biting and similar estimated absolute bite force between *Chiropotes* and *Cacajao*, although estimations for *Cacajao* had higher results than *Chiropotes* (Ledogar et al., 2018). However, the MA and large jaw adductor CSA observed in this study is broadly in line with an adaptive morphocline for these species, which proposes that *Cacajao* is the most extreme pitheciine seed predator in terms of its adaptations for high bite force (Kinzey, 1992). Patterns

between *Chiropotes* and *Pithecia* are more surprising given their previously observed dietary differences (Norconk and Veres, 2011). It is also interesting that *Pithecia*, the smallest of the three pitheciines, has a higher scaled gape height than *Chiropotes.* This may be a consequence of a slight increase in prognathism in this primate, allowing it to maintain high gape relative to its body size (see Ch. 2, 2.5.2). Slightly elevated MA may compensate for lower CSA in *Chiropotes*, indeed *Chiropotes* and *Pithecia* are estimated to have very similar bite force. It is also possible that further measurements are needed for *Chiropotes,* as past work has noted the high MA on the medial-pterygoid in this primate which may provide some compensation (Püschel et al., 2018). This same past work also did not find *Cacajao* to have exceptional performance (Püschel et al., 2018), in direct contrast to this study. Previous studies used only two specimens of each species examined, and one specimen for each species was of unknown sex (Püschel et al., 2018). This study finds differences between sexes in pitheciines in a range of measurements (see below, 3.5.3), which paired with a larger sample size may explain the difference in results. Overall, in this study *Cacajao* has exceptional performance but varies on several parameters compared with other pitheciines.

*Sapajus* is a seasonal seed predator which feeds on a range of mechanically foods, including hard palm seeds and a range of extremely tough foods (Izawa and Mizuno, 1977; Terborgh, 1984; Wright, 2005). Chapter 2 found a very significant degree of convergence between *Sapajus* and the pitheciine seed predators (see Ch. 2, 2.4.2). Results here show that there are a range of similarities in masticatory morphology for high MA and gape in *Sapajus* and the pitheciines, especially in *Cacajao*. Absolute linear gape in these two primates is near identical, and MA values are also very similar, although *Sapajus* has elevated MA on the incisor for the temporalis while *Cacajao* has elevated MA on other measurements. *Sapajus* and *Cacajao* also perform very similarly for muscle stretch and muscle CSA. Bite force estimates consider many of these similarities as one total output, and indeed find that *Sapajus* and *Cacajao* have similar estimates, with slightly higher bite force predicted for *Cacajao.* Numerous past studies have suggested that *Sapajus* displays adaptations for hard object feeding (e.g. Lambert et al., 2004; Wieczkowski, 2009; Daegling et al., 2011; McGraw et al., 2011). Past work has found high values in *Sapajus* for MA without gape (Wright, 2005) and for muscle PCSA (Taylor and Vinyard, 2013). Additional measurements in this study, taking gape into account, show that *Sapajus* has adaptations which facilitate high bite force

relative to a broad primate sample, and that *Sapajus* and intensive seed predator *Cacajao* share numerous masticatory features.

The morphology observed in seasonal seed predator *Mandrillus* is very different to that of the platyrrhine seed predators (pitheciines and *Sapajus*). As highlighted above (3.5.1) this very large-bodied papionin is extremely prognathic, therefore having an exceptionally long out-lever and the lowest MA of the sample. However, *Mandrillus* has absolutely very wide linear gape and very large CSA, both absolutely and scaled. Little is known about the feeding behaviours of *Mandrillus,* although crushed seeds found in mandrill faeces show that seed predation is a seasonally intense behaviour (Hoshino, 1985; Lahm, 1986; Hongo et al., 2017). Despite low MA, the large body size and associated very large CSA result in estimations of very high bite force in *Mandrillus*. It is also important to note that this primate engages in very wide gape display and aggression behaviours (Ravosa, 1990; Leigh et al., 2005; Hylander, 2013). As such, there are certainly numerous factors strongly influencing mandrill morphology.

In contrast to *Mandrillus* is intensive seed predator *Cercocebus.* As reviewed (3.1.2), the majority component of the entire annual diet of *Cercocebus* consists of the exceptionally hard *Sacoglottis* seeds (Daegling et al., 2011; McGraw et al., 2011; McGraw et al., 2014; Geissler et al., 2020). Overall results for *Cercocebus* do not suggest exceptional performance on any of the measured parameters. There are, however, some additional aspects of the performance in *Cercocebus* to consider. Past work has suggested that *Cercocebus* is able to process its challenging diet by virtue of having a body size which results in adequate muscle mass to produce high bite force (Taylor et al., 2018). *Cercocebus* does have low MA within the sample but has high MA relative to *Mandrillus* due to a considerably less prognathic morphology (Singleton, 2002, 2005). Past GMM work has predicted this morphology and this study quantifies these predictions (Singleton, 2002, 2005). Furthermore, while *Cercocebus* has low linear gape relative to *Mandrillus, Theropithecus,* and *Pan,* it has absolutely wider gape than the smaller-bodied platyrrhine seed predators. Similarly, *Cercocebus* has low stretch compared with the platyrrhine seed predators, and larger muscle CSA (absolutely). As such, while the performance of *Cercocebus* is not highest in the sample on any single parameter, it remains middling across most measurements. Other seed predators have considerably lower performance on either MA (*Mandrillus*) or CSA and

slightly lower estimated bite force (platyrrhines), although the estimated bite force for *Cercocebus* is relatively low within the wider sample. Despite this, the combination of features observed in *Cercocebus*, while not exceptional, clearly is adequate permits *Cercocebus* to feed on hard seeds.

### 3.5.3 Objective 5. Evaluate any differences between the sexes within the seed predator groups.

Examining the results from both sexes shows that, in most cases, females follow similar trends to males within species. There are, however, some differences in masticatory morphology between the sexes. These results match predictions (H2), as the sexes differ but both show some adaptations for high bite force at wide gape. Notably, absolute values in males are higher for most measurements and most species, especially for muscle CSA and estimated bite force, regardless of diet.

In platyrrhine seed predators (*Cacajao, Chiropotes, Pithecia, Sapajus*) females have smaller absolute gape height, a greater increase in muscle length, and a lower muscle CSA. In the pitheciines the female and male MA values are extremely similar. All male platyrrhines are estimated to have a higher bite force than females. A particularly strong difference in sexes is in the capuchins, where male *Sapajus* has considerably higher MA for the temporalis than female *Sapajus*. *Sapajus apella* is more sexually dimorphic in cranial form than other capuchin species (Masterson, 1997), but past studies examining MA in this species have not separated results by sex (Wright, 2005). This dimorphism includes multiple biomechanically relevant variables, including increased bizygomatic breadth in males which is predicted to facilitate relatively greater muscle mass (Masterson, 1997). Sex-based differences in *Sapajus apella* diet have been suggested (Janson, 1990; Gunst et al., 2007, 2010), but are not well understood, and the material properties of these dietary differences are yet to be quantified. Sex-based differences in diet are also possible in the pitheciines, although this has only been the subject of one past study (Bowler and Bodmer, 2011), which found male *Cacajao* to have a more extreme diet than female *Cacajao* in terms of seed size and hardness. As such, the likely decrease in bite force in female pitheciines relative to males is due to reduced muscle CSA while retaining similar MA.

A different pattern is seen between sexes in *Cercocebus*. Although female *Cercocebus* have an absolutely smaller CSA than male *Cercocebus*, females have one of the largest CSA sizes relative to body mass. This is not the case in male *Cercocebus,* which has a relatively low CSA after scaling (Fig. 3.22). Additionally, *Cercocebus* females have higher MA than males (Figs. 3.13 – 3.14), and for the masseter have relatively high MA within the entire sample. Measurements of lever lengths highlight that male *Cercocebus* has a relatively long out-lever, while female *Cercocebus* does not stand out in terms of out-lever length (Fig. 3.15). This long out-lever is due to a higher degree of prognathism in males and is the cause of low MA in male *Cercocebus*, while females are less prognathic. While the increased MA and relatively large CSA in female *Cercocebus* results in a very similar estimated bite force to female *Mandrillus,* relatively high within the female sample, this is still considerably lower than the estimated bite force for males. Male *Cercocebus* do have a slightly increased quantity of hard *Sacoglottis* in their diet relative to females (McGraw et al., 2011; Geissler et al., 2020). Some studies have also suggested females may process foods differently, perhaps softening seeds in a cheek pouch (McGraw et al., 2011). Other primate species (*Macaca fuscata*) also vary in their hard seed processing by sex (Tamura, 2020), and such positional behaviours may facilitate hard diets in species with different masticatory capabilities.

It may be expected, based on the performance in *Cercocebus* females as compared with *Cercocebus* males, that *Mandrillus* follows a similar pattern between the sexes. However, this is not the case. The two sexes have very similar MA for the temporalis, and within each sex these are the lowest MA values of the sample. Female *Mandrillus* has slightly higher MA for the masseter than male *Mandrillus*, but the differences between sexes are very small. Given the previously detailed high degree of prognathism and very large muscle CSA in *Mandrillus,* as well as the differences between sexes in *Cercocebus* MA, this is a surprising result. The impact on bite force is that female *Mandrillus* is predicted to have exceptionally lower bite force capability than male *Mandrillus*. As discussed (Ch. 2, 2.5.3) although little is known about the feeding behaviours of mandrills, it is possible that males feed on a very different diet to females, and that females consume a much higher proportion of soft fruits than males (Lahm, 1986; Stammbach, 1986). It is noteworthy that female *Mandrillus* muscle CSA is also still amongst the largest of the female sample, both scaled and unscaled, and although the female bite force is estimated to be considerably lower than the male, it is still

amongst the highest of the female sample. Both a less mechanically challenging diet and the large muscle CSA due to large body size may explain the pattern in female *Mandrillus*.

## 3.5.4 Bite force and functional equivalence

Results indicate that seed predators are not functionally equivalent, instead vary across a range of performance-indicating variables relating to bite force, and in terms of estimated bite force. It is evident that both body size and phylogeny play key roles here. Results show that large-bodied African seed predator primates (*Mandrillus,* and to a certain degree, *Cercocebus*) have large muscle CSA and meet some predictions for wide gape (low stretch, low condyle height in *Mandrillus*). While some African primates have relatively high MA on the masseter (*Cercocebus*, especially females), all have low MA on the temporalis. In contrast, smaller-bodied South American seed predator primates (*Cacajao, Chiropotes, Pithecia, Sapajus*) primarily have high MA, although notably male *Cacajao* also has high CSA for its body size. There may be a degree of functional equivalence between some of these seed predators, with high MA compensating for absolutely smaller muscle mass in smaller-bodied primates, and with large muscle mass compensating for low MA in larger primates, notably *Mandrillus*. A similar pattern is seen between sexes, especially noteworthy in *Cercocebus* as females and males show a sharp contrast between high MA in females and large muscle CSA in males.

However, bite force estimates emphasise the importance of body size. The results of this study do not suggest that seed predators have functional equivalence in terms of their bite force. Similar examples can be seen in other animals, in example past studies have found a durophagous shark (*Heterodontus francisci*) to have high MA and overall a high bite force relative to its body size (Huber et al., 2005). These adaptations are linked with the durophagous diet of *H. francisci*, but although this is an extreme diet it is noted that there are other animals with absolutely higher bite force due to the effects of body size and scaling on bite force (Huber et al., 2005). Such a relationship can be observed here, as the very large-bodied mandrill has large masticatory muscle mass and can therefore generate a higher bite force than a smaller primate such as *Cacajao*, despite the impressively high MA and large muscle CSA relative to body mass observed in *Cacajao*. Similarly, despite the adaptations observed in numerous seed predators, body size and phylogeny across primates

can result in primates with less mechanically challenging diets having absolutely higher bite forces than seed predators. *Pan* is an example of this, being of large body size and having high MA as a result of low prognathism, and with an exceptionally high estimated bite force in both sexes. The adaptations observed in many of the primate seed predators in this study may produce a high bite force relative to body size, producing ample bite force to facilitate access to hard seeds. However, many larger-bodied primates possess absolutely higher bite force, regardless of diet.

## 3.5.5 Model unknowns

The relationship between MA, gape, and bite force was a key consideration in this study. MA was found to decrease with jaw opening, and the highest bite force across the sample was found to be at occlusion, followed by a very gradual decrease in bite force as jaw opening increased. Occlusion is not the optimal operating length for the muscles of mastication, nor is maximum gape (Santana, 2015; and see review in 1.6.4). As length-tension curves for the muscles of mastication have only been produced for a small number of primates (i.e. Eng et al., 2009) it is not currently possible to know the gape at which the primates in this sample would produce their maximum biting force. It can be expected that the trajectory of true bite force follows a different path to the estimates made in this study, increasing up to the point of optimal muscle stretch, then decreasing sharply. Further research on muscle stretch in primates is key to better understanding the relationship between gape and bite force. By incorporating models of MA at different gape heights such as the present study with species-specific muscle stretch, a more accurate prediction of the gape at which primates have their highest bite force capability can be made.

In all cases, this modelling work can also continue to work further towards realism. In this study, to test predictions and measure masticatory parameters on numerous primate species it was necessary to make simplifications to the model which may have affected results. For measuring MA decisions made in selecting in-lever and out-lever measurements affect results. For the in-lever it is important to note that this study only took the most anterior muscle line of action into account. Muscle fibre length can vary in different muscle portions (Terhune et al., 2015; Taylor et al., 2018, 2019), and while it is common practice to measure and model MA using one muscle line of action (e.g. O'Connor et al., 2005; Godinho

et al., 2018), this does not represent the full function of the muscle. In humans the MA of posterior temporalis is considerably lower than that of anterior temporalis (Throckmorton and Dean, 1994). It would be interesting to assess if a similar pattern is seen in all primates, especially given the diversity of primate cranial morphology. Posterior and middle temporalis are also less affected by muscle stretch than anterior temporalis (Eng et al., 2009), and by only estimating muscle length increase at anterior temporalis the stretch prediction for this muscle only quantifies the most extreme value.

Decisions which could affect results also had to be made when measuring the out-lever lengths. In this study the out-lever was measured as the perpendicular distance from the fulcrum to a vector which represents the vertical component of the bite vector (Fig. 3.8, van Eijden, 1991; O'Connor et al., 2005; Dickinson et al., 2018; Godinho et al., 2018). However, this is not the only approach used to measure the out-lever length in primates. Another option is to measure the distance from the fulcrum to the tooth without using a horizontal vector (i.e. Taylor et al., 2018). Such an approach will capture information relating to varying dental heights and orientations between specimens, which may affect MA but is not represented by the measurements used in this study. Further work would benefit from a comparison of out-lever measurement methods to consider the potential impact of these different approaches.

Related to the choices made for the measurements used to calculate MA, future work could take additional steps to approach reality. Past work has suggested that MA calculated using lever arm lengths measured using similar approaches to those in this study overestimates MA in fish (Westneat, 2003). By using a model which measures effective MA for multiple muscles, incorporating the transmission and motion of force in the estimation of MA, estimations can come closer to reality (Westneat, 2003). Such an approach has yet to be applied to the primate masticatory system. It would be interesting to examine the impact of including these additional variables on primate MA in future work.

Other simplifications are evident in the method used for calculating CSA and bite force. Past studies have shown that 2D methods typically overestimate masseter-pterygoid muscle force and underestimate temporalis, so if temporalis contributes an especially large amount of muscle force to feeding in these primates then estimates may be low (Davis et al., 2010). The measurements used in this study also did not take internal fibre architecture into

account (Taylor and Vinyard, 2013). As discussed above, past studies have shown that the optimal zones in sarcomere operating ranges can vary to a great degree between different primate species, even those that are closely related (Eng et al., 2009), so it is possible that the pitheciine intensive seed predators have internal muscle architecture which is advantageous for maintaining high force at wide gape, as has been observed for *Sapajus apella* (Taylor and Vinyard, 2009). Increased understanding of muscle architecture in primate jaw adductors would increase accuracy in future models. Bite force estimates as used here are also affected by these concerns. The values presented here are very useful as comparative values within the sample, and 2D methods have been shown to produce "reasonable" estimates of bite force in bats (Davis et al., 2010). However, 2D CSA measurements methods are less accurate than PCSA (Davis et al., 2010), and the selection of lever arm measurements may also affect results. While the lever measurements used in this study may more closely measure the true morphology of the specimens in the sample than the 2D measures made using photographs used in past bite force estimation studies (Thomason, 1991; Davis et al., 2010), the impact of combining 2D CSA with 3D levers is unknown, particularly with regard to the simplistic masseter-medial pterygoid muscle mass estimate used in this study. Future work could explore this relationship by comparing fully 2D and 3D bite force estimates, and by using alternative muscle CSA estimates which separate masseter and medial pterygoid. Taken together, and as pointed out in past work examining other mammals (Demes and Creel, 1988; Wroe et al., 2005a; Dumont et al., 2009), estimates of bite force and muscle mass as produced for this study are very useful for comparisons of performance within the sample, but should not be interpreted as true bite force values.

Finally, muscle architecture data is not the only unknown information in the context of primate feeding biomechanics. Positional behaviours likely affect feeding in other primates as well, both in relation to necessary gape for feeding and force to access foods. As discussed (3.1.2), *Chiropotes* feeds on hard-shelled fruits with a breadth of up to 220mm, but is a mid-sized primate (Norconk and Veres, 2011). Such large fruits are larger than the entire crania of *Chiropotes* and *Pithecia* (see Fig. 3.2), and this study predicts a maximum gape height of 34-37mm in *Chiropotes* (Fig. 3.12, Appendix 6 Table A6.1). However, a combination of dental morphology and positional feeding behaviours enable access to

nutritious seeds through the hard pericarp, in combination with high MA even at large gapes (Norconk et al., 2009). This is especially the case in the pitheciines, which are noted for a range of dental adaptations which are predicted to facilitate feeding on large and hard fruits (Kinzey, 1992; Rosenberger, 1992; Bowler and Bodmer, 2011; Norconk and Veres, 2011; Norconk et al., 2013; Barnett et al., 2016). The primate seed predators in this study show a range of adaptations to improve bite force, but this information is incomplete without understanding dentition and other aspects which affect feeding behaviour.

## 3.5.6 Future model applications

Given the challenges in accessing detailed primate muscle architecture data there are many values which may not be known for many years, or may never be obtainable, particularly for endangered species. As such, models based on the available information, such as the one tested in this study, remain necessary. There are additional benefits to developing such a modelling approach. This method is flexible, allowing new specimens or additional measurements to be added. Future research could apply this model to the study of feeding biomechanics in fossil specimens, for which muscle architecture data can never be known. This can improve predictions of fossil diet and feeding ecology, particularly in the context of how biomechanically relevant variables change with gape, a subject which has so far rarely been explored. More theoretical work could also explore the impact of changes in morphology on the feeding biomechanics of an individual specimen. Variables such as mandible length, dental position or TMJ height, which directly relate to feeding biomechanics, can easily be altered in this model. Certain variables, particularly prognathism, vary widely within the sample tested in this study, as explored in Chapter 2. Investigating the impact of changing prognathism on MA, gape, and muscle stretch within the sample would be an interesting exploration of how increasing jaw length relates to changes in masticatory function. A similar approach could also explain the range of variation between sexes, particularly interesting due to the poorly understood sex-based differences in primate diet even amongst primates with extreme diets (see 3.5.3). Finally, the model also has the potential to work with new data, for example using a developmental sample to understand how biomechanically relevant variables change with growth. Sub-adult primates including *Cercocebus atys* and *Sapajus libidinosus* are known to have a different diet to adults (Daegling et al., 2011; Chalk et al, 2016). While changes in dentition (Swan, 2016),

mechanical advantage (Fitton et al., 2015), and food material properties (Chalk et al., 2016) are known to occur during the development of these species, the impact of changes during development on a wide range of biomechanical variables is not fully understood. Developing a model such as the one in this study creates the potential for application to diverse areas of further study.

## 3.5.7 Conclusions

Taken together, the results partially support the prediction that primate seed predators have morphologies which enable high bite force and wide gape. The contrast between African and South American seed predators highlights that increasing muscle size or MA present two avenues for increasing bite force, although the results do not indicate that these two avenues have the same bite force performance. Instead, although some seed predators have exceptionally high MA and large muscle CSA relative to body size, those primates with larger body size are estimated to have ultimately higher bite force. It is also clear that females and males show differences, and while some females show increased adaptations for high bite force, others show a reduction. Past research has suggested that after a certain threshold, adaptations for increasing bite force may not be needed, as body size alone will in most cases guarantee a high bite force due to absolutely larger masticatory muscle mass (Taylor et al., 2018). Smaller-bodied primates with extreme diets, such as the pitheciines, show adaptations for exceptionally high MA in some cases, as well as relatively high CSA after scaling, suggesting that some primate seed predators, most especially *Cacajao*, do show adaptations for their diet. Larger-bodied *Cercocebus* does show adaptations relative so closely related but larger-bodied *Mandrillus* in terms of its MA, although its MA is still low relative to many other primates.

It is possible that seed predators, including *Cercocebus*, employ other strategies such as foraging on weakened seeds to reduce force in feeding on their hard diet. It is also possible seed predators have an advantageous dental morphology in order to cope with dietary challenges. Past studies have found dental form and diet provide more conclusive links than musculoskeletal form and diet (Terhune, Cooke, et al., 2015). The relationship between dental form and force to fracture in hard-shelled seeds will be explored in the next chapter to determine if seed predators have advantageous dentition for the processing of seeds.

# Chapter 4 - The impact of dental form on stress-resistant food breakdown: how to crack a nut

## 4.1 Introduction

Past chapters have demonstrated that primate seed predators show some, but not universal convergence in masticatory form (Ch. 2), and that although some seed predators show adaptations to increase bite force, seed predators are not functionally equivalent in terms of their estimated bite force (Ch. 3). However, these chapters have not considered the part of the masticatory system which directly contacts food: the teeth. Teeth can be seen as tools for breaking down food, and their different shapes may reflect a range of requirements these tools must fulfil (Evans and Sanson, 2003; Lucas, 2004; Anderson and Labarbera, 2008; Anderson, 2009; Crofts and Summers, 2014; Berthaume et al., 2020). Dental morphology varies both between species and within the mouth of an individual, with different functions typically associated with anterior and posterior dentition (as reviewed in Ch. 1, 1.2.3). If teeth are conceived of as the tools required to access and process the diet of an individual then a clear relationship between dental structure and function can be expected: the material properties of foods vary in association with dental form (Lucas, 2004).

Links between dental form and function, measured by correlating diet with dental shape metrics, are often considered more clearly observable than those between cranial form and diet (e.g. Kay, 1975; Ledogar et al., 2013; Terhune et al., 2015; Ungar et al., 2016). Theoretical functional explanations of dental form have been made for a wide range of animals, especially for primates, to some degree of success (e.g. Kay, 1975; Bunn et al., 2011; Winchester et al., 2014; Allen et al., 2015). However, these studies cannot inform directly on how changing dental form relates to fracture mechanics of different food types. Changing the shape of this tool will alter the fracture of the food being eaten, potentially reducing the force required to access certain food items (Lucas, 2004). This could be highly advantageous for species which feed on mechanically challenging foods such as seeds which require a high force to access nutrients through hard external layers (Norconk et al., 2013; Barnett et al., 2016). Testing the force required to access different foods and resulting fracture patterns using real or stylised hypothetical teeth is a practical and macro approach

to directly test and compare dental performance (e.g. Anderson, 2009; Berthaume et al., 2010; Crofts and Summers, 2014; Barnett et al., 2016; Swan, 2016).

The manner in which the shapes of primate teeth relate to the force to fracture and fragmentation behaviour in different food objects is generally not known. Past chapters have highlighted that not all seed predators meet predictions of primate seed predator masticatory form (*Cercocebus atys*). It is possible that the teeth of this primate facilitate access to such a challenging diet by reducing the work required to fracture seeds. By contrast, smaller-bodied platyrrhine primates have high mechanical advantage but relatively small muscle cross-sectional area compared to larger-bodied primates with less challenging diets. The dental form of these primates is highly specialised (Kinzey, 1992) and may facilitate food access at relatively lower force than other primates. This chapter seeks to test the link between these dental forms and their function in seed feeding. Physical testing using the teeth of primate seed predators and comparison species will be used to fracture hard objects in order to quantify seed predator dental function.

## 4.1.1 Dental form and diet in primates

A common approach for understanding the links between dental form and diet is to quantify whole tooth form with a range of measures then link observed shapes with known dietary categories (e.g. Kay, 1975; Bunn et al., 2011; Winchester et al., 2014; Allen et al., 2015; Terhune et al., 2015). The postcanine teeth have been the focus of the majority of these past studies. Postcanine teeth exhibit different numbers of cusps which range from being high and sharp to low and rounded (Constantino et al., 2016). Variation in cusp size and shape has been linked with major dietary categories in primates (Kay, 1975). Unicuspid teeth, such as the incisors and canines of many species, also vary significantly in length, curvature and size (Koenigswald, 2011). However, although some primate species use their anterior teeth for feeding, only few studies have focussed explicitly on anterior tooth form in primates (e.g. Hylander, 1975).

The methods used to quantify whole tooth form include measuring the length of the tooth and occlusal surface area (Kay, 1975), geometric morphometrics (Terhune, Cooke, et al., 2015), and measures such as shearing quotient to quantify molar cutting edges, Dirichlet normal energy to quantify surface curvature, relief index to quantify surface relief, and

orientation patch count to quantify surface complexity (Boyer, 2008; Bunn et al., 2011; Winchester et al., 2014; Allen et al., 2015). Some of these measures have successfully demonstrated links between general primate molar form and the major primate dietary categories of folivory, frugivory, and insectivory (Kay, 1975; Winchester et al., 2014; Terhune, Cooke, et al., 2015). Insectivores show adaptations for puncturing and crushing with relatively large crushing and grinding surfaces, high sharp cusps, and relatively long shearing surfaces, although the height of the shearing crests varies in extremity with the type of insect consumed (Kay, 1975; Winchester et al., 2014; Terhune, Cooke, et al., 2015). Folivores show similarities to insectivores, with long shearing crests and relatively large crushing and grinding surfaces for facilitating the comminution of leaves for digestion (Kay, 1975; Winchester et al., 2014; Terhune, Cooke, et al., 2015). Primates with more frugivorous diets have shorter and lower shearing crests than either folivores or frugivores with low, bulbous cusps, and relatively large crushing basins for processing fruits (Kay, 1975; Norconk et al., 2013; Winchester et al., 2014; Allen et al., 2015; Terhune, Cooke, et al., 2015). Taken together a range of measures have been used to broadly classify the dental form of some primates into shape-diet groups.

These studies are valuable for understanding the correlation between shape and diet. However, very few studies have examined what these shapes mean in terms of function. The effect of altering dental forms on food fracture is generally not known (Anderson and Labarbera, 2008; Anderson, 2009; Berthaume, 2016). This is especially challenging because the whole tooth shape may not directly relate to the contact surface area of the tooth with the food during feeding: especially hard, brittle foods may not touch the entire occlusal surface and instead may be fragmented on specific cusps (Berthaume et al., 2020).

Further issues also relate to categorising primate diets. Broad dietary categories such as 'folivory' may not accurately reflect the material properties of the diet of an individual (Coiner-Collier et al., 2016). This is because the material properties within a dietary category vary, for example, leaves have varying degrees of toughness (Coiner-Collier et al., 2016). Additionally, most primates feed on foods from a range of dietary categories (Coiner-Collier et al., 2016). As such, teeth are unlikely to be optimised for all objects eaten by an individual. Seasonality introduces further variation and some seasons may include a higher proportion of mechanically challenging foods in months when preferable resources are only

sparsely available (Rosenberger, 1992; Marshall and Wrangham, 2007). As such, dental form may not always reflect the most frequently consumed object in the diet. Instead, the most extreme objects and fallback foods may exert the main pressures (Constantino et al., 2009; Terhune, Cooke, et al., 2015). This is one reason why primates which face extreme dietary challenges are considered useful for studying dental function: the exceptional demands faced by these primates may produce strong selective pressure for advantageous dental morphology to aid in the processing of their challenging diet (Rosenberger, 1992; Coiner-Collier et al., 2016).

Another complication in studying dental form is that it is not constant. Both the thickness of dental enamel and the overall dental form change over time due to dental wear throughout the life of an individual, gradually flattening teeth (Ungar, 2004). The relationship between dental wear and dental function is rarely examined. In some primates, wear may be advantageous, altering the occlusal surface to take on a secondary morphology as seen in some ungulates (Luke and Lucas, 1983; Venkataraman et al., 2014). This process reveals enamel crests which increase efficiency in the processing of tough grasses by *Theropithecus gelada* (Luke and Lucas, 1983; Venkataraman et al., 2014). This relationship changes as wear continues during aging as very advanced wear is known to reduce feeding efficiency in *Theropithecus gelada* and multiple strepsirrhine primates (King et al., 2005; Cuozzo and Sauther, 2006; Venkataraman et al., 2014). Past work has drawn these links by observing food particle size in faeces changing alongside dental wear, indicating reduced efficiency associated with changes in dental form (Venkataraman et al., 2014). The present study does not seek to quantify the effects of dental wear within an individual. However, a better understanding of how different dental forms directly affect dental function may contribute to predictions of how function may change with wear.

Two other major variables must also be considered in the context of dental form in primates: body mass and phylogeny. Body mass and posterior tooth size are correlated, with primate dental size typically scaling with negative allometry (Lucas, 2004). Phylogeny also affects dentition, both in terms of the number of teeth present and the shape of those teeth, although the correlations between phylogeny, diet, and morphology are not yet fully understood (Swindler, 2002; Ungar, 2004; Terhune, Cooke, et al., 2015; Berthaume et al., 2020). Some broad dental variation due to phylogeny is clear, as in the difference in tooth

number between catarrhine and platyrrhine primates (Swindler, 2002). Catarrhines have lost an additional premolar (as reviewed in Ch. 1, 1.6.2; Swindler, 2002). The form of individual teeth also varies with phylogeny. Shearing crest length has been found to be greater in African primates than in South American primates independent of diet, complicating predictions of extinct diets and associations of dental form with diet (Ungar, 2004). As of yet no study has investigated if this variation results in a functional difference while feeding, although there is overlap in the types of foods eaten by primates on both continents (Kay, 1975).

## 4.1.2 Fracture mechanics and occlusal morphology

Foods have a range of material properties, which will affect both the force required to access them and the manner of their fracture (see Ch. 1, 1.3.2 for review). Some objects are especially mechanically challenging to feed on: notably, large and hard foods will require high forces to access (Strait, 1997; Lucas, 2004; Lucas et al., 2008). Generating sufficient bite force at high gape is not the only challenge here, as such challenging foods may also present a challenge for tooth integrity. The forces required to feed on very hard foods, such as certain seed types as observed in some primate, may cause cracking of the dental enamel (Lucas et al., 2008; Lawn et al., 2009). The high forces required to access hard foods have led to these foods frequently being described as stress-limited, a term which highlights that the major challenge in accessing these foods is generating enough stress to initiate a crack (Lucas, 2004).

The shape of the tool used to fracture an object will affect how the object fractures (see Ch. 1, 1.6.2 for review; Lucas, 2004). In the case of feeding, this means that the shape of the tooth has a relationship with how the object deforms and ultimately fractures under loading. Theoretically efficient dental forms for foods with different material properties have been predicted and tested. A narrow and sharp cusp will concentrate stress in a small area, which some have predicted may reduce the force required to access brittle foods (Strait, 1997). However, very sharp cusps supress cracking, as the application of stress to such a small area will result in plastic deformation instead of propagating a crack (Lucas, 2004). A blunter cusp with a wider angle can spread the stress more widely and thereby better promote crack propagation (Lucas, 2004; Berthaume et al., 2020). This tooth shape

may also reduce the risk of tooth failure and damage which is an important consideration for maintaining function (Chai et al., 2009; Berthaume et al., 2010; Ungar, 2015). A sharp cusp is prone to failure or rapid wear and flattening resulting in reduced sharpness as it wears– while blunter cusps may better resist both wear and catastrophic failure (Luke and Lucas, 1983; Crofts and Summers, 2014). As such, teeth must both facilitate food breakdown and resist excessive wear.

Additional complexity in the dentition of most mammals also exists due to the wide range of possible variation in cusp number and form. Studies have attempted to link optimal dental form with function using simulation, modelling, and direct testing methods (see 4.1.5 for review; Evans and Sanson, 2003; Anderson and Labarbera, 2008; Anderson, 2009; Berthaume et al., 2013; Berthaume, 2014; Crofts and Summers, 2014; Swan, 2016). Cusp number, shape, and arrangement affects both food breakdown and tooth safety (Constantino et al., 2016; Berthaume et al., 2020). When food is in contact with multiple cusps the load is spread, which can reduce the risk of damage to the tooth (Constantino et al., 2016). The shape, number, and arrangement of cusps also affects the contact surface area between the tooth and the food (Berthaume et al., 2010, 2013). As such changing cusp morphology is expected to affect the fracture behaviour of food (Lucas, 2004; Berthaume et al., 2010, 2013).

## 4.1.2.1 Optimal dental form for hard foods?

Hard-object feeding has been a particular focus for studies examining the links between cusp morphology and function (Berthaume et al., 2010, 2013; Crofts and Summers, 2014; Swan, 2016). Feeding on hard objects presents a particular dietary challenge due to the high forces required to access these foods (Strait, 1997; Norconk and Veres, 2011; Santana et al., 2012; Crofts and Summers, 2014). Hard-object feeders are often predicted to have dental forms which are either advantageous for hard food fracture, reducing the force required to access challenging foods by concentrating stress on the food object, or teeth which protect against catastrophic dental failure (Berthaume et al., 2010, 2020; Crofts and Summers, 2014; Swan, 2016). Protection from tooth damage or failure is particularly important when the foods are both large and hard (Lucas et al., 2008; Lawn et al., 2009). Enamel thickness is a key consideration for large objects which require high forces in feeding, as thicker enamel

can protect the tooth against wear (Lucas et al., 2008; Lawn et al., 2009). Orangutans, which feed on large and very hard-shelled seeds, present an example of thick enamel which is thought to prevent enamel failure (Lucas et al., 2008). Dental microstructure also plays a role, and enamel rods can be decussated to prevent cracks propagating through the enamel (Lucas et al., 2008). Both thick enamel and decussated enamel rods are predicted to be advantageous when feeding on large and hard food items (Lucas et al., 2008).

Non-primate hard object feeders have been observed to have a wide range of dental forms, including flat plates or dome-like shapes in marine species, or low, rounded cusps in otters (Constantino et al., 2011; Crofts and Summers, 2014). For primate hard-object feeders the optimal cusp arrangement has been predicted through modelling to be a "Complex Cusp" arrangement featuring teeth with multiple asymmetrical cusps which include both sharp and dull cusps (Berthaume et al., 2013, 2020; Berthaume, 2014). This shape is thought to both transfer maximal pressure to the food and stabilise the food during feeding which protects teeth from excessive stress which could cause damage (Berthaume et al., 2013, 2020; Berthaume, 2014). However, this hypothetical shape does not match the dental form observed in hard-object feeding primate molars which are generally low-crowned and bulbous (Constantino et al., 2011; Berthaume et al., 2020). Primate molars are also not the only teeth used in seed predation as some primates use their anterior dentition to access hard seeds (Norconk et al., 2013). What is more, there are primates with very different dental forms such as the high-crested molar teeth of lowland gorillas which, on rare occasion, have been observed to exploit very hard seeds (van Casteren et al., 2019). High estimated bite forces are thought to aid the lowland gorilla in accessing this hard seed but its dental form does not match any predictions of a seed predator (van Casteren et al., 2019). It is possible that past models of optimal hard-object feeder form are incorrect or that the area of the tooth which is in contact with the food during feeding differs to that which has previously been modelled.

### 4.1.3 Extractive foraging – accessing seed nutrients

A special feature of a seed-based diet is that many seeds are encased in some kind of protection, whether that is a hard, brittle seed-casing shell or a thick, hard, and tough pericarp layer (See reviews in Ch. 1, 1.5; Lucas et al., 1991; Norconk et al., 2013). The plant

embryo within this protective casing is typically relatively soft and nutrient rich but must be accessed via this challenging exterior (Lucas et al., 1991; Norconk et al., 2013). This feeding pathway is sometimes referred to as extractive foraging, referencing the encased or encapsulated nature of the nutrients (Tamura, 2020). The primary challenge is gaining access to the protected seed. These defences can be very difficult to overcome, with past work drawing similarities between the fracture resistant properties of dental enamel and the arrangements of fibres within seed shells (Lucas et al., 2008).

Primate seed predators feed on a wide range of seeds which may have hard and brittle or hard and tough casings of variable thickness (Daegling et al., 2011; Norconk et al., 2013). Internal morphology also varies, ranging from multiple seeds encased in tough honeycomb structures to single seeds encased in a single layer of shell (as depicted in Fig. 1.7, section 1.5.2; Daegling et al., 2011; Norconk et al., 2013). Accessing such foods requires a range of feeding behaviours. Seed predators are known to carefully place foods in the mouth in specific positions relative both to seed morphology and their own dental morphology (Barnett et al., 2016; Geissler et al., 2020; Tamura, 2020). It has been suggested that these positions are related to sites of natural weakness in seeds, sites from which the cotyledon would sprout if the seed were not consumed thereby reducing the force required to access nutrients within (Lucas et al., 1994; Lucas, 2004; Barnett et al., 2016). Seeds are also not chosen randomly and some seeds are rejected after an attempted bite for unknown reasons (Barnett et al., 2016; Geissler et al., 2020; Tamura, 2020). For those seeds which are successfully fractured, multiple feeding modes may be possible. While feeding on hard-shelled walnuts *Macaca fuscata* individuals have been shown to produce a range of fracture patterns, varying by individual and sex (Tamura, 2020). Initial fractures to damage seed casing may be large, bilateral cracks or small "hole-punch" fractures which are then propagated with additional cracking bites (Tamura, 2020). The seed is extracted from its casing for chewing and digestion, although evidence from the faeces of other primates indicates that often some fibrous elements or even seed shells are processed along with the seed (Hoshino, 1985; Tamura, 2020).

## 4.1.4 Seed predator dental form: Advantages relative to sympatric primates with other diets?

Given the links between dental form and function it is possible that primate seed predators have teeth which facilitate extractive foraging by having optimal contact surface area with seeds to reduce force for repeated feeding. This group of primates is unified by a diet of hard seeds, although they vary in their dental morphology and feeding positions (detailed below; Fig. 4.1). Some seed predators focus on this food type very intensively, to the point that these hard foods make up the vast majority of their diet, whereas for others they are processed seasonally (see review in Ch. 2, 2.1.2) (Norconk et al., 2013). The hard foods in the diets of these primates have been measured in terms of their material properties and have been found to present similar challenges (Norconk and Veres, 2011; Norconk et al., 2013).

Feeding position divides seed predators into anterior-feeders, which practice sclerocarpy, and posterior-feeders, which use durophagy. Sclerocarpic feeding involves extracting seeds from husks or shells with the anterior dentition, while durophagous individuals use crushing bites on posterior dentition to access foods (Norconk et al., 2013). However, primates which access hard foods using their anterior dentition also chew on their posterior dentition, while posterior feeders also use their incisors in food preparation and, on rare occasions, have been observed to use their canines in food access (Plavcan and Ruff, 2008; McGraw et al., 2011). Primate feeding observations which describe food positioning behaviours in the wild are relatively rare and, especially for posterior bites, it is nearly impossible to know exactly where on the tooth the food has been positioned (Laird et al., 2020). Dental contact points will affect force to fracture so quantifying the effect of different feeding positions is key to understanding primate feeding.

A closer examination of the dental form of anterior-feeding seed predators- the pitheciine primates (*Cacajao, Chiropotes,* and *Pithecia*) shows enlarged and unusual anterior dentition (Kinzey, 1992; Rosenberger, 1992; Norconk and Veres, 2011; Barnett et al., 2015). These species have narrow, tall, procumbent and proclivious incisors and mesiodistally large, laterally splayed canines (Fig. 4.1; Kinzey, 1992; Rosenberger, 1992; Norconk and Veres, 2011; Barnett et al., 2015). The incisors of these species have been found to be exceptionally procumbent and their canines exhibit pronounced mesial crown curvature

relative to primates with other feeding strategies (Deane, 2012). In particular, these very robust canines are used to extract large and hard seeds from hard pericarps (husks) and have high bending strength to facilitate this behaviour (Plavcan and Ruff, 2008; Norconk and Veres, 2011; Deane, 2012). After initial seed access these species use their postcanine dentition to masticate the seed. Their postcanine dental form has been found to group on low and short shearing crests relative to other dietary groupings, as well as bulbous, low and rounded cusps, and wide basins providing expanded occlusal surfaces (Ledogar et al., 2013; Winchester et al., 2014; Allen et al., 2015). Interestingly, the pitheciines also have a relatively large last premolar, which has been associated with seed retention and mastication after it has been extracted from the hard pericarp (Kinzey, 1992; Norconk and Veres, 2011). It has been predicted that this unusual dentition facilitates feeding on large, hard-shelled seeds (Kinzey, 1992; Norconk and Veres, 2011) but the relationship has yet to be quantified.
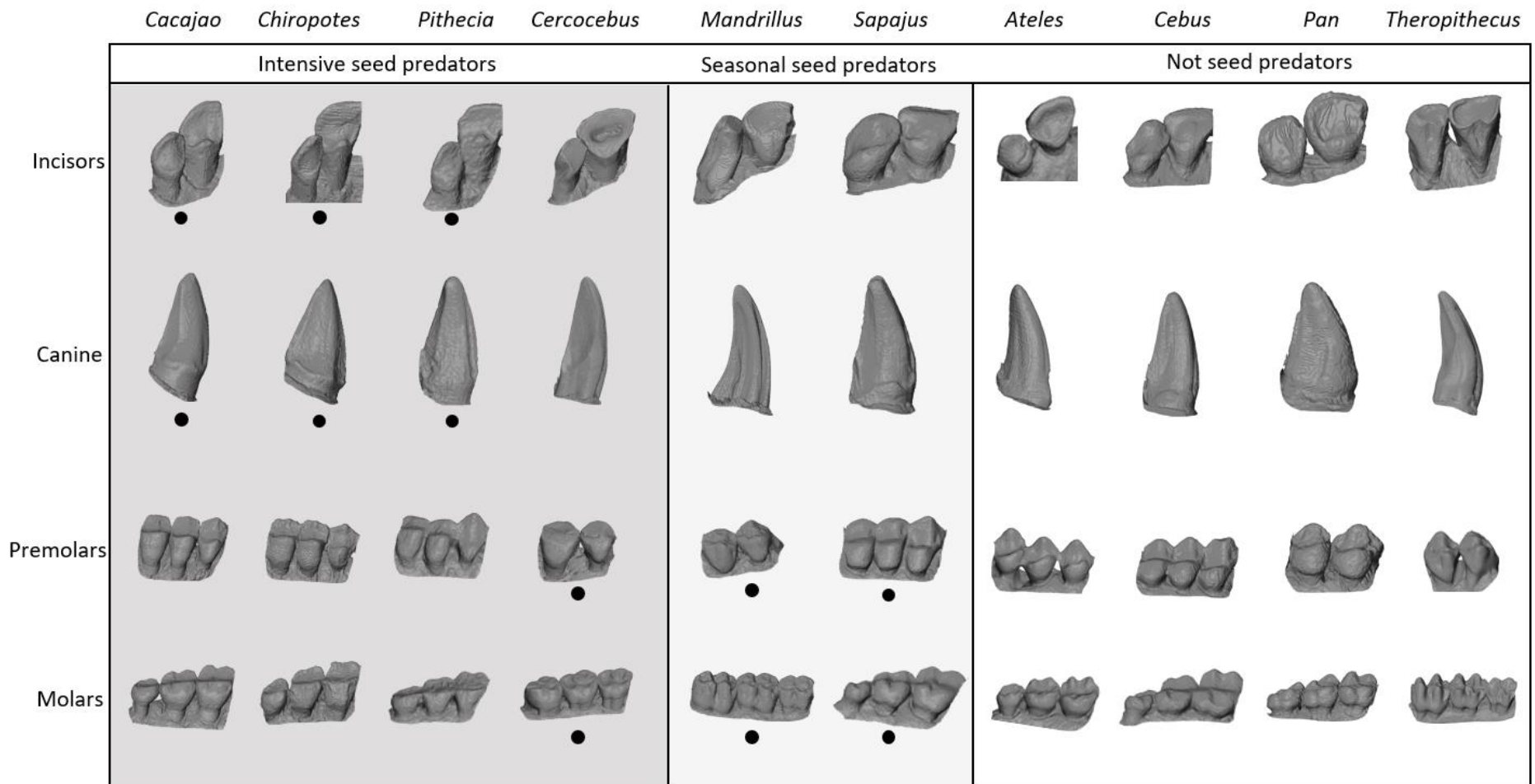
**Figure 4.1 Figure which shows variation in the incisors, canine, premolars, molars in intensive and occasional seed predator primates as well as comparison species with different diets (diets of all groups reviewed in Ch. 2, sections 2.1.2 and 2.1.7). Within seed predators there is also variation in feeding position along the dental row. Typical seed feeding positions are marked with dot symbol. Images not to scale.**

Posterior feeding seed predators can be found in both Africa and South America, and include *Cercocebus atys, Mandrillus sphinx,* and *Sapajus apella*. Both *Cercocebus* and *Mandrillus* both have an enlarged second premolar, which in *Cercocebus* is used for a powerful isometric bite on large seeds (Fig. 4.1; Daegling et al., 2011; McGraw et al., 2011). The posterior teeth of *Cercocebus atys* wear extremely quickly from eruption on, with four high, sharp cusps on the freshly erupted first molar wearing to a relatively flat surface surrounded by an enamel ridge by the age of 5, with increased flattening and dentine exposure as the individual ages (Swan, 2016). This form may aid in the processing of the hard *Sacoglottis* seeds which make up a large proportion of the diet of this species, but past studies have yet to test this. In contrast with anterior-feeding seed predators, canine bites by this species are very rare. The incisors are used for various feeding actions, including scraping and puncturing, although not for the crushing bites which open hard foods (McGraw et al., 2011).

The feeding behaviours of seasonal seed predator *Mandrillus* are less known due to the challenges of studying this primate in the wild (Astaras, 2009). While the similarity in second premolar form has been used as evidence that mandrills likely feed on seeds in a similar manner to *Cercocebus,* this has yet to be directly observed (Fleagle and McGraw, 2002). In contrast with *Cercocebus* the mandrill mandibular first premolar is elongated, with a crown that extends to the mesiobuccal root, a shape which has been associated with large body size in papionins (Fig. 4.1; Swindler, 2002; Lucas, 2004). Another interesting feature in the dentition of this primate is the exceptionally long canine in males, the length of which is closely associated with rank and reproductive fitness (Leigh et al., 2005; Plavcan and Ruff, 2008).

A final example of a posterior-feeding primate is *Sapajus apella*, which feeds on hard palm seeds seasonally, predominantly with their posterior dentition (Martin et al., 2003). Interestingly, *Sapajus* shows an unusual degree of variability in seed processing, as some populations of *Sapajus* also use tools or manual dexterity to process the palm seeds, and while the posterior dentition is most commonly used when biting directly on seeds there are some reports of these capuchins using their canines to penetrate the eye-hole of hard palm fruits (Izawa and Mizuno, 1977; Izawa, 1979; Spencer, 2003). The molars of this species (fig. 4.1) have thick enamel with relatively large, bunodont cusps with wide talonid basins

(Rosenberger, 1992; Delgado and Galbany, 2015). The M3 is quite reduced while the premolars are broad, as are the incisors (Rosenberger, 1992). This thickly enamelled molar shape has been interpreted as advantageous for hard object feeding but has yet to be tested as such (Daegling et al., 2011).

Not all primates feed on hard seeds, including some primates which are sympatric with seed predators or are close relatives of seed predators. For example, soft-fruit feeding *Ateles paniscus,* with which both *Pithecia pithecia* and *Chiropotes satanas* are sympatric, uses its anterior dentition for fruit processing (Swindler, 2002; Norconk and Veres, 2011; Delezene et al., 2016). *Ateles* uses its broad, spatulate incisors (Fig. 4.1) to peel fruit exocarp and scoop out soft flesh (Swindler, 2002; Norconk and Veres, 2011; Delezene et al., 2016). Despite being sympatric and of much larger body size *Ateles* does not consume the hard fruits eaten by *Chiropotes* and *Pithecia* (Norconk and Veres, 2011)*.* Also sympatric with some pitheciine seed predators is *Cebus olivaceus*, a gracile capuchin and close relative of *Sapajus apella* which feeds on seeds that are already damaged and therefore structurally weakened (Terborgh, 1984; de Sousa, 2009; Martins-Junior et al., 2018). The dental morphology of robust and gracile capuchins (Fig. 4.1) has been directly compared, finding enlarged molar cusps and wider talonid basins in robust capuchins, a difference which has been linked with the more extreme diet of robust capuchins (Delgado and Galbany, 2015). By contrast, *Pan troglodytes verus*, is sympatric with *Cercocebus atys* but instead of practicing durophagy this primate feeds on *Sacoglottis* with nut-cracking tools (Boesch and Boesch, 1982). This primate has relatively thin dental enamel, which some have linked with the relatively soft chimpanzee diet, where hard objects encountered are generally very small grit particles (Lawn et al., 2009). The dental form of closely related *Pan troglodytes troglodytes* (Fig. 4.1) was found to have less occlusal relief, shorter shearing crests and lower cusps than more folivorous gorillas, resulting in a flatter molar surface predicted to be more optimal for breaking down fruit pulp (Ungar and M'Kirera, 2003). Finally, a papionin primate, *Theropithecus gelada*, presents a prominent contrast in terms of dental form (Fig. 4.1). This primate has a very unusual feeding ecology, relying intensively on grasses (Dunbar and Dunbar, 1974; Iwamoto et al., 1996). In this primate the teeth wear in such a way that a secondary morphology emerges, as is seen in herbivores, exposing compensatory enamel shearing crests (Venkataraman et al., 2014). Such a specialist diet with very different

material properties to primate seed predators would be expected to relate to a very different dental function.

## 4.1.5 Testing dental form and function

A range of methods can be used to bridge the gap between understanding dental form and dental function, including computer modelling and physical testing. Numerous metrics can be explored, including the force required to fracture a given food with a given real or hypothetical tooth (e.g. Anderson and Labarbera, 2008; Anderson, 2009; Berthaume et al., 2010; Crofts and Summers, 2014; Barnett et al., 2015; Anderson et al., 2016; Swan, 2016) and the efficiency of food fragmentation (Lucas et al., 2002; Laird et al., 2016).

Finite Element Analysis (FEA) is a computer modelling method which has been employed to map the stress produced by teeth on virtual food objects or vice versa (Berthaume et al., 2010; Anderson and Rayfield, 2012; Berthaume, 2014; Constantino et al., 2016). This approach can observe the relationship between food item size, cusp number, and dental radius of curvature. However, past studies highlight that while FEA is a valuable tool for testing hypothetical scenarios with full control of variables, the complexities of biological materials are challenging to perfectly replicate (Anderson and Rayfield, 2012). Seeds are an especially complex physical object, consisting of multiple layers with varying material properties in each (Lucas et al., 1994; Lucas, 2004).

Instead, the most direct method of measuring feeding performance involves active participants chewing food and permitting dental measurements (Lucas et al., 2002; Laird et al., 2016). This approach can be used to compare dental efficiency and the effect of varying dental morphology directly on food objects (Lucas et al., 2002; Laird et al., 2016). This can only be examined in compliant test subjects, as participants need to chew and then remove the food from the mouth. More indirect methods are used to examine fracture efficiency in non-human species, including fragmentation quantification of food particles in faeces (Venkataraman et al., 2014). If sufficient material is available it is possible to compare food particle size in faeces with dental form, as has been quantified for different stages of dental wear in *Theropithecus gelada* (Venkataraman et al., 2014). However, to quantify the relationship between dental form and function additional direct testing is needed.

Physical testing methods can be used to test predictions relating to dental function which would be impossible to test in reality using stylised cusp tips or blades to physically crush or puncture a range of foods or food replicas (Fig. 4.2; (Anderson and Labarbera, 2008; Anderson, 2009; Berthaume et al., 2010; Crofts and Summers, 2014; Barnett et al., 2015; Anderson et al., 2016; Swan, 2016). This approach facilitates comparisons of force to fracture and other aspects of fracture behaviour. In such studies researchers have varied the cusp or blade morphology to test predictions of form and function (Evans and Sanson, 1998; Anderson, 2009; Crofts and Summers, 2014; Anderson et al., 2016). Modelling teeth based on knowledge of dental morphology and engineering principles to design the most optimal tooth found a close match between models and real mammalian teeth (Evans and Sanson, 2003). Results were especially successful in matching 'ideal' teeth to real teeth associated with tough foods, particularly for species with carnivorous diets but less so for species with hard diets which may have additional constraints (Evans and Sanson, 2003). When examining teeth linked with hard diets by testing a series of hypothetical cusps, results showed that tall or skinny cusp replicas fracture hard snail shell replicas at the lowest force (Crofts and Summers, 2014). However, the fact that this morphology is very rare in nature suggests that tooth safety is an essential component of dental form, as tall and skinny cusps are prone to rapid catastrophic failure (Crofts and Summers, 2014). Indeed, modelling and experimental work suggests that there are strong relationships between food size, material properties and enamel thickness (Lucas et al., 2008; Lawn and Lee, 2009; Lawn et al., 2009). Small and hard items such as the grit encountered during feeding will cause surface yield on the tooth surface, damaging the tooth more slowly with wear such as pitting (Lucas et al., 2008; Lawn et al., 2009). For large and hard items, such as some seeds eaten by primates, cracks in the enamel likely first arise from the enamel base and radiate up to the surface of the tooth (Lucas et al., 2008; Lawn et al., 2009). In either case thick enamel was found to be of benefit, reducing the impact of gradual wear in those which eat small, hard objects and preventing catastrophic damage to the tooth in those feeding on large and hard objects (Lucas et al., 2008; Lawn et al., 2009).

**Figure 4.2 Examples of physical testing of dental form and function, showing a. Rig for testing hominin dental row force to fracture on a hard and brittle replica object (Berthaume et al, 2010); b. Hypothetical cusp tips used to examine the relationship between cusp morphology and hard food breakdown (Swan, 2016); and c. Rig set-up for comparing durophagous stingray morphology in crushing hard objects, in this case a hard snail replica (Kolmann et al., 2015).**

A domed or flat tooth may provide a compromise between lower force to fracture and tooth safety (Crofts and Summers, 2014). Hypothetical cusps modelled on *Cercocebus atys* teeth found that cusp morphology has a significant effect on force to fracture hard food replicas, as well as on fragmentation behaviour (Swan, 2016). Notably, a blunter cusp did require more force to initiate a crack than a sharp cusp, but examining food fragmentation revealed an additional effect, that blunter cusps also had a higher degree of food fragmentation (Swan, 2016). This is an important observation, as crack propagation after initial fracture is important for actually accessing the food for feeding, but very few studies have quantified food fragmentation alongside force or energy to fracture (Swan, 2016). In addition to stylised cusps tips, different blade shapes have been tested, representing a range of sharp teeth including carnivoran carnassials (Anderson and Labarbera, 2008; Anderson, 2009). Results have found a prominent effect when changing the shape of the blades (Anderson and Labarbera, 2008; Anderson, 2009). Notably however, the material properties of the food being fractured had a pronounced effect on which hypothetical tooth shape is most advantageous (Anderson and Labarbera, 2008; Anderson, 2009). This further highlights the strong relationship between optimal dental form and food material property.

Past work suggests that changing a single cusp can have a significant impact on tooth performance. To understand non-hypothetical tooth shape function, it is possible to manufacture dental replicas from full or partial real dental rows and use these to crush real foods or food replicas, recording the force or energy to fracture (Lucas et al., 1994; Berthaume et al., 2010; Barnett et al., 2015, 2016). Testing with real teeth is a potentially destructive process: specimens are likely to be damaged by repeated loading, or the teeth may wear during testing, altering dental topography. Instead, studies typically work with dental replicas. A range of materials and methods have been used in the past to manufacture dental models, including casting in cobalt-chrome (Lucas et al., 1994), cast in nickel-cobalt (Barnett et al., 2015), or cast iron (Berthaume et al., 2010). Some studies have also used CNC machining on steel (Swan, 2016) or milled aluminium (Crofts and Summers, 2014; Kolmann et al., 2015). The key uniting need of the dental material used is the ability to accurately represent dental form and resist deformation so that the replicated dental form remains constant during testing.

Testing with dental replicas has examined force to fracture in isolated teeth and full dental rows in a small number of studies (Lucas et al., 1994; Berthaume et al., 2010; Barnett et al., 2015, 2016). The force required to penetrate fruit using an isolated canine replica of the seed predating *Cacajao* was compared with a standard fruit penetrometer, finding that the dental replica required less force to access hard fruits than the penetrometer (Barnett et al., 2015). This very interesting finding requires further exploration to compare performance in *Cacajao* to other primates. Full dental rows have been tested for Orang-utan dentition, exploring the force to fracture hard seeds (Lucas et al., 1994). Results indicated that Orang-utans would need to generate a very high force (>2000N) to fracture seeds they are known to consume (Lucas et al., 1994). The only other study to test a full primate dental row examined predictions of past diet using metal casts of hominin mandibular dentition to fracture hard, brittle synthetic food replicas (Berthaume et al., 2010). Results found that neither blunt nor pointed cusps were of obvious advantage in this fracture, but that the presence of multiple cusps is likely functionally important (Berthaume et al., 2010).

Taken together, a significant body of dental functional research exists, both quantifying whole dental shape and matching form or hypothetical form to function. However, many questions remain unanswered. Studies which test full and opposing dental rows are very

rare, and those which have been carried out do not consider the role of gape (Lucas et al., 1994). As the mandible rotates and translates during jaw opening the occlusal surfaces and thereby the tooth-food-tooth contact changes (Carlson, 1977). The inclusion of gape is therefore a key component of modelling dental fracture performance. What is more, to date no study has tested a broad comparative sample of primate dental replicas. There is still no understanding of how the dental forms of known dietary specialists such as primate seed predators perform compared to other species.

## 4.2 Aims and hypotheses

Teeth are a key part of the masticatory system: Dental form which improves dental performance may form part of a suite of adaptations to facilitate access to mechanically challenging foods, or indeed may provide another pathway for many-to-one mapping in primate seed predators. Previous chapters have considered other components of the masticatory system (Chapters 2 and 3) and found some evidence of advantageous masticatory morphologies especially in the smaller-bodied seed predator primates in the sample. Certain dental forms have been hypothesised to better promote crack propagation (Lucas, 2004), which would promote easy access to the nutrients within the seed casing.

This chapter aims to compare fracture performance (force to initiate fracture, fragmentation, and tooth contact with food) between primate seed predators and primates with non-seed diets by simulating feeding on a hard food object. It is predicted that seed predators will have advantageous dental adaptations to facilitate their access to hard foods in their diet. This prediction will be investigated by using physical testing of primate dentition to simulate bites on a hard seed at multiple positions along the dental row. Given the challenges of feeding on large, hard seeds (Norconk et al., 2013; Tamura, 2020) and the strong links between dental form and diet (Lucas, 2004) it is predicted that the dental form of primate seed predators will both reduce the force to fracture when feeding on a large hard item. As seed predators feed in different positions along the dental row this prediction is made for at least one bite position (tooth), not for feeding on all teeth.

**H1**. **Primate seed predators will initiate the fracture of a large, hard seed at a consistent lower force relative to primates with other diets when simulating feeding. This will be the case on at least one bite position along the dental row.**

Additionally, given the feeding ecology of primate seed predators (see section 4.1.4), the most advantageous feeding position for each seed predator is expected to relate to real feeding position. Anterior-feeding seed predators are expected to have advantageous feeding on the anterior dentition, and posterior-feeding seed predators on the posterior dentition.

**H2**. **Within primate seed predators the tooth which facilitates the lowest force to initial fracture will be the tooth most often used to access large hard objects.**

A further prediction is made regarding the contact between food object and the teeth. Based on previous reviews indicating there may be optimal tooth design for hard-object feeding it is predicted that when feeding on large hard foods there will be similarities (number and size of contact points) in the tooth-food contact of seed predator primates which will facilitate reduced force to initial fracture. The optimal tooth design for hard-object feeding is unknown, but it is predicted that such a shape will result in a lower force to initiate fracture. To understand this relationship the tooth-food contact at initial fracture will be extracted and compared.

These predictions will be tested using physical replicas of primate teeth (upper and lower dental rows) modelling bites on a hard-shelled seed (pecan). This seed will be compressed between teeth along the dental row (anterior; incisors and canines, posterior; premolar and M1) after mandible rotation to simulate gape. For all bites fragmentation patterns will additionally be observed and recorded to determine if fracture of the seed shell has occurred. It has been shown that primates feeding on hard-shelled seeds will initiate seed feeding with a range of crack types (Tamura, 2020). The type of fragmentation event for each initial fracture will be recorded, and all events which penetrate the seed casing will be evaluated statistically to validate or falsify hypotheses.

## 4.3 Materials and methods

## 4.3.1 Sample selection

Ten primate species were used in this study (*Ateles, Cacajao, Cebus, Cercocebus, Chiropotes, Mandrillus, Pan, Pithecia, Sapajus, Theropithecus*). The primates span a range of diets, including seed predators and primates with no seeds in their diets (Table 4.1; see Ch. 2, 2.3.1 for additional details). Seed predators included vary in their feeding behaviour: Some seed predators (*Cacajao, Chiropotes, Pithecia*) feeding predominantly on their anterior dentition while others (*Sapajus, Cercocebus, Mandrillus*) feed on seeds primarily using their posterior dentition (Table 4.1). Seed predators also vary by the intensity of their diet. Some species (*Cacajao, Chiropotes, Pithecia, Cercocebus*) feed on hard seeds with great intensity and regularity, while others (*Mandrillus, Sapajus*) feed on hard seeds occasionally, as part of their seasonal diet (Table 4.1, Norconk et al., 2013).

Mandibles and crania had previously been collected, digitized (either with MicroCT, structured light surface scanner, or medical CT; Table 2.2), reconstructed into virtual models, and aligned in occlusion using Avizo (v9.2, FEI, Thermo Fischer Scientific) as part of Chapter 2 (see 2.3.2 and 2.3.3 for data acquisition and preparation, Appendix 1 for full specimen database, and Appendix 2, A2.2 and A.2.3 for further details on specimen preparation).Using the morphospace in Chapter 2 as a guide (Fig. 2.11 in section 2.4.1), one adult male individual was chosen from the centre of the distribution for each species. Unlike previous chapters note that *Saimiri* is not included as there was a size limitation in the manufacturing process of dental models. A male rather than female individual was chosen for this study as past comparisons of dietary differences between sexes have found males to be more extreme in terms of diet, consuming a higher proportion of harder foods in at least some species (Bowler and Bodmer, 2011).

All specimens included are adults with minimal dental damage, presented no abnormal dental wear and were not heavily aged based on their teeth. While not abnormal, the *Cercocebus atys* specimen C13.21 possessed a significant amount of wear (assessed by examining dentine exposure) on both upper and lower post-canine teeth. However, this species is known for rapid and extreme dental wear (Swan, 2016). A past study which quantified dental wear in *Cercocebus atys* included this specimen (C13.21), finding it to be

both fully mature and at a relatively early stage of wear (Swan, 2016). As such C13.21 was deemed a suitable specimen for this study. Some damage remained on a small number of the specimens, but this was easily digitally repaired (Ch2, section 2.3.4.1 and Table 4.1).

Only one side of the dental arch was used for this study as one-sided bites were simulated. It was decided based on reduced damage in the majority of the sample that the right side would preferentially be used. For two specimens the left side was used (Table 4.1) and mirrored after model processing.

**Table 4.1 Specimens used for physical testing, denoting their seed predator status and whether seeds are processed with the anterior or posterior dentition, the modality of their scan, the working bite side used, and the extent of reconstruction carried out. See Appendix 1 (specimen database) for scan resolution and details on specimen source.**

| Genus | Species | Museum accession number | Seed predator | Anterior or posterior | Imaging Modality | Side | Reconstruction / damage |
|-------|---------|-------------------------|---------------|-----------------------|------------------|------|-------------------------|
| *Cacajao* | *Cacajao calvus rubicundus* | 5496 | Yes, intensive | Anterior | MicroCT | Right | No |
| *Chiropotes* | *Chiropotes chiropotes* | 406582 | Yes, intensive | Anterior | MicroCT | Right | No |
| *Pithecia* | *Pithecia pithecia* | 38461 | Yes, intensive | Anterior | Surface scan | Left | No |
| *Cercocebus* | *Cercocebus atys* | C13.21 | Yes, intensive | Posterior | MicroCT | Right | No |
| *Mandrillus* | *Mandrillus sphinx* | 2056 | Yes, occasional | Posterior | MicroCT | Right | No |
| *Sapajus* | *Sapajus apella* | 90010 | Yes, occasional | Posterior | Surface scan | Right | Yes, lower right M3 |
| *Ateles* | *Ateles paniscus* | 39427 | No | NA | Surface scan | Left | Yes, upper left canine and cavity on lower left M2 |
| *Cebus* | *Cebus olivaceus* | 224 | No | NA | Surface scan | Right | Yes, lower right canine (not reconstructed) |
| *Pan* | *Pan troglodytes verus* | 383 | No | NA | Medical CT | Right | No |
| *Theropithecus* | *Theropithecus gelada* | 72190 | No | NA | Surface scan | Right | No |

## 4.3.2 Creation of dental models to be used in the physical testing

A range of materials and methods have been used in the past to manufacture dental models (Lucas et al., 1994; Berthaume et al., 2010; Crofts and Summers, 2014; Kolmann et al., 2015; Swan, 2016). This study takes advantage of recent advances in 3D printing technology and uses 3D printed dental replicas made of a steel-bronze alloy. A tooth printed using this method was compared to a CNC machined steel model of the same tooth in its performance fracturing hard food replicas, finding no statistical difference in performance (Camp, 2019). Before the 3D scans of the mandibular and maxillary teeth could be physically manufactured the scans previously collected in Chapter 2 needed to be further processed.

The models previously created from MicroCT and Medical CT scans were first solidified in Avizo. In doing so all materials (trabecular bone, tooth roots, air) were treated as the same solid material (Fig. 4.3). The reason for this was to create a solid model that would be structurally sound when manufactured in metal. The solidification process required additional segmentation. The steps taken in segmentation altered the model position in the global coordinate system, meaning that solidified surfaces were no longer in occlusion. To re-align the surfaces, a rigid landmark warp in Avizo was carried out, placing landmarks on identical points on the original and solidified models, then warping the solidified model to the original.
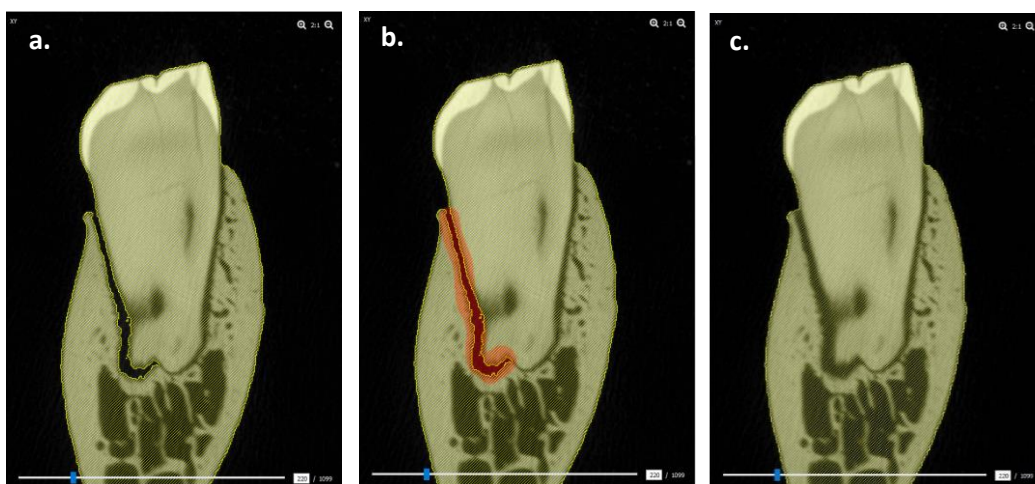


**Figure 4.3 MicroCT scan (specimen *Cercocebus* C13.21) demonstrating model solidification. From left: a. the trabecular bone has already been added to the main bone material (yellow), but a channel still goes along the tooth root, which b. is highlighted. Finally, c. the highlighted material is added so that a solid structure remains.**

The models created via the surface scans required only minimal preparation because this scan modality does not capture internal architecture removing the need to solidify models. Small holes did remain on models because surface scanners cannot pick up excessively dark areas or highly reflective surfaces (Fig. 4.4). Great care was taken while scanning to avoid any errors on the occlusal surfaces, although very small holes were, in some cases, unavoidable. Models were imported into Geomagic (Geomagic Studio, 3D Systems), where they were cleaned with the "Meshdoctor" tool, which carried out minor repairs such as flipping inverted vertices. This step was essential because only clean models with no such errors could be manufactured. Holes in non-occlusal regions were repaired individually and semi-manually so that geometry was minimally altered.
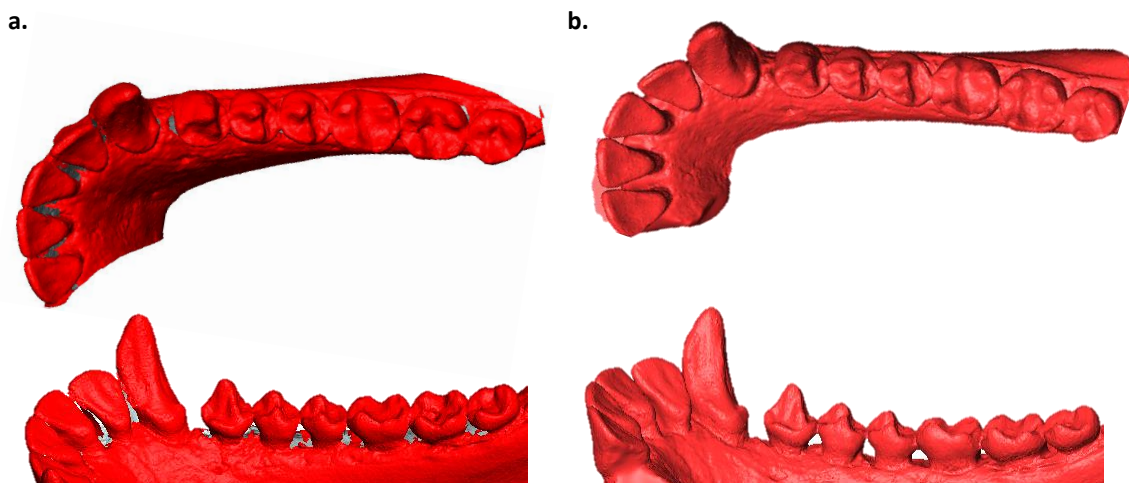


**Figure 4.4 Example of hole repair on a surface scanned model (specimen *Ateles* 39427). Showing specimen unrepaired (a.) and repaired (b.). The occlusal surface is not affected, but the spaces between teeth were in to facilitate the manufacture of a closed surface. Note additionally that the cavity on M2 was repaired on this specimen.**

## 4.3.2.1 Repairing damage

Three models had damage which needed to be addressed due to its effect on dental topography. Two models were repaired using bilateral symmetry (*Ateles* 39427 and *Sapajus* 90010). Both were missing one full tooth (Table 4.1), and *Ateles* 39427 additionally had a small cavity on one tooth. Mirroring was used for all repairs, as the damage was one-sided. For missing teeth, using Geomagic the missing tooth was segmented from the other side of

the dental row, mirrored, then positioned and merged (Fig. 4.5). To repair the cavity the intact tooth on the other side of the dental row was also segmented and fit to the damaged tooth, then used as a guide to fill in the cavity. One additional model (*Cebus*) had bilateral dental damage on its lower canines. This damage could not be repaired as there was no undamaged side to use as a mirror. This damage is taken into account in interpreting results on this tooth for this specimen.
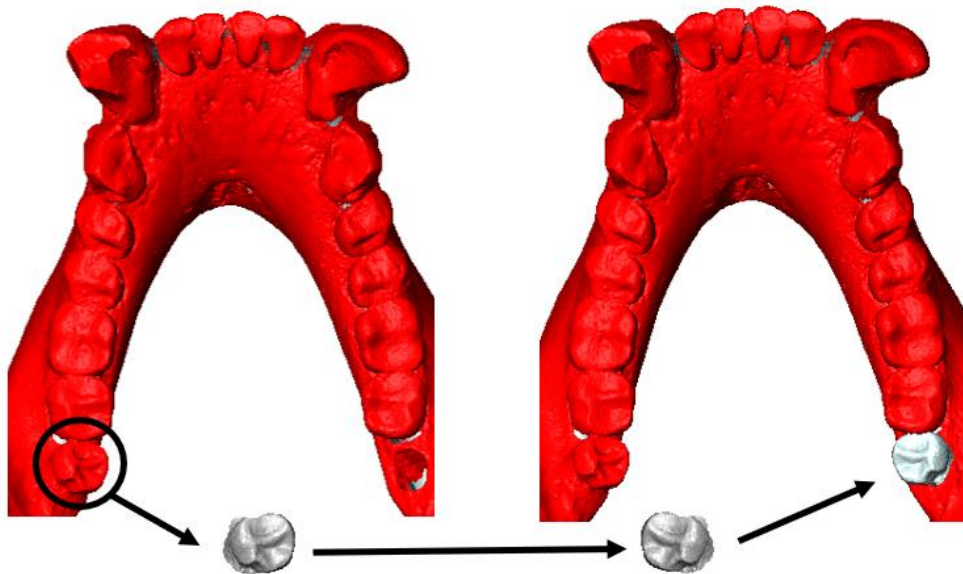


**Figure 4.5 Repair of the M3 in *Sapajus* 90010. The intact molar on the left side was segmented, mirrored, then translated into position on the right side using Geomagic and Avizo. Note this specimen also presented damage on its left side (canine). It was preferable to repair M3 as this bite point was not directly tested while canine was.**

## 4.3.2.2 Mounting dental models

The next step in model manufacture was to create flat plates upon which dental rows (mandibular and maxillary) would be mounted. The plates were designed to serve as attachment points to a universal physical testing machine and to help maintain accurate occlusion once the upper and lower models were manufactured. For the mandibular dental row, a simple flat plate was designed SolidWorks (v2017, Dassault Systems) with a thickness of 4 mm (Fig. 4.6a). The plate for the maxillary dental row was 12 mm thick and featured a pilot hole (depth 8.5 mm) with a reinforcing cylinder (10 mm diameter) at the point of origin. This pilot hole (6 mm diameter) was located at the model origin and would become the point of the attachment of the model to the physical testing machine. A master set of

plates with these attributes was made with excessively large dimensions (150 x 200 mm) so that they could be virtually trimmed to fit each specimen. An additional simple plate was made to raise the mandibular row for specimens if the canine came into contact with the physical testing machine base plate (*Ateles, Cercocebus, Sapajus,* and *Theropithecus*).

In order for the teeth to compress vertically when attached to the universal tester, simulating a realistic bite, they needed to be aligned parallel to the plates. The dental models were therefore re-aligned to an occlusal plane based on the third molars (left and right) and incisor. This standardised model orientation between specimens while also creating a common point of origin for each mandible and cranium pair on their respective flat plates. To move models to this position each specimen was transformed (rotated and translated) using rigid landmarks in Avizo. The transformation moved models so that 0,0,0 (x,y,z) in the global registration system was positioned at the third molar on the working biting side (Table 4.1), with an axis running between the third molars and in the direction of the incisors. To reduce torsion during loading the model was further translated along the y axis to move the global origin to the halfway point along the y-axis and M3 on the working biting side.

To reduce the physical size of the model, and by result the manufacturing costs, material extraneous to the dental row was virtually trimmed (Fig. 4.6b). The unused side of the dental row and any excess skeletal material surrounding the working side dental row were removed in Geomagic. At this point those dental rows with a left working side were mirrored to facilitate a standardised model orientation during testing.

The master files for the flat plates were imported and trimmed to fit the dental rows, retaining identical dimensions in the upper and lower plates for each specimen. The virtual dental models were merged with the respective flat plate using a Boolean union in Geomagic (Fig. 4.6c). At the time of manufacture 3D print companies only processed file sizes of up to 50mb and/or with a polygon limit of 1000000 triangles. To meet this manufacturing requirement all non-dental structures were selected and decimated to a very high degree, while decimation on the teeth was kept to an absolute minimum avoiding quality loss on the occlusal surface.
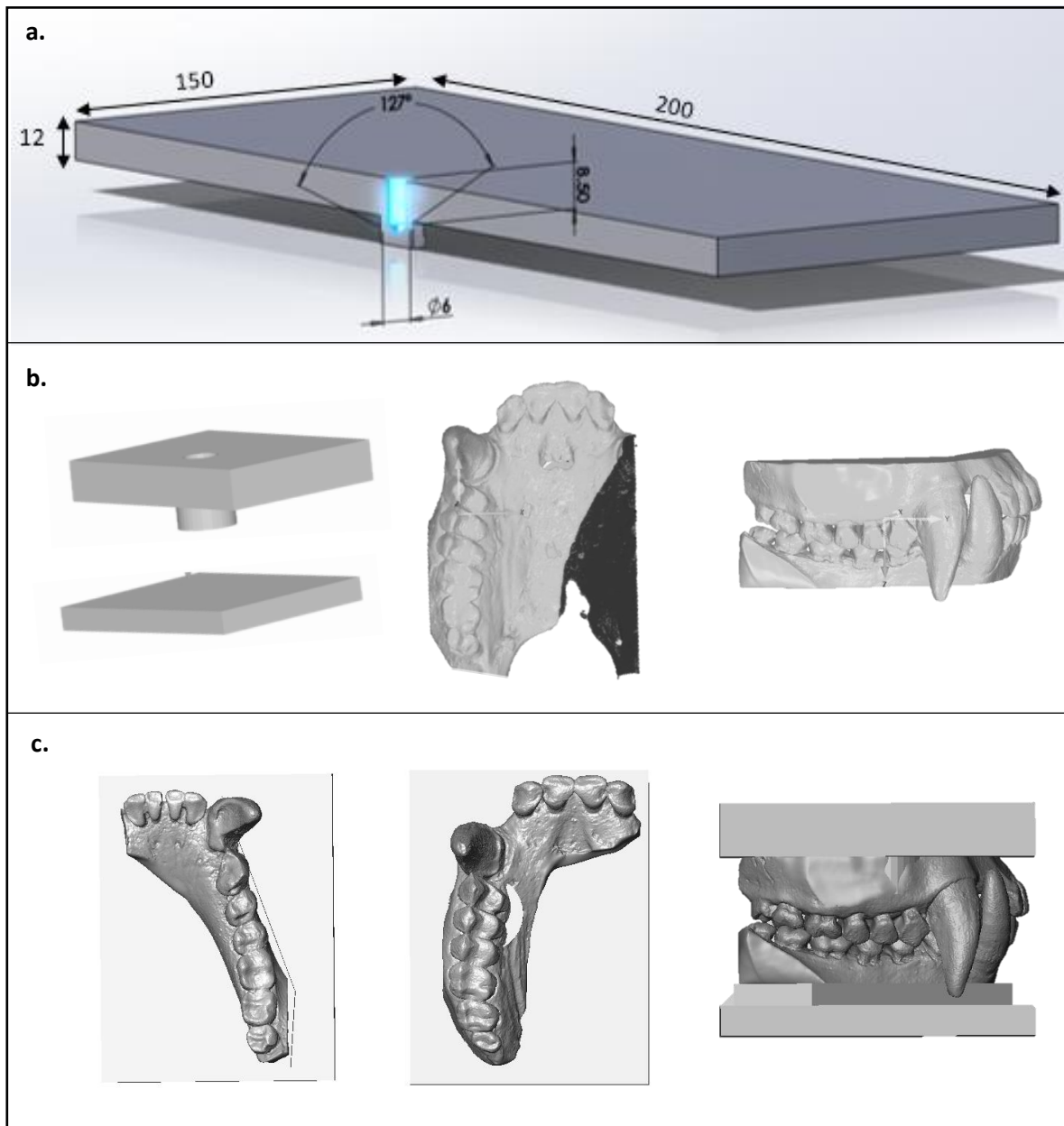
**Figure 4.6 Virtual steps in dental model manufacture for the specimen *Sapajus* 90010. Showing: a. flat plate basic design (upper) with size specifications including pilot hole; b. finalising the flat plates and preparation of dental rows. From left: completed upper flat plate with pilot hole (top) and plain lower flat plate (bottom); trimming of maxillary dental row, dark region being removed; trimmed mandibular and maxillary virtual dental models before attachment to plates; c. completed virtual models separated and with jaw closed in occlusion.**

## 4.3.2.3 3D printing process

The final models were sent to commercial companies for manufacture (Fig. 4.7). An additive manufacturing process of 3D printing called binder jetting was chosen for the study. This is a

process by which layers of steel powder are printed and infused with a glue, then the model is solidified with copper in a furnace, which burns away the glue and leaves the metal composite product. The material selected was a metal which is 60% stainless steel 420 with 40% bronze infiltrate. Two companies were used to manufacture 3D printed models: Sculpteo (https://www.sculpteo.com/en/) for *Cercocebus, Mandrillus, Theropithecus,* and *Pan* and Shapeways (https://www.shapeways.com/) for *Ateles, Cacajao, Chiropotes, Pithecia, Cebus,* and *Sapajus*. Price and turnaround time made using two different companies a necessity, however both companies use printers and materials from the same original manufacturing company (ExOne Systems, USA). The same datasheet of material properties was given by both at the time of printing (April – June 2017), which states the material has a Young's modulus of 147 GPa. Minor shrinkage was expected in model manufacture, with Sculpteo citing +/- 2-3%, and Shapeways +/- 5%.

A sensitivity study examining the effect of using 3D printed teeth from these two manufacturers was previously carried out by another researcher (Camp, 2019). In this experiment, the same single tooth was 3D printed by both Sculpteo and Shapeways and compared alongside the same tooth made using CNC machining. Results found that the tooth printed by each manufacturer or manufacturing method produced no statistically significant differences in performance (force to fracture) when tested in the fracture of identical (synthetic) hard food replicas.
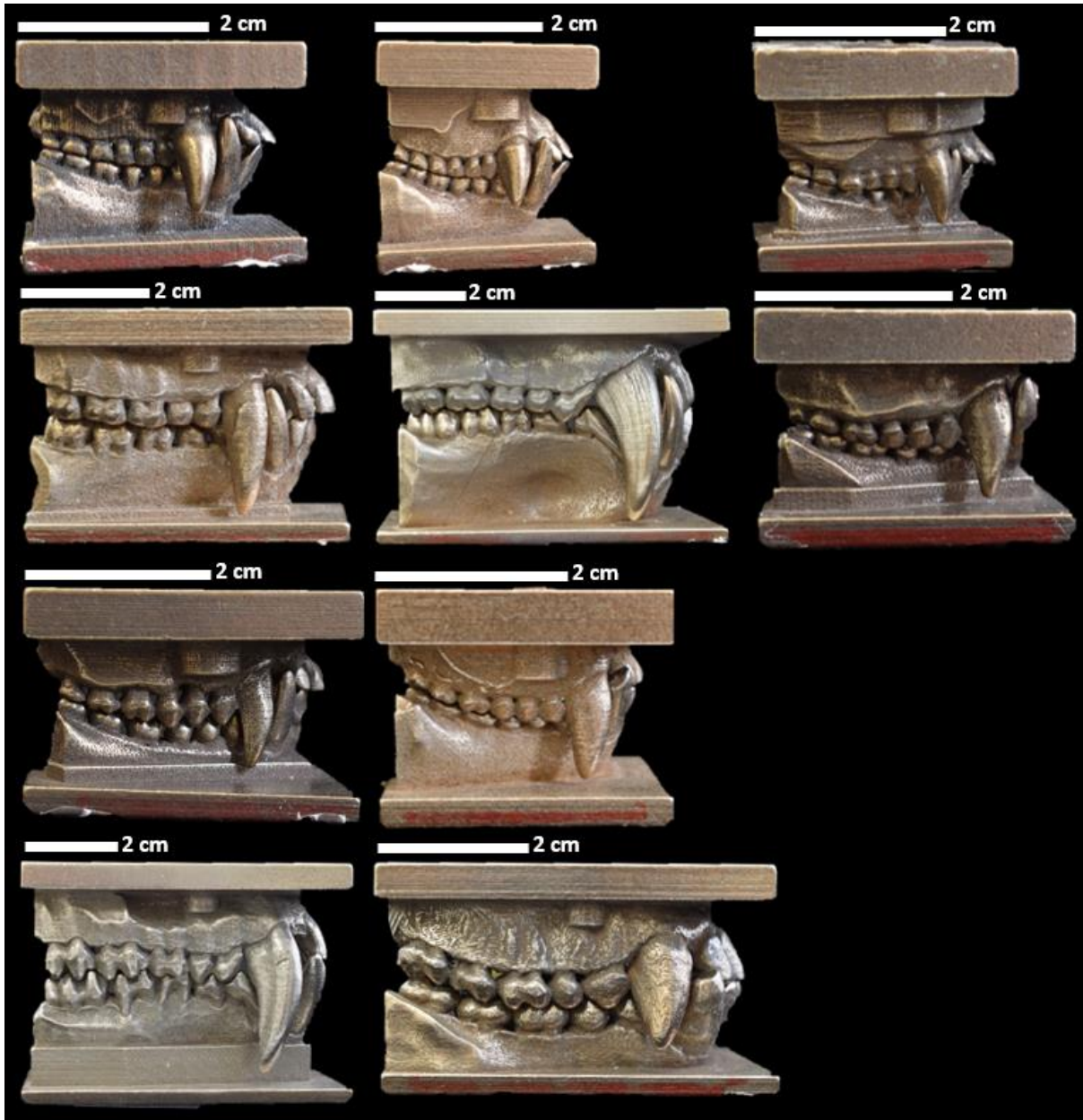
**Figure 4.7 All completed physical dental model. Showing from top left:** *Cacajao, Chiropotes, Pithecia, Cercocebus, Mandrillus, Sapajus, Ateles, Cebus, Theropithecus, Pan.*

### 4.3.3 Physical testing machine set-up

All compression experiments were carried out with a universal materials tester (Mecmesin MultiTest 2.5-*i*). This physical testing machine allows pure compression to be applied between a load cell and a base plate. In its basic setup, the mandible is attached to the lower plate and the upper dental row to the upper load cell. The upper row is lifted and a food item placed between the teeth. Four bites were simulated: Two anterior (incisor and canine) and two posterior (premolar and molar).

## 4.3.3.1 Attachment of dental models to physical testing machine

The dental models had to be very securely fastened to the physical testing machine to avoid slippage during testing as well as to minimise deflection. The lower dental row was, in all cases, fixed to the base plate directly with a specialised glue (X60, HBM UK Ltd., cold-curing methylmetacrylate-based glue designed for strain gauges) which is extremely resistant to compressive force. The upper dental row was designed for attachment via an M7 thread tapped into the pilot hole (as shown in Fig. 4.6). In larger specimens (dental row length > 3.5 cm) the most anterior and posterior bites were too far from this central point and bending occurred which was deemed problematic for machine, model, and results integrity. Instead, for large specimens a large flat plate was attached directly to the machine, and the specimen was fixed to the plate using the same specialised glue as for the mandible.

Correct occlusion was taken into account during model attachment to the physical testing machine. The dental models were designed in occlusion (as shown in Fig. 4.6 and with identically sized upper and lower base plates for each specimen. Using a custom alignment tool with a 90 degree angle the upper and lower base plates were kept in alignment during attachment (Fig. 4.8). For fitting small specimens attached directly with the tap, the upper dental row was attached first. The alignment tool was used to guide the placement of the lower dental row before fixing it with the same specialised glue. In large specimens the mandible plate was attached first before using the alignment tool to orient the cranium plate, which was affixed to the flat plate using the specialised glue and clamped during curing.
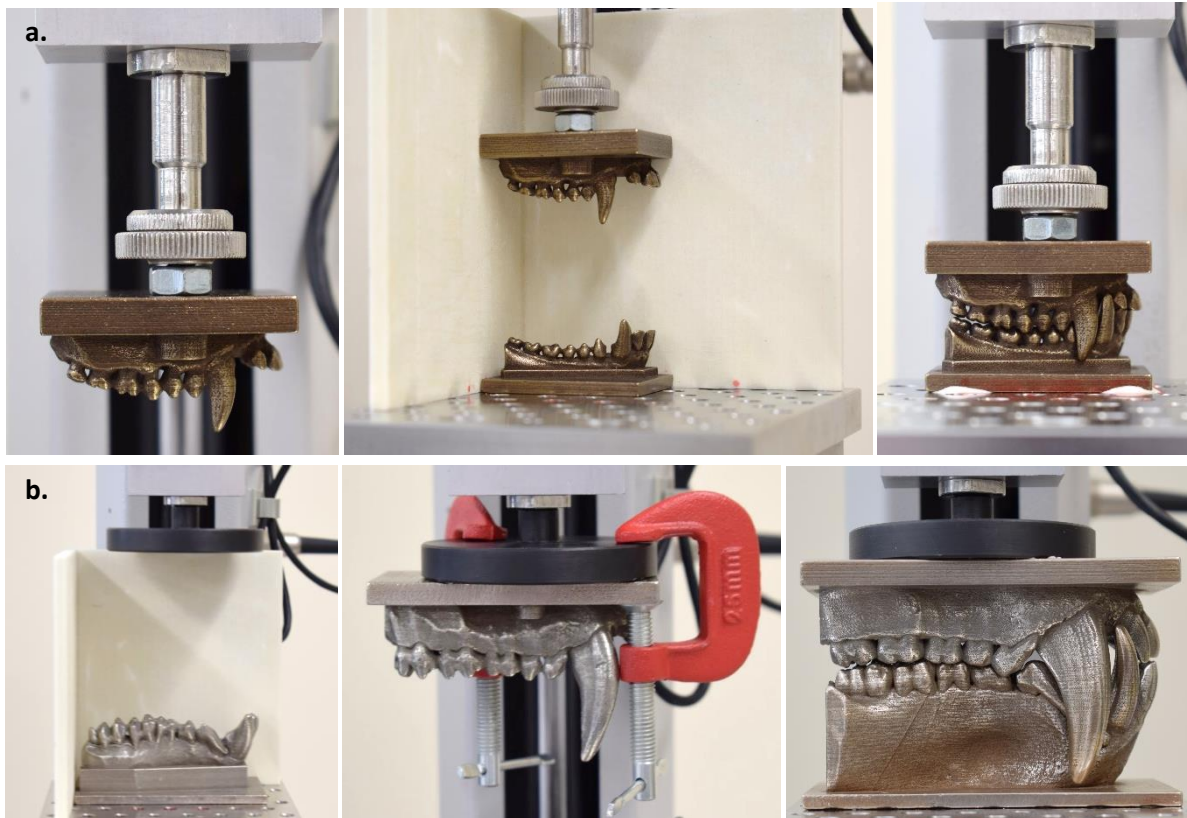
**Figure 4.8 Attachment of dental models to the physical testing machine. Showing a. attachment of small specimens using the tap. The maxillary dental model was attached directly to the machine (left), the alignment tool was used to centre the mandibular dental model (centre) so that the model was in correct occlusion (right); and b. attachment of large specimens with flat plate. The mandibular dental model was fixed to the machine plate (left), with the alignment tool left on to guide the position of the maxillary dental model, which was fixed in place using clamps while the adhesive dried (centre) to result in correct occlusion (right).**

## 4.3.4 Simulation of gape

To replicate realistic tooth-food-tooth contact the amount of rotation and translation required to place the food item between each tooth was calculated. These values are specific to each individual, and to each tooth. A rig which can rotate and translate was designed, and subsequently manufactured by Mecmesin (Mecmesin Ltd., UK) and modified by the Biology Mechanical Workshop (University of York). The rig (Fig. 4.9) attaches directly to the physical testing machine base plate, and the mandibular dental model attaches to the rig.
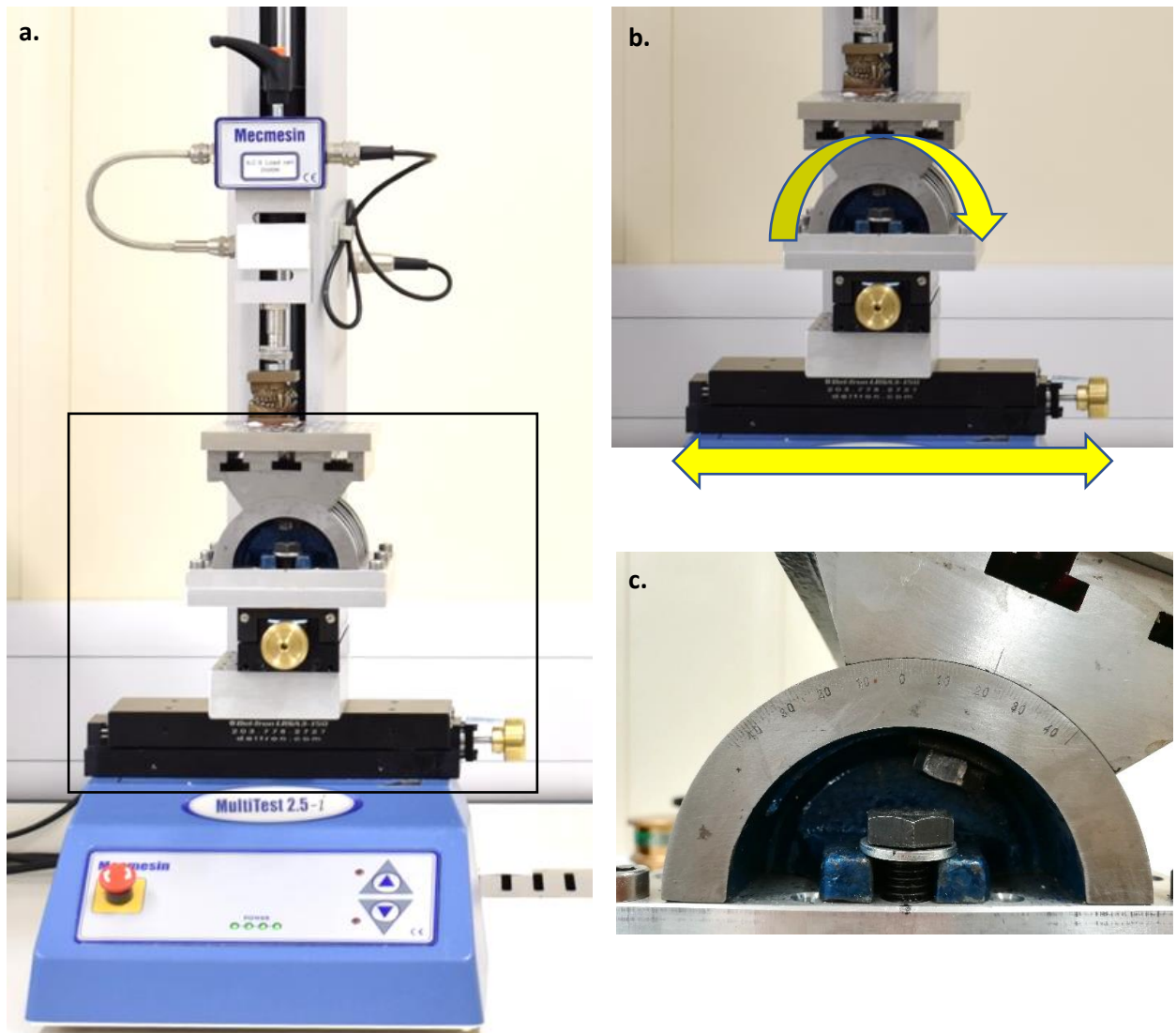
**Figure 4.9 Rig to rotate and translate mandible fixed on to physical testing machine (Mecmesin MultiTest 2.5-i), shown with *Sapajus* 90010. Showing a. physical tester with rig fixed and teeth attached, box highlighting position of rig. The rig features multiple moving components: The mandible is affixed to a flat plate which sits atop an angle block which can rotate forwards to imitate pitch. At the base of the rig and additional translation plate translates left and right, with each rotation equivalent to 2 mm translation and with markings for every 0.5 mm; b. focus on rig, with arrows showing the angle plate rotation direction for jaw opening and translation plate for anterior translation and c. Angle plate rotated by 20°.**

Gape angle was calculated for each specimen and bite virtually using Avizo, using the protocol used for calculation of mechanical advantage (Ch. 3, 3.2.1). The gape angle at a linear gape height of 2cm was extracted from this existing dataset for bites on each tooth (incisor, canine, PM1, M1) for use in this chapter. This height was measured using an

automated script (RStudio, Ch. 3, 3.2.1.8 and Appendix 4 for code) which rotated mandibular landmark points while measuring the linear gape between points on the teeth.

Anterior translation of the mandible at a given gape angle was also calculated. The length of the glenoid was used to determine the extent of anterior translation. This length was measured as the distance from the deepest point of the mandibular fossa to the most anterior point on the articular surface of the glenoid (Terhune, 2011). A proportion of the length relative to degree of jaw opening was then applied as anterior translation to the mandible. A maximal degree of jaw rotation had to be determined in order to calculate the correct proportion of glenoid length for translation. For all specimens 40 degrees was taken as a maximal degree of jaw rotation: this value is an estimate of maximum functional gape (as reviewed in 3.1.1). Numerous primates can attain considerably higher maximum gape, up to approximately 74 degrees in male African primates (Herring and Herring, 1974; Hylander, 2013). However, the functional range of gape is thought to be considerably lower, between 28-55 degrees for optimal gape in different primate species (Eng et al., 2009). As such, 40 degrees was taken as an estimate of maximum functional gape range for this study. After rotation, the mandible was anteriorly translated a proportion of the glenoid length relative to the degree of jaw opening, taking 40 degrees as the maximum opening. In practice this meant that if the mandible was rotated 20 degrees, the mandible was then translated anteriorly by 50% of the length of the glenoid. This simplified estimate allowed standardisation while replicating the natural state of translation and rotation in jaw opening.

## 4.3.4.1 Simulation of gape: virtual to physical

The physical models required additional adjustment after attachment to the machine and rotation on the rig. The rig had a different centre of rotation than the virtual models used to produce the dental models, with the result that mandibular dental models were not aligned to the maxillary model after rotation was applied. The mandibular dental model was translated to restore it to the correct position. A to-scale image of the virtual models in Avizo positioned in the correct rotation and translation position was taken and used as a guide for alignment (Fig 4.10). The flat plates on both the virtual and physical models

permitted precise alignment using the translation component of the testing rig. The distance translated was recorded for repeatability.
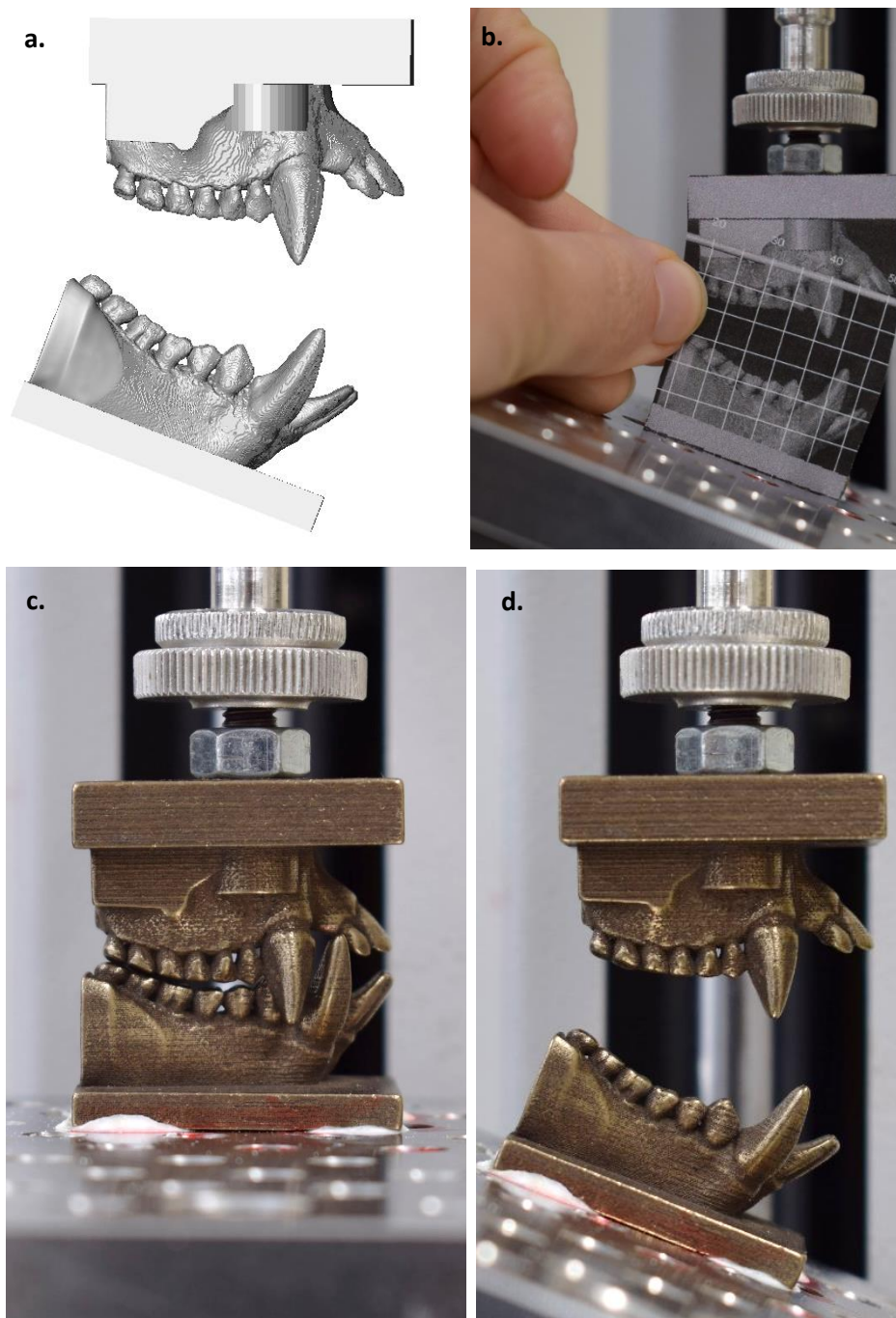


**Figure 4.10 Recreating physical gape height using virtual dental model using *Chiropotes* 406582. Showing a. virtual dental model at linear gape height of 2cm for incisors; b. scaled and printed image of virtual dental model printed and held to physical model to guide alignment; c. physical dental model closed and in occlusion; and d. physical dental model at linear gape height of 2cm for incisors, aligned to position using printed guide.**

## 4.3.5 Selection of food

In order to simulate biting on a large hard food item two option were available, to use a real large hard seed (similar in size and properties to those consumed by the primates in this study) or to use additive manufacturing to create repeatable prints of a standardised large sphere. Synthetic food replicas have the advantage that they can be manufactured so that each piece is identical in shape and material properties, removing some of the noise in testing (Berthaume et al., 2010; Crofts and Summers, 2014; Swan, 2016). However, synthetic foods cannot capture the complexity of real seeds, which consist numerous layers with differing material properties (Lucas et al., 1994; Lucas, 2004).

Pilot studies were conducted using the physical testing machine and one of the dental model sets (*Sapajus*). This dental model was used to test force to fracture and fragmentation behaviour in a selection of real seeds (hazelnut, Brazil nut, and pecan) and 3D printed seed replicas in the form of 2cm diameter spheres made using additive manufacturing (Zprint 350, 3D Systems). Interestingly all the real seed types were found to have advantages over 3D printed seed replicas in pilot testing. 3D prints broke slowly, with extensive deformation, which resulted in deflection of the machine head and attached maxillary dental model, potentially affecting results (Berthaume et al., 2010). The various seeds types deformed less and were more brittle, resulting in less deflection. Additionally, the real seeds were easier to place on the teeth and were more easily gripped than the 3D printed foods. This improved repeatability and reliability of results, increasing test speed. Real seeds also had a lower cost of procurement and lower preparatory time which allowed for a much larger number of repeats to be carried out.

Of the real seeds tested, pecans were found to perform most consistently in an additional study, with the lowest standard deviation (data collected in collaboration with Mariana Fogaça, and see Appendix 7 for plot of results). Pecan size (mean diameter = 20.79 mm, SD = 0.88; mean length = 40.7 mm, SD= 2.9; n = 150) is also close in shape and size to food items in the diet of some hard object feeders. This includes the *Sacoglottis* seed (mean diameter 24mm, mean length 32 mm, n = 9; McGraw et al., 2011) eaten by *Cercocebus*, the *Astrocaryum* palm seed (mean diameter = 28 mm, mean length = 46 mm, n = 12; Visalberghi et al., 2008) eaten by *Sapajus* (Terborgh, 1984), and the Brazil nut (mean diameter =23 mm,

mean length =39 mm, n =150) eaten by *Cacajao* (Norconk et al., 2013)*.* The Brazil nut was considered for this study but was found to have a much less consistent performance than the pecan (Appendix 7). Other hard seeds and fruits eaten by primate seed predators can be much larger in diameter than pecans, up to 220 mm in *Chiropotes* (Norconk et al., 2009)*.* However, such foods are only processed on anterior teeth and would not provide a suitable comparison for posterior bites, nor was it possible to gain access to these seeds for a UK-based study. As such pecans were used as the test food object in this study (Fig. 4.11).



**Figure 4.11 Pecan seed external and internal morphology. Showing (from top) intact external seed, internal seed wall through longitudinal and transverse section, hollow seed casings showing internal divisions in seed, and pecan seed outside of shell.**

## 4.3.5.1 Seed preparation

Unshelled pecans (*Carya illinoinensis*) used in this study were sourced from Scarlett's Parrot Essentials UK. All pecans were from the same recent crop and stored together in dry warehouse conditions prior to shipping. To improve consistency and homogeneity in testing all pecans were visually examined. Any pecan with a visual deformity was removed from the sample, as this could indicate rot or damage to the seed during transportation, both of which could affect results. Pecans were numbered, measured and their length and diameter recorded (Fig. 4.12). The line at the join of the seed on both sides of its longitudinal axis, termed 'the sulcus', was identified. This sulcus line was marked on one side. The centre point along the longitudinal axis was marked on both sides. This enabled consistent seed positioning during testing (Fig. 4.12).



**Figure 4.12 Preparation of foods for physical testing. Showing (left) seeds randomly selected from a large quantity, then measured. A line is drawn along the sulcus and a marking was made halfway along the length of the seed on both sides to aid in placement. Seeds laid out after measuring, drawing centre-point and sulcus line, and numbering (right).**

### 4.3.6 Biting positions: seed placement

Four bite positions were tested: One each on the incisors, canines, premolars, and molars (Figs. 4.13 – 4.16). For each bite point the marked sulcus line was placed facing the mandible. The marked centre points on the seed were aligned to pre-determined positions for each bite point in order to standardise seed position. Seed position was standardised because past work has indicated that seeds are not homogenous in their material properties: the region from which the cotyledon sprouts has a different microstructure to other parts of the seed in at least some seeds (Lucas et al., 1994).

In all bite positions the seed was positioned with the sulcus marking facing the mandible. For the incisor bite position the seed was placed with the sulcus marking between the left and right lower first incisors (Fig. 4.13). For the canine bite, the upper and lower canine tips were placed on the centre point markings on the seeds (Fig. 4.14). The premolar bite was centred between the first and second mandibular premolars, positioning the seed at the most distal premolar position possible (Fig. 4.15). It is noted that catarrhine and platyrrhine primates differ in their number of premolar teeth (as reviewed in Ch. 1, 1.2.3). For consistency, the first premolar in all species will henceforth be referred to as PM1. The canine shape restricts anterior food placement on the premolars in some species (Fig. 4.15). The molar bite was centred on the mandibular M1 (Fig 4.16). The large gape needed to place the seed on M1 excluded smaller specimens from this test. Seeds were consistently placed on *Ateles, Mandrillus, Pan,* and *Theropithecus* and placed partially on *Cebus* and *Sapajus*, for whom some seed placements failed, resulting in slippage.
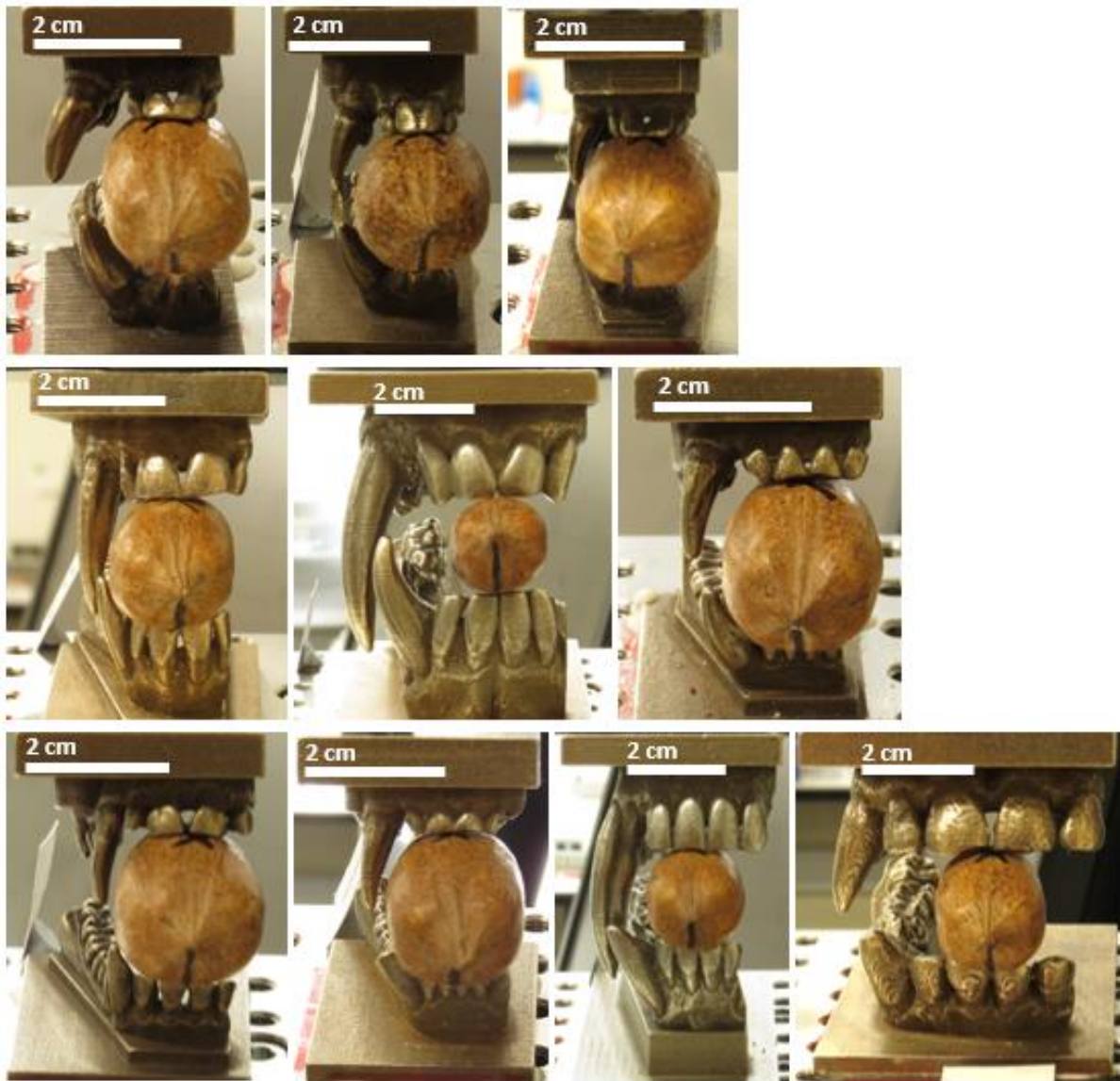
**Figure 4.13 Seed placement for incisor bites. Showing, from top left:** *Cacajao, Chiropotes, Pithecia, Cercocebus, Mandrillus, Sapajus, Ateles, Cebus, Theropithecus, Pan*. **Scale bar marks 2cm. The centre point along the sulcus marking was placed directly between the lower first two incisors. The upper seed centre point was placed as close to being between the upper first two incisors as was possible without altering the lower alignment.**
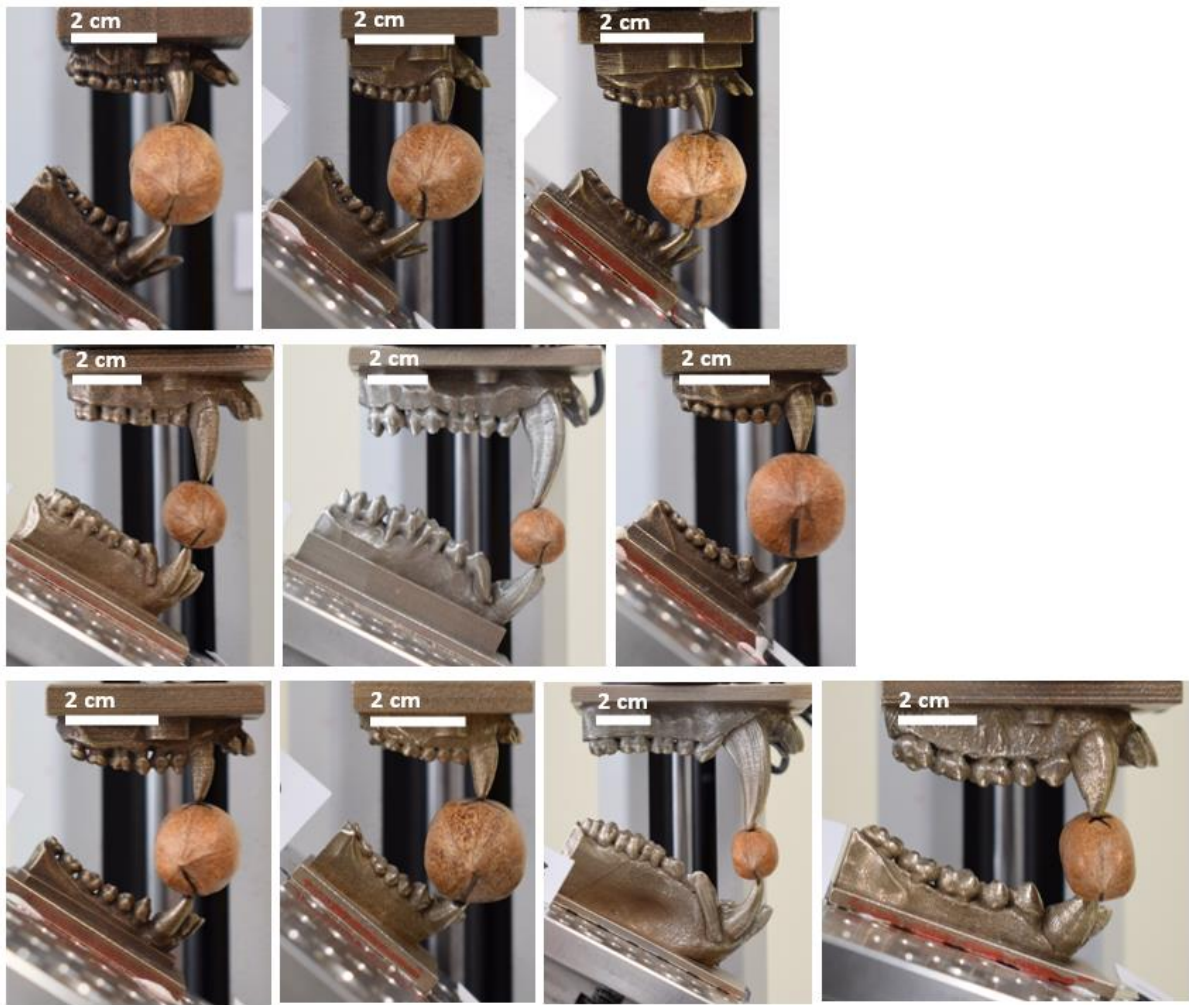
**Figure 4.14 Seed placement for canine bites. Showing, from top left** *Cacajao, Chiropotes, Pithecia, Cercocebus, Mandrillus, Sapajus, Ateles, Cebus, Theropithecus, Pan*. **Scale bar marks 2cm. The sulcus line and centre point were aligned to the mandibular canine tip, the upper seed centre point was placed as close as possible to the upper canine tip without altering lower alignment.**
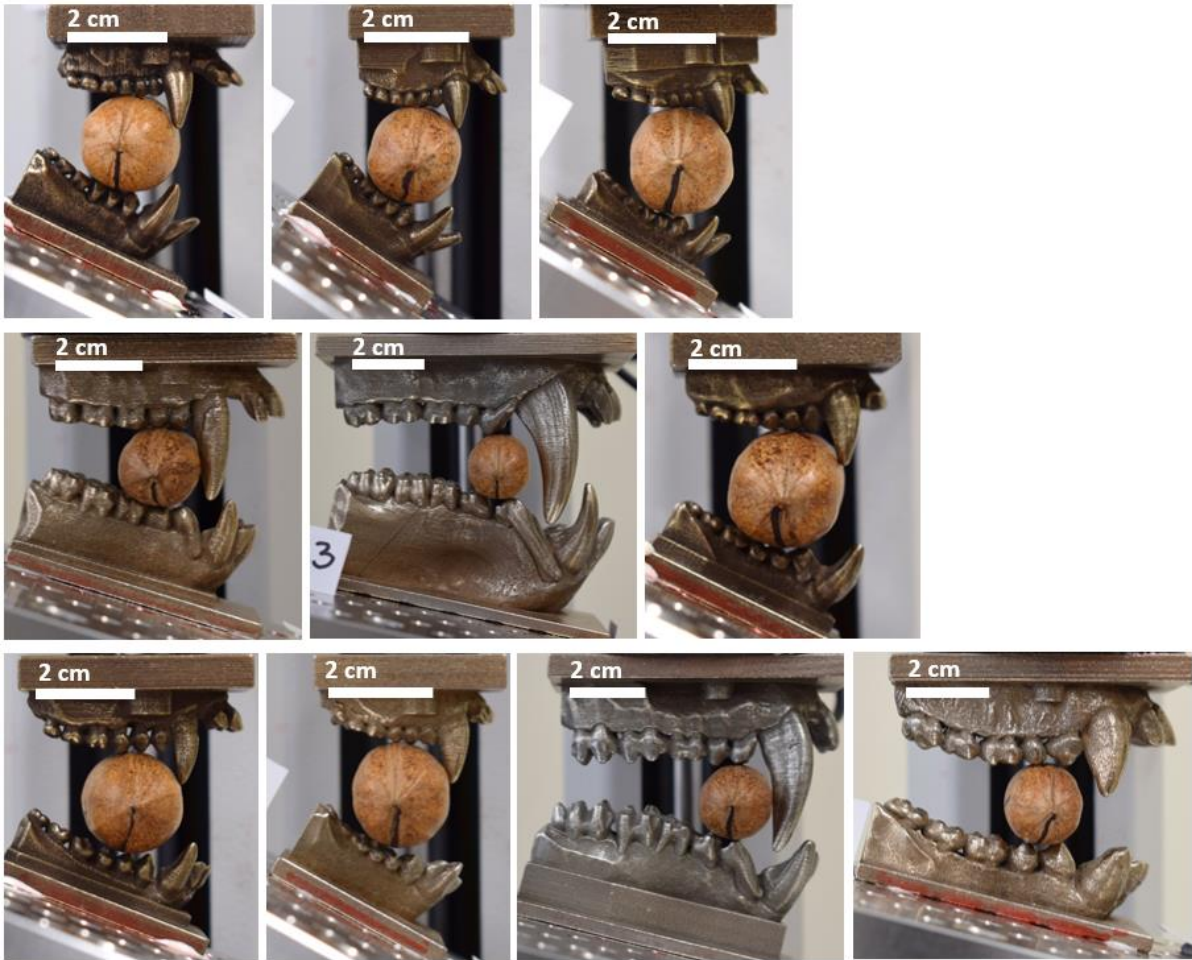
**Figure 4.15 Seed placement for premolar bites. Showing, from top left: *Cacajao, Chiropotes, Pithecia, Cercocebus, Mandrillus, Sapajus, Ateles, Cebus, Theropithecus, Pan* Scale bar marks 2cm. The centre point along the sulcus marking was aligned between the first and second lower premolars, although canine position limited anterior placement on some specimens, notable on *Ateles.* The opposing centre point was aligned towards the first and second maxillary premolar without altering the mandibular alignment.**
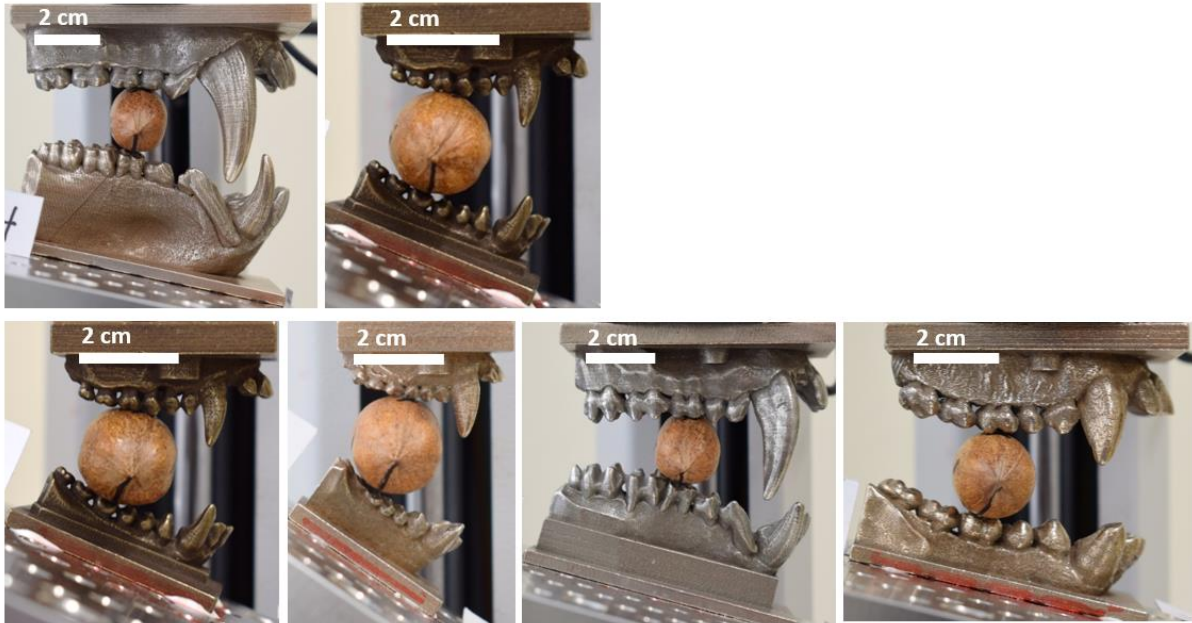
**Figure 4.16 Seed placement for molar bites. Showing, from top left _Mandrillus, Sapajus, Ateles, Cebus, Theropithecus, Pan._ Note that this seed placement was only possible on these specimens. Scale bar marks 2cm. The marked sulcus centre point was aligned to the mandibular M1, and the opposing centre point was aligned as closely as possible to the maxillary M1 without altering the mandibular position.**

## 4.3.7 Data collection

For incisor and premolar bites 30 repeats were made. Pilot testing revealed challenges in placement when testing on canine and molar. In both cases seed placement was challenging and time-consuming. As such, 10 repeats were made on these bites. In total there were 80 tests per specimen, totalling 800 tests in total.

## 4.3.7.1 Physical testing

The physical testing machince used for this experiment (Mecmesin MultiTest 2.5-_i_) consists of a crosshead which is lowered to compress the test object. Force and displacement are recorded. The machine runs on a test program which determines its speed, as well as the conditions to end each test. The crosshead speed for all tests in this experiment was set to 10 mm/min. A range of speeds have been used in past physical testing experments, and the value used is often not reported (Berthaume, 2016). Primate seed predation speed is virtually unknown, but limited video evidence and observations indicate that this is a slow and careful process (McGraw et al., 2011; Norconk et al., 2013) and seed predation in primates has previously been modelled as a static load (Lucas et al., 1994). As such, a speed

which is relatively slow was selected. 10 mm/min is faster than the 5 mm/min used in the first primate seed predation physical testing study (Lucas et al., 1994) but is the lowest speed used while testing a range of food objects (Williams et al., 2005).

The test program for running the physical testing machine was set to allow tests to run to the point of fracture without continuing to run beyond the point of fracture. This design prevented continued crushing of the seed after initial fracture. Following extensive pilot testing several halting conditions were set up in the test program. The main test-halting criteria was the break percentage, which is calculated by measuring the drop in force relative to maximum force during a test. At a drop in force equal to or greater than 40% of the total force the test was halted. Pilot testing determined that this value captured the vast majority of initial fractures. This test program was used for all tests. Additionally, all tests were automatically halted at 2000 N for safety reasons, as this value approaches the limits of the load cell. A displacement limit was also set, and all tests automatically halted after reaching a displacement of 4mm. This displacement limit was chosen for multiple reasons. The experiment was designed to model static loading during seed feeding, as has previously been tested for primates (Lucas et al., 1994). As such the experiment was not designed to model natural jaw kinematics with mandibular translation during jaw closing (Iriarte-Diaz et al., 2017), instead modelling initial dental contact and fracture. A consequence of this design was the risk of the upper and lower third molars coming into contact on some specimens with high gape. As such the 4mm displacement served as an additional safety limit to prevent this potentially damaging contact. However, this limit was rarely met as pilot tests found that the majority of seeds fractured at < 4mm.

During testing the force and displacement values were recorded using the software associated with Mecmesin's physical tester, Emperor (v.1.18-408, Mecmesin, UK) at a sampling rate of 1000 Hz. These values were then exported as raw data for further analysis. The key value of interest to this study was the force at initial fracture (Fig. 4.17). The displacement at force to fracture, the depth to which the cranium plate was pushed into the seed was additionally recorded and exported (Appendix 8; Figs. A7.1-A7.4 and data tabulated, Table A7.1).
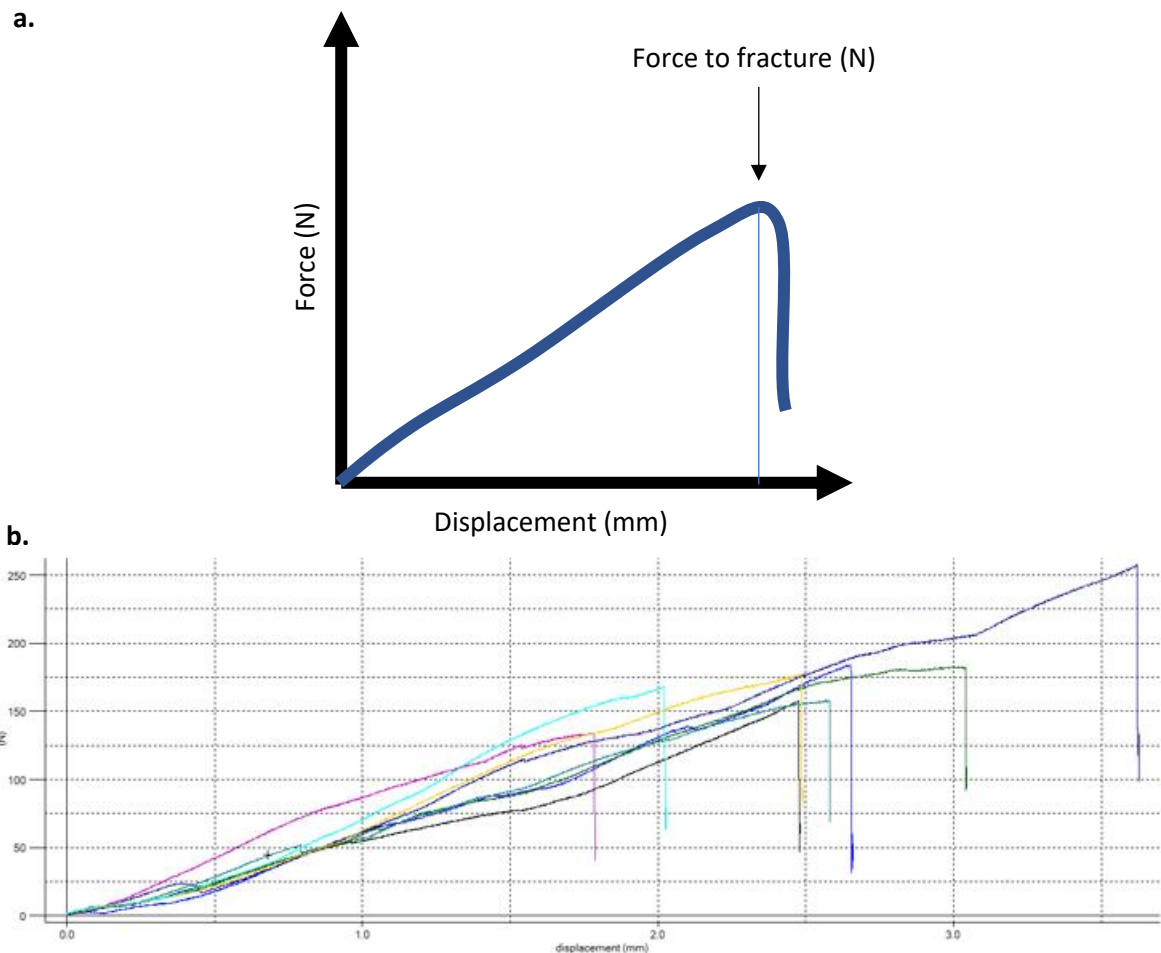
**Figure 4.17 Values measured during physical testing. Showing a. schematic of force-displacement plot as produced by the machine, highlighting force to fracture and b. graph of force-displacement data as it appears in the testing system, showing data for *Cercocebus* on incisor.**

Seed placement during data collection required minor adjustment as a result of the natural variations in seed width. This was because gape angle was calculated for precisely 2cm, but because pecan diameter ranged from 1.81cm – 2.29cm (n = 150 seeds) the fit at 2cm with most seeds was not perfect. The maxillary dental row, attached to the machine crosshead, was raised or lowered to fit the seed. All movements were recorded and reset after each test. Additionally, to prevent slippage of the seed in the initial test stages, the maxillary dental row was lowered to the point of 'grip' with the seed, meaning light force contact. The force used for gripping was recorded for each test, and in no case exceeded 5N.

Every test was photographed from a frontal and lateral view before the test was carried out. Additionally, each completed group of fractured seed repeats for each bite point on each specimen was photographed. Video recordings were made of some tests, randomly selecting a pre-determined number of samples on each biting position for each specimen

(random sample selection for recording using random.org, Randomness and Integrity Ltd. Services, 2019). The higher number of repeats for incisor and premolar bites led to a higher number of recordings for those bites (n = 4 videos per bite position and per specimen) and fewer for canine and molar bites (n = 2 videos per bite position and per specimen).

## 4.3.7.2 Fragmentation quantification and test fail conditions

Fragmentation was recorded during testing by noting and drawing fracture type to ensure that the tests recorded represented a fractured seed. Each seed was evaluated on the following criteria: no crack (no damage, sample was not fractured, no clear fault with seed – see below), crack (a crack was propagated in the seed) and pierced (seed shell punctured with a hole but crack not propagated). It has been shown that individuals may use different methods for accessing hard walnut seeds, as some macaques initiated walnut access with large cracks and others with a "hole-punch" pierce in the shell which was then expanded (Tamura, 2020). As such both the crack and pierce breaks were considered an initial fracture in the results, but these fragmentation types are distinguished as they represent different access modes. 'No crack' results are also recorded as primates are known to attempt fracture and reject some seeds, although the reason for the rejection of specific seeds is generally not known (Terborgh, 1984; Geissler et al., 2020). As these attempts did not result in fracture they could not be statistically evaluated. All break types were recorded directly following tests, and a drawn record of the fracture line was made.

A small number of tests had to be removed from the sample due to occasional faults with the seeds. Seeds were inspected (as described in 4.3.5.1) but some seed defects were missed in the initial inspection. If the seed performed in a manner indicating a seed fault (instantaneous or near-instantaneous low force break along a clear line) it was removed from the sample after inspection for the fault origin. Taken together, these faults comprised a total of 18 tests which were removed from the sample.

## 4.3.7.3 Contact surface area

The contact surface area of each tooth during biting was estimated using a 3D model of a pecan seed of average size. This representative seed model was made using photogrammetry (PhotoScan Professional, Agisoft LLC) to create a virtual replica which

could be fit to virtual dental models. In order to validate the fit between seed and dentition in the virtual models the seed was also 3D printed (Zprint 350, 3D Systems) and fit to the physical dental replicas matching the positions of the real seeds. The 3D printed seed was placed on each bite point for each physical dental model and photographed. The physical testing machine was then run to a displacement of 1mm for a 3D print on each bite point. The dental imprints made by the teeth onto this pliable 3D printed material were recorded using photography, drawing, and written description.

To estimate contact surface area, virtual dental models were rotated and translated to the positions used in testing in Avizo. The seed model was warped to each bite point using two landmarks placed at the centre points on the longitudinal axis along the sulcus. The photographs of the 3D printed seed positioned on the physical dental model were used to guide additional rotation to the correct orientation on the virtual models (Fig. 4.18). Models with the seed correctly positioned were exported to Geomagic and the upper and lower dental rows were each displaced 0.5 mm into the seed, for a total of 1mm displacement. This depth was selected to show the initial contact of the teeth with the seed. The seed was clipped to expose the dental area in contact with the seed at this displacement teeth (Fig 4.18). This area was segmented and its surface area ($mm^2$) measured. This virtual dental contact surface area was compared with the dental imprints made on the 3D printed seed which was tested on the physical models to ensure the virtual method reflected the physical contact. Given the challenges in seed placement for the molar bite contact surface area was not calculated for this bite.
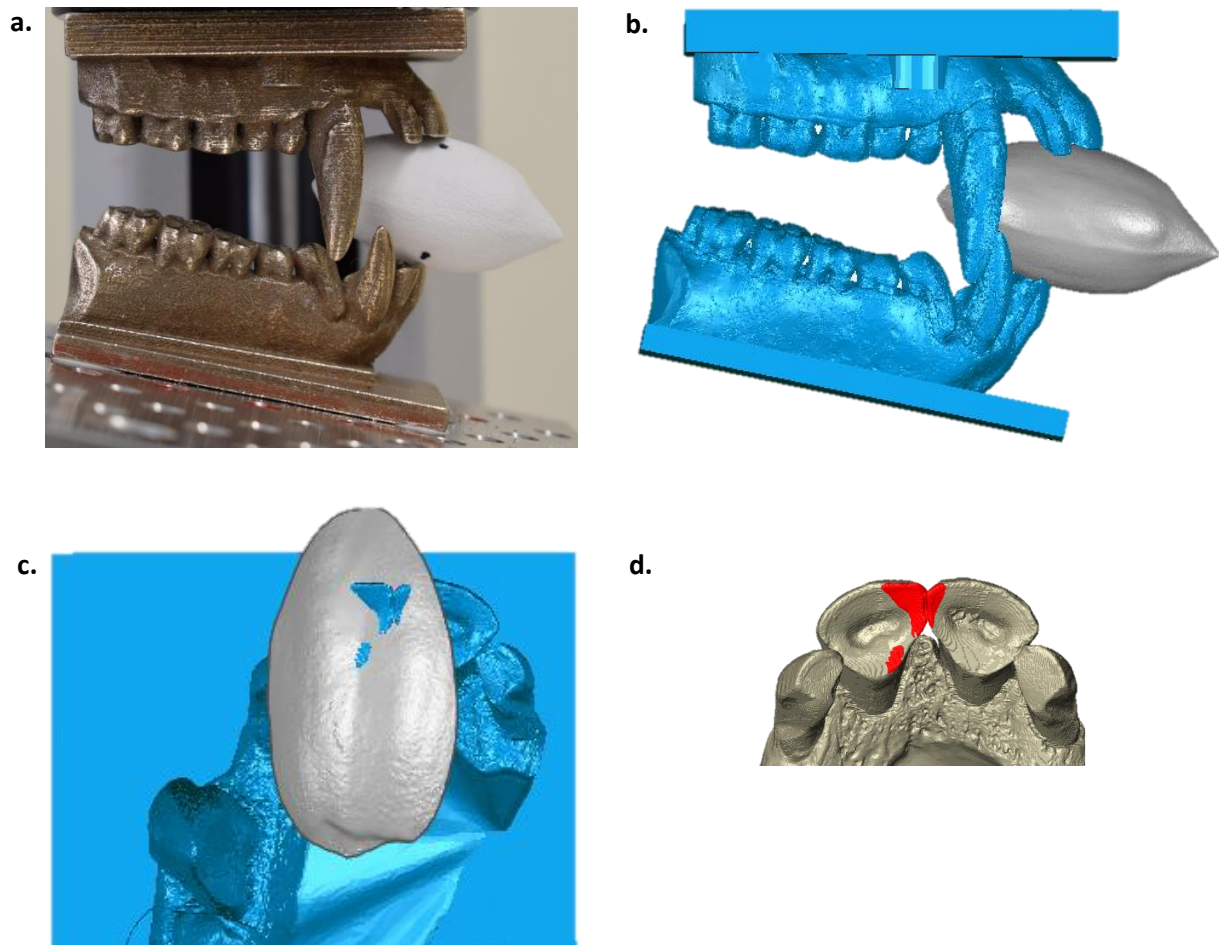
**Figure 4.18 Contact surface area measurement process, shown on *Cercocebus*. Images show a. 3D printed pecan is placed for an incisor bite, image used to guide virtual model placement; b. virtual models of the teeth and the pecan are positioned to match the physical model; c. after displacing the teeth 0.5 mm into the pecan, the pecan is clipped to the surfaces which penetrate the seed (inferior view of maxillary teeth shown); and d. after segmenting this area, it can be overlaid on the virtual dental models, here showing contact surface area on maxillary incisor bite.**

## 4.3.8. Data analysis

The force to fracture data was extracted semi-automatically. The majority of samples had a sufficient drop in force at the moment of fracture that the break percentage of the test program correctly halted the test at peak force. In this case, the value could be automatically extracted using RStudio (v1.1.442, RStudio Team 2016). However, in some cases the seed fractured but force did not drop sufficiently to halt the test and the force continued to rise meaning that the highest force recorded was not the moment of first fracture. These instances were noted during testing and correct values were manually

extracted using Emperor by extracting the highest force at initial fracture. Timestamps of audio and visual observations of fracture recording during data collection as well as the drop in force following fracture recorded by the testing software facilitated the extraction of this data. Displacement at peak force was extracted in the same manner. Displacement was recorded and exported and include as an appendix (Appendix 8) for reference.

Before further analysis was carried out the force results were scaled to account for the possible effect of pecan size on force. Measurements of pecan size (length x width) were recorded at the point of data preparation (4.3.5.1). Each force result was then divided by the size of the pecan. Scaled force results are displayed alongside a table showing unscaled (raw) force to fracture results.

Additional processing, statistical testing, and visualisation of force and displacement results was carried out in RStudio (v1.1.442, RStudio Team 2016), using the packages ggplot2 (Wickham, 2016), dplyr (Wickham et al., 2021), tidyverse (Wickham et al., 2019), car (Fox and Weisberg, 2019) and moments (Komsta and Novomestky, 2015). Statistical testing was only carried out on the incisor and premolar data as the molar and canine sample sizes were too small (see 4.3.7). Normality of the scaled force data was assessed using a Shapiro-Wilk test which showed that not all data was normally distributed: the results for the incisor tests showed a positive skew. This was corrected with a log 10 transformation. Levene's test for equality of variance indicated that both the incisor and premolar data were also not homogenously variable. As such, independent samples t-tests which do not assume equal variances (Welch's t-test) were used to make comparisons between groups. The groups of interest for these tests were based on diet and feeding position. All seed predators were compared to the sample with non-seed diets for the first test. For the second test, only those seed predators for which the tooth dataset being tested represents the tooth most often used in their diet (i.e. anterior feeders on incisor) were compared against primates which do not eat seeds. Following these tests, further comparisons between individual species were conducted using pairwise comparisons with Welch's test. A Bonferroni correction was carried out to adjust for potential errors in multiple comparisons (critical alpha $p$ = 0.05). Outliers, values which were either above or below 1.5 times the interquartile range (n = 17), were removed from the force data ahead of statistical testing. Significance test and reports on data values were calculated based on results with successful

crack propagation. This means that while results with only a pierced seed and no crack propagation were recorded and reported these results were not used for significance testing because they do not reflect crack propagation. An exception was made for reporting canine values because the majority of results were pierced with no crack propagation, however in this case the small sample size precluded statistical testing.

## 4.3 Results

It was predicted that seed predators will require a consistently lower force to fracture than primates with other diets on at least one bite position (H1). It was additionally predicted that within seed predators the tooth which facilitates the lowest force to initial fracture will be the tooth most often used to fracture hard seeds in their diet (H2). In order to address these hypotheses results will be examined for each tooth separately, starting with force results (scaled force, Fig. 4.19 – 4.20 and raw force, Table 4.2) and followed by contact surface area measurements (Fig. 4.22 – 4.24 and Table 4.3). Results comprise four bite positions: incisor, canine, premolar, and molar. However, both canine and molar bites were affected by methodological challenges. Only limited results can be presented for these bite positions.

## 4.3.1 Force to initial fracture results on individual teeth

*Incisor:* Across all of the species *Cebus* has the highest mean force to initiate fracture on incisor (194.98N) while *Cacajao* has the lowest (109.83N) (Table 4.2). Between all species, including within seed predators, there is variability (Fig. 4.19). Differences between the seed predator group and the comparison no-seed group are indeed significant (t(221.7)= 2.97, *p* = 0.003). As such, the mean force to fracture is significantly higher in the no-seed group (no seed group mean = 157.41N, seed predator mean = 136.15N – for standard deviations see Table 4.2). This supports predictions for H1 for this bite position.

Further comparisons clarify the source of differences. While the seed predator group has an overall lower mean force to fracture seeds than the no-seed diet group, results are not uniformly spread across seed predators. Posterior-feeding seed predators (*Cercocebus, Mandrillus, Sapajus*) as a group require a higher mean force to fracture seeds (155.56N) than anterior-feed seed predators (*Cacajao, Chiropotes, Pithecia*; 116.96N) regardless of whether they are intensive or occasional seed predators (Fig. 4.19, Table 4.2). The mean force to fracture for anterior-feeding seed predators is also significantly lower than the force required by the no-seed group (t(157.4) = -6.49, *p* < 0.000). This also highlights the lower mean force to fracture in the anterior-feeding seed predator group relative to the posterior-feeding seed predators. Posterior-feeding seed predators have a near-identical mean to initiate fracture to the non-seed feeder group (155.56N for posterior seed feeders, 157.41N

for no-seed feeders). Notably, the intensive seed predator *Cercocebus* has a higher mean force to fracture (155.58N) than the majority of the sample and groups closely with posterior-feeding occasional seed predators *Sapajus* and *Mandrillus*.

Additional comparisons between individuals are necessary to further understand differences between groups. The lowest mean force to fracture in the sample on incisor is found in *Cacajao* (109.83N), followed by *Chiropotes* and *Pithecia* which are near identical (120.98N and 120.42N, respectively). However, the values for *Chiropotes* and *Pithecia* are also near identical to results for *Pan,* which is not a seed predator but has the fourth lowest mean force to fracture in the sample (128.07N). Pairwise comparisons confirm that the differences between both *Chiropotes* and *Pithecia* with *Pan* are not significantly different (*Chiropotes*: $p$ = 1; *Pithecia*: $p$ = 1). Although *Cacajao* does have a somewhat lower mean force to fracture than *Pan* this difference is also not significant ($p$ = 0.403). The difference in force between *Cacajao* and *Ateles* is significant ($p$ = 0.007), but the difference is not significant between *Chiropotes* and *Ateles* ($p$ = 1) or *Pithecia* and *Ateles* ($p$ = 0.84). As such, although the data fail to falsify the predication made by H2, as anterior-feeding seed predators do outperform the remaining sample on incisor, the differences between groups are not significant in all cases.

These results also highlight the broad range of force to fracture observed in non-seed predators for bites on incisor. Notably especially *Cebus* required a very high mean force to fracture seeds and has very variable results (SD = 64.13). By contrast, *Cacajao* shows the most consistent fracture of the sample with the lowest variability in force to initiate fracture on incisor (SD = 23.73). This pattern does not hold for all anterior seed predators, or all seed predators as a group (Table 4.2). Fracture mode is also not necessarily more consistent in seed predators. Across the sample only a very small number of seeds were not cracked (n = 5, Table 4.2), but *Cacajao* and *Chiropotes* each have bites in this category. *Cacajao* and *Chiropotes* also had more variable fracture, with especially *Cacajao* having a notably high proportion of pierced seeds (Table 4.2). This goes against predictions of consistent fracture mode in all seed predators (H1).

*Canine:* As stated above, due to methodological challenges only limited results will be presented for the canine. Across all of the species *Cercocebus* has the highest mean force to initiate fracture on canine (68.6N) while *Cebus* has the lowest (53.45N), however these means span a small range (Fig. 4.19, Table 4.2). The mean force to initiate fracture required by the seed predator group (61.6N, SD = 14.64) is near identical to that required by the no seed group (60.24N, SD = 11.14). This result does not support H1, as seed predators do not have a lower force to initiate fracture than non-seed predators. The mean force to initiate fracture is slightly lower in the anterior-feeding group (58.95N, SD = 11.25), but the mean force to initiate fracture on canine is extremely similar across all groups. As such these results also do not support H2.

A closer examination of the individuals within each grouping highlights that there are differences within categories which obscure any clear trends. Anterior-feeding seed predator *Cacajao* has a low mean force to fracture relative to the majority of the sample (Table 4.2, 52.25, SD = 9.14), while another anterior-feeding seed predator, *Chiropotes*, has one of the highest mean values of the sample (67.68N, SD = 6.73). The differences between these two primates in the same dietary group also shows the lack of clear pattern for canine bites and the small range in results on this bite position. Notably a large number of bites on this tooth, across the full sample, did not result in a fracture of any kind, and a relatively high proportion of results were pierced without crack propagation (Table 4.2).

*Premolar:* Across all of the species *Pithecia* has the highest mean force to initiate fracture on the premolars (166.22N) while *Mandrillus* has the lowest (94.7N). Results are variable between all species, including within seed predators (Fig. 4.20, Table 4.2). Differences between seed predators (all) and comparison no-seed group are not significant (t(201.8)= -1.21, *p* = 0.227). The mean force to fracture in each group is nearly identical, although the seed predator group mean (141.46N) is slightly higher than the no seed group mean (140.9N). This does not meet predictions for H1. Further comparisons are however necessary in order to examine the distribution amongst individual primates. Although the posterior seed predator group requires a slightly lower mean force to initiate fracture (136.74N) than the no-seed group (14.0.9N), these means are near identical. The differences between these groups are not significant (t(148.6)= -1.16, *p* = 0.248). This finding does not support H2.

However, as was also the case with the incisor bite these group comparisons mask individual differences in the sample. By having the lowest mean force of the sample (94.7N), the performance of posterior-feeding occasional seed predator *Mandrillus* supports predictions for its diet. The second-lowest mean force to fracture of the sample is seen in the no-seed group by *Theropithecus* (115.75N). Although *Mandrillus* requires a lower force, the difference between *Mandrillus* and *Theropithecus* is not significant ($p = 1$). The remaining no-seed group require relatively higher force to initiate fracture. However, it is noteworthy that the highest force to fracture in the no-seed group (*Ateles,* mean = 161.06N) is nearly identical to mean force to fracture in the remaining posterior-feeding sample (*Cercocebus* 158.89N and *Sapajus* 157.39). These values are also nearly equal to the highest force to initiate fracture in the entire sample, observed in intensive anterior-feeding seed predator *Pithecia* (166.22N). *Mandrillus* is therefore the only specimen to conform to predictions on this bite, although it is an occasional seed predator while *Cercocebus*, which required a relatively high force to initiate fracture, is an intensive seed predator.

Despite the low force performance by *Mandrillus* on premolar bites, the fracture performance on this tooth is not consistent. *Mandrillus* has a near equal split between cracked and pierced seeds (Table 4.2) indicating not all the seeds were fractured in the same manner despite the low force. *Theropithecus,* in the non-seed group yet with a relatively low force, also shows an inconsistent fracture behaviour, and notably also had a high proportion of seeds with neither a crack nor a pierce propagated (Table 4.2, n = 6). By contrast, the specimens identified above as requiring the highest force to initiate fracture consistently cracked all seeds with no pierces or lack of fracture. This applies both to the seed predators (*Cercocebus, Sapajus,* and *Pithecia*) and the non-seed predator (*Ateles*) with the highest force in the sample.

*Molar:* As stated above, due to methodological challenges only limited results will be presented for molar. Molar bites could not be placed on intensive seed predators, and of the seed predators in the sample could only be placed for the occasional seed predators (*Mandrillus, Sapajus*). The mean force to initiate fracture required by the seed predator group (Fig. 4.20, Table 4.2, 141.5N, SD = 39.07) is lower than that required by the no seed group (157.11N, SD = 44). However, within group performance is not entirely consistent with these group mean comparisons. The highest force to initiate fracture is held by a no

seed diet individual (*Pan*, mean = 175.4N, SD = 52.99), but the lowest force to initiate fracture is also held by a no seed diet individual (*Cebus*, mean = 123.5N, SD = 10.94). As such, results do not support predictions.

Additionally, the type of fracture on M1 bites is variable by species but does not follow a clear trend by dietary category (Table 4.2). Occasional seed predator *Mandrillus* consistently cracked all seeds, while occasional seed predator *Sapajus* had varied results and did not initiate a crack or pierce the shell in the majority (n = 6) of tests. Results also vary in the no-seed group (table x), and while most specimens (*Ateles, Pan, Theropithecus*) initiated a crack in the majority of samples, *Cebus* had a relatively high rate of no crack or pierce initiations (n = 3).
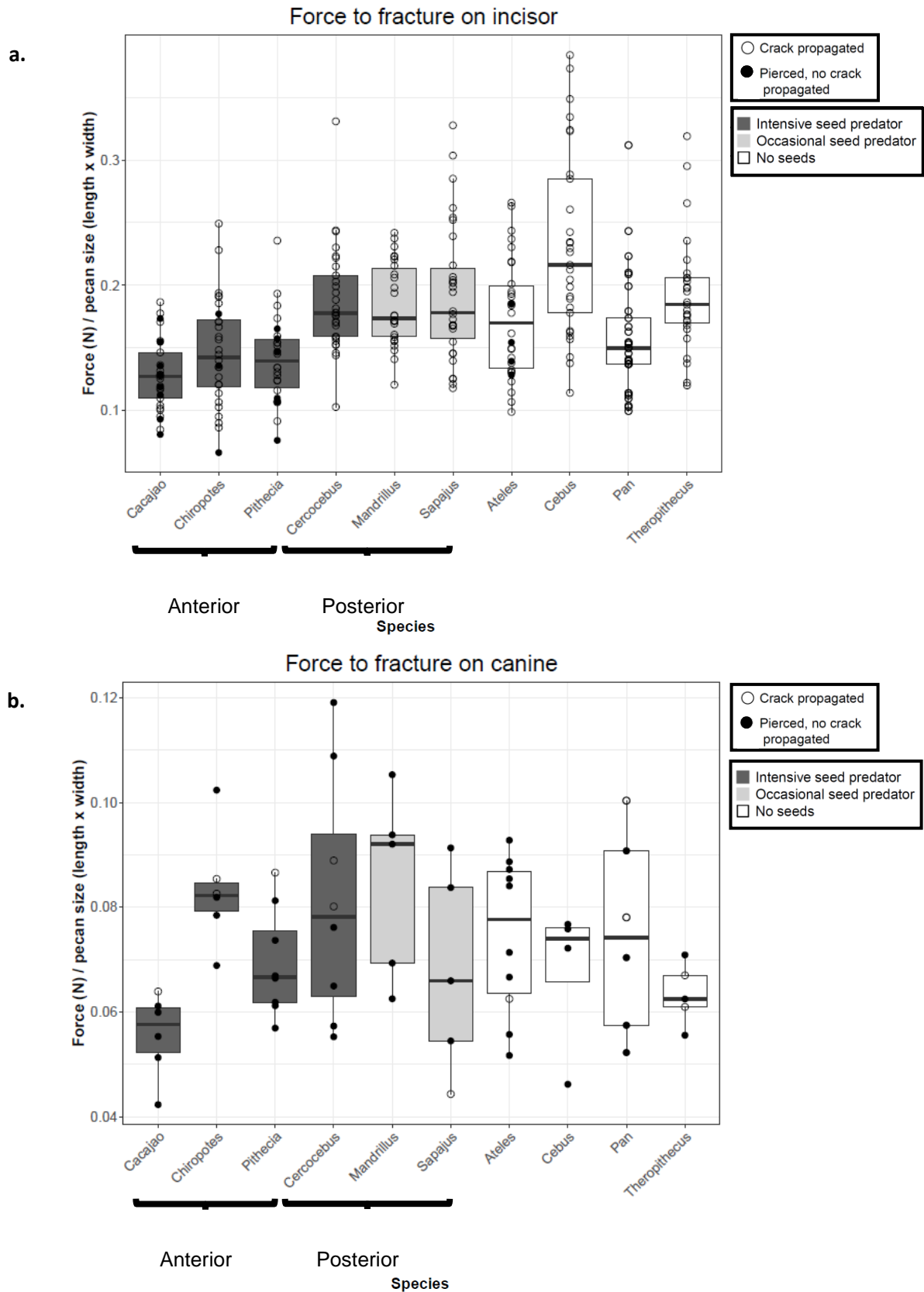
**Figure 4.19 Boxplot showing force to fracture divided by a measure of pecan size on anterior bites (a. incisor and b. canine) for all species. Intensive and occasional seed predators, as well as species with no seeds are denoted by boxplot colour. All test results are included. Samples where a crack was propagated are marked with a clear circle, samples which were pierced without crack propagation are marked with a dark circle.**
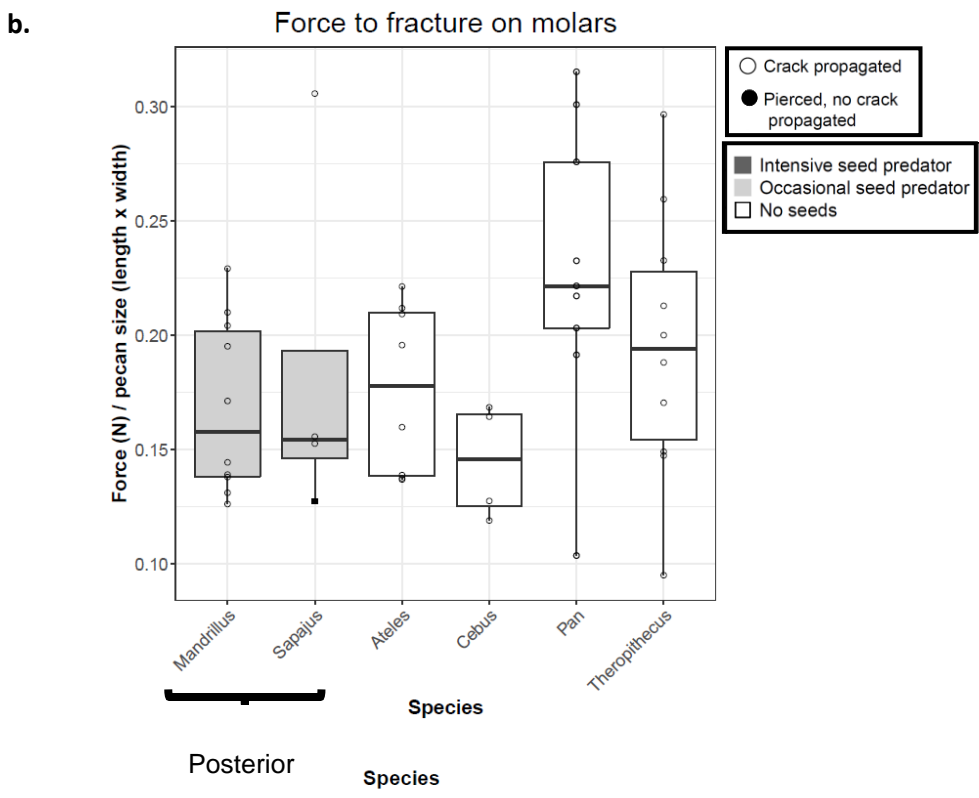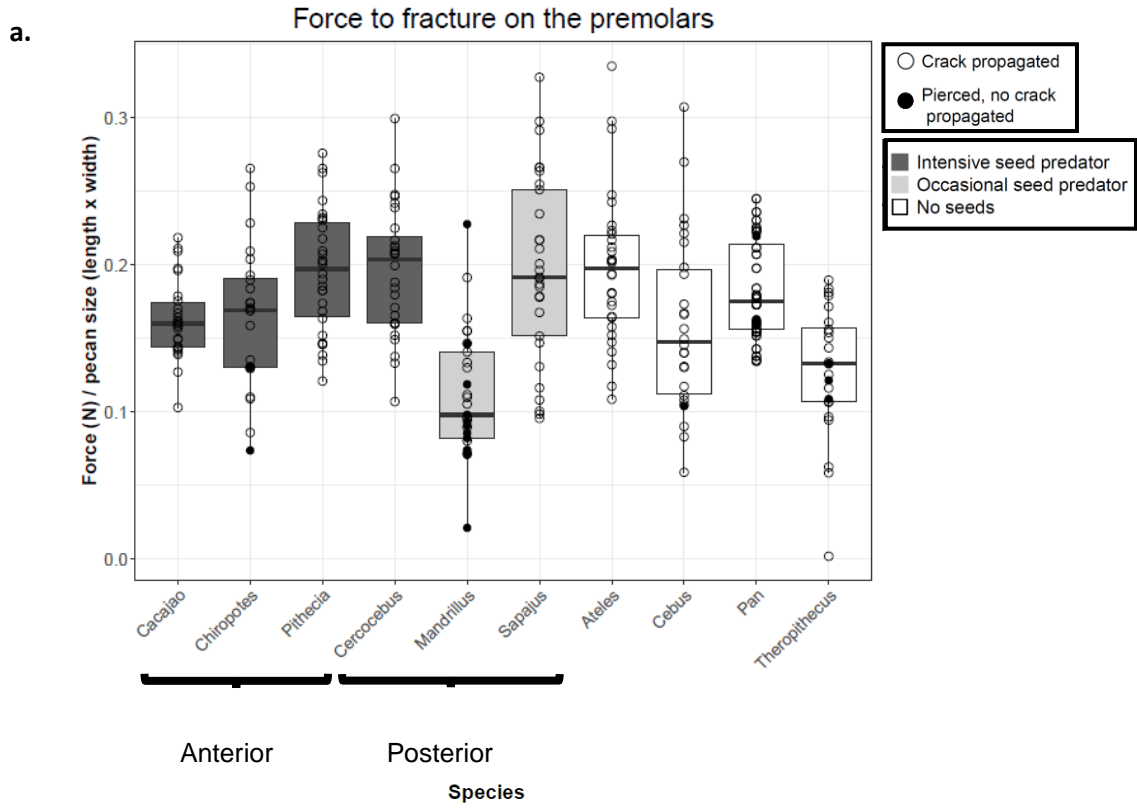
**Figure 4.20 Boxplot showing force to fracture divided by a measure of pecan size on posterior bites (a. premolar and b. molar) for all species. Intensive and occasional seed predators, as well as species with no seeds are denoted by boxplot colour. Samples where a crack was propagated are marked with a clear circle, samples which were pierced without crack propagation are marked with a dark circle.**

**Table 4.2 Mean and median force to fracture (absolute force, in newton), and standard deviation (SD) for each species on each bite point, and quantification of fracture type for each bite point.**

| Species | Tooth | Results: Force (N) | | | Results: Fracture type (count and percentage total successful tests) | | |
|---------|-------|------|--------|-----|-------|--------|----------|
| | | Mean | Median | SD | Crack | Pierce | No crack |
| *Cacajao* | Incisor | 109.83 | 108.60 | 23.73 | 20 (66.6%) | 9 (30%) | 1 (3.3%) |
| | Canine | 49.53 | 52.25 | 9.14 | 2 (20%) | 5 (50%) | 3 (30%) |
| | Premolar | 137.12 | 135.00 | 21.36 | 29 (100%) | 0 | 0 |
| | Molar | NA | NA | NA | NA | NA | NA |
| *Chiropotes* | Incisor | 120.98 | 121.90 | 34.17 | 25 (83.3%) | 3 (10%) | 2 (6.6%) |
| | Canine | 67.68 | 65.75 | 6.73 | 2 (20%) | 5 (50%) | 3 (30%) |
| | Premolar | 132.15 | 121.05 | 37.58 | 24 (88.8%) | 2 (7.4%) | 1 (3.7%) |
| | Molar | NA | NA | NA | NA | NA | NA |
| *Pithecia* | Incisor | 120.42 | 121.30 | 26.48 | 29 (100%) | 0 | 0 |
| | Canine | 59.46 | 55.15 | 10.48 | 3 (30%) | 4 (40%) | 3 (30%) |
| | Premolar | 166.22 | 165.25 | 30.10 | 30 (100%) | 0 | 0 |
| | Molar | NA | NA | NA | NA | NA | NA |
| *Cercocebus* | Incisor | 155.58 | 153.20 | 29.11 | 30 (100%) | 0 | 0 |
| | Canine | 68.60 | 73.20 | 14.29 | 2 (20%) | 6 (60%) | 2 (20%) |
| | Premolar | 158.89 | 160.45 | 29.08 | 29 (100%) | 0 | 0 |
| | Molar | NA | NA | NA | NA | NA | NA |
| *Mandrillus* | Incisor | 153.38 | 149.05 | 25.25 | 26 (86.6%) | 2 (6.6%) | 2 (6.6%) |
| | Canine | 72.38 | 72.30 | 19.94 | 0 | 5 (55.5%) | 4 (44.4%) |
| | Premolar | 94.70 | 93.90 | 29.96 | 16 (55.2%) | 13 (44.8%) | 0 |
| | Molar | 143.63 | 139.55 | 40.26 | 10 (100%) | 0 | 0 |
| *Sapajus* | Incisor | 156.16 | 145.70 | 38.37 | 30 (100%) | 0 | 0 |
| | Canine | 50.18 | 46.90 | 13.57 | 1 (10%) | 4 (40%) | 5 (50%) |
| | Premolar | 157.39 | 158.10 | 48.72 | 29 (100%) | 0 | 0 |
| | Molar | 136.18 | 121.25 | 41.21 | 3 (30%) | 1 (10%) | 6 (60%) |
| *Ateles* | Incisor | 145.44 | 139.15 | 38.14 | 26 (86.6%) | 4 (13.3%) | 0 |
| | Canine | 64.55 | 65.95 | 9.69 | 1 (10%) | 7 (70%) | 2 (20%) |
| | Premolar | 161.06 | 159.90 | 38.27 | 30 (100%) | 0 | 0 |
| | Molar | 150.39 | 158.15 | 26.60 | 9 (100%) | 0 | 0 |
| *Cebus* | Incisor | 194.98 | 183.00 | 64.13 | 29 (100%) | 0 | 0 |
| | Canine | 53.45 | 55.55 | 10.67 | 0 | 5 (50%) | 5 (50%) |
| | Premolar | 129.01 | 133.40 | 39.02 | 25 (83.3%) | 4 (13.3%) | 1 (3.3%) |
| | Molar | 123.50 | 124.45 | 10.94 | 4 (57.2%) | 0 | 3 (42.8%) |
| *Pan* | Incisor | 128.07 | 121.90 | 33.31 | 29 (100%) | 0 | 0 |
| | Canine | 62.85 | 65.05 | 13.42 | 3 (30%) | 4 (40%) | 3 (30%) |
| | Premolar | 151.91 | 149.45 | 23.97 | 25 (86.2%) | 4 (13.8%) | 0 |
| | Molar | 175.40 | 179.80 | 52.99 | 9 (90%) | 0 | 1 (10%) |
| *Theropithecus* | Incisor | 161.86 | 159.50 | 32.71 | 28 (100%) | 0 | 0 |
| | Canine | 53.90 | 52.90 | 8.37 | 3 (30%) | 3 (30%) | 4 (40%) |
| | Premolar | 115.75 | 120.90 | 27.80 | 21 (70%) | 3 (10%) | 6 (20%) |
| | Molar | 157.64 | 152.40 | 48.51 | 10 (100%) | 0 | 0 |

## 4.3.2 Force to initial fracture across all teeth

Force results across multiple bite positions (Figs. 4.19 and 4.20) show that seed predators do not necessarily initiate force at a lower fracture at any one bite position, relative to primates with other diets. Results also do not fully support the prediction that the lowest force to initial fracture would be the tooth most frequently used to access large hard objects. Anterior-feeding seed predators, as a group, have the lowest force of the sample for bites on incisor (Fig. 4.19), and for *Cacajao* and *Pithecia* this feeding position requires a lower force to fracture than the premolar (Fig. 4.21). This is not the case for *Chiropotes*, which requires a near equivalent median force to fracture on incisor and premolar (Fig. 4.21). Posterior-feeding seasonal seed predator *Mandrillus* also meets predictions, having the lowest force to initiate fracture on premolar both within the sample and relative to its own performance on incisor (Fig. 4.21). *Sapajus*, a posterior-feeding seasonal seed predator, does not have the lowest force of the sample on premolar, but does have a lower force to initiate fracture when biting on premolar relative to incisor (Fig. 4.21). Finally, *Cercocebus* meets no predictions, having relatively high force to fracture on all bites and requiring a higher force to initiate fracture on premolar than on incisor (Fig. 4.21).
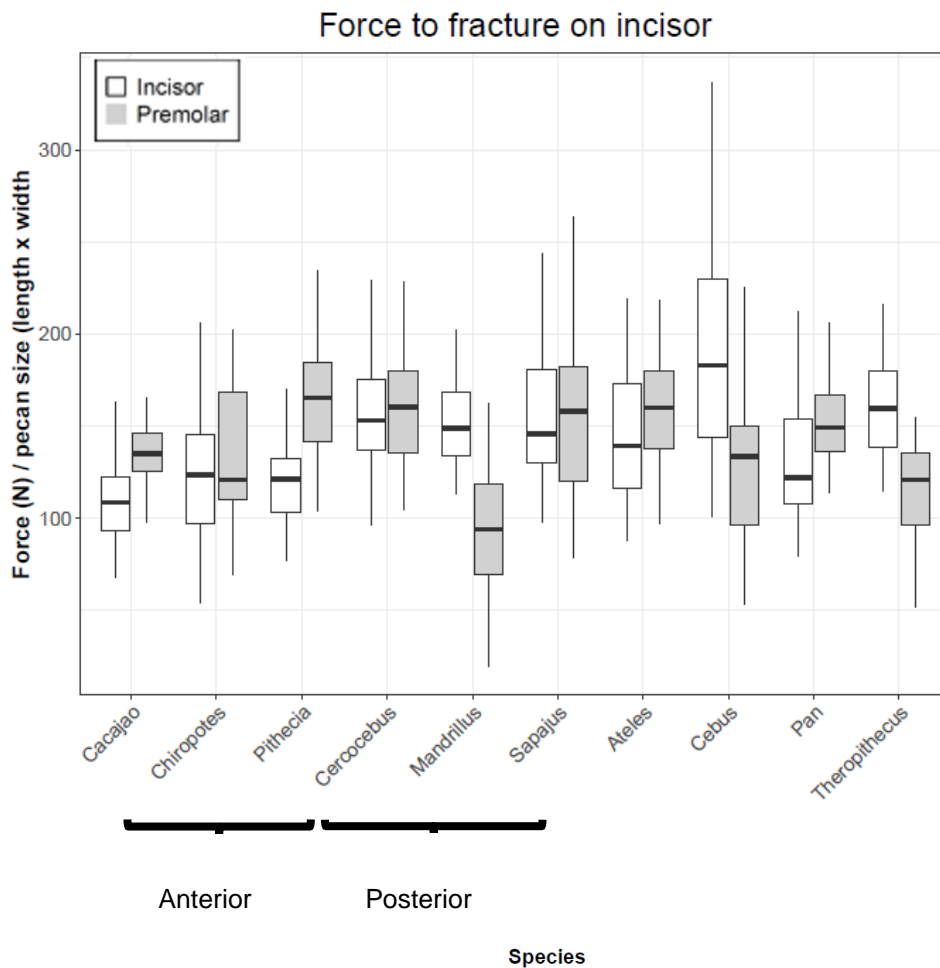
**Figure 4.21 Grouped boxplot showing force to fracture on anterior and posterior bites (incisor and premolar) for all species.**

## 4.3.3 Contact surface area

It was predicted that, to facilitate the fracture of hard objects at a lower force, seed predators will show similarities (number and size of contact points) in the area of their dentition in contact with foods. Dental areas of initial contact were quantified and visualised for each bite point with the exception of molar due to the methodological issues with seed placement on numerous specimens for this position.

*Incisor:* Dental contact surface with the seed on incisor is not uniform in all seed predators (Fig. 4.22, Table 4.3). Above results show that the three anterior-feeding intensive seed predators (*Cacajao, Chiropotes,* and *Pithecia*) have lowest force to initial fracture. The contact surface area in this group shows a broad area of contact along the incisor row. This is especially the case in their maxillary incisors, which show contact on both the incisal edges and some of the lingual fossa, including on the lingual tubercle on all three (Fig. 4.22).

Contact with the incisal edge and lingual tubercle creates four points of contact on the first maxillary incisors in all three species. *Cacajao* and *Chiropotes* additionally show a small area of contact on their second maxillary incisors. In all three species there is contact with multiple mandibular incisors, forming a long narrow surface. For *Cacajao* the measured tooth-food contact on incisor results in a very large contact surface area on the maxillary teeth (20.83mm$^2$, Table 4.3). This large area is only superseded by one other specimen, no seed group specimen *Ateles* (28.62 mm$^2$, Table 4.3). However, the large contact surface area in *Ateles* is not matched by a similar shape to the anterior-feeding seed predators, instead showing contact along the concave lingual and mesial surfaces of both first maxillary incisors, spanning the large gap between these teeth (Fig. 4.22). Contact surface area is relatively smaller in the other anterior-feeding seed predators, despite similarities in contact surface shape to *Cacajao*. This is especially the case in *Pithecia* which has the smallest total incisor contact surface area of the entire sample (12.72 mm$^2$).

A range of forms are observed in the poster-feeding seed predators. *Cercocebus*, which has relatively high force to fracture on incisor (Fig. 4.19), shows prominent differences in contact surface area to the anterior-feeding seed predators. On the maxillary teeth *Cercocebus* shows contact on the mesial and incisal edges and a small area at the base of the lingual fossa, and on the mandibular teeth a broad region across the incisal edges of the first two incisors (Fig. 4.22). *Mandrillus,* which grouped closely with *Cercocebus,* has a similar number of contact points although spread on a smaller contact area of both maxillary and mandibular incisors (Fig. 4.22, Table 4.3). By contrast the contact surface area observed in *Sapajus* shows contact on the relatively broad and flat show lingual aspects of both left and right first incisor, both upper and lower. This is a similar contact area to a no-seed group primate, *Cebus*, which had both the highest mean force to initiate fracture on incisor and very variable performance on this bite, although *Cebus* shows a more flattened incisal edge forming to a ridge which had contact with the seed than *Sapajus*. Finally, also notable is *Pan*, which performed with the lowest force to fracture of the no seed diet group and with similar performance to the anterior-feeding group. *Pan* has three points of contact with the food item, the mesial incisal edges on the maxillary first left incisor and mandibular first incisors.
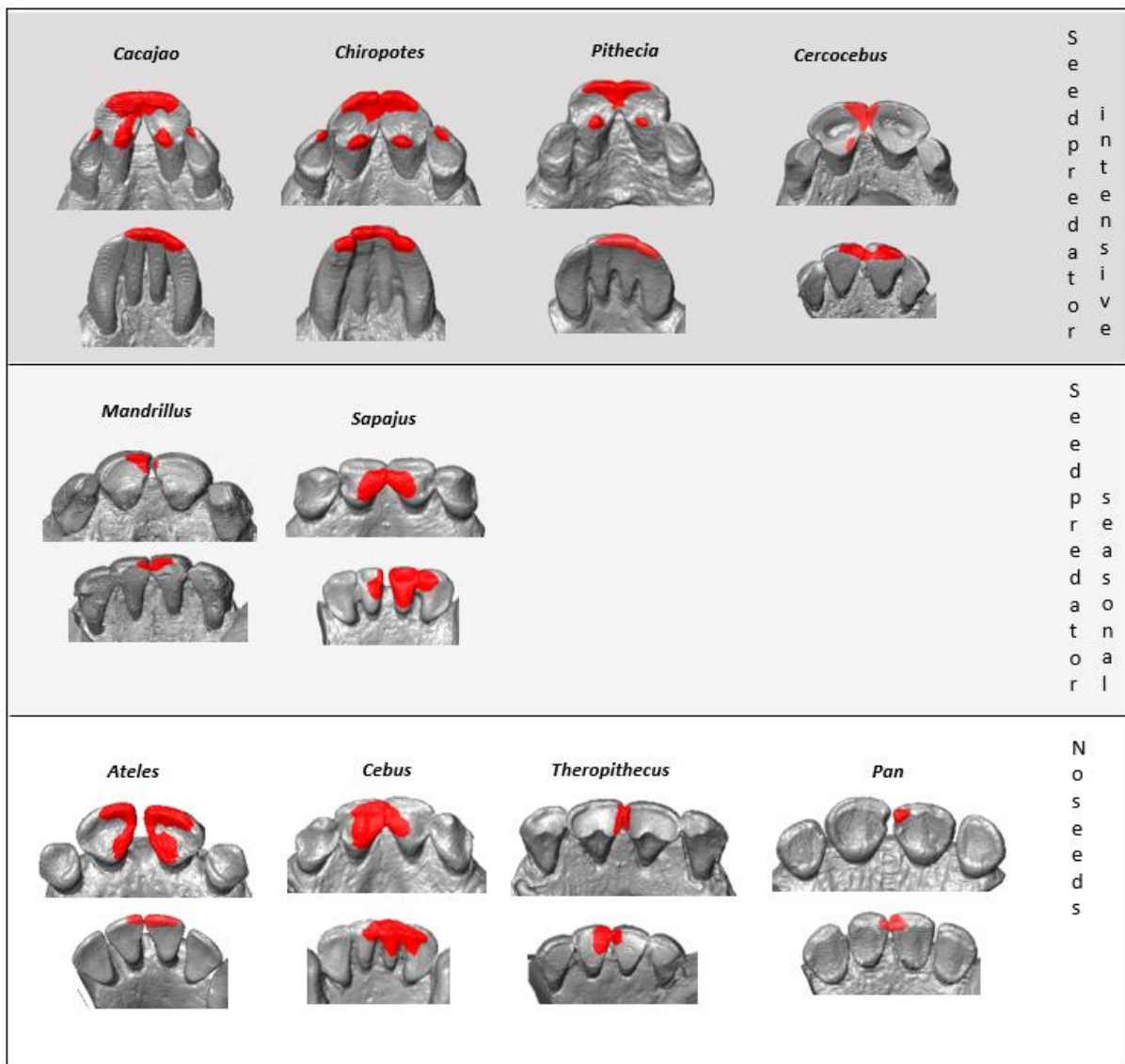
**Figure 4.22 Contact surface area of pecan seed for incisor bites for each species, showing contact on the maxillary (top) and mandibular (bottom) dental row. Anterior-feeding seed predators are *Cacajao*, *Chiropotes*, and *Pithecia*, posterior-feeding seed predators are *Cercocebus*, *Mandrillus*, and *Sapajus*.**

*Canine:* As noted above (4.3) bites on canine were faced with methodological challenges. Seed predators did not group on a low force to fracture, although the anterior-feeding seed predators (*Cacajao*, *Chiropotes*, and *Pithecia*) do show a very similar canine contact shape (Fig. 4.23). All three have a relatively small region of their canines in contact with the seed at fracture (6.67 mm$^2$, 4.62mm$^2$, and 4.8mm$^2$ in *Cacajao*, *Chiropotes*, and *Pithecia* respectively, Table 4.3), with seed contact spreading along the sharp distolingual border on the mandibular canine in all three cases. Posterior-feeding seed predators *Cercocebus* and *Mandrillus* have narrow and sharp canine tips, although the flattened mesial edge on the

*Mandrillus* canine and the overall large size of this tooth results in a relatively large surface area (11.7 mm$^2$).

Of the no-seed group *Pan* is again notable, in this case due to having the largest contact surface area on canine bites in the sample (15.21 mm$^2$, total surface area 18.71 mm$^2$). This is due to the large flat surface on the lower canine. Another noteworthy result in the no-seed group is *Cebus,* which exclusively had pierced fracture results on canine (Fig. 4.19). *Cebus* has a very flat mandibular canine surface paired with a sharp upper canine.
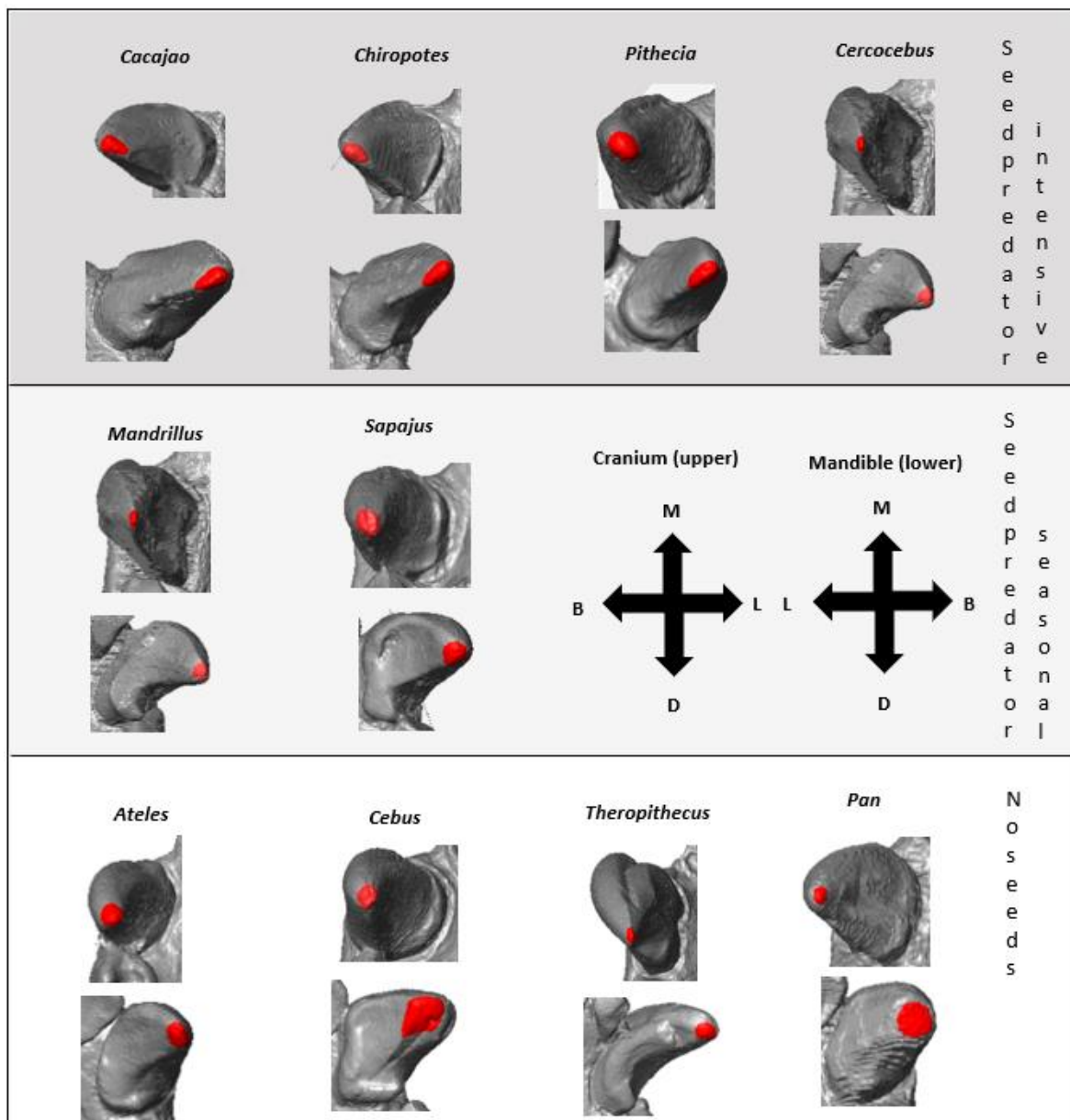


**Figure 4.23 Contact surface area of pecan seed for canine bites for each species, showing contact on the maxillary (top) and mandibular (bottom) dental row. Anterior-feeding seed predators are *Cacajao, Chiropotes,* and *Pithecia,* posterior-feeding seed predators are *Cercocebus, Mandrillus,* and *Sapajus.***

**Premolar:** Dental contact surface with the seed on premolar is not uniform in all seed predators (Fig. 4.24, Table 4.3). For one, the orientation of the canine constrains seed placement (as shown in Fig. 4.15, section 4.3.6). This position, as well as the range of absolute tooth sizes and number of premolars present in the sample, affects tooth contact with the seed across the seed predators (Fig. 4.24). In anterior-feeding seed predators (*Cacajao, Chiropotes, Pithecia*) the contact surface area includes maxillary and mandibular PM2 and PM3 in cases, along the protocristid as well as touching the metaconid and protoconids. There is also a small region of contact with PM1 in *Chiropotes* and with M1 in *Pithecia*. Posterior-feeding *Sapajus* has a similar region of contact but contact with fewer teeth, with seed contact on the PM1 protoconid and the most mesial PM2 surface on the mandibular teeth, and maxillary paracone (PM1). By contrast *Cercocebus* has contact on PM2 and M1, while *Mandrillus* has contact on maxillary PM1 and mandibular PM1 and PM2.

The number of contact points and size of contact area between tooth and seed for premolar bites. The anterior-feeding seed predators have as many as 8 contact point with the seed along the dental row in these species (Fig. 4.24). *Mandrillus*, a posterior-feeding seed predator which had the lowest force to fracture in the sample, has a very different contact arrangement to the other seed predators, with just three points of contact including a small point on its narrow and elevated PM1. *Theropithecus,* which had the second lowest force to fracture but is not a seed predator, shows a similar contact surface area with the addition of the maxillary protocone (PM1). Despite this additional tooth contact point *Mandrillus* still has a larger total contact surface area than *Theropithecus* ($24.81mm^2$ in *Mandrillus*, $18.74mm^2$ in *Theropithecus,* Table 4.3). *Sapajus*, which requires a relatively high force to initiate fracture, also has three points of contact but on different teeth (as above), and this contact in *Sapajus* results in a much smaller contact surface area ($8.65 mm^2$). By contrast, the intensive posterior-feeding seed predator *Cercocebus*, which requires a similarly high force as *Sapajus* to initiate fracture, has a relatively broad area of contact for both mandible and cranium. This is also reflected in its contact surface area measurement, which is highest in the group both individually for maxillary tooth contact and for its total contact surface area ($13.11mm^2$ and $28.23mm^2$, respectively). This large area shows contact along the flattened surfaces along the premolars and M1 in *Cercocebus*.
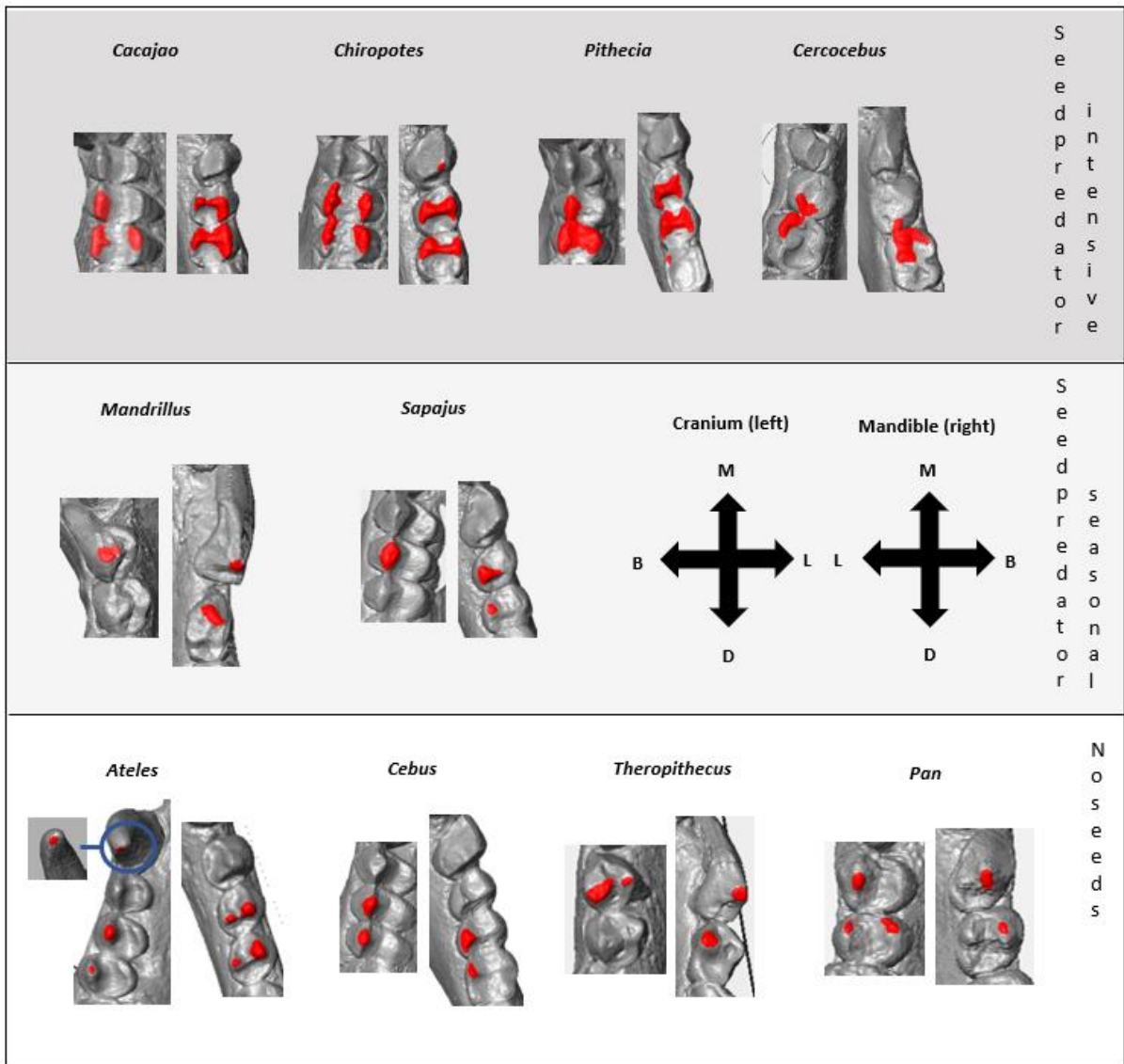
**Figure 4.24 Contact surface area of pecan seed for premolar bites for each species, showing contact on the maxillary (top) and mandibular (bottom) dental row. Anterior-feeding seed predators are *Cacajao, Chiropotes,* and *Pithecia,* posterior-feeding seed predators are *Cercocebus, Mandrillus,* and *Sapajus.***

**Table 4.3 Contact surface area mm² for all specimens on each measured tooth.**

| Species | Tooth | Mandible | Cranium | Total |
|---|---|---|---|---|
| *Cacajao* | Incisor | 20.83 | 8.89 | 29.72 |
| | Canine | 3.23 | 3.44 | 6.67 |
| | Premolar | 9.74 | 13.96 | 23.70 |
| *Chiropotes* | Incisor | 12.90 | 7.49 | 20.39 |
| | Canine | 1.88 | 2.74 | 4.62 |
| | Premolar | 9.32 | 8.32 | 17.65 |
| *Pithecia* | Incisor | 7.60 | 5.12 | 12.72 |
| | Canine | 2.46 | 2.35 | 4.80 |
| | Premolar | 10.07 | 8.61 | 18.67 |
| *Cercocebus* | Incisor | 13.60 | 14.08 | 27.68 |
| | Canine | 1.61 | 2.31 | 3.92 |
| | Premolar | 13.11 | 15.12 | 28.23 |
| *Mandrillus* | Incisor | 11.31 | 10.74 | 22.04 |
| | Canine | 6.36 | 5.35 | 11.70 |
| | Premolar | 9.45 | 15.36 | 24.81 |
| *Sapajus* | Incisor | 11.94 | 13.79 | 25.74 |
| | Canine | 3.59 | 3.26 | 6.85 |
| | Premolar | 4.51 | 4.14 | 8.65 |
| *Ateles* | Incisor | 28.62 | 8.17 | 36.79 |
| | Canine | 2.83 | 2.74 | 5.57 |
| | Premolar | 3.32 | 6.64 | 9.96 |
| *Cebus* | Incisor | 13.96 | 10.98 | 24.94 |
| | Canine | 2.42 | 6.59 | 9.02 |
| | Premolar | 4.19 | 3.83 | 8.02 |
| *Pan* | Incisor | 7.00 | 11.67 | 18.67 |
| | Canine | 3.21 | 15.21 | 18.41 |
| | Premolar | 11.21 | 7.50 | 18.71 |
| *Theropithecus* | Incisor | 8.13 | 10.85 | 18.98 |
| | Canine | 2.85 | 5.49 | 8.34 |
| | Premolar | 9.84 | 8.90 | 18.74 |

## 4.5 Discussion

Primate seed predators were predicted to show advantageous dental performance in terms of force to fracture relative to primates with less challenging diets (H1). Additionally, it was predicted that the within primate seed predators the tooth which facilitates the lowest force to initial fracture will be the tooth most often used to access large hard objects (H2). These predictions were partially met. Some primates, especially the anterior-feeders, do require less force to initiate fracture than primates with other diets. For these primates their most advantageous feeding position relates to their known feeding behaviour. This was not the case for all specimens however and most posterior-feeding primates did not meet predictions. As such the results only partially support the hypotheses. There are multiple possible explanations for these results. Due to the methodological issues faced in testing on the molar and canine bites this discussion will focus primarily on the wider context of the incisor and premolar bite results (but see 4.5.4 below).

## 4.5.1 Advantageous morphology, advantageous fracture?

The primates which meet predictions (H1 and H2) include both those which feed on their anterior and those which feed on their posterior dentition. The anterior-feeding pitheciine primates are known to use their specialised incisors and canines to extract seeds from hard-shelled fruits as part of their regular diet (Norconk and Veres, 2011). Collectively these primates had the lowest force to fracture on incisor, with *Cacajao*, thought to feed on the most extreme foods within this group, having the lowest force to fracture (Fig. 4.19). This group also differed from the remaining sample by having unusual incisor contact surface area which included a lingual tubercle, a shared derived characteristic of pitheciines (Kinzey, 1992). This increased both the surface area in contact with the seed and the number of points of contact, distributing load broadly over the surface of the seed. Notably although these primates are amongst the smallest of the sample (Table 3.2; Smith and Jungers, 1997) they had some of the largest contact surface areas, indicating that the shape of their incisors facilitates a broad contact surface area with the food eaten. *Cacajao*, with the largest contact surface area, also had the lowest force of this group (Figs. 4.19 and 4.22). These results suggest that the unusual dental form in the pitheciines provides advantageous fracture of a hard and brittle food item, although it must be noted that the seed modelled

does not represent the full spectrum of foods eaten by these primates (see 4.5.4). It must also be noted that although by comparison with all other species the force to fracture was lowest on incisor in the pitheciine group, it was not significantly lower than all comparison groups. While even relatively small differences in force may make a considerable difference in repeated bites as needed for seed-intensive diets, this was unexpected. The contact arrangement in *Pan,* comprising three relatively small points of contact with the seed, resulted in very similar force to initiate fracture to two of the pitheciines (Fig. 4.19). It would be valuable to investigate if this relationship holds when comparing a wider range of food sizes and types in a future study.

Another surprising result in this group is the fact that despite similarities in both the number and shape of contact surface areas, it is notable that *Chiropotes* does not meet predictions for H2, unlike *Cacajao* and *Pithecia*, as it has near identical force to initiate fracture on both incisor and premolar (Fig. 4.21). This is due to better performance on the premolars in *Chiropotes* relative to the other pitheciines, not lower performance on incisor (Table 4.2). Although contact surface area is similar in shape between these groups on premolar it is notable that a small area of the sharp mandibular first premolar protoconid is in contact with the seed in *Chiropotes* (Fig. 4.24). This adds an additional sharp contact point to this complex multi-cusped contact arrangement, potentially lowering the force to fracture. The premolar shape may still produce an advantageous fragmentation formation which could be beneficial in seed mastication after initial access. For initial seed access pitheciines access hard foods with their incisors and canines, not premolars. The hard fruits and seeds eaten by these primates are very large, especially relative to the small pitheciine body size (Norconk et al., 2009). Both the procumbent incisors and laterally splayed canines in these primates are thought to reduce the required gape for feeding on large foods relative to species with more upright dentition (Ledogar et al., 2018). Pitheciine postcanine dentition is thought to be used more in chewing seeds post-extraction from their hard casings (Kinzey, 1992; Norconk and Veres, 2011).

Besides the pitheciine group one other primate met predictions: seasonal seed predator *Mandrillus*, which had the lowest force to fracture on premolar. There are multiple factors to consider on this bite. For one, although *Mandrillus* produced a low force to fracture, the mode of fracture was not consistent, with a near equal split between seed cracks and seed

pierces (Table 4.2). The feeding ecology of *Mandrillus* is less well-known than that of other primates (Astaras, 2009). It is unclear where in the mouth mandrills place the seeds that form part of their diet, although their morphological similarities to *Cercocebus* in their expanded second premolar have been taken as evidence of feeding on this tooth (Fleagle and McGraw, 1999). The sharp mandibular PM1 protoconid likely contributed to the pierced seed results in this study and contributed to a three-point arrangement with two blunt and one sharp contact points for the mandrill bites (Fig. 4.24). While this arrangement may be advantageous for crack initiation, the high proportion of pierced results suggests it is may not be advantageous for crack propagation after initiation. Interestingly a similar contact arrangement was found in *Theropithecus*, and although *Theropithecus* required a higher force to initiate fracture than *Mandrillus* it was not significantly different (4.20). *Theropithecus* does have a fourth point of contact with the seed on the maxillary protocone, and also shows a difference in fragmentation: while *Theropithecus* had fewer pierced results it also had a high proportion of uncracked seeds. *Theropithecus* has a very different diet to all other primates in the sample, feeding primarily on grasses (Dunbar and Dunbar, 1974; Iwamoto et al., 1996). This overall similar performance may be due to phylogeny and body size, as it has been observed that very large-bodied papionins such as *Mandrillus* and *Theropithecus* have greatly extended first premolars, with crowns that extend to the mesiobuccal root (Swindler, 2002). A scaling relationship has been suggested for both species in this context. Posterior dentition size tends to scale with negative allometry (Lucas, 2004). As a result, primates with large body mass will either have a sizeable space between the last molar and mandibular ramus, or a diastema with extended premolar length (Lucas, 2004).

The extended premolar in both *Mandrillus* and *Theropithecus* may fracture seeds at low force but may also pierce them and not propagate a crack. This feeding position is not thought to relate to the ecology of *Theropithecus*, which feeds on grasses primarily on the second premolar and molars with their enamelled shearing crests (Venkataraman et al., 2014). *Mandrillus* is thought to seasonally feed on hard seeds but given both the large body size and accompanying high bite force in mandrills, alongside their high degree of prognathism and canine-necessitated high gape (Hylander, 2013) it is entirely possible that the mandrills place seeds more posteriorly on their molars. Molar bites presented

challenges in placement for this study, but data could be obtained for *Mandrillus* and show consistent crack propagation when biting on the molars. The force to fracture on molar for is relatively low and well and likely within their bite force capabilities. It is therefore possible that the premolar position tested in this study does not represent the natural feeding position of this primate, and that instead it feeds more posteriorly, on the molars. Given the numerous reports of crushed seed casings in mandrill faeces (Hoshino, 1985; Hongo et al., 2017) it can be assumed that seed feeding is not a challenge for these primates, and it can be predicted that the molar teeth are used in seasonal seed feeding.

## 4.5.2 High force to fracture in seed predators

Not all seed predators met predictions. This includes intensive seed predator *Cercocebus atys*, known to crush hard *Sacoglottis* seeds on its expanded posterior dentition (Fleagle and McGraw, 1999). *Cercocebus* had relatively very high force to initiate force to fracture on its natural posterior feeding position (Fig. 4.20). This is the dental region in which *Cercocebus* is known to feed directly on seeds, and unlike seasonal seed predators *Mandrillus* and *Sapajus* the sooty mangabey feeds very intensively on this hard diet. Multiple explanatory angles can be considered. For one, this is a mid-sized primate, and although it has been shown to have neither exceptionally high mechanical advantage or muscle size (Taylor et al., 2018), it is of a large enough body size that is still estimated to surpass the pitheciines in terms of absolute bite force. Past work has suggested that after passing a body size threshold it may be possible to meet the demands of mechanically challenging diet without additional specialisations, instead relying on body size to produce adequate bite force (Taylor et al., 2018).

The contact surface area with the seed for *Cercocebus* may cause the high force required on premolar bites. *Cercocebus* undergoes rapid and intensive dental wear, attributed to its diet (Swan, 2016). The specimen used for the dental model was identified as a young, yet mature adult with a relatively low degree of wear within a comparative sample (Swan, 2016). Freshly erupted post-canine teeth in this species feature sharp cusps, but even by the onset of full maturity these cusps are worn to the relatively flat surface present on the specimen in this sample, and wear continues on to create a concave dentine centre surrounded by an enamel rim (Swan, 2016). Despite this, the *Sacoglottis* seed is consumed very intensively

from a relatively young age and throughout the lives of *Cercocebus* individuals of both sexes (McGraw et al., 2011). Seed placement in this study closely correlates with the feeding position identified in past studies, on the PM2-M1 complex (Daegling et al., 2011; McGraw et al., 2011), as the relatively straight canine in this primate prevents the placement of the seed further forward on the dental row (Fig. 4.15). The contact surface on this bite shows opposing relatively broad and flat surfaces (4.24). This may spread the load relatively evenly, and indeed *Cercocebus* produced a crack on all seeds, in stark contrast to *Mandrillus* (Table 4.2). As such, this feeding position may allow for a consistent fracture even if that fracture is at relatively high force. Given adequate bite force to access seeds due to body size such a fragmentation may be advantageous for repeated fracture on hard seeds.

The same explanation does not suffice for seasonal posterior seed predator *Sapajus*. This specimen had amongst the highest forces to initial fracture of the sample (Fig. 4.21). This is surprising as *Sapajus* uses its postcanine teeth for fracturing hard palm seeds and is a mid-sized primate with less body mass than *Cercocebus*. Also surprising is the fact that the gracile capuchin *Cebus*, close relative of *Sapajus* with a less mechanically challenging diet, had a lower median force to fracture on the premolars than *Sapajus*. The behaviour of *Sapajus apella* is unusual in that some populations using tools or manual dexterity to open seeds instead of crushing bites to open hard palm seeds, while others bite directly on the seed (Izawa and Mizuno, 1977; Izawa, 1979; Terborgh, 1984; Spencer, 2003). Additionally, *Sapajus* feeds on a large proportion of exceptionally tough foods using its anterior dentition and is known for an exceptionally mechanically advantageous temporalis muscle (Ch. 3, 3.4.2; Wright, 2005). This primate also has large muscle PCSA and is predicted to have large bite force (Taylor and Vinyard, 2009). It is possible that the advantageous non-dental morphology of *Sapajus* is sufficient for enabling hard seed process. It is also possible that as these seeds are only seasonally eaten in relatively small quantities there are other elements in the *Sapajus* diet which provide stronger constraints. While *Sapajus* is certainly capable of occasionally feeding on this seed it is ultimately a highly opportunistic species with a very broad diet which may present conflicting demands.

### 4.5.3 Dental crown safety

Although having dental form which facilitates low force fracture initiation was predicted to be advantageous for seed predators, the role of dental crown safety must also be considered. There is a trade-off between shapes which promote fracture at a low force and shapes which resist failure of the tooth itself (Lucas, 2004; Crofts and Summers, 2014). As such, crown safety is thought to play a role in the dental form of hard object feeders, as extremely high force can risk chipping or even catastrophic tooth failure (Chai et al., 2009). A potential explanation for the high force to fracture seen in *Cercocebus* is the prioritising of crown safety over minimising force to fracture. *Cercocebus* has very thick dental enamel and post-canine teeth which wear incredibly quickly from sharp cusps to a flat surface (W. Scott McGraw et al., 2014; Swan, 2016). Thick enamel in particular is considered advantageous for species which feed on hard objects, as it can protect the tooth from damage and extend the lifetime of the tooth (Lucas et al., 2008; Lawn et al., 2009). Thick enamel is not present in all primates, for example *Pan* is noted to have relatively thin enamel and does not directly feed on hard seeds, instead experiencing more gradual wear from the presence of abrasive grit in its diet (Lawn et al., 2009). Object size also has a relationship with dental safety (Lucas et al., 2008; Lawn et al., 2009). If enamel thickness and object size is known, the type of damage which can occur to the tooth with increasing loading can be predicted (Lucas et al., 2008; Lawn et al., 2009). Objects which are both large and hard may first cause the tooth surface to yield but will cause the enamel to crack at high forces (Lucas et al., 2008; Lawn et al., 2009). Smaller objects are more likely to cause more gradual, minor wear due to surface yield (Lawn and Lee, 2009). Particularly for objects which are large and require high forces to access, thicker enamel is key for protecting the tooth from catastrophic fracture (Lawn et al., 2009).

The seeds eaten by the primates in this sample are both large and hard. The observed large contact surface in some seed predators spreads forces widely on the teeth, creating less pressure on an individual point – on one hand, this should increase the force to fracture an object, but it also reduces the risk of failure as the force is not concentrated in one small area of the tooth. While high, sharp cusps can pierce foods at low force, not only are they are not best for crack propagation after initiation but also are quick to wear (Lucas, 2004; Crofts and Summers, 2014). The large, relatively flat contact surface area observed in

*Cercocebus* may therefore provide an alternative advantage than low force, instead protecting the longevity of the tooth. Results may support the idea that crown protection is key in some hard-object feeders, and that maintaining the ability to consume a food for a long time is more important than minimising force to fracture – this may especially be the case because seeds are such a high-energy food item. Larger tooth size may prevent catastrophic tooth failure when biting at high forces by spreading the load broadly, although relationships between dental size and diet are not clear or universal (Lucas, 2004; Constantino and Wright, 2009; Norconk et al., 2013). It has been predicted that tooth size affects the likely tooth failure mode: with a constant enamel thickness, a larger-sized tooth is likely to undergo a radial crack before it yields, with final failure in the form of radial cracking, whereas smaller teeth are expected to first yield, then experience a crack which emerges at the enamel-dentine junction (Lawn and Lee, 2009). Given the large, hard objects which are part of the seed predator diet and the presence of thick enamel in at least some species, future work could pair physical testing data with models of tooth failure at different object sizes.

## 4.5.4 Challenges with modelling reality

Although this study was able to take novel steps towards modelling real feeding by including both full dental rows and gape at initial contact, there were inevitable simplifications and simulations. The impact of these choices on the results must be considered. Given that two bite positions presented unique issues they are also evaluated in this context. Especially the challenges with these bites may prove formative for future studies.

## 4.5.4.1 Reality of seed modelling

It is important to consider that no primate in the sample feeds on pecans, instead the pecan seed was used as a model for seed predation on a hard and brittle seed. It is therefore possible that this seed does not provide an accurate model of seed predation for all or some of the primates in this sample, or that it reflects only some of the objects eaten by seed predators. The pecan is very similar in size to seeds eaten by several primates in the sample (the *Sacoglottis* eaten by *Cercocebus*, Brazil nuts eaten by *Cacajao*, palm seed eaten by *Sapajus*) but these seeds are not identical in their internal morphology (see Ch. 1 review and figure, section 1.5 and Fig. 1.7). Pecans also showed themselves to be quite brittle: Fracture

of this thin, hard shell occurred after relatively low displacement (see Appendix 8 for displacement results) but many foods eaten by these primates may require a much further displacement. Hard-shelled fruits eaten by *Cacajao* have been measured and found to have variably thick pericarps, with some being 0.5mm thick at their thinnest region but others with having a mean thickness of 11mm (Barnett et al., 2016). Displacement for contact surface area measurements in the present study is at the lowest end of these measurements due to the thin and relatively brittle pecan shell. This has permitted the modelling of initial contact at realistic gape on a hard and brittle seed but does not necessarily replicate bites with extensive displacement on tough and hard foods.

Some aspects of model design must also be considered for their potential impact. The usage of metal dental replicas is well-established as a safe and reliable alternative to using rare and breakable real teeth (Lucas et al., 1994; Berthaume et al., 2010; Barnett et al., 2015; 2016; Swan, 2016). However, at the time of model manufacture metal 3D printing methods were relatively novel, and model manufacturing limitations resulted in the usage of two suppliers (see section 4.3.2.3). These two suppliers use the same machine source and therefore the same materials (see 4.3.2.3) but may vary in their printing process, which could affect results. A past sensitivity study found that printing the same tooth once each from the two suppliers produced highly similar results in physical testing (Camp, 2019). It is also reassuring that clear trends were observed on one tooth (incisor), but not on another (premolar), indicating there is no single unifying pattern across tests which links to print supplier. However, it is still possible that the results in this study were affected by the choice of model manufacturer. Future studies can hopefully benefit from rapid and considerable improvements in 3D printing technology and avoid this limitation.

Another point to consider is the placement of the seed. Past studies modelling real teeth have worked with no gape (Lucas et al., 1994) and single dental rows (Berthaume et al., 2010), or single teeth (Barnett et al., 2015, 2016). By using the full dental row at natural gape a more realistic contact surface area can be modelled, but natural seed placement is challenging to model and indeed is often not known for primates. Primates may not naturally place seeds in the positions modelled in this study. What is more, due to the variable body size in the sample the seed touched different teeth in different primates, particularly evident in the premolar contact in *Mandrillus*. This may have affected

comparisons, as it was not physically possible to place seeds more anteriorly on other primates due to the canine shape and position.

## 4.5.4.2 Canine and molar bites

Canine and molar bites faced different methodological issues. For canines, the high number of unbroken seeds presented a challenge for the interpretation of force results and the majority of seeds which could be fractured were punctured without crack propagation. Future studies would benefit from repeated bite simulations or from allowing additional displacement into the seed to attempt to fracture a higher number of seeds or propagate a higher number of cracks. In this regard the static loading model presented another challenge, as the 4mm displacement limit did not include dynamic mandible movement with biting. In consequence the last molars on some specimens would come into contact after great displacement, limiting the possible displacement in the study. Despite these issues, the contact surface area on canine highlighted some interesting relationships. Although anterior-feeding pitheciines did not show a clear pattern in force results as a group, the pitheciines do group on contact surface area. Due to the lateral splay of the canines the sharp distolingual border of the canine quickly comes into contact with the seed (Fig. 4.23). This tooth-food contact indicates that the canines of these species could work as a sharp wedge which is driven into hard foods to propagate cracks. This shape is unlike any other in the sample as the majority of the remaining sample showed contact on just the canine tip due to the less laterally splayed canine shape. An exception to this is *Pan,* which has relatively stout and less sharp canines (Fig. 4.23). *Pan* has previously been documented to have rounder and less obtuse canines than other apes (Swindler, 2002). The functional implications of this shape cannot be interpreted from the limited results, as is the case for the pitheciine seed predators, leaving this as an open topic for future investigations.

Issues with molar bites were instead due to seed placement. It was not possible to place the seeds for all specimens in the study. This is partially due to body size, as for the pitheciines the placement of the 2cm seed on the molar required a tremendous gape. As a result the dental row was steeply angled and the seed could not remain in position on the molar. However, dental shape and dental row curvature (curve of Spee) likely also affected seed positioning on the molar bite. The dental row of pitheciine primates is not in a flat plane,

255

instead it features a pronounced curvature. This additional height on the molars relative to the front of the dental row may have posed an additional challenge for seed placement. By contrast, *Cercocebus* has a relatively flat dental plane and is of relatively large body size, but it was not possible for the seed to remain in place on M1. In this case the flattened cusps contributed to a failure to grip the seed. Natural feeding behaviours such as gripping the seed while biting may hold the seed in place. However, these issues could also be related to modelling problems such as the shape of the pecan seed and the simulation of gape.

## 4.5.5 How hard is a seed really?

A final consideration concerns past measurements of seeds eaten by primates and the potential range of material properties present in seeds. The predictions of this study, and those of many past studies focussing on primate seed predators, are based on past measurements of the hardness of the seeds in their diet. However, recent work is increasingly suggesting that positional behaviours in feeding likely contribute to the force required to fracture these foods (Barnett et al., 2016; Laird et al., 2020). The *Sacoglottis* eaten by *Cercocebus* contains a larger number of small kernels in a star-like shape suspended within a fibrous internal structure (van Casteren, pers. Comm). It is possible that *Cercocebus* may perform better when feeding on *Sacoglottis*, or indeed that movements made within the mouth and during feeding – as the food is often moved around and generally is positioned carefully (van Casteren, pers. Comm). What is more, it is possible that the seeds eaten by *Cercocebus* may require less force to fracture than reported measurements suggest. There are multiple reasons for this. For one, *Cercocebus* forages on the forest floor, which has high humidity, and may also moisten the seeds in cheek pouches prior to eating (McGraw et al., 2014). Increased humidity reduces force to fracture in some seeds (Williamson and Lucas, 1995), so the seeds processed may be less hard then when their properties are measured in the field.

Additionally, it has been shown that processing seeds along different orientations can take advantage of natural weaknesses and reduce force to fracture, which may also lower the force required to access the foods for seed predators (Williamson and Lucas, 1995; Barnett et al., 2016). Cheek pouches may be used by the sooty mangabey to store seeds before feeding, moistening them to reduce force to fracture (W. Scott McGraw et al., 2014). Seeds

on the forest floor may also be affected by insect damage, which has been suggested to reduce the force to fracture (Terborgh, 1984; Lucas et al., 1991). Examining the effect of varying moisture conditions and seed orientation on force to fracture would be a valuable contribution to understanding the possible effects of these variables on primate seed predator feeding, as lab measurements may overestimate the force required to fracture seeds. This has been demonstrated for *Cacajao* by comparing the force to fracture required with a dental replica relative to a standard fruit penetrometer (Barnett et al., 2015). *Cacajao* is known to bite into the weakest area of the husk, significantly reducing the force required to access the nutrients within (Barnett et al., 2016). Past measurements of fruit hardness were made with standardised measurement tools may inflate the force required to access both due to the implement used and the position where the measurement was taken (Barnett et al., 2015). What is more, due to their large size and thick pericarp additional displacement of the tooth into the seed is likely, altering the tooth contact with the food, and increasing the gape to further alter the contact area. Results here suggest that pitheciines have an advantageous morphology for reducing force to fracture on one type of seed, it would be of great interest to explore this relationship further with a broader sample of foods.

## 4.5.6 Conclusions

Diversity in seed predator dental forms also results in diverse performance when fracturing a hard, brittle object. Some seed predators meet predictions and have relatively low force to initiate fracture on the bite position which relate to their natural feeding ecology. Other primates do not. This may be due to a dental form which prioritises safety over advantageous crack propagation. It is also possible that the experiment does not fully represent seed fracture, or indeed that seeds eaten by some or all seed predators are less challenging than previously thought. Body size, muscle arrangement, and bite force may also play a role, and it is possible that primates which do not gain an advantage from their dentition in terms of force to fracture are still able to feed on these items without specialised teeth. Taken together, there are multiple possible approaches for seed predators, and results highlight that primates with large body sizes can circumvent the need for special adaptations.

# Chapter 5 – Discussion: Different solutions to different mechanical challenges?

This thesis has considered the functional morphology of primate seed predators from multiple angles: first, by comparing the masticatory shapes of seed predators to primates with other diets and by testing for convergence within seed predators (Ch. 2); next, by quantifying key biomechanical parameters to determine if seed predators have advantageous mechanical advantage, muscle cross sectional areas, bite force, and gape abilities both within their dietary grouping and relative to other primates (Ch. 3); and finally, by evaluating the role of dental morphology by measuring the force required to initiate fracture on a hard, brittle seed in both seed predators and comparison species (Ch. 4). An examination of the results of these experiments viewed collectively serves to highlight the observation that the majority of seed predators display advantageous performance on at least some mechanically relevant components relative to primate with non-seed primates. However, there is variation between species, suggesting there is no common approach to seed predation.

## 5.1 Primate seed predators: advantageous anatomies for seed access

The multiple pathways for seed predation include a combination of high mechanical advantage (MA), large muscle cross-sectional area (CSA), and dentition which facilitates reduced force to fracture on hard seeds. Mid-sized platyrrhine primates all have relatively high MA on all teeth at wide gapes, and some males have relatively high muscle CSA for their body size (Ch. 3, see sections 3.4.2 and 3.4.4). Of the pitheciines, *Cacajao* has the most advantageous performance both in terms of multiple biomechanically relevant parameters and for dental fracture. This is consistent with past predictions that *Cacajao* is the most extreme pitheciine seed predator due to the observation of its robust cranial morphology (Kinzey, 1992). All three pitheciine primates (*Cacajao, Chiropotes, Pithecia*) were found to be convergent with *Sapajus* (Ch. 2, see sections 2.4.4 – 2.4.5). From the GMM shape analysis it was predicted that all pitheciines, but especially *Cacajao*, may be grouping with *Sapajus* in the morphospace associated with relatively high MA (Ch. 2, see section 2.4.1). Quantifying measurements of biomechanical predictors (Ch. 3) found this to indeed be the case in both sexes, especially for measurements on anterior bites and for the temporalis in males. A

difference between these groups, however, is that pitheciines additionally have highly advantageous dentition for initiating fracture in a hard, brittle seed (Ch. 4, see section 4.3.1). *Sapajus* feeds on hard palm seeds posteriorly and tough, fibrous foods anteriorly (Wright, 2005), and did not have advantageous force to fracture on a hard, brittle food in either position.

No convergence was found with *Mandrillus* and the other seed predators. Examining the results of quantified measurements underscores the effect of the highly prognathic shape observed in *Mandrillus* (Ch. 3, see section 3.4). While large-bodied *Mandrillus* has a tremendous gape and very large muscle CSA, it has a very low MA. This large-bodied primate feeds on hard seeds seasonally when fruits are scarce, although many key details describing its feeding behaviours are unknown, such as the material properties of the seeds it consumes and exactly where in the mouth it positions the seeds when feeding (Hoshino, 1985; Lahm, 1986; Astaras, 2009; Hongo et al., 2017). *Mandrillus* is likely capable of accessing hard seeds by virtue of its body size increasing absolute muscle CSA, resulting in a high estimated bite force. The extremely long rostrum in this primate, which produces a very long out-lever, is closely associated with the non-feeding behaviours of aggression and sexual display. The exceptionally large *Mandrillus* canine is a key feature in these paramasticatory activities, and there are clear links between large canine height and wide gape ability (Leigh et al., 2005; Hylander, 2013). An interesting result was the finding that *Mandrillus* induced fracture on the premolar at a very low force. If indeed this is a regular feeding position for *Mandrillus*, it may have an excellent advantage in seed predation by combining teeth which initiate fracture at low force with large muscle mass. The large gape and body size (Ravosa, 1990; Hylander, 2013) in this primate and its enlarged second premolar (Fleagle and McGraw, 2002) may also facilitate a more posterior feeding position.

Body size may also be a solution for mid-sized *Cercocebus* (Taylor et al., 2018), resulting in a larger muscle mass than the smaller-bodied seed predators in the sample. While *Cercocebus* has a low MA relative to most other seed predators (Ch. 3, Fig. 3.16 in section 3.4.2) and relative to some other papionins (Taylor et al., 2018) it in fact has a high MA when compared against *Mandrillus.* Past work has predicted this relationship due to the facial and palatal shortening in *Cercocebus* relative to other papionins (Singleton, 2002, 2005)*. Cercocebus* does not display the extremity of specialism which may be expected in such an

intensely hard diet, although it does have improved MA in comparison to some other papionins. This improved MA comes, however, at the cost of a considerable loss in maximum gape in *Cercocebus* relative to *Mandrillus* (Ch. 3, section 3.4.1), while not precluding the ability of *Cercocebus* to produce gapes in the range of 20mm on the premolars/M1 complex and feed on its habitual dietary of *Sacoglottis* seeds (McGraw et al., 2011; W.S. McGraw et al., 2014; Geissler et al., 2020).

Given the lack of exceptional MA or muscle CSA in *Cercocebus*, resulting in low bite force estimates relative to other primates such as *Mandrillus*, it is surprising that the well-documented seed feeding position of *Cercocebus* (McGraw et al., 2011; W.S. McGraw et al., 2014; Geissler et al., 2020) does not relate to advantageous fracture performance. The contact surface area measurements highlight the essentially flat plate surface of *Cercocebus* premolars. This is a shape which spreads force across a broad area, resulting in the relatively high force to fracture. Despite this 'poor' force performance it is noteworthy that the *Cercocebus* premolar consistently propagated cracks on seeds, in contrast to the frequent seed piercing seen in *Mandrillus*. This may facilitate rapid access to seeds despite the high force required to initiate this fracture. Interestingly, the dental wear in *Cercocebus* is very rapid, with post-canine cusps nearly entirely flattened by the on-set of adulthood (Swan, 2016). Some mammals, including *Theropithecus* and a range of ungulates, have dentition which wears to expose a beneficial secondary morphology which then improves efficiency in feeding (Luke and Lucas, 1983; Koenigswald, 2011; Venkataraman et al., 2014). However, such a pattern has only been previously observed in species which specialise on grasses and leaves. Dental safety is another possible explanation for the morphology in *Cercocebus,* as such a flat postcanine shape may protect the postcanine teeth against catastrophic tooth failure (Ungar and Williamson, 2000; Ungar and M'Kirera, 2003; Chai et al., 2009; Ungar, 2015).

It is also possible that the dental and masticatory muscle morphology in *Cercocebus* is simply not advantageous, and dental wear in this species is simply the consequence of extremely intensive feeding on hard *Sacoglottis*. Other mangabey species, such as the Tana River mangabey, *Cercocebus galeritus*, also eat mechanically challenging foods, including relatively hard seeds, but feed on a much broader diet than *Cercocebus atys* (Wieczkowski, 2009)*.* Observations of the extreme *C. atys* diet are relatively recent and focus on the Tai

forest population (Daegling et al., 2011; McGraw et al., 2011; W.S. McGraw et al., 2014; Geissler et al., 2020) – such an extraordinary reliance on *Sacoglottis* may be a recent behavioural development. This is especially so because *C. atys* is considered a vulnerable species, and lives in fragmented, damaged habitats with extensive destruction of both primary and secondary forest (Ferreira da Silva et al., 2020). It is possible that environmental degradation has influenced the extreme reliance on very hard seeds observed in this primate. Taken together, *Cercocebus atys* does not fully meet expectations for a primate seed predator. Expectations of the masticatory requirements of a primate seed predator may be wrong, or may not be analogous in all primates, or indeed, other environmental and behavioural factors may also contribute to seed predation in *Cercocebus atys*.

Another interesting and unexpected finding is the difference in extremism observed between individuals of different sex within most of the species studied. The differences between female and male seed predator diets are not well-known (see Ch. 2, 2.5.3; Norconk and Veres, 2011), although it has been observed that male *Cacajao* eats a higher proportion of harder seeds than females (Bowler and Bodmer, 2011). A similar relationship has been observed in *Cercocebus* (McGraw et al., 2011; Geissler et al., 2020)*,* and may also exist in *Mandrillus* (Stammbach, 1986)*.* Females and males occupied different positions in shape space (Ch. 2, section 2.4.1), with male platyrrhine seed predators (*Cacajao, Chiropotes, Pithecia, Sapajus*) grouping with features associated with high MA, and male papionin seed predators (*Cercocebus, Mandrillus*) showing greater prognathism than females. Quantifying differences (Ch. 3) highlighted higher MA and larger muscle CSA in male platyrrhines, and lower MA and larger muscle CSA in male papionins, although the overall picture shows higher bite force estimates for males. While the higher MA in female papionins (notably in *Cercocebus*) may contribute significantly towards functional equivalence between sexes, estimates suggest that the absolutely much larger muscle CSA in males results in considerably higher bite force in males.

These anatomical features match the findings of the small number of studies which consider the differences in material properties or quantity of challenging foods eaten by different seed predator sexes (Bowler and Bodmer, 2011; McGraw et al., 2014; Geissler et al., 2020). Further research into sex-based differences in diets would be of great value to better

understand these relationships. Future studies could also consider female dental form. In the present study, only males were used in physical testing. Pitheciine female and male seed predators have very have similar dental specialisations across sexes (Kinzey, 1992; Rosenberger, 1992; Norconk et al., 2013), which may result in similar dental function in both sexes. Female *Cercocebus atys* is known to show similarly intensive dental wear patterns to males (Swan, 2016) so may also have a similarly high force to fracture performance on premolar bites. Quantification and functional testing of dental form for both sexes in these primates would be an interesting topic for further study.

Despite the differences measured between female and male seed predators it is important to consider the fact that females in all seed predator species examined do still consume hard seeds. Beyond the sample of this study, it has recently been demonstrated that there is sex-based variation in the processing behaviours of hard walnuts by *Macaca fuscata* individuals (Tamura, 2020). Both sexes feed on the hard seeds, but females manipulate walnuts to a greater degree in feeding which may reduce the force required to access the encased nut, compensating for smaller female body size and expected lower bite force (Tamura, 2020). Food manipulation and processing behaviours may have a major impact on accessing challenging foods (see below, 5.2). Food selection may also vary between sexes in manners which have yet to be quantified. Studies of primate ontogeny highlight that small-bodied juvenile *Sapajus libidinosus* consumes similarly tough foods to adults but select smaller foods items (Chalk et al., 2016). Changes in food selection and feeding behaviour may therefore be another route for species and sexes with a less mechanically advantageous masticatory apparatus to process challenging food types.

At the outset of this thesis a key aim was to investigate for the possibility of many-to-one mapping in primate seed predators. Taken together, results underpin the idea that there are many ways to be a seed predator, but that these many morphologies do not map to one output even under a very broad interpretation of many-to-one mapping. Some primate seed predators seem to converge on a similar muscular configuration but have different dentition (pitheciines and *Sapajus*). Other seed predators have very large body size and correspondingly very large predicted bite force (*Mandrillus*). Still others are surprising in that they have morphologies associated with seed predation (expanded premolars in

*Cercocebus*) but do not display the exceptional MA or advantageous fracture results one would predict to be associated with such an extreme diet.

## 5.2 Are 'hard' foods more easily and frequently consumed than we anticipate?

An interesting result of this study was the repeated observation that *Pan* has excellent performance across multiple variables (Ch. 3 and Ch. 4). *Pan troglodytes verus* was selected for this study because it is sympatric with *Cercocebus atys* but is not typically thought to feed on *Sacoglottis* without the help of tools (Boesch and Boesch, 1982). Reports of this behaviour state *Sacoglottis* seeds are only rarely consumed despite their abundance in chimpanzee habitats (Boesch and Boesch, 1982). Other seeds are processed more frequently in some seasons, using tools in a skilled manner which requires a high degree of manual dexterity and planning to source fittingly shaped stone 'hammerstones' and 'anvils' (Boesch and Boesch, 1982; Carvalho et al., 2008; Haslam et al., 2009). However, despite occasional feeding on *Sacoglottis* with the aid of tools, *Pan* had higher performance than *Cercocebus* on all variables, with higher MA, muscle CSA, and requiring lower force to fracture hard seeds. This brings into consideration factors such as intelligence and material culture. Another angle to consider is that of dental adaptations which could not be accounted for in this study, specifically enamel thickness. It has previously been noted that chimpanzees have relatively thin enamel which may not be able to withstand the high forces encountered during seed feeding using teeth, not tools (Lawn et al., 2009). As such, although chimpanzees may be able to produce the forces needed to feed on hard seeds, they may have a dental constraint which limits their diet. These topics are beyond this scope of this study, but raise interesting questions regarding how and why *Cercocebus atys* frequently consume these hard food items directly - while *Pan troglodytes verus* will not or cannot.

Seeds are a good source of nutrition, being high in energy, lipids, and protein (Norconk et al., 2013). It is possible that many larger-bodied primates feed on seeds regularly, without this activity having been observed or recorded doing so or are capable of feeding on seeds but select other foods such as leaves and tubers when fruits are scarce. A degree of seed predation is present in the diets of many primates, but the behaviour is poorly understood

in the diets of some larger primates such as orangutans (Norconk et al., 2013), and even *Mandrillus sphinx*, about which records of seed predation are only known through faecal data (Hongo et al., 2017). Other primates may also turn to seeds when necessary, as a recent documentation of gorillas feeding on very hard *Coula edulis* demonstrates (van Casteren et al., 2019). This highly folivorous primate, which has masticatory adaptations associated with tough feeding, is an example of the fact that large-bodied primates are freed from some dietary constraints and can delve into a wide range of resources when necessary (van Casteren et al., 2019). This is likely also the case with frugivorous *Pan,* but the regularity of tool use in *Pan* enables this primate to bypass the need to gain access to these seeds using the masticatory apparatus (Boesch and Boesch, 1982; Carvalho et al., 2008; Haslam et al., 2009). Indeed, the observation that not all gorilla or chimpanzee populations appear to consume seeds, whether in the mouth or with tools, has been taken to suggest that this is a learned and shared behaviour in some primates (McGrew et al., 1997; van Casteren et al., 2019). This may be another reason why not all primate populations feed on seeds: they may not have the knowledge this is an available resource, leaving primates such as *Cercocebus* to their niche of hard seeds.

What remains exceptional in the intensive seed predators is the volume and frequency of seeds in their diets. Other primates may be capable of feeding on seeds but use them as rare, extra resources in certain seasons when preferred resources are not available. These primates do not make seeds their dominant diet, unlike primates such as *Cacajao* and *Cercocebus.*

*Cacajao* met most biomechanical predictors of an intensive hard-object feeder but *Cercocebus* did not. As such it is important to consider how *Cercocebus* is able to feed on such a mechanically challenging diet. Although *Sacoglottis* seeds are measured as requiring over 2000N to fracture (Daegling et al., 2011), it could be that the seeds eaten by *Cercocebus* are not, in fact, as extremely hard as expected: it has been proposed that small invertebrates or fungi can weaken seeds casings, as can humidity (Terborgh, 1984; Williamson and Lucas, 1995). Seed shells are also not uniformly hard and may contain lines of natural weakness (Lucas et al., 1994; Williamson and Lucas, 1995; Lucas, 2004) which are not necessarily taken into account when measuring hardness. When suitably oriented in the mouth to access the weak points in the natural structure, or following environmental

damage, seeds may require less force to fracture. Food positioning is known to affect the force required by *Cacajao* to access some hard-shelled fruits. A study examining bite positions used by *Cacajao* relative to seed anatomy found that *Cacajao* bites hard fruits and seeds along natural lines of seed weakness (Barnett et al., 2015). Examples from the diets of other primates show that insects and humidity can weaken seed casings, for example making hard palm seeds accessible to *Cebus* when undamaged seeds are thought to only be eaten by *Sapajus* (Terborgh, 1984)*.*

Positional behaviours in feeding are also important to understanding seed feeding. Primates do not place seeds in the mouth randomly, which is important given the variable material properties along the surface of seeds (Lucas et al., 1994; Lucas, 2004; Norconk et al., 2009). Additionally, primates perform a tremendous range of seed processing behaviours, even within the cracking of a single seed type within a single population, as recently observed in walnut-feeding macaques (Tamura, 2020). One capuchin species, *Sapajus libidinosus,* has been shown to carry out a series of ingestive behaviours ahead of feeding on a Piaçava nut (Laird et al., 2020). There are multiple manual food processing steps before the seed is eaten which may facilitate seed feeding (Laird et al., 2020). Such behaviours are only beginning to be understood, but likely affect the ability of a species to access foods. *Cercocebus* is known to use its incisors to prepare seeds ahead of performing the crushing bite on its posterior dentition. They also have been recorded to store seeds in their cheek pouch in advance to crushing, whereby moisture may cause a weakening of the seed casing prior to crushing (Williamson and Lucas, 1995; McGraw et al., 2011). Only a small number of studies have investigated the impact of moisture content and seed positioning on fracture (Lucas et al., 1994; Williamson and Lucas, 1995; Barnett et al., 2015, 2016). This is not to say that *Sacoglottis* seeds pose no mechanical challenge, but this and other seeds may be less mechanically challenging to access than past measurements suggest.

## 5.3 Masticatory requirements for tough and hard diets

Another important consideration is the role of toughness in seed predation. Some of the seeds eaten by pitheciine primates are described as hard and brittle, others as hard and tough (Norconk and Veres, 2011; Norconk et al., 2013; Barnett et al., 2016). A combination of these properties may be present in many seeds, combining a hard and brittle external seed casing with hard and tough endocarp as seen in the *Sacoglottis* eaten by *Cercocebus*

(Daegling et al., 2011). The quantification of these measurements is known to be notoriously difficult (Berthaume, 2016), and only a small number of the items consumed by primates have had their material properties measured. Both hardness and toughness are likely to influence morphology, and there may be shared adaptations for high toughness and high hardness.

Previous research predicted that *Chiropotes* and *Sapajus* may be convergent due to their mutual need to feed on tough foods by utilizing high force on the anterior dentition (Wright, 2005). Highly significant convergence was indeed found between *Sapajus* and *Chiropotes,* as well as between *Sapajus* with both *Cacajao* and *Pithecia* (Ch. 2). Particularly *Cacajao* and *Sapajus* had very similar performance across a range of variables (Ch. 3; MA, gape height, muscle CSA), these variables being very relevant to feeding ability. Both must produce high forces on their anterior dentition, and while *Sapajus* feeds on hard and brittle food only on posterior teeth, the shared feeding behaviour of consuming very tough foods using the anterior dentition may cause this similar pattern. Dental performance varied in these groups, highlighting that differences remain. While both may have adaptations for toughness, *Sapajus* had poor fracture performance when simulating bites on a brittle hard food on its anterior dentition, unlike the pitheciines. Further explorations of these relationships, perhaps by physically testing primate dentition with a range of tough foods, could further explore this interesting relationship.

## 5.4 Implications for interpreting fossil diets

Hard-object feeding is a dietary specialisation which has been considered to be a key explanation for the extreme craniofacial robusticity found in some fossil hominin species (Teaford and Ungar, 2000). The robust australopith *Australopithecus boisei* was nicknamed the "nutcracker man" upon its discovery. *A. robustus* and *A. boisei* have similar craniofacial forms, possessing features such as flared zygomatic arches, sagittal crests, and postcanine megadontia (Rak, 1983; Wood and Constantino, 2007) resulting in predictions of mechanical exceptionalism and high biting forces (Demes and Creel, 1988). Despite these predictions, results of recent palaeodiet reconstructions using isotope analysis (Sponheimer et al., 2006), measurements of dental microwear (Scott et al., 2005; Ungar et al., 2008) and dental chipping analysis (Constantino et al., 2010) reveal contradictions in their previously assumed dietary predictions. One theory, based on dental wear complexity and dental pitting

patterns, is that *A. robustus* used hard, brittle foods as fall-back foods in times of resource scarcity (Ungar et al., 2008). Such a pattern has recently been observed in extant gorillas, although notably the dental morphology of gorillas does not conform to the expected morphology for such a diet (van Casteren et al., 2019). A different prediction is made for *A. boisei,* and despite the even greater extremity of craniofacial robusticity in this species, it was found to have parallel scratch markings and practically no pitting on its teeth when examined for microwear (Ungar et al., 2008). Isotope analysis suggests that this species had a diet more similar to *Theropithecus gelada,* consisting of grasses and sedges (Grine et al., 2012; Fashing et al., 2014). Difficulties in inferring dietary categories from craniofacial morphology alone are seen in the results of this present study. Both tough foods and hard foods could result in similar anatomical configurations, and multiple morphologies are linked to hard object feeding behaviours.

Predictions of past diet based on extant morphology are further complicated by the fact that extant species do not always conform to functional predictions. The combination of premolar expansion with a large, hard diet in *Cercocebus atys* has led to comparisons with *A. africanus,* which has megadontia and premolar expansion (Strait et al., 2009; Daegling et al., 2011). However, this study reveals that despite intensive feeding on large and hard seeds *C. atys* appears to lack dental or craniofacial mechanical specialisations to facilitate such a diet. Seed hardness may be lower than measured due to environmental factors and positional feeding behaviours may ease access, but in either case, *C. atys* does not have the functional morphology that would be expected for a hard seed specialist. As others have previously suggested, body size may be key in facilitating hard diets without further adaptations (Taylor et al., 2018). This finding may also apply to fossil hominins, and australopithecines may easily have consumed large 'hard' objects in their diet without needing to possess many of the derived features.

## 5.5 Conclusions

This study has not found primate seed predators to have a common solution to the challenges of feeding on large, hard seeds. Instead, it would appear that there are, in fact, many ways to be a primate nutcracker. Some primates have a large body size, others have a combination of high leverage and advantageous dental morphology, and still others appear to succeed despite middling results on all values. Is this many-to-one-mapping on a broad

scale? The presence of high mechanical advantage with advantageous dentition in some primates and large muscle size in others does show multiple paths to the shared outcome of seed predation, but these morphologies do not have an equivalent result. Primate solutions to nut-cracking are diverse – as are primate habitats, life histories, and evolutionary histories. There is no one tool to do the job, nor is there even necessarily one job.

# References

Adams, D. C., Collyer, M. L. and Kaliontzopoulou, A. (2020) 'Geomorph: Software for geometric morphometric analyses. R package version 3.2.1.' Available at: https://cran.r-project.org/package=geomorph.

Adler, D. and Murdoch, D. (2020) 'rgl: 3D Visualization Using OpenGL'. Available at: https://cran.r-project.org/package=rgl.

Aguirre, L. F., Herrel, A., vn Damme, R. and Matthysen, E. (2003) 'The implications of food hardness for diet in bats', *Functional Ecology*, 17(2), pp. 201–212. doi: https://doi.org/10.1046/j.1365-2435.2003.00721.x.

Alfaro, J. W. L., Silva, J. de S. E. and Rylands, A. B. (2012) 'How Different Are Robust and Gracile Capuchin Monkeys? An Argument for the Use of Sapajus and Cebus', *American Journal of Primatology*, 74(4), pp. 273–286. doi: 10.1002/ajp.22007.

Alfaro, M. E., Bolnick, D. I. and Wainwright, P. C. (2005) 'Evolutionary Consequences of Many-to-One Mapping of Jaw Morphology to Mechanics in Labrid Fishes', *The American Naturalist*, 165(6), pp. 140–154. doi: https://doi.org/10.1086/429564.

Allen, K. L., Cooke, S. B., Gonzales, L. A. and Kay, R. F. (2015) 'Dietary inference from upper and lower molar morphology in platyrrhine primates', *PLoS ONE*, 10(3), pp. 1–22. doi: 10.1371/journal.pone.0118732.

Anapol, F. and Herring, S. W. (1989) 'Length-tension relationships of masseter digastric muscles of miniature swine during ontogeny', *Journal of Experimental Biology*, 143, pp. 1–16.

Anapol, F. and Lee, S. (1994) 'Morphological adaptation to diet in platyrrhine primates', *American Journal of Physical Anthropology*, 94(2), pp. 239–261. doi: 10.1002/ajpa.1330940208.

Anapol, F., Shahnoor, N. and Ross, C. F. (2008) 'Scaling of Reduced Physiologic Cross-Sectional Area in Primate Muscles of Mastication', in Vinyard, C., Ravosa, M. J., and Wall, C. E. (eds) *Primate Craniofacial Function and Biology*. Springer US, pp. 201–216. doi: 10.1007/978-0-387-76585-3_10.

Anderson, P. S. L. (2009) 'The effects of trapping and blade angle of notched dentitions on fracture of biological tissues', *Journal of Experimental Biology*, 212(22), pp. 3627–3632. doi: 10.1242/jeb.033712.

Anderson, P. S. L., Claverie, T. and Patek, S. N. (2014) 'Levers and Linkages: Mechanical trade-offs in a power-amplified system', *Evolution*, 68(7), pp. 1919–1933. doi: 10.1111/evo.12407.

Anderson, P. S. L. and Labarbera, M. (2008) 'Functional consequences of tooth design : effects of blade shape on energetics of cutting', *Journal of Experimental Biology*, 211, pp. 3619–3626. doi: 10.1242/jeb.020586.

Anderson, P. S. L., Lacosse, J. and Pankow, M. (2016) 'Point of impact: The effect of size and speed on puncture mechanics', *Interface Focus*, 6(3). doi: 10.1098/rsfs.2015.0111.

Anderson, P. S. L. and Rayfield, E. J. (2012) 'Virtual experiments , physical validation : dental morphology at the intersection of experiment and theory', *Journal of the Royal Society Interface*, 9(73), pp. 1846–1855. doi: doi:10.1098/rsif.2012.0043.

Anderson, P. S. L. and Westneat, M. W. (2007) 'Feeding mechanics and bite force modelling of the skull of Dunkleosteus terrelli , an ancient apex predator', *Biology Letters*, 3(1), pp. 76–79. doi: 10.1098/rsbl.2006.0569.

Anderson, R. A., Mcbrayer, L. D. and Herrel, A. (2008) 'Bite force in vertebrates : opportunities and caveats for use of a nonpareil whole-animal performance measure', *Biological Journal of the Linnean Society*, 93(4), pp. 709–720. doi: https://doi.org/10.1111/j.1095-8312.2007.00905.x.

Ang, K. Y., Lucas, P. W. and Tan, H. T. W. (2006) 'Incisal orientation and biting efficiency', *Journal of Human Evolution*, 50(6), pp. 663–672. doi: 10.1016/j.jhevol.2006.01.003.

Anton, S. C. (1999) 'Macaque masseter muscle: internal architecture, fiber length and cross-sectional area', *International Journal of Primatology*, 20(3), pp. 441–462. doi: 10.1023/A:1020509006259.

Anton, S. C. (2000) 'Macaque pterygoid muscle: internal architecture, fiber length and cross-sectional area', *International Journal of Primatology*, 21(1), pp. 131–156. doi: https://doi.org/10.1023/A:1005431831444.

Arbour, J. H. and Brown, C. M. (2014) 'Incomplete specimens in geometric morphometric analyses', *Methods in Ecology and Evolution*, 5(1), pp. 16–26. doi: 10.1111/2041-210X.12128.

Aristide, L., Furtado, S., Machado, A. C., Lima, I., Lopes, R. T. and Perez, S. I. (2016) 'Brain shape convergence in the adaptive radiation of New World monkeys', *Proceedings of the National Academy of Sciences*, 113(8), pp. 2158–2163. doi: 10.1073/pnas.1514473113.

Armstrong, W. P. (2002) *Fruit Terminology (Part 4)*. Available at: https://www2.palomar.edu/users/warmstrong/termfr4.htm (Accessed: 1 August 2020).

Armstrong, W. P. (2005) *Brazil Nut, Paradise Nut & Cashew*. Available at: https://www2.palomar.edu/users/warmstrong/ecoph1.htm (Accessed: 1 August 2020).

Armstrong, W. P. (2009) *Fruits Called Nuts*. Available at: https://www2.palomar.edu/users/warmstrong/ecoph8.htm#walnut (Accessed: 1 August 2020).

Astaras, C. (2009) *Ecology and Status of the Drill*. PhD Thesis. Georg-August-University of Göttingen.

Awono, A., Djouguep, A., Zapfack, L. and Ndoye, O. (2009) 'The Potential of Irvingia Gabonensis: Can it Contribute to the Improvement of the Livelihoods of Producers in Southern Cameroon?', *International Journal of Social Forestry*, 2(1), pp. 67–85. Available at: http://ijsf.org/site/index.php/ijsf/article/view/21 (Accessed: 4 November 2021).

Ayres, J. M. (1989) 'Comparative feeding ecology of the Uakari and Bearded Saki, Cacajao and Chiropotes', *Journal of Human Evolution*, 18(7), pp. 697–716. doi: 10.1016/0047-2484(89)90101-2.

Barnett, A. A., Bezerra, B. M., Santos, P. J. P., Spironello, W. R., Shaw, P. J. A., MacLarnon, A. and Ross, C. (2016) 'Foraging with finesse: A hard-fruit-eating primate selects the weakest areas as bite sites', *American Journal of Physical Anthropology*, 160(1), pp. 113–125. doi: 10.1002/ajpa.22935.

Barnett, A. A., Santos, P. J. P., Boyle, S. A. and Bezerra, B. M. (2015) 'An Improved Technique Using Dental Prostheses for Field Quantification of the Force Required by Primates for the Dental Penetration of Fruit', *Folia Primatologica*, 86(4), pp. 398–410. doi: 10.1159/000434677.

Bates, K. T. and Falkingham, P. L. (2012) 'Estimating maximum bite performance in Tyrannosaurus rex using multi-body dynamics', *Biology Letters*, 8(4), pp. 660–664. doi: doi:10.1098/rsbl.2012.0056.

Berkovitz, B. K. B. and Shellis, R. P. (2018) *The teeth of mammalian vertebrates*. Academic Press.

Berthaume, M. A. (2014) 'Tooth cusp sharpness as a dietary correlate in great apes', *American Journal of Physical Anthropology*, 153(2), pp. 226–235. doi: 10.1002/ajpa.22424.

Berthaume, M. A. (2016) 'Food mechanical properties and dietary ecology', *American Journal of Physical Anthropology*, 159(S61), pp. 79–104. doi: 10.1002/ajpa.22903.

Berthaume, M. A., Dumont, E. R., Godfrey, L. R. and Grosse, I. R. (2013) 'How does tooth cusp radius of curvature affect brittle food item processing?', *Journal of the Royal Society Interface*, 10(84), pp. 20–24. doi: 10.1098/rsif.2013.0240.

Berthaume, M. A., Lazzari, V. and Guy, F. (2020) 'The landscape of tooth shape: Over 20 years of dental topography in primates', *Evolutionary Anthropology*, 29(5), pp. 245–262. doi: 10.1002/evan.21856.

Berthaume, M., Grosse, I. R., Patel, N. D., Strait, D. S., Wood, S. and Richmond, B. G. (2010) 'The effect of early hominin occlusal morphology on the fracturing of hard food items', *Anatomical Record*, 293(4), pp. 594–606. doi: 10.1002/ar.21130.

Bjarnason, A., Soligo, C. and Elton, S. (2015) 'Phylogeny , Ecology , and Morphological Evolution in the Atelid Cranium', *International Journal of Primatology*, 36(3), pp. 513–529. doi: 10.1007/s10764-015-9839-z.

Boesch, C. and Boesch, H. (1982) 'Optimisation of Nut-Cracking with Natural Hammers by Wild Chimpanzees', *Behaviour*, 83(3), pp. 265–286. doi: doi.org/10.1163/156853983X00192.

Boinski, S. and Cropp, S. J. (1999) 'Disparate Data Sets Resolve Squirrel Monkey (Saimiri) Taxonomy: Implications for Behavioral Ecology and Biomedical Usage', *International Journal of Primatology*, 20(2), pp. 237–256. doi: 10.1023/A:1020522519946.

Botton-Divet, L. É. O., Cornette, R., Houssaye, A., Fabre, A. and Herrel, A. (2017) 'Swimming and running : a study of the convergence in long bone morphology among semi-aquatic mustelids ( Carnivora : Mustelidae )', *Biological Journal of the Linnean Society*, 121(1), pp. 38–49. doi: https://doi.org/10.1093/biolinnean/blw027.

Boubli, J. P. (1999) 'Feeding ecology of black-headed uacaris (Cacajao melanocephalus melanocephalus) in Pico da Neblina National Park, Brazil', *International Journal of Primatology*, 20(5), pp. 719–749. doi: 10.1023/a:1020704819367.

Bowler, M. and Bodmer, R. E. (2011) 'Diet and Food Choice in Peruvian Red Uakaris (Cacajao calvus ucayalii): Selective or Opportunistic Seed Predation?', *International Journal of Primatology*, 32(5), pp. 1109–1122. doi: 10.1007/s10764-011-9527-6.

Boyer, D. M. (2008) 'Relief index of second mandibular molars is a correlate of diet among prosimian primates and other euarchontan mammals', *Journal of Human Evolution*, 55(6), pp. 1118–1137. doi: 10.1016/j.jhevol.2008.08.002.

Braus, H. (1921) 'Anatomie des Menschen: Ein Lehrbuch für Studierende und Aerzte', in. Springer Verlag. Available at: https://archive.org/details/anatomiedesmenschen1921v1.

Bunn, J. M., Boyer, D. M., Lipman, Y., St. Clair, E. M., Jernvall, J. and Daubechies, I. (2011) 'Comparing Dirichlet normal surface energy of tooth crowns, a new technique of molar shape quantification for dietary inference, with previous methods in isolation and in combination', *American Journal of Physical Anthropology*, 145(2), pp. 247–261. doi: 10.1002/ajpa.21489.

Butynski, T. M. and Koster, S. H. (1994) 'Distribution and conservation status of primates in Bioko island, Equatorial Guinea', *Biodiversity and Conservation*, 3(9), pp. 893–909. doi: 10.1007/BF00129665.

Buzi, C., Micarelli, I., Profico, A., Conti, J., Grassetti, R., Vincenzo, F. Di, Tafuri, M. A., Manzi, G., Ambientale, B., Università, S., Università, S., Università, S. and Giuseppe, A. (2018) 'Measuring the shape : performance evaluation of a photogrammetry improvement applied to the Neanderthal skull Saccopastore 1', *Acta Imeko*, 7(3), pp. 79–85.

Camp, S. (2019) *Functional implications of size reduction in molar dentition during human evolution using 3D printed models*. MSc by Thesis. Hull York Medical School.

Campbell, K. M. and Santana, S. E. (2017) 'Do differences in skull morphology and bite performance explain dietary specialization in sea otters?', *Journal of Mammalogy*, 98(5), pp. 1408–1416. doi: 10.1093/jmammal/gyx091.

Cardini, A. and Elton, S. (2008) 'Variation in guenon skulls (II): sexual dimorphism', *Journal of Human Evolution*, 54(5), pp. 638–647. doi: 10.1016/j.jhevol.2007.09.023.

Cardini, A. and Elton, S. (2009) 'Geographical and taxonomic influences on cranial variation in red colobus monkeys (Primates , Colobinae): introducing a new approach to " morph " monkeys', *Gobal Ecology and Biogeography*, 18(2), pp. 248–263. doi: 10.1111/j.1466-8238.2008.00432.x.

Carlson, D. S. (1977) 'Condylar translation and the function of the superficial masseter muscle in the rhesus monkey(M. mulatta)', *American Journal of Physical Anthropology*, 47(1), pp. 53–63. doi: 10.1002/ajpa.1330470111.

Carvalho, S., Cunha, E., Sousa, C. and Matsuzawa, T. (2008) 'Chaînes opératoires and resource-exploitation strategies in chimpanzee (Pan troglodytes) nut cracking', *Journal of Human Evolution*, 55(1), pp. 148–163. doi: 10.1016/j.jhevol.2008.02.005.

van Casteren, A., Wright, E., Kupczik, K. and Robbins, M. M. (2019) 'Unexpected hard-object feeding in Western lowland gorillas', *American Journal of Physical Anthropology*, 170(3), pp. 433–438. doi: 10.1002/ajpa.23911.

Chai, H., Lee, J. J. W., Constantino, P. J., Lucas, P. W. and Lawn, B. R. (2009) 'Remarkable resilience of teeth', *Proceedings of the National Academy of Sciences of the United States of America*, 106(18), pp. 7289–7293. doi: 10.1073/pnas.0902466106.

Chalk, J., Wright, B. W., Lucas, P. W., Schuhmacher, K. D., Vogel, E. R., Fragaszy, D., Visalberghi, E., Izar, P. and Richmond, B. G. (2016) 'Age-related variation in the mechanical properties of foods processed by Sapajus libidinosus', *American Journal of Physical Anthropology*, 159(2), pp. 199–209. doi: 10.1002/ajpa.22865.

Chen, J. (2009) 'Food oral processing-A review', *Food Hydrocolloids*, 23(1), pp. 1–25. doi: 10.1016/j.foodhyd.2007.11.013.

Christiansen, P. and Adolfssen, J. S. (2005) 'Bite forces, canine strength and skull allometry in carnivores (Mammalia, Carnivora)', *Journal of Zoology*, 266(2), pp. 133–151. doi: 10.1017/S0952836905006643.

Christiansen, P. and Wroe, S. (2007) 'Bite forces and evolutionary adaptations to feeding ecology in carnivores', *Ecology*, 88(2), pp. 347–358. doi: https://doi.org/10.1890/0012-9658(2007)88[347:BFAEAT]2.0.CO;2.

Clee, P. R. S., Abwe, E. E., Ambahe, R. D., Anthony, N. M., Fotso, R. and Locatelli, S. (2015) 'Chimpanzee population structure in Cameroon and Nigeria is associated with habitat variation that may be lost under climate change', *BMC evolutionary biology*, 15(2), pp. 2–15. doi: 10.1186/s12862-014-0275-z.

Close, R. I. (1972) 'Dynamic Mammalian Properties of Skeletal Muscles', *Physiological Reviews*, 52(1), pp. 129–183.

Coiner-Collier, S. *et al.* (2016) 'Primate dietary ecology in the context of food mechanical properties', *Journal of Human Evolution*, 98, pp. 103–118. doi: 10.1016/j.jhevol.2016.07.005.

Constantino, P. J., Bush, M. B., Barani, A. and Lawn, B. R. (2016) 'On the evolutionary advantage of

multi-cusped teeth', *Journal of the Royal Society Interface*, 13(121), pp. 1–8. doi: 10.1098/rsif.2016.0374.

Constantino, P. J., Lee, J. J., Morris, D., Lucas, P. W., Hartstone-Rose, A., Lee, W., Dominy, N. J., Cunningham, A., Wagner, M. and Lawn, B. R. (2011) 'Adaptation to hard-object feeding in sea otters and hominins', *Journal of Human Evolution*, 61(1), pp. 89–96. doi: 10.1016/j.jhevol.2011.02.009.

Constantino, P. J., Lee, J. J. W., Chai, H., Zipfel, B., Ziscovici, C., Lawn, B. R. and Lucas, P. W. (2010) 'Tooth chipping can reveal the diet and bite forces of fossil hominins', *Biology Letters*, 6(6), pp. 826–829. doi: 10.1098/rsbl.2010.0304.

Constantino, P. J., Lucas, P. W., Lee, J. J. W. and Lawn, B. R. (2009) 'The influence of fallback foods on great ape tooth enamel', *American Journal of Physical Anthropology*, 140(4), pp. 653–660. doi: 10.1002/ajpa.21096.

Constantino, P. J. and Wright, B. W. (2009) 'The Importance of Fallback Foods in Primate Ecology and Evolution', *American Journal of Physical Anthropology*, 140(4), pp. 599–602. doi: 10.1002/ajpa.20978.

Cooke, B. and Terhune, C. E. (2015) 'Form , Function , and Geometric Morphometrics', *The Anatomical Record*, 298(1), pp. 5–28. doi: 10.1002/ar.23065.

Couette, S. and White, J. (2010) '3d GMM and missing data can extant taxa give clues for fossil primates', *Comptes Rendus - Palevol*, 9(6), pp. 423–433. doi: 10.1016/j.crpv.2010.07.002.

Cox, P. G., Rayfield, E. J., Fagan, M. J., Herrel, A., Pataky, T. C. and Jeffery, N. (2012) 'Functional Evolution of the Feeding System in Rodents', *PLoS ONE*, 7(4), p. e36299. doi: 10.1371/journal.pone.0036299.

Crofts, S. B., Neenan, J. M., Scheyer, T. M. and Summers, A. P. (2016) 'Tooth occlusal morphology in the durophagous marine reptiles, Placodontia (Reptilia: Sauropterygia)', *Paleobiology*, 43(1), pp. 114–128. doi: 10.1017/pab.2016.27.

Crofts, S. B. and Summers, A. P. (2014) 'How to best smash a snail: The effect of tooth shape on crushing load', *Journal of the Royal Society Interface*, 11(92). doi: 10.1098/rsif.2013.1053.

Crompton, A. W. (1962) 'The Evolution of the Mammalian Jaw', *Evolution*, 17(4), pp. 431–439.

Cuozzo, F. P. and Sauther, M. L. (2006) 'Severe wear and tooth loss in wild ring-tailed lemurs (Lemur catta): A function of feeding ecology, dental structure, and individual life history', *Journal of Human Evolution*, 51(5), pp. 490–505. doi: 10.1016/j.jhevol.2006.07.001.

Curtis, N., Fitton, L. C., Watson, P. J., Gro, F., Herrel, A., Mccormack, S. W., Fagan, M. J. and Watson, P. J. (2014) 'Masticatory biomechanics in the rabbit : a multi-body dynamics analysis', *Journal of the Royal Society Interface*, 11(99), p. 20140564. doi: https://doi.org/10.1098/rsif.2014.0564.

Curtis, N., Jones, M. E. H., Evans, S. E., Shi, J. F., O'Higgins, P. and Fagan, M. J. (2009) 'Predicting muscle activation patterns from motion and anatomy: Modelling the skull of Sphenodon (Diapsida: Rhynchocephalia)', *Journal of the Royal Society Interface*, 7(42), pp. 153–160. doi: 10.1098/rsif.2009.0139.

Curtis, N., Kupczik, K., Higgins, P. O., Moazen, M., Fagan, M. and Al, C. E. T. (2008) 'Predicting Skull Loading : Applying Multibody Dynamics Analysis to a Macaque Skull', *The Anatomical Record*, 291(1), pp. 491–501. doi: 10.1002/ar.20689.

Daegling, D. J. and McGraw, W. Scott (2007) 'Functional morphology of th emangabey mandibular corpus', *American Journal of Physical Anthropology*, 134, pp. 50–62. doi: 10.1002/ajpa.

Daegling, D. J. and McGraw, W Scott (2007) 'Functional Morphology of the Mangabey Mandibular Corpus : Relationship to Dental Specializations and Feeding Behavior', *American Journal of Physical Anthropology*, 134(1), pp. 50–62. doi: DOI 10.1002/ajpa.20621.

Daegling, D. J., McGraw, W. S., Ungar, P. S., Pampush, J. D., Vick, A. E. and Bitty, E. A. (2011) 'Hard-object feeding in sooty mangabeys (Cercocebus atys) and interpretation of early hominin feeding ecology', *PLoS ONE*, 6(8), p. e23095. doi: 10.1371/journal.pone.0023095.

Davis, J. L., Santana, S. E., Dumont, E. R. and Grosse, I. R. (2010) 'Predicting bite force in mammals: two-dimensional versus three-dimensional lever models', *Journal of Experimental Biology*, 213(11), pp. 1844–1851. doi: 10.1242/jeb.041129.

Deane, A. S. (2012) 'New evidence for canine dietary function in Afropithecus turkanensis', *Journal of Human Evolution*, 62(6), pp. 707–719. doi: 10.1016/j.jhevol.2012.03.004.

Dechow, P. C. and Carlson, D. S. (1990) 'Occlusal Force and Craniofacial Biomechanics During Growth in Rhesus Monkeys', *American Journal of Physical Anthropology*, 83(2), pp. 219–237. doi: https://doi.org/10.1002/ajpa.1330830211.

Delezene, L. K., Teaford, M. F. and Ungar, P. S. (2016) 'Canine and Incisor Microwear in Pitheciids and Ateles Reflects Documented Patterns of Tooth Use', *American Journal of Physical Anthropology*, 161(1), pp. 6–25. doi: 10.1002/ajpa.23002.

Delgado, M. N. and Galbany, J. (2015) 'Taxonomic Implications of Molar Morphology Variability in Capuchins', *International Journal of Primatology*, 36(4), pp. 707–727. doi: 10.1007/s10764-015-9850-4.

Demes, B. and Creel, N. (1988) 'Bite force, diet, and cranial morphology of fossil hominids', *Journal of Human Evolution*, 17(7), pp. 657–670. doi: https://doi.org/10.1016/0047-2484(88)90023-1.

Dew, J. L. (2005) 'Foraging , Food Choice , and Food Processing by Sympatric Ripe-Fruit Specialists : Lagothrix lagotricha poeppigii and Ateles belzebuth belzebuth', *International Journal of Primatology*, 26(5), pp. 1107–1135. doi: 10.1007/s10764-005-6461-5.

Dickinson, E., Fitton, L. C. and Kupczik, K. (2018) 'Ontogenetic changes to muscle architectural properties within the jaw-adductor musculature of Macaca fascicularis', *American Journal of Physical Anthropology*, 167(2), pp. 291–310. doi: 10.1002/ajpa.23628.

Diogo, R. and Wood, B. A. (2012) *Comparative Anatomy and Phylogeny of Primate Muscles and Human Evolution*. CRC Press.

Doran, D. (1997) 'Influence of Seasonality on Activity Patterns , Feeding Behavior , Ranging , and Grouping Patterns in Tai Chimpanzees', *International Journal of Primatology*, 18(2), pp. 183–206.

Dumont, E. R., Davis, J. L., Grosse, I. R. and Burrows, A. M. (2011) 'Finite element analysis of performance in the skulls of marmosets and tamarins', *Journal of Anatomy*, 218(1), pp. 151–162. doi: 10.1111/j.1469-7580.2010.01247.x.

Dumont, E. R., Grosse, I. R. and Slater, G. J. (2009) 'Requirements for comparing the performance of finite element models of biological structures', *Journal of Theoretical Biology*, 256(1), pp. 96–103. doi: 10.1016/J.JTBI.2008.08.017.

Dumont, E. R. and Herrel, A. (2003) 'The effects of gape angle and bite point on bite force in bats', *The Journal of Experimental Biology*, 206(13), pp. 2117–2123. doi: 10.1242/jeb.00375.

Dunbar, R. I. M. and Dunbar, E. P. (1974) 'Ecological Relations and Niche Separation between Sympatric Terrestrial Primates in Ethiopia', *Folia Primatologica*, 21(1), pp. 36–60. doi: 10.1159/000155595.

van Eijden, T. M. G. J. (1991) 'Three-dimensional analyses of human bite-force magnitude and moment', *Archives of Oral Biology*, 36(7), pp. 535–539. doi: 10.1016/0003-9969(91)90148-N.

Elton, S. (2006) 'Forty years on and still going strong : the use of hominin- cercopithecid comparisons in palaeoanthropology', *Journal of the Royal Anthropological Institute*, 12, pp. 19–38.

Eng, C. M., Ward, S. R., Vinyard, C. J. and Taylor, A. B. (2009) 'The morphology of the masticatory apparatus facilitates muscle force production at wide jaw gapes in tree-gouging common marmosets (Callithrix jacchus)', *Journal of Experimental Biology*, 212(24), pp. 4040–4055. doi: 10.1242/jeb.029983.

Ennos, A. R. (2012) *Solid Biomechanics*. Princeton: Princeton University Press.

Evans, A. R. and Pineda-Munoz, S. (2018) 'Inferring mammal dietary ecology from dental morphology', in *Vertebrate Paleobiology and Paleoanthropology*. Springer, pp. 37–51. doi: 10.1007/978-3-319-94265-0_4.

Evans, A. R. and Sanson, G. D. (1998) 'The effect of tooth shape on the breakdown of insects', *Journal of Zoology*, 246(4), pp. 391–400. doi: https://doi.org/10.1111/j.1469-7998.1998.tb00171.x.

Evans, A. R. and Sanson, G. D. (2003) 'The tooth of perfection: Functional and spatial constraints on mammalian tooth shape', *Biological Journal of the Linnean Society*, 78(2), pp. 173–191. doi: 10.1046/j.1095-8312.2003.00146.x.

Evin, A., Souter, T., Hulme-Beaman, A., Ameen, C., Allen, R., Viacava, P., Larson, G., Cucchi, T. and Dobney, K. (2016) 'The use of close-range photogrammetry in zooarchaeology: Creating accurate 3D models of wolf crania to study dog domestication', *Journal of Archaeological Science: Reports*, 9, pp. 87–93. doi: 10.1016/j.jasrep.2016.06.028.

Evison, S. E. F., Gallagher, J. D., Thompson, J. J. W., Siva-Jothy, M. T. and Armitage, S. A. O. (2017) 'Cuticular colour reflects underlying architecture and is affected by a limiting resource', *Journal of Insect Physiology*, 98, pp. 7–13. doi: 10.1016/j.jinsphys.2016.11.005.

Ewédjè, E.-E. B. K., Parmentier, I., Natta, A., Ahanchédé, A. and Hardy, O. J. (2012) 'Morphological variability of the tallow tree, Pentadesma butyracea Sabine (Clusiaceae), in Benin', *Genetic Resources and Crop Evolution 2012 59:4*, 59(4), pp. 625–633. doi: 10.1007/S10722-012-9802-1.

Fashing, P. J., Nguyen, N., Venkataraman, V. V. and Kerby, J. T. (2014) 'Gelada feeding ecology in an intact ecosystem at Guassa, Ethiopia: Variability over time and implications for theropith and hominin dietary evolution', *American Journal of Physical Anthropology*, 155(1), pp. 1–16. doi: 10.1002/ajpa.22559.

Feldhammer, G. A. L., Drickamer, L. C., Vessey, S. H., Merritt, J. F. and Krajewski, C. (2007) *Mammalogy: Adaptation, Diversity, Ecology*. Baltimore: John Hopkins University Press.

Ferreira da Silva, M. J., Paddock, C., Gerini, F., Borges, F., Aleixo-Pais, I., Costa, M., Colmonero-Costeira, I., Casanova, C., Lecoq, M., Silva, C., Bruford, M. W., Varanda, J. and Minhós, T. (2020) 'Chasing a ghost: notes on the present distribution and conservation of the sooty mangabey (Cercocebus atys) in Guinea-Bissau, West Africa', *Primates*, 61(3), pp. 357–363. doi: 10.1007/s10329-020-00817-2.

Fitton, L., Dickinson, E., Swan, K. and Cobb, S. (2015) 'Functional Integration During Development Within The Masticatory Apparatus', *The FASEB Journal*, 29(S1), p. 865.15. doi: 10.1096/FASEBJ.29.1_SUPPLEMENT.865.15.

Fleagle, J. G. (2013) *Primate Adaptation and Evolution*. Academic Press.

Fleagle, J. G. and McGraw, W. S. (1999) 'Skeletal and dental morphology supports diphyletic origin of

baboons and mandrills.', *Proceedings of the National Academy of Sciences of the United States of America*, 96(3), pp. 1157–1161. doi: 10.1073/pnas.96.3.1157.

Fleagle, J. G. and McGraw, W. S. (2002) 'Skeletal and dental morphology of African papionins: unmasking a cryptic clade', *Journal of Human Evolution*, 42(3), pp. 267–292. doi: 10.1006/jhev.2001.0526.

Fox, J. and Weisberg, S. (2019) *An {R} Companion to Applied Regression*. Third. Thousand Oaks {CA}: Sage. Available at: https://socialsciences.mcmaster.ca/jfox/Books/Companion/.

Fragaszy, Dorothy M and Boinski, S. (1995) 'Patterns of Individual Diet Choice and Efficiency of Foraging in Wedge-Capped Capuchin Monkeys ( Cebus olivaceus )', 109(4), pp. 339–348.

Fragaszy, Dorothy M. and Boinski, S. (1995) 'Patterns of Individual Diet Choice and Efficiency of Foraging in Wedge-Capped Capuchin Monkeys (Cebus olivaceus)', *Journal of Comparative Psychology*, 109(4), pp. 339–348. doi: 10.1037/0735-7036.109.4.339.

Francois, R. (2020) 'bibtex: Bibtex Parser'. Available at: https://cran.r-project.org/package=bibtex.

Fricano, E. E. I. and Perry, J. M. G. (2018) 'Maximum Bony Gape in Primates', *The Anatomical Record*, 302(2), pp. 625–635. doi: 10.1002/ar.23897.

Frost, S. R., Marcus, L. F., Bookstein, F. L., Reddy, D. P. and Delson, E. (2003) 'Cranial Allometry, Phylogeography, and Systematics of Large-Bodied Papionins (Primates: Cercopithecinae) Inferred from Geometric Morphometric Analysis of Landmark Data', *The Anatomical Record*, 275A(2), pp. 1048–1072. doi: 10.1002/ar.a.10112.

Galetti, M., Pedroni, F. and Pedronit, F. (1994) 'Seasonal Diet of Capuchin Monkeys (Cebus apella) in a Semideciduous Forest in South-East Seasonal diet of capuchin monkeys (Cebus apella) in a semideciduous forest in south-east Brazil', *Journal of Tropical Ecology*, 10(1), pp. 27–39.

Galland, M. and Friess, M. (2016) 'A three-dimensional geometric morphometrics view of the cranial shape variation and population history in the New World', *American Journal of Human Biology*, 28(5), pp. 646–661. doi: 10.1002/ajhb.22845.

Geissler, E., Daegling, D. J., Polvadore, T. A. and Mcgraw, W. S. (2020) 'Seed choice differs by sex in sooty mangabeys (Cercocebus atys)', *Primates*, 62, pp. 361–367. doi: 10.1007/s10329-020-00863-w.

Giacomini, G., Scaravelli, D., Herrel, A., Veneziano, A. and Russo, D. (2019) '3D Photogrammetry of Bat Skulls : Perspectives for Macro-Evolutionary Analyses', *Evolutionary Biology*, 46(3), pp. 249–259. doi: 10.1007/s11692-019-09478-6.

Gibb, S. and Strimmer, K. (2012) '{MALDI}quant: a versatile {R} package for the analysis of mass spectrometry data', *Bioinformatics*, 28(17), pp. 2270–2271. doi: 10.1093/bioinformatics/bts447.

Gippoliti, S. (2010) 'Theropithecus gelada distribution and variations related to taxonomy : history, challenges and implications for conservation', *Primates*, 51, pp. 291–297. doi: 10.1007/s10329-010-0202-x.

Godinho, R. M., Fitton, L. C., Toro-Ibacache, V., Stringer, C. B., Lacruz, R. S., Bromage, T. G. and O'Higgins, P. (2018) 'The biting performance of Homo sapiens and Homo heidelbergensis', *Journal of Human Evolution*, 118, pp. 56–71. doi: 10.1016/j.jhevol.2018.02.010.

Greaves, W. S. (1978) 'The jaw lever system in ungulates: a new model', *Journal of Zoology*, 184(2), pp. 271–285. doi: https://doi.org/10.1111/j.1469-7998.1978.tb03282.x.

Grine, F. E., Sponheimer, M., Ungar, P. S., Lee-Thorp, J. and Teaford, M. F. (2012) 'Dental microwear and stable isotopes inform the paleoecology of extinct hominins', *American Journal of Physical*

*Anthropology*, 148(2), pp. 285–317. doi: 10.1002/ajpa.22086.

Grossnickle, D. M. (2020) 'Feeding ecology has a stronger evolutionary influence on functional morphology than on body mass in mammals', *Evolution*, 74(3), pp. 610–628. doi: 10.1111/evo.13929.

Gunst, N., Boinski, S. and Fragaszy, D. M. (2007) 'Acquisition of foraging competence in wild brown capuchins (Cebus apella), with special reference to conspecifics' foraging artefacts as an indirect social influence', *Behaviour*, 145(2), pp. 195–229. doi: 10.1163/156853907783244701.

Gunst, N., Leca, J., Boinski, S. U. E. and Fragaszy, D. (2010) 'The Ontogeny of Handling Hard-to-Process Food in Wild Brown Capuchins ( Cebus apella apella ): Evidence From Foraging on the Fruit of Maximiliana maripa', *American Journal of Primatology*, 72(1), pp. 960–973. doi: 10.1002/ajp.20856.

Habegger, M. L., Motta, P. J., Huber, D. R. and Dean, M. N. (2012) 'Feeding biomechanics and theoretical calculations of bite force in bull sharks (Carcharhinus leucas) during ontogeny', *Zoology*, 115(6), pp. 354–364. doi: 10.1016/j.zool.2012.04.007.

Harding, R. S. (1973) 'Predation by a Troop of Olive Baboons (Papio anubis)', *American Journal of Physical Anthropology*, 38(2), pp. 587–591.

Hartstone-Rose, A., Deutsch, A. R., Leischner, C. L. and Pastor, F. (2018) 'Dietary Correlates of Primate Masticatory Muscle Fiber Architecture', *Anatomical Record*, 301(2), pp. 311–324. doi: 10.1002/ar.23715.

Hartstone-Rose, A., Parkinson, J. A., Criste, T. and Perry, J. M. G. (2015) 'Comparing apples and oranges - The influence of food mechanical properties on ingestive bite sizes in lemurs', *American Journal of Physical Anthropology*, 157(3), pp. 513–518. doi: 10.1002/ajpa.22726.

Haslam, M. *et al.* (2009) 'Primate archaeology', *Nature*, 460(7253), pp. 339–344. doi: 10.1038/nature08188.

Herrel, A., Vincent, S. E., Alfaro, M. E., Wassenbergh, S. Van, Vanhooydonck, B. and Irschick, D. J. (2008) 'Morphological convergence as a consequence of extreme functional demands: examples from the feeding system of natricine snakes', *Journal of Evolutionary Biology*, 21(5), pp. 1438–1448. doi: 10.1111/j.1420-9101.2008.01552.x.

Herring, S. W. (1972) 'The Role of Canine Morphology in the Evolutionary Divergence of Pigs and Peccaries', *American Society of Mammalogists*, 53(3), pp. 500–512.

Herring, S. W. and Herring, S. E. (1974) 'The Superficial Masseter and Gape in Mammals', *The American Naturalist*, 108(962), pp. 561–576.

Herzog, W. (2007) 'Muscle', in Nidd, B. and Herzog, W. (eds) *Biomechanics of the Musculo–skeletal System*. Wiley, pp. 169–225.

Hiiemae, K. and Kay, R. F. (1972) 'Trends in the evolution of primate mastication', *Nature*, 240(5382), pp. 486–487. doi: 10.1038/240486a0.

Hiiemae, K. M. and Crompton, A. W. (1985) 'Mastication, Food Transport, and Swallowing', in Hildebrand, M., Bramble, D. M., Liem, K. F., and Wake, D. B. (eds) *Functional Vertebrate Morphology*. Harvard: Harvard University Press, pp. 262–290.

Hongo, S., Nakashima, Y., Akomo-Okoue, E.-F. and Mindonga-Nguelet, F. L. (2017) 'Seasonal Change in Diet and Habitat Use in Wild Mandrills (Mandrillus sphinx)', *International Journal of Primatology*, 38(1), pp. 1–22. doi: 10.1007/s10764-017-0007-5.

Hoshino, J. (1985) 'Feeding ecology of mandrills (Mandrillus sphinx) in campo animal reserve, Cameroon', *Primates*, 26(3), pp. 248–273. doi: 10.1007/BF02382401.

Huber, D. R., Eason, T. G., Hueter, R. E. and Motta, P. J. (2005) 'Analysis of the bite force and mechanical design of the feeding mechanism of the durophagous horn shark Heterodontus francisci', *Journal of Experimental Biology*, 208(18), pp. 3553–3571. doi: 10.1242/jeb.01816.

Humle, T. (2011) 'The Chimpanzees of Bossou and Nimba', *Folia Primatologica*, 82(4–5), pp. 246–247. doi: 10.1159/000336262.

Humle, T. and Matsuzawa, T. (2004) 'Oil palm use by adjacent communities of chimpanzees at Bossou and Nimba Mountains, West Africa', *International Journal of Primatology*, 25(3), pp. 551–581. doi: 10.1023/B:IJOP.0000023575.93644.f4.

Hylander, W L (1975) 'Incisor size and diet in anthropoids with special reference to Cercopithecidae Incisor Size and Diet in Anthropoids with Special Reference to Cercopithecidae', *Science*, 189(4208), pp. 1095–1098. doi: 10.1126/science.808855.

Hylander, W. L. (1975) 'The Human Mandible: Lever', *American Journal of Physical Anthropology*, 43(2), pp. 227–242.

Hylander, W. L. (1979) 'The Functional Significance of Primate Mandibular Form', *Journal of Morphology*, 160(2), pp. 223–240.

Hylander, W. L. (2006) 'Functional anatomy and biomechanics of the masticatory apparatus', in Laskin, D. M., Greene, C. S., and Hylander, W. L. (eds) *Temporomandibular disorders: an evidenced approach to diagnosis and treatment*. New York: Quitessence Pub Co, pp. 3–34.

Hylander, W. L. (2013) 'Functional Links Between Canine Height and Haw Gape in Catarrhines with Speical Reference to Early Hominins', *Vertebrate Paleobiology and Paleoanthropology*, 150(2), pp. 247–259. doi: 10.1002/ajpa.22195.

Iriarte-Diaz, J., Terhune, C. E., Taylor, A. B. and Ross, C. F. (2017) 'Functional correlates of the position of the axis of rotation of the mandible during chewing in non-human primates', *Zoology*, 124(Oct), pp. 106–118. doi: 10.1016/j.zool.2017.08.006.

Iwamoto, T., Mori, A., Kawai, M. and Bekele, A. (1996) 'Anti-predator Behavior of Gelada Baboons', *Primates*, 37(4), pp. 389–397.

Izawa, K. (1979) 'Foods and feeding behavior of wild black-capped capuchin (Cebus apella)', *Primates*, 20(1), pp. 57–76. doi: 10.1007/BF02373828.

Izawa, K. and Mizuno, A. (1977) 'Palm-fruit cracking behavior of wild black-capped capuchin (Cebus apella)', *Primates*, 18(4), pp. 773–792. doi: 10.1007/BF02382930.

Janson, C. H. (1990) 'Social correlates of individual spatial choice in foraging groups of brown capuchin monkeys, Cebus apella', *Animal Behaviour*, 40(5), pp. 910–921. doi: 10.1016/S0003-3472(05)80993-5.

Johnston, E. (2003) *Papio anubis skull*. Available at: http://rafael.glendale.edu/skull/papio_anubis/right.htm (Accessed: 1 June 2020).

Katz, D. and Friess, M. (2014) 'Technical note: 3D from standard digital photography of human crania - A preliminary assessment', *American Journal of Physical Anthropology*, 154(1), pp. 152–158. doi: 10.1002/ajpa.22468.

Kay, R. F. (1975) 'The functional adaptations of primate molar teeth', *American Journal of Physical Anthropology*, 43(2), pp. 195–215. doi: 10.1002/ajpa.1330430207.

King, S. J., Arrigo-nelson, S. J., Pochron, S. T., Semprebon, G. M., Godfrey, L. R., Wright, P. C. and Jernvall, J. (2005) 'Dental senescence in a long-lived primate links infant survival to rainfall', *Proceedings of the National Academy of Sciences*, 102(46), pp. 16579–16583.

King, S. J., Boyer, D. M., Tecot, S., Strait, S. G., Zohdy, S., Blanco, M. B., Wright, P. C. and Jernvall, J. (2012) 'Lemur Habitat and Dental Senescence in Ranomafana', *American Journal of Physical Anthropology*, 148(2), pp. 228–237. doi: 10.1002/ajpa.21589.

Kinzey, W. G. (1992) 'Dietary and dental adaptaions in the Pitheciinae', *American Journal of Physical Anthropologyournal of physical anthropology*, 88(4), pp. 499–514.

Kinzey, W. G. and Norconk, M. a. (1993) 'Physical and chemical properties of fruit and seeds eaten byPithecia andChiropotes in Surinam and Venezuela', *International Journal of Primatology*, 14(2), pp. 207–227. doi: 10.1007/BF02192632.

Kinzey, W. G. and Norconk, M. A. (1990) 'Hardness as a Basis of Fruit Choice in Two Sympatric Primates', *American Journal of Physical Anthropology*, 81(1), pp. 5–15.

Koenigswald, W. Von (2011) 'Diversity of hypsodont teeth in mammalian dentitions – construction and classification', *Palaeontographica*, 294(1–3), pp. 63–94. doi: 10.1127/pala/294/2011/63.

Kolmann, M. A., Crofts, S. B., Dean, M. N., Summers, A. P. and Lovejoy, N. R. (2015) 'Morphology does not predict performance : jaw curvature and prey crushing in durophagous stingrays', *Journal of Experimental Biology*, 218(24), pp. 3941–3949. doi: 10.1242/jeb.127340.

Komsta, L. and Novomestky, F. (2015) 'moments: Moments, cumulants, skewness, kurtosis and related tests'. Available at: https://cran.r-project.org/package=moments.

Koolstra, J. H. and van Eijden, T. M. G. J. (1992) 'Application and validation of a three-dimensional mathematical model of the human masticatory system in vivo', *Journal of Biomechanics*, 25(2), pp. 175–187. doi: 10.1016/0021-9290(92)90274-5.

Koolstra, J. H. and van Eijden, T. M. G. J. (1997) 'Dynamics of the human masticatory muscles during a jaw open-close movement', *Journal of Biomechanics*, 30(9), pp. 883–889.

Koolstra, J. H. and Van Eijden, T. M. G. J. (1995) 'Biomechanical Analysis of Jaw-closing Movements', *Journal of Dental Research*, 74(9), pp. 1564–1570. doi: 10.1177/00220345950740091001.

Koops, K., McGrew, W. C. and Matsuzawa, T. (2013) 'Ecology of culture: Do environmental factors influence foraging tool use in wild chimpanzees, Pan troglodytes verus?', *Animal Behaviour*, 85(1), pp. 175–185. doi: 10.1016/j.anbehav.2012.10.022.

Koyabu, D. B. and Endo, H. (2009) 'Craniofacial variation and dietary adaptations of African colobines', *Journal of Human Evolution*, 56(6), pp. 525–536. doi: 10.1016/j.jhevol.2008.12.009.

Koyabu, D. B. and Endo, H. (2010) 'Craniodental mechanics and diet in Asian colobines: Morphological evidence of mature seed predation and sclerocarpy', *American Journal of Physical Anthropology*, 142(1), pp. 137–148. doi: 10.1002/ajpa.21213.

Lahm, S. (1986) 'Diet and habitat preference of Mandrillus sphinx in Gabon: implications of foraging strategy', *American Journal of Primatology*, 26(11), pp. 9–26. doi: 10.1002/ajp.1350110103.

Laird, M. F., Vogel, E. R. and Pontzer, H. (2016) 'Chewing efficiency and occlusal functional morphology in modern humans', *Journal of Human Evolution*, 93(4), pp. 1–11. doi: 10.1016/j.jhevol.2015.11.005.

Laird, M. F., Wright, B. W., Rivera, A. O., Fogaça, M. D., Casteren, A. Van, Fragaszy, D. M., Izar, P., Visalberghi, E., Scott, R. S., Strait, D. S., Ross, C. F. and Wright, K. A. (2020) 'Ingestive behaviors in

bearded capuchins (Sapajus libidinosus)', *Scientific Reports*, 10(1), p. 20840. doi: 10.1038/s41598-020-77797-2.

Lambert, J. E., Chapman, C. A., Wrangham, R. W. and Conklin-Brittain, N. Lou (2004) 'Hardness of cercopithecine foods: Implications for the critical function of enamel thickness in exploiting fallback foods', *American Journal of Physical Anthropology*, 125(4), pp. 363–368. doi: 10.1002/ajpa.10403.

Langenbach, G. E. J. and Hannam, A. G. (1999) 'The role of passive muscle tensions in a three-dimensional dynamic model of the human jaw', *Archives of Oral Biology*, 44(7), pp. 557–573. doi: 10.1016/S0003-9969(99)00034-5.

Lawn, B. R. and Lee, J. J. W. (2009) 'Analysis of fracture and deformation modes in teeth subjected to occlusal loading', *Acta Biomaterialia*, 5(6), pp. 2213–2221. doi: 10.1016/j.actbio.2009.02.001.

Lawn, B. R., Lee, J. J. W., Constantino, P. J. and Lucas, P. W. (2009) 'Predicting failure in mammalian enamel', *Journal of the Mechanical Behavior of Biomedical Materials*, 2(1), pp. 33–42. doi: 10.1016/j.jmbbm.2008.05.007.

Ledogar, J. A., Luk, T. H. Y., Perry, J. M. G., Neaux, D. and Wroe, S. (2018) 'Biting mechanics and niche separation in a specialized clade of primate seed predators', *PLoS ONE*, 13(1), pp. 1–26. doi: 10.1371/journal.pone.0190689.

Ledogar, J. A., Winchester, J. M., St. Clair, E. M. and Boyer, D. M. (2013) 'Diet and dental topography in pitheciine seed predators', *American Journal of Physical Anthropology*, 150(1), pp. 107–121. doi: 10.1002/ajpa.22181.

Lee-Thorp, J. (2011) 'The demise of "Nutcracker Man"', *Proceedings of the National Academy of Sciences of the United States of America*, 108(23), pp. 9319–9320. doi: 10.1073/pnas.1105808108.

Leigh, S. R., Setchell, J. M. and Buchanan, L. S. (2005) 'Ontogenetic Bases of Canine Dimorphism in Anthropoid Primates', *American Journal of Physical Anthropology*, 127(3), pp. 296–311. doi: 10.1002/ajpa.20096.

Lima, E. M. and Ferrari, S. F. (2003) 'Diet of a free-ranging group of squirrel monkeys (Saimiri sciureus) in Eastern Brazilian Amazonia', *Folia Primatologica*, 74(3), pp. 150–158. doi: 10.1159/000070648.

Losos, J. B. (2011) 'Convergence, Adaptation, and Constraint', *Evolution*, 65(7), pp. 1827–1840. doi: 10.1111/j.1558-5646.2011.01289.x.

Lucas, P., Constantino, P., Wood, B. and Lawn, B. (2008) 'Dental enamel as a dietary indicator in mammals', *BioEssays*, 30(4), pp. 374–385. doi: 10.1002/bies.20729.

Lucas, P. W. (1982) 'An analysis of the canine tooth size of old world higher primates in relation to mandibular length and body weight', *Archives of Oral Biology*, 27(6), pp. 493–496. doi: 10.1016/0003-9969(82)90090-5.

Lucas, P. W. (2004) *Dental Functional Morphology: How Teeth Work*. Cambridge: Cambridge University Press. doi: 10.26575/daj.v18i2.137.

Lucas, P. W., Lowreytt, T. K., Pereira, B. P. and Sarafjsw, V. (1991) 'The ecology of Mezzettia leptopoda1 (Hk. f. et Thoms.) Oliv. (Annonaceae) seeds as viewed from a mechanical perspective', *Functional Ecology*, 5(4), pp. 545–553.

Lucas, P. W., Peters, C. R. and Arrandale, S. R. (1994) 'Seed-breaking forces exerted by orang-utans with their teeth in captivity and a new technique for estimating forces produced in the Wild', *American Journal of Physical Anthropology*, 94(3), pp. 365–378. doi: 10.1002/ajpa.1330940306.

Lucas, P. W., Prinz, J. F., Agrawal, K. R. and Bruce, I. C. (2002) 'Food physics and oral physiology', *Food Quality and Preference*, 13(4), pp. 203–213. doi: 10.1016/S0950-3293(00)00036-7.

Luke, D. A. and Lucas, P. W. (1983) 'The significance of cusps', *Journal of Oral Rehabilitation*, 10(3), pp. 197–206. doi: 10.1111/j.1365-2842.1983.tb00113.x.

Madeira, M. and De Oliveira, A. (1979) 'Anatomical Aspects of the Masticatory Muscles of the Tufted Capuchin (Cebus Apella)', *Okajimas Folia Anatomica Japonica*, 56(1), pp. 35–44. doi: 10.2535/ofaj1936.56.1_35.

Makedonska, J., Wright, B. W. and Strait, D. S. (2012) 'The Effect of Dietary Adaption on Cranial Morphological Integration in Capuchins (Order Primates, Genus Cebus)', *PLoS ONE*, 7(10), pp. 20–24. doi: 10.1371/journal.pone.0040398.

Marcé-Nogué, J., Püschel, T. A. and Kaiser, T. M. (2017) 'A biomechanical approach to understand the ecomorphological relationship between primate mandibles and diet', *Scientific Reports*, 7(1), pp. 1–12. doi: 10.1038/s41598-017-08161-0.

Marshall, A. J. and Wrangham, R. W. (2007) 'Evolutionary Consequences of Fallback Foods', *International Journal of Primatology*, 28(6), pp. 1219–1235. doi: 10.1007/s10764-007-9218-5.

Martin, L. B., Olejniczak, A. J. and Maas, M. C. (2003) 'Enamel thickness and microstructure in pitheciin primates, with comments on dietary adaptations of the middle Miocene hominoid Kenyapithecus', *Journal of Human Evolution*, 45(5), pp. 351–367. doi: 10.1016/j.jhevol.2003.08.005.

Martinez, C. M. and Sparks, J. S. (2017) 'Malagasy cichlids differentially limit impacts of body shape evolution on oral jaw functional morphology', *Evolution*, 71(9), pp. 2219–2229. doi: 10.1111/evo.13298.

Martins-Junior, A. M. G., Carneiro, J., Sampaio, I., Ferrari, S. F. and Schneider, H. (2018) 'Phylogenetic relationships among Capuchin (Cebidae , Platyrrhini) lineages : An old event of sympatry explains the current distribution of Cebus and Sapajus', *Genetics and Molecular Biology*, 41(3), pp. 699–712.

Masterson, T. J. (1997) 'Sexual dimorphism and interspecific cranial form in two capuchin species: Cebus albifrons and C. apella', *American Journal of Physical Anthropology*, 104(4), pp. 487–511. doi: 10.1002/(SICI)1096-8644(199712)104:4<487::AID-AJPA5>3.0.CO;2-P.

Maughan, R. J., Watson, J. S. and Weir, J. (1983) 'Strength and cross-sectional area of human skeletal muscle.', *The Journal of Physiology*, 338(1), pp. 37–49. doi: 10.1113/jphysiol.1983.sp014658.

Maynard Smith, J. and Savage, R. J. G. (1957) 'The Mechanics of Mammalian Jaws', *The School Science Review*, 141, pp. 289–301.

McGraw, W. Scott, van Casteren, A., Kane, E., Geissler, E., Burrows, B. and Daegling, D. J. (2014) 'Feeding and oral processing behaviors of two colobine monkeys in Tai Forest, Ivory Coast', *Journal of Human Evolution*, 98, pp. 90–102. doi: 10.1016/j.jhevol.2015.06.001.

McGraw, W. S., Vick, A. E. and Daegling, D. J. (2011) 'Sex and age differences in the diet and ingestive behaviors of sooty mangabeys (Cercocebus atys) in the Tai forest, Ivory coast', *American Journal of Physical Anthropology*, 144(1), pp. 140–153. doi: 10.1002/ajpa.21402.

McGraw, W.S., Vick, A. E. and Daegling, D. J. (2014) 'Dietary variation and food hardness in sooty mangabeys (Cercocebus atys): Implications for fallback foods and dental adaptation', *American Journal of Physical Anthropology*, 154(3), pp. 413–423. doi: 10.1002/ajpa.22525.

Mcgrew, W. C., Baldwin, P. J. and Tutin, C. E. G. (1988) 'Diet of Wild Chimpanzees (Pan troglodytes verus) at Mt. Assirik, Senegal: I. Composition', *American Journal of Primatology*, 16(3), pp. 213–226. doi: https://doi.org/10.1002/ajp.1350160304.

McGrew, W. C., Ham, R. M., White, L. J. T., Tutin, C. E. G. and Fernandez, M. (1997) 'Why don't chimpanzees in Gabon crack nuts?', *International Journal of Primatology*, 18(3), pp. 353–374. doi: 10.1023/A:1026382316131.

Metzger, K. A. and Herrel, A. (2005) 'Correlations between lizard cranial shape and diet : a quantitative , phylogenetically informed analysis', *Biological Journal of the Linnean Society*, 86(4), pp. 433–466. doi: https://doi.org/10.1111/j.1095-8312.2005.00546.x.

Mitteroecker, P. and Gunz, P. (2009) 'Advances in Geometric morphometrics', *Evolutionary Biology*, 36(2), pp. 235–247. doi: 10.1007/s11692-009-9055-x.

Moazen, M., Curtis, N., Evans, S. E., O'Higgins, P. and Fagan, M. J. (2008) 'Rigid-body analysis of a lizard skull: Modelling the skull of Uromastyx hardwickii', *Journal of Biomechanics*, 41(6), pp. 1274–1280. doi: 10.1016/j.jbiomech.2008.01.012.

Moen, D. S., Irschick, D. J., Wiens, J. J. and Moen, D. S. (2013) 'Evolutionary conservatism and convergence both lead to striking similarity in ecology , morphology and performance across continents in frogs', *Proceedings of the Royal Society B: Biological Sciences*, 280(1773), p. 20132156. doi: http://dx.doi.org/10.1098/rspb.2013.2156.

Moore, K. L. (2014) *Clinically oriented anatomy*. Lippincott Williams & Wilkins.

Morales-Jimenez, A. L., Disotell, T. and Di, A. (2015) 'Molecular Phylogenetics and Evolution Revisiting the phylogenetic relationships , biogeography , and taxonomy of spider monkeys (genus Ateles) in light of new molecular data', *Molecular Phylogenetics and Evolution*, 82(1), pp. 467–483. doi: 10.1016/j.ympev.2014.09.019.

Morgan, B., Ford, A. L. J. and Smith, M. J. (2019) 'Standard methods for creating digital skeletal models using structure-from-motion photogrammetry', *American Journal of Physical Anthropology*, 169(1), pp. 152–160. doi: 10.1002/ajpa.23803.

Morris, P. J. R., Cobb, S. N. F. and Cox, P. G. (2018) 'Convergent evolution in the Euarchontoglires', *Biology Letters*, 14(8), pp. 9–12. doi: 10.1098/rsbl.2018.0366.

Neeser, R., Ackermann, R. R. and Gain, J. (2009) 'Comparing the accuracy and precision of three techniques used for estimating missing landmarks when reconstructing fossil hominin crania', *American Journal of Physical Anthropology*, 140(1), pp. 1–18. doi: 10.1002/ajpa.21023.

Norconk, M. A., Grafton, B. A. and McGraw, W. S. (2013) 'Morphological and ecological adaptations to seed predation - a primata - wide perspective', *Evolutionary Biology and Conservation of Titis, Sakis and Uacaris*, 29(1), pp. 160–178.

Norconk, M. A., Raghanti, M. A., Martin, S. K., Grafton, B. W., Gregory, L. T. and De Dijn, B. P. E. (2003) 'Primates of Brownsberg Natuurpark, Suriname, With Particular Attention To the Pitheciins', *Neotropical Primates Fundação Biodiversitas*, 11(2), pp. 215–222.

Norconk, M. A. and Veres, M. (2011) 'Physical properties of fruit and seeds ingested by primate seed predators with emphasis on sakis and bearded sakis', *Anatomical Record*, 294(12), pp. 2092–2111. doi: 10.1002/ar.21506.

Norconk, M. A., Wright, B. W., Conklin-brittain, N. L. and Vinyard, C. J. (2009) 'Mechanical and Nutritional Properties of Food as Factors in Platyrrhine Dietary Adaptations', in Garber, P. A., Estrada, A. E., Bicca-Marques, J. C., and Heymann, E. W. (eds) *South American Primates: Comparative Perspectives in the Study of Behaviour, Ecology, and Conservation*. New York: Springer, pp. 279–314. doi: 10.1007/978-0-387-78705-3.

O'Connor, C. F., Franciscus, R. G. and Holton, N. E. (2005) 'Bite force production capability and

efficiency in neandertals and modern humans', *American Journal of Physical Anthropology*, 127(2), pp. 129–151. doi: 10.1002/ajpa.20025.

O'Higgins, P. (2000) 'The study of morphological variation in the hominid fossil record: biology, landmarks and geometry', *Journal of Anatomy*, 197(1), pp. 103–120. doi: 10.1046/j.1469-7580.2000.19710103.x.

O'Higgins, P., Cobb, S. N., Fitton, L. C., Gröning, F., Phillips, R., Liu, J. and Fagan, M. J. (2011) 'Combining geometric morphometrics and functional simulation: an emerging toolkit for virtual functional analyses', *Journal of Anatomy*, 218(1), pp. 3–15. doi: 10.1111/j.1469-7580.2010.01301.x.

O'Higgins, P., Fitton, L. C., Phillips, R., Cobb, S. N. and Fagan, M. J. (2012) 'Virtual Functional Morphology: Novel Approaches to the Study of Craniofacial Form and Function', *Evolutionary Biology*, 39(4), pp. 521–535. doi: 10.1007/s11692-012-9173-8.

Okecha, A. A. and Newton-Fisher, N. E. (2006) 'The Diet of Olive Baboons (Papio anubis) in the Budongo Forest', in Newton-Fisher, N. E., Notman, H., Reynolds, V., and Paterson, J. D. (eds) *Primates of Western Uganda*. New York.

de Oliveira, S. G., Lynch Alfaro, J. W. and Veiga, L. M. (2014) 'Activity budget, diet, and habitat use in the critically endangered Ka'apor capuchin monkey (Cebus kaapori) in Para State, Brazil: A preliminary comparison to other capuchin monkeys', *American Journal of Primatology*, 76(10), pp. 919–931. doi: 10.1002/ajp.22277.

Olsen, A. (2016) '{linkR}: 3D Lever and Linkage Mechanism Modeling'. Available at: https://aaronolsen.github.io/software/linkr.html.

Olsen, A. (2018) 'bezier: Toolkit for Bezier Curves and Splines'. Available at: https://cran.r-project.org/package=bezier.

Olsen, A. M. (2017) 'Feeding ecology is the primary driver of beak shape diversification in waterfowl', *Functional Ecology*, 31(10), pp. 1985–1995. doi: 10.1111/1365-2435.12890.

Osborn, J. W. (1987) 'Relationship between the mandibular condyle and the occlusal plane during hominid evolution: Some of its effects on jaw mechanics', *American Journal of Physical Anthropology*, 73(2), pp. 193–207. doi: 10.1002/ajpa.1330730206.

Page, C. E. and Cooper, N. (2017) 'Morphological convergence in "river dolphin" skulls', *PeerJ*, 5, p. e4090. doi: 10.7717/peerj.4090.

Palmqvist, P., Martínez-navarro, B., Pérez-claros, J. A., Torregrosa, V., Figueirido, B., Jiménez-arenas, J. M., Espigares, M. P., Ros-montoya, S. and Renzi, M. De (2011) 'The giant hyena Pachycrocuta brevirostris : Modelling the bone-cracking behavior of an extinct carnivore', *Quaternary International*, 243(1), pp. 61–79. doi: 10.1016/j.quaint.2010.12.035.

Pampush, J. D., Daegling, D. J., Vick, A. E., Mcgraw, W. S., Covey, R. M. and Rapoff, A. J. (2011) 'Technical Note : Converting Durometer Data into Elastic Modulus in Biological Materials', *American Journal of Physical Anthropology*, 146(9), pp. 650–653. doi: 10.1002/ajpa.21628.

Pampush, J. D., Duque, A. C., Burrows, B. R., Daegling, D. J., Kenney, W. F. and McGraw, W. S. (2013) 'Homoplasy and thick enamel in primates', *Journal of Human Evolution*, 64(3), pp. 216–224. doi: 10.1016/j.jhevol.2013.01.009.

Pearson, O. M. and Lieberman, D. E. (2004) 'The Aging of Wolff's " Law ": Ontogeny and Responses to Mechanical Loading in Cortical Bone', *Yearbook of Physical Anthropology*, 125(S39), pp. 63–99. doi: 10.1002/ajpa.20155.

Peck, C. C., Langenbach, G. E. J. and Hannam, A. G. (2000) 'Dynamic simulation of muscle and

articular properties during human wide jaw opening', *Archives of Oral Biology*, 45(11), pp. 963–982. doi: 10.1016/S0003-9969(00)00071-6.

Peres, C. A. (1991) 'Seed Predation of Cariniana micrantha (Lecythidaceae) by Brown Capuchin Monkeys in Central Amazonia', *Biotropica*, 23(3), pp. 262–270.

Peres, C. A. (1993) 'Notes on the Ecology of Buffy Saki Monkeys (Pithecia albicans, Gray 1860): A Canopy Seed-Predator', *American Journal of Primatology*, 31(2), pp. 129–140. doi: 10.1002/ajp.1350310205.

Perry, J. M. G. (2018) 'Inferring the Diets of Extinct Giant Lemurs from Osteological Correlates of Muscle Dimensions', *Anatomical Record*, 301(2), pp. 343–362. doi: 10.1002/ar.23719.

Perry, J. M. G. and Hartstone-Rose, A. (2011) 'The Jaw Adductors of Strepsirrhines in Relation to Body Size, Diet, and Ingested Food Size', *The Anatomical Record*, 294(4), pp. 712–728. doi: 10.1002/ar.21354.

Perry, J. M. G. and Wall, Christine E. (2008) 'Scaling of the Chewing Muscles in Prosimians', in Vinyard, C., Ravosa, M. J., and Wall, C. E. (eds) *Primate Craniofacial Function and Biology*. Springer US, pp. 217–240. doi: 10.1007/978-0-387-76585-3_11.

Plavcan, J. M. and Ruff, C. B. (2008) 'Canine Size , Shape , and Bending Strength in Primates and Carnivores', *American Journal of Physical Anthropology*, 136(1), pp. 65–84. doi: 10.1002/ajpa.20779.

Port-Carvalho, M., Ferrari, S. F. and Magalhaes, C. (2003) 'Predation of Crabs by Tufted Capuchins (Cebus apella) in Eastern Amazonia', *Folia Primatologica*, 75(3), pp. 1–12. doi: 10.1159/0000XXXXX.

Profico, A., Buzi, C., Melchionna, M., Piras, P., Raia, P. and Veneziano, A. (2019) 'Arothron: Geometric Morphometrics Analysis and Virtual Anthropology'. Available at: https://cran.r-project.org/package=Arothron.

Püschel, T. A., Marcé-Nogué, J., Kaiser, T. M., Brocklehurst, R. J. and Sellers, W. I. (2018) 'Analyzing the sclerocarpy adaptations of the Pitheciidae mandible', *American Journal of Primatology*, 80(5), pp. 1–16. doi: 10.1002/ajp.22759.

Raadsheer, M. C., van Eijden, T. M., van Ginkel, F. C. and Prahl-Andersen, B. (1999) 'Contribution of jaw muscle size and craniofacial morphology to human bite force magnitude', *Journal of Dental Research*, 78(1), pp. 31–42. doi: 10.1177/00220345990780010301.

Rak, Y. (1983) *The Australopithecine Face*, *The Australopithecine Face*. New York: Academic Press. doi: 10.1016/c2013-0-07547-0.

Ravosa, M. J. (1990) 'Functional Assessment of Subfamily Variation in Maxillomandibular Morphology Among Old World Monkeys', *American Journal of Physical Anthropology*, 82(2), pp. 199–212.

Ravosa, M. J., Vinyard, C. J. and Gagnon, M. (2000) 'Evolution of Anthropoid Jaw Loading and Kinematic Patterns', *American Journal of Physical Anthropology*, 112(4), pp. 493–516.

Revell, L. J. (2012) 'phytools: An R package for phylogenetic comparative biology (and other things).', *Methods in Ecology and Evolution*, 3, pp. 217–223.

Robinson, C. and Terhune, C. E. (2017) 'Error in geometric morphometric data collection: Combining data from multiple sources', *American Journal of Physical Anthropology*, 164(1), pp. 62–75. doi: 10.1002/ajpa.23257.

van Roosmalen, M. G. M. (1985) 'Habitat preferences, diet, feeding strategy, and social organisation of the black spider monkey [Ateles paniscus paniscus Linneaeus 1758] in Surinam', *Acta Amazonica*,

15(3–4), pp. 1–236.

Rosenberger, A. L. (1992) 'Evolution of Feeding Niches in New-World Monkeys', *American Journal of Physical Anthropology*, 88(4), pp. 525–562. doi: 10.1002/ajpa.1330880408.

Ross, C. (1995) 'Muscular and osseous anatomy of the primate anterior temporal fossa and the functions of the postorbital septum', *American Journal of Physical Anthropology*, 98(3), pp. 275–306. doi: 10.1002/ajpa.1330980304.

Ross, C. F., Berthaume, M. A., Dechow, P. C., Iriarte-Diaz, J., Porro, L. B., Richmond, B. G., Spencer, M. and Strait, D. (2011) 'In vivo bone strain and finite-element modeling of the craniofacial haft in catarrhine primates', *Journal of Anatomy*, 218(1), pp. 112–141. doi: 10.1111/j.1469-7580.2010.01322.x.

Ross, C. F., Dharia, R., Herring, S. W., Hylander, W. L., Liu, Z.-J., Rafferty, K. L., Ravosa, M. J. and Williams, S. H. (2007) 'Modulation of mandibular loading and bite force in mammals during mastication', *Journal of Experimental Biology*, 210(6), pp. 1046–1063. doi: 10.1242/jeb.02733.

Ross, C. F. and Iriarte-diaz, J. (2014) 'What Does Feeding System Morphology Tell Us About Feeding?', 23(3), pp. 105–120. doi: 10.1002/evan.21410.

Ross, C. F. and Iriarte-Diaz, J. (2014) 'What does feeding system morphology tell us about feeding?', *Evolutionary Anthropology*, 23(3), pp. 105–120. doi: 10.1002/evan.21410.

Ross, C. F. and Iriarte-Diaz, J. (2019) 'Evolution, constraint, and optimality in primate feeding systems', in Bels, V. and Whishaw, I. Q. (eds) *Feeding in Vertebrates*. Springer International Publishing, pp. 787–829. doi: 10.1007/978-3-030-13739-7.

Ross, C. F., Iriarte-Diaz, J. and Nunn, C. L. (2012) 'Innovative Approaches to the Relationship Between Diet and Mandibular Morphology in Primates', *International Journal of Primatology*, 33(3), pp. 632–660. doi: 10.1007/s10764-012-9599-y.

Ross, C. F., Iriarte-Diaz, J., Platts, E., Walsh, T., Heins, L., Gerstner, G. E. and Taylor, A. B. (2017) 'Scaling of rotational inertia of primate mandibles', *Journal of Human Evolution*, 106, pp. 119–132. doi: 10.1016/j.jhevol.2017.02.007.

Ross, C. F., Iriarte-Diaz, J., Reed, D. A., Stewart, T. A. and Taylor, A. B. (2016) 'In vivo bone strain in the mandibular corpus of Sapajus during a range of oral food processing behaviors', *Journal of Human Evolution*, 98, pp. 36–65. doi: 10.1016/j.jhevol.2016.06.004.

Rowland, C., Fitton, L. C. and Oa, M. P. R. (2015) 'The Impact of Simplifications on the Performance of a Finite Element Model of a Macaca fascicularis Cranium', *The Anatomical Record*, 298(1), pp. 107–121. doi: 10.1002/ar.23075.

de Ruiter, J. R. (1986) 'The Influence of Group Size on Predator Scanning and Foraging Behaviour of Wedgecapped Capuchin Monkeys', *Behaviour*, 98(1), pp. 240–258.

Russo, S. E., Campbell, C. J., Dew, J. L., Stevenson, P. R. and Suarez, S. A. (2005) 'A Multi-Forest Comparison of Dietary Preferences and Seed Dispersal by Ateles spp.', *International Journal of Primatology*, 26(5), pp. 1017–1037. doi: 10.1007/s10764-005-6456-2.

Sampaio, D. T. (2005) 'Predation of an Infant Titi Monkey (Callicebus moloch) by a Tufted Capuchin (Cebus apella)', *Folia Primatologica*, 76, pp. 113–115. doi: 10.1159/000083617.

Santana, S. E. (2016) 'Quantifying the effect of gape and morphology on bite force: Biomechanical modelling and in vivo measurements in bats', *Functional Ecology*, 30(4), pp. 557–565. doi: 10.1111/1365-2435.12522.

Santana, S. E. and Cheung, E. (2016) 'Go big or go fish: Morphological specializations in carnivorous bats', *Proceedings of the Royal Society B: Biological Sciences*, 283(1830). doi: 10.1098/rspb.2016.0615.

Santana, S. E. and Dumont, E. R. (2009) 'Connecting behaviour and performance : the evolution of biting behaviour and bite performance in bats', *Journal of Evolutionary Biology*, 22(11), pp. 2131–2145. doi: 10.1111/j.1420-9101.2009.01827.x.

Santana, S. E., Dumont, E. R. and Davis, J. L. (2010) 'Mechanics of bite force production and its relationship to diet in bats', *Functional Ecology*, 24(4), pp. 776–784. doi: 10.1111/j.1365-2435.2010.01703.x.

Santana, S. E., Grosse, I. R. and Dumont, E. R. (2012) 'Dietary hardness, loading behaviour, and the evolution of skull form in bats', *Evolution*, 66(8), pp. 2587–2598. doi: 10.5061/dryad.d548646j.

Schlager, S. (2017) 'Morpho and Rvcg -- Shape Analysis in {R}', in Zheng, G., Li, S., and Szekely, G. (eds) *Statistical Shape and Deformation Analysis*. Academic Press, pp. 217–256.

Schumacher, G. H. (1961) *Funktionelle Morphologie der Kaumuskulatur*, *VEB G*. Jena: Fischer Verlag.

Scott, R. S., Ungar, P. S., Bergstrom, T. S., Brown, C. A., Grine, F. E., Teaford, M. F. and Walker, A. (2005) 'Dental microwear texture analysis shows within-species diet variability in fossil hominins', *Nature*, 436(7051), pp. 693–695. doi: 10.1038/nature03822.

Sellers, W. I. and Crompton, R. H. (2004) 'Using sensitivity analysis to validate the predictions of a biomechanical model of bite forces', *Annals of Anatomy*, 186(1), pp. 89–95. doi: 10.1016/S0940-9602(04)80132-8.

Setchell, J. M., Lee, P. C., Wickings, E. J. and Dixson, A. F. (2001) 'Growth and Ontogeny of Sexual Size Dimorphism in the Mandrill (Mandrillus sphinx)', *American Journal of Physical Anthropology*, 115(4), pp. 349–360.

Sherratt, E., Rasmussen, A. R. and Sanders, K. L. (2018) 'Trophic specialization drives morphological evolution in sea snakes', *Royal Society Open Science*, 5(3), p. 172141. doi: http://dx.doi.org/10.1098/rsos.172141.

Shi, J., Curtis, N., Fitton, L. C., O'Higgins, P. and Fagan, M. J. (2012) 'Developing a musculoskeletal model of the primate skull: Predicting muscle activations, bite force, and joint reaction forces using multibody dynamics analysis and advanced optimisation methods', *Journal of Theoretical Biology*, 310, pp. 21–30. doi: 10.1016/j.jtbi.2012.06.006.

Singleton, M. (2002) 'Patterns of cranial shape variation in the Papionini (Primates : Cercopithecinae)', *Journal of Human Evolution*, 42(5), pp. 547–578. doi: 10.1006/jhev.2001.0539.

Singleton, M. (2005) 'Functional Shape Variation in the Cercopithecine Masticatory Complex', in Slice, D. (ed.) *Modern Morphometrics in Physical Anthropology*. New York: Kluwer Academic, pp. 319–348.

Singleton, M. (2015) 'Functional Geometric Morphometric Analysis of Masticatory System Ontogeny in Papionin Primates', *The Anatomical Record*, 298(1), pp. 48–63. doi: 10.1002/ar.23068.

Slice, D. E. (2007) 'Geometric Morphometrics', *Annual Review of Anthropology*, 36(1), pp. 261–81. doi: 10.1146/annurev.anthro.34.081804.120613.

Slowikowski, K. (2020) 'ggrepel: Automatically Position Non-Overlapping Text Labels with "ggplot2"'. Available at: https://cran.r-project.org/package=ggrepel.

Smith, A. L., Benazzi, S., Ledogar, J. A., Tamvada, K., Smith, L. C. P., Weber, G. W., Spencer, M. A.,

Lucas, P. W., Michael, S., Shekeban, A. L. I., Madden, R. H., Richmond, B. G. and Wright, B. W. (2015) 'The Feeding Biomechanics and Dietary Ecology of Paranthropus boisei', *The Anatomical Record*, 298(1), pp. 145–167. doi: 10.1002/ar.23073.

Smith, R. J. and Jungers, W. L. (1997) 'Body mass in comparative primatology', *Journal of Human Evolution*, 32(6), pp. 523–559.

de Sousa, J. and S. (2009) 'Taxonomy and geographic distribution of the species of the Pitheciidae', in Veiga, L. M., Barnett, A. A., Ferrari, S. F., and Norconk, M. A. (eds) *Evolutionary Biology and Conservation of Titis, Sakis and Uacaris*. Cambridge University Press, pp. 31–44.

Spencer, M. A. (2003) 'Tooth-Root Form and Function in Platyrrhine Seed-Eaters', *American Journal of Physical Anthropology*, 122(4), pp. 325–335. doi: 10.1002/ajpa.10288.

Spencer, M. A. and Demes, B. (1993) 'Biomechanical Analysis of Masticatory System Configuration in Neandertals and Inuits', *American Journal of Physical Anthropology*, 91(1), pp. 1–20.

Sponheimer, M., Passey, B. H., De Ruiter, D. J., Guatelli-Steinberg, D., Cerling, T. E. and Lee-Thorp, J. A. (2006) 'Isotopic evidence for dietary variability in the early hominin Paranthropus robustus', *Science*, 314(5801), pp. 980–982. doi: 10.1126/science.1133827.

Stammbach, E (1986) '10. Desert, Forest and Montane Baboons: Multilevel-Societies', in Smuts, B., Cheney, D., Seyforth, R., and Wrangham, R. (eds) *Primate Societies*. Chicago: University Chicago Press, pp. 112–145.

Stayton, C. T. (2008) 'Is convergence surprising? An examination of the frequency of convergence in simulated datasets', *Journal of Theoretical Biology*, 252(1), pp. 1–14. doi: 10.1016/j.jtbi.2008.01.008.

Stayton, C. T. (2015a) 'The definition, recognition, and interpretation of convergent evolution, and two new measures for quantifying and assessing the significance of convergence', *Evolution*, 69(8), pp. 2140–2153. doi: 10.1111/evo.12729.

Stayton, C. T. (2015b) 'What does convergent evolution mean? The interpretation of convergence and its implications in the search for limits to evolution', *Interface Focus*, 5(6), p. 20150039. doi: 10.1098/rsfs.2015.0039.

Stayton, C. T. (2018) 'convevol: Analysis of Convergent Evolution'. Available at: https://cran.r-project.org/package=convevol.

Strait, D. S. *et al.* (2009) 'The feeding biomechanics and dietary ecology of Australopithecus africanus', *Proceedings of the National Academy of Sciences*, 106(7), pp. 2124–2129. doi: https://doi.org/10.1073/pnas.0808730106.

Strait, S. G. (1997) 'Tooth use and the physical properties of food', *Evolutionary Anthropology*, 5(6), pp. 199–211. doi: 10.1002/(sici)1520-6505(1997)5:6<199::aid-evan2>3.0.co;2-8.

Sugiyama, Y. (1987) 'A Preliminary List of Chimpanzees ' Alimentation at Bossou , Guinea', *Primates*, 28(1), pp. 133–147.

Swan, K. R. (2016) *Dental morphology and mechanical efficiency during development in a hard object feeding primate (Cercocebus atys)*. PhD Thesis. Hull York Medical School.

Swindler, D. (2002) *Primate Dentition: An Introduction to the Teeth of Non-Human Primates*. Cambridge: Cambridge University Press. doi: 10.26575/daj.v16i2.161.

Swindler, D. R. and Wood, C. D. (1973) 'Atlas of Primate Gross Anatomy'. University of Washington Press.

Tamura, M. (2020) 'Extractive foraging on hard - shelled walnuts and variation of feeding techniques in wild Japanese macaques (Macaca fuscata)', *American Journal of Primatology*, 82(6), pp. 1–14. doi: 10.1002/ajp.23130.

Tanner, J. B., Dumont, E. R., Sakai, S. T., Lundrigan, B. L. and Holekamp, K. E. (2008) 'Of arcs and vaults: The biomechanics of bone-cracking in spotted hyenas (Crocuta crocuta)', *Biological Journal of the Linnean Society*, 95(2), pp. 246–255. doi: 10.1111/j.1095-8312.2008.01052.x.

Taylor, A. B. (2002) 'Masticatory Form and Function in the African Apes', *American Journal of Physical Anthropology*, 117(2), pp. 133–156. doi: 10.1002/ajpa.10013.

Taylor, A. B., Eng, C. M., Anapol, F. C. and Vinyard, C. J. (2009) 'The functional correlates of jaw-muscle fiber architecture in tree-gouging and nongouging callitrichid monkeys', *American Journal of Physical Anthropology*, 139(3), pp. 353–367. doi: 10.1002/ajpa.20991.

Taylor, A. B., Terhune, C. E., Toler, M., Holmes, M., Ross, C. F. and Vinyard, C. J. (2018) 'Jaw-Muscle Fiber Architecture and Leverage in the Hard-Object Feeding Sooty Mangabey are not Structured to Facilitate Relatively Large Bite Forces Compared to Other Papionins', *Anatomical Record*, 301(2), pp. 325–342. doi: 10.1002/ar.23718.

Taylor, A. B., Terhune, C. E. and Vinyard, C. J. (2019) 'The influence of masseter and temporalis sarcomere length operating ranges as determined by laser diffraction on architectural estimates of muscle force and excursion in macaques (Macaca fascicularis and Macaca mulatta)', *Archives of Oral Biology*, 105, pp. 35–45. doi: 10.1016/j.archoralbio.2019.05.015.

Taylor, A. B. and Vinyard, C. J. (2004) 'Comparative analysis of masseter fiber architecture in tree-gouging (Callithrix jacchus) and nongouging (Saguinus oedipus) callitrichids', *Journal of Morphology*, 261(3), pp. 276–285. doi: 10.1002/jmor.10249.

Taylor, A. B. and Vinyard, C. J. (2009) 'Jaw-muscle fiber architecture in tufted capuchins favors generating relatively large muscle forces without compromising jaw gape', *Journal of Human Evolution*, 57(6), pp. 710–720. doi: 10.1016/j.jhevol.2009.06.001.

Taylor, A. B. and Vinyard, C. J. (2013) 'The relationships among jaw-muscle fiber architecture, jaw morphology, and feeding behavior in extant apes and modern humans', *American Journal of Physical Anthropology*, 151(1), pp. 120–134. doi: 10.1002/ajpa.22260.

Taylor, Andrea B., Yuan, T., Ross, C. F. and Vinyard, C. J. (2015) 'Jaw-muscle force and excursion scale with negative allometry in platyrrhine primates', *American Journal of Physical Anthropology*, 158(2), pp. 242–256. doi: 10.1002/ajpa.22782.

Taylor, Andrea B, Yuan, T., Ross, C. F. and Vinyard, C. J. (2015) 'Jaw-Muscle Force and Excursion Scale With Negative Allometry in Platyrrhine Primates', *American Journal of Physical Anthropology*, 158(2), pp. 242–256. doi: 10.1002/ajpa.22782.

Teaford, M. F. and Ungar, P. S. (2000) 'Diet and the evolution of the earliest human ancestors.', *Proceedings of the National Academy of Sciences*, 97(25), pp. 13506–13511. doi: 10.1073/pnas.260368897.

Telfer, P. T., Souquiere, S., Clifford, S. L., Abernethy, A., Bruford, M. W., Disotell, T. R., Sterner, K. N., Roques, P., Marx, P. A. and Wickings, E. J. (2003) 'Molecular evidence for deep phylogenetic divergence in Mandrillus sphinx', *Molecular Ecology*, 12(7), pp. 2019–2024. doi: 10.1046/j.1365-294X.2003.01877.x.

Terborgh, J. (1984) *Five New World primates: a study in comparative ecology.* Princeton University Press.

Terhune, C. E. (2011) 'Dietary correlates of temporomandibular joint morphology in new world monkeys', *American Journal of Physical Anthropology*, 150(2), pp. 260–272. doi: 10.1002/ajpa.22204.

Terhune, C. E. (2013) 'How effective are geometric morphometric techniques for assessing functional shape variation? An example from the great ape temporomandibular joint', *Anatomical Record*, 296(8), pp. 1264–1282. doi: 10.1002/ar.22724.

Terhune, C. E., Cooke, S. B. and Otrola-Castillo, E. (2015) 'Form and Function in the Platyrrhine Skull: A Three-Dimensional Analysis of Dental and TMJ Morphology', *Anatomical Record*, 298(1), pp. 29–47. doi: 10.1002/ar.23062.

Terhune, C. E., Hylander, W. L., Vinyard, C. J. and Taylor, A. B. (2015) 'Jaw-muscle architecture and mandibular morphology influence relative maximum jaw gapes in the sexually dimorphic Macaca fascicularis', *Journal of Human Evolution*, 82, pp. 145–158. doi: 10.1016/j.jhevol.2015.02.006.

Terhune, C. E., Iriarte-Díaz, J., Taylor, A. B. and Ross, C. F. (2011) 'The instantaneous center of rotation of the mandible in nonhuman primates.', *Integrative and comparative biology*, 51(2), pp. 320–32. doi: 10.1093/icb/icr031.

Thiery, G., Guy, F. and Lazzari, V. (2017) 'Investigating the dental toolkit of primates based on food mechanical properties: Feeding action does matter', *American Journal of Primatology*, 79(6), pp. 1–15. doi: 10.1002/ajp.22640.

Thomason, J. J. (1991) 'Cranial strength in relation to estimated biting forces in some mammals', *Canadian Journal of Zoology*, 69(9), pp. 2326–2333. doi: 10.1139/z91-327.

Thompson, C. J., Ahmed, N. I., Veen, T., Peichel, C. L., Hendry, A. P., Bolnick, D. I. and Stuart, Y. E. (2017) 'Many-to-one form-to-function mapping weakens parallel morphological evolution', *Evolution*, 71(11), pp. 2738–2749. doi: 10.1111/evo.13357.

Throckmorton, G. S. and Dean, J. S. (1994) 'The relationship between jaw-muscle mechanical advantage and activity levels during isometric bites in humans', *Archives of Oral Biology*, 39(5), pp. 429–437. doi: 10.1016/0003-9969(94)90174-0.

Toro-Ibacache, V., Zapata Muñoz, V. and O'Higgins, P. (2016) 'The relationship between skull morphology, masticatory muscle force and cranial skeletal deformation during biting', *Annals of Anatomy*, 203, pp. 59–68. doi: 10.1016/j.aanat.2015.03.002.

Toro-Ibacache, V., Zapata, V. and Noz, M. U. (2015) 'The Predictability from Skull Morphology of Temporalis and Masseter Muscle Cross-Sectional Areas in Humans', *The Anatomical Record*, 298(7), pp. 1261–1270. doi: 10.1002/ar.23156.

Tyler, C. L; Stafford, E.S; Leighton, L. R. (2014) 'The utility of wax replicas as a measure of crab attack frequency in the rocky intertidal', *Journal of Marine Biological Association of the United Kingdom*, 95(2), pp. 361–369. doi: 10.1017/S0025315414001210.

Ungar, P. s. (2004) 'Dental Functional Morphology - the known, the unknown, and the unknowable', *Dental Functional Morphology*. doi: 10.1017/cbo9780511735011.

Ungar, P. S. (2010) *Mammal Teeth: Origin, Evolution, and Diversity*. Baltimore: John Hopkins Press.

Ungar, P. S. (2015) 'Mammalian dental function and wear: A review', *Biosurface and Biotribology*, 1(1), pp. 25–41. doi: 10.1016/j.bsbt.2014.12.001.

Ungar, P. S., Grine, F. E. and Teaford, M. F. (2008) 'Dental Microwear and Diet of the Plio-Pleistocene Hominin Paranthropus boisei', *PLoS ONE*, 3(4), p. e2044. doi: 10.1371/journal.pone.0002044.

Ungar, P. S., Healy, C., Karme, A., Teaford, M. and Fortelius, M. (2016) 'Dental topography and diets of platyrrhine primates', *Historical Biology*, 2963(November), pp. 1–12. doi: 10.1080/08912963.2016.1255737.

Ungar, P. S. and M'Kirera, F. (2003) 'A solution to the worn tooth conundrum in primate functional anatomy', *Proceedings of the National Academy of Sciences of the United States of America*, 100(7), pp. 3874–3877. doi: 10.1073/pnas.0637016100.

Ungar, P. S. and Sponheimer, M. (2011) 'The diets of early hominins', *Science*, 334(6053), pp. 190–193. doi: 10.1126/science.1207701.

Ungar, P. and Williamson, M. (2000) 'Exploring the effects of tooth wear on functional morphology: A preliminary study using dental topographic analysis', *Palaeontologia Electronica*, 3(1), pp. 1–18.

Veneziano, A., Landi, F. and Profico, A. (2018) 'Surface smoothing, decimation, and their effects on 3D biological specimens', *American Journal of Physical Anthropology*, 166(2), pp. 473–480. doi: 10.1002/ajpa.23431.

Venkataraman, V. V, Glowacka, H., Fritz, J., Clauss, M., Seyoum, C., Nguyen, N. and Fashing, P. J. (2014) 'Effects of Dietary Fracture Toughness and Dental Wear on Chewing Efficiency in Geladas (Theropithecus gelada)', *American Journal of Physical Anthropology*, 155(1), pp. 17–32. doi: 10.1002/ajpa.22571.

Verderane, M., Izar, P., Visalberghi, E. and Fragaszy, D. (2013) 'Socioecology of wild bearded capuchin monkeys (Sapajus libidinosus): An analysis of social relationships among female primates that use tools in feeding', *Behaviour*, 150(6), pp. 659–689. doi: 10.1163/1568539X-00003076.

Vinyard, C. J., Taylor, A. B., Teaford, M. F., Glander, K. E., Ravosa, M. J., Rossie, J. B., Ryan, T. M. and Williams, S. H. (2011) 'Are we looking for loads in all the right places? New research directions for studying the masticatory apparatus of New World monkeys', *Anatomical Record*, 294(12), pp. 2140–2157. doi: 10.1002/ar.21512.

Vinyard, C. J., Wall, C. E., Williams, S. H. and Hylander, W. L. (2003) 'Comparative functional analysis of skull morphology of tree-gouging primates', *American Journal of Physical Anthropology*, 120(2), pp. 153–170. doi: 10.1002/ajpa.10129.

Vinyard, C. J., Wall, C. E., Williams, S. H. and Hylander, W. L. (2008) 'Patterns of variation across primates in jaw-muscle electromyography during mastication', *American Zoologist*, 48(2), pp. 294–311. doi: 10.1093/icb/icn071.

Visalberghi, E. Ã., Sabbatini, G., Spagnoletti, N., Andrade, F. R. D., Ottoni, E. and Izar, P. (2008) 'Physical Properties of Palm Fruits Processed With Tools by Wild Bearded Capuchins (Cebus libidinosus)', *American Journal of Primatology*, 70(9), pp. 884–891. doi: 10.1002/ajp.20578.

Wainwright, P. C. (2009) 'Innovation and diversity in functional morphology', in Laubichler, M. D. and Maienschein, J. (eds) *Form and Function in Development Evolution*. Cambridge University Press, pp. 132–152.

Wainwright, P. C., Alfaro, M. E., Bolnick, D. I. and Hulsey, C. D. (2005) 'Many-to-One Mapping of Form to Function: A General Principle in Organismal Design?', *Integrative and Comparative Biology*, 45(2), pp. 256–262. doi: 10.1093/icb/45.2.256.

Wall, C. E. (1999) 'A model of temporomandibular joint function in anthropoid primates based on condylar movements during mastication', *American Journal of Physical Anthropology*, 109(1), pp. 67–88. doi: 10.1002/(SICI)1096-8644(199905)109:1<67::AID-AJPA7>3.0.CO;2-F.

Wall, C. E., Vinyard, C. J., Johnson, K. R., Williams, S. H., Hylander, W. L. and Carolina, N. (2006)

'Phase II Jaw Movements and Masseter Muscle Activity During Chewing in Papio anubis', *American Journal of Physical Anthropology*, 120(2), pp. 215–224. doi: 10.1002/ajpa.20290.

Watson, P. J., Gröning, F., Curtis, N., Fitton, L. C., Herrel, A., McCormack, S. W. and Fagan, M. J. (2014) 'Masticatory biomechanics in the rabbit: A multi-body dynamics analysis', *Journal of the Royal Society Interface*, 11(99). doi: 10.1098/rsif.2014.0564.

Weber, G. W. (2015) 'Virtual Anthropology', *American Journal of Physical Anthropology*, 156(S59), pp. 22–42. doi: 10.1002/ajpa.22658.

Weijs, W. A., Brugman, P. and Grimbergen, C. A. (1989) 'Jaw movements and muscle activity during mastication in growing rabbits', *The Anatomical Record*, 224(3), pp. 407–416. doi: 10.1002/ar.1092240309.

Westneat, M. W. (2003) 'A biomechanical model for analysis of muscle force, power output and lower jaw motion in fishes', *Journal of Theoretical Biology*, 223(3), pp. 269–281. doi: 10.1016/S0022-5193(03)00058-4.

Wickham, H. (2016) *ggplot2: Elegant Graphics for Data Analysis*. Springer-Verlag New York. Available at: https://ggplot2.tidyverse.org.

Wickham, H. (2019) 'stringr: Simple, Consistent Wrappers for Common String Operations'. Available at: https://cran.r-project.org/package=stringr.

Wickham, H. *et al.* (2019) 'Welcome to the {tidyverse}', *Journal of Open Source Software*, 4(43), p. 1686. doi: 10.21105/joss.01686.

Wickham, H., Francois, R., Henry, L. and Mueller, K. (2021) 'dplyr: A Grammar of Data Manipulation'. Available at: https://cran.r-project.org/package=dplyr.

Wieczkowski, J. (2003) *Aspects of the ecological flexibility of the Tana Mangabey (Cercocebus galeritus) in its fragmented habitat, Tana River, Kenya*. PhD Thesis. University of Georgia.

Wieczkowski, J. (2009) 'Brief communication: Puncture and crushing resistance scores of Tana River mangabey (Cercocebus galeritus) diet items', *American Journal of Physical Anthropology*, 140(3), pp. 572–577. doi: 10.1002/ajpa.21132.

Williams, S. H., Wright, B. W., den Truong, V., Daubert, C. R. and Vinyard, C. J. (2005) 'Mechanical Properties of Foods Used in Experimental Studies of Primate Masticatory Function', *American Journal of Primatology*, 1222(11), pp. 1210–1222. doi: 10.1002/ajp.

Williamson, L. and Lucas, P. (1995) 'The effect of moisture content on the mechanical properties of a seed shell', *Journal of Materials Science*, 30(1), pp. 162–166.

Winchester, J. M., Boyer, D. M., St. Clair, E. M., Gosselin-Ildari, A. D., Cooke, S. B. and Ledogar, J. A. (2014) 'Dental topography of platyrrhines and prosimians: Convergence and contrasts', *American Journal of Physical Anthropology*, 153(1), pp. 29–44. doi: 10.1002/ajpa.22398.

Wood, B. and Constantino, P. (2007) 'Paranthropus boisei: Fifty years of evidence and analysis', *American Journal of Physical Anthropology*, 134(S45), pp. 106–132. doi: 10.1002/ajpa.20732.

Wood, B. and Strait, D. (2004) 'Patterns of resource use in early Homo and Paranthropus', *Journal of Human Evolution*, 46(2), pp. 119–162. doi: 10.1016/j.jhevol.2003.11.004.

Wright, B. W. (2005) 'Craniodental biomechanics and dietary toughness in the genus Cebus', *Journal of Human Evolution*, 48(5), pp. 473–492. doi: 10.1016/j.jhevol.2005.01.006.

Wroe, S., McHenry, C. and Thomason, J. (2005a) 'Bite club: APPENDIX', *Proceedings of the Royal*

*Society B: Biological Sciences*, 272(1563), pp. 619–625. doi: 10.1098/rspb.2004.2986.

Wroe, S., McHenry, C. and Thomason, J. (2005b) 'Bite club: Comparative bite force in big biting mammals and the prediction of predatory behaviour in fossil taxa', *Proceedings of the Royal Society B: Biological Sciences*, 272(1563), pp. 619–625. doi: 10.1098/rspb.2004.2986.

Wroe, S., McHenry, C. and Thomason, J. (2005c) 'Bite club appendix', *Proceedings of the Royal Society B: Biological Sciences*, 272(1563), pp. 619–625. doi: 10.1098/rspb.2004.2986.

Yamakoshi, G. (1998) 'Dietary Responses to Fruit Scarcity of Wild Chimpanzees at Bossou , Guinea : Possible Implications for Ecological Importance of Tool Use', *American Journal of Physical Anthropology*, 295(April), pp. 283–295.

Young, R. L., Haselkorn, T. S. and Badyaev, A. V (2007) 'Functional Equivalence of Morphologies Enables Morphological and Ecological Diversity', *Evolution*, 61(11), pp. 2480–2492. doi: 10.1111/j.1558-5646.2007.00210.x.

# Appendix 1 - Specimen database

The specimen database is supplied via an online spreadsheet.

[Please click here to access the spreadsheet of specimen data for this appendix.](#)

The link will take you to a spreadsheet uploaded as a google spreadsheet. No log-ins are required.

The spreadsheet lists: specimen names, museum accession numbers, sex, whether the specimen was selected as the representative individual for tests which did not use the full sample, modality of scan, CT resolution (if CT), continent and location of origin of specimen, specimen source, whether a composite model was used for alignment to occlusion, specimen side (left or right) used for one-sided analyses, the number of missing landmarks, specimen source DOI (if available), media number (for Morphosource specimens), and funding information (where present).

# Appendix 2 - Data collection and preparation, including sensitivity studies (mixed imaging modalities and intraobserver error).

## A2.1 Data collection: Scan modalities

Samples for this study were collected from four different imaging modalities: Medical CT scans, MicroCT scans, structured-light surface scans, and photogrammetry (Fig. A2.1). These methods all result in 3D data, but with differences between modalities. Medical and MicroCT scans are volume scans which retain both the internal and external structure (Weber, 2015). The methods attain images with similar methods but MicroCT has a much higher resolution. Photogrammetry and surface scans only capture the external structure of objects. Photogrammetry uses a series of 2D digital photographs to produce a 3D model, taking a series of photographs with significant overlap which is then used to create a point cloud which can be triangulated to create a 3D surface (Katz and Friess, 2014; Evin et al., 2016). Surface scanners can use various methods, this study used a structured light scanner to collect data (Breuckmann SmartScan 3D), which creates 3D objects by measuring the deformation of a projected pattern of light on an object (Weber, 2015).
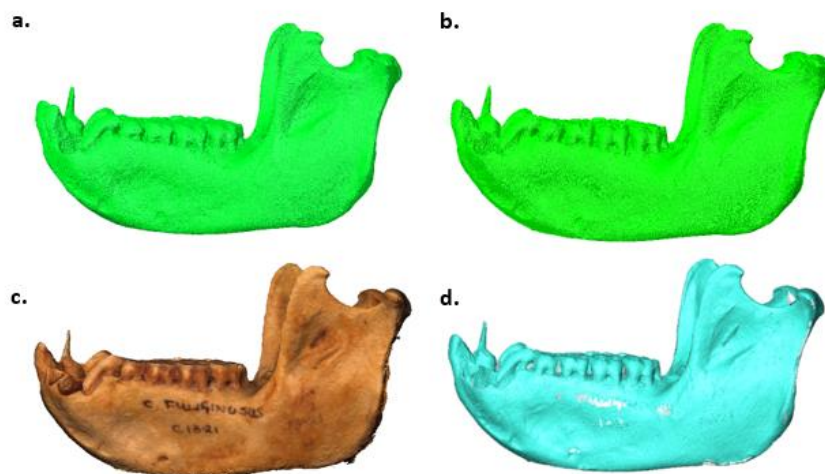


**Figure A2.1 A *Cercocebus* mandible in the four imaging modalities used for data analysis, showing: a. medical CT, b. microCT, c. photogrammetry, and d. surface scanner. Please note: the medCT scan pre-dates all other scans, and the specimen suffered the loss of an additional incisor after this scan was made.**

## A2.1.1 Scan processing: Medical and Micro-CT scans

Medical CT and MicroCT scans were obtained from a range of sources (Appendix 1). Of these, *Pan troglodytes* and *Cercocebus atys* were collected as Medical CT scans, and *Cacajao calvus, Cercocebus atys, Chiropotes satanas, Sapajus apella, Mandrillus sphinx, Pithecia pithecia* and *Saimiri sciureus* as MicroCT. Scans were processed and prepared by segmentation in Avizo (v9.2, Visualization Sciences Group, Burlington, MA, USA). An additional step was taken with some MicroCT scans, as due to extremely large file sizes for many scans it was necessary to reduce the voxel size via downsampling (Appendix 1). Voxel size was reduced to a compromise between the highest possible quality scan and a scan of a size that could easily be processed on the available computing facilities.

Following this preparatory step, scans were processed to create separate and cleaned surfaces of mandible and cranium using threshold-based segmentation. The maximum threshold value was left on the highest available value for all specimen, as the upper threshold ranges contained only anatomical material. The selection of the minimum threshold was guided the pterygoid plates of the cranium and the condyles of the mandible, two structures with relatively thin cortical bone. The highest threshold which left these two regions fully intact was selected. Following threshold selection, the mandible and cranium were separated (if necessary) and any extraneous material remaining after thresholding was cleaned.

## A2.1.2 Scan processing: Photogrammetry

Photogrammetry models were created using data collected at the Museum für Naturkunde, Berlin for *Ateles paniscus, Cacajao calvus, Cebus apella, Chiropotes satanas, Pithecia pithecia, Saimiri sciureus, Sapajus apella,* and *Theropithecus gelada.* A 24.3 mega-pixel digital single-lens reflex (DSLR) Nikon D5300 camera was used, mounted with a Nikon AF-P 18-55 mm f/5.6 lens. Mandible and crania were scanned separately to allow for capture of the entirety of the object, and in addition to this a 'composite' model of the mandible and cranium in occlusion was to guide alignment to occlusion. For photography, objects were placed in a light box with opaque but thin white walls, diffusing light to evenly illuminate the object. The entirety of the box and turntable for rotating the object were lined with black cloth to improve masking. Lights were placed on either side of the box as well as above the

box, facing downwards to illuminate the object from all angles. Camera settings were strictly controlled and set to match the environment, with a low ISO (125), aperture stop set at f/5.6, and a relatively fast shutter speed (1/25). Focus was manually adjusted at the start of each rotation-set of images. For both mandible and crania photographs were taken in three views. For composite models in occlusion only one view was photographed.

Photographs were imported into Agisoft PhotoScan (Professional Edition, v1.3.2, Agisoft LLC, St. Petersburg, Russia). Before processing, a mask was generated from the background of each image set and applied to the entire set of images. A standardised tolerance threshold for the mask was applied, which was only altered when necessary to process unusually coloured specimens. Features were always constrained to mask in the processing. Settings used for model processing were standardised across all objects and were kept on high quality settings, with high key and tie point limits increased to 80 000 and 8 000, respectively. The next step was to scale the models, which was done following the protocol recorded in Katz and Friess (2014). Three standardised measurements running in three directions were taken on the object using high precision digital callipers, measurements were then made on the model in Agisoft and applied while still holding the specimen. Models were exported without texture as texture could not be used in later steps of model processing.

### A2.1.3 Surface scans

Surface scans were collected at the Museum für Naturkunde, Berlin for *Ateles paniscus, Cacajao calvus, Cebus apella, Chiropotes satanas, Pithecia pithecia, Saimiri sciureus, Sapajus apella,* and *Theropithecus gelada*). A Breuckman Smartscan 3D (www.aicon.com) was used for all scans. This scanner was mounted with optical lenses of a medium size within the possible lenses for this system, which feature a diagonal scope of 250mm and an average spatial precision of 18 µm. Pilot work found these lenses to be an adequate size for the range of specimens scanned. Mandible and crania were scanned separately to allow for capture of the entirety of the object. The surface scanner was set up to face a darkened photography box, with black cloth lining the base and back wall of the box to produce an optimal background for masking. Between the scanner and this photography box a black, opaque curtain was hung to keep the light level stable and low inside the box. The object to

be scanned was placed on a black turntable, which was rotated to capture the entire object. Artificial lighting in the lab room was switched off to improve scan quality, only indirect natural light was present during scanning.

Approximately 35 individual scan-images were taken of each object, varying with specimen size. Each individual scan-image was taken at a high-quality setting and was produced from a series of three individual photographs in varying exposure levels. Automatic exposure was used to set lighting and exposure. The scanner was regularly calibrated to maintain accuracy. Completed scans were aligned and then merged to form a single surface file in the Breuckmann scanner's own software, Optocat (Breuckmann, 2014). Following data export the meshes were repaired without altering surface anatomy in Geomagic (Geomagic Studio, 3D Systems) with the aim of i.e. eliminating intersecting triangles.

## A2.2 Sensitivity: Imaging modalities

A sensitivity study was carried out to test the potential impact of using 3D scans from multiple modalities. The test aimed to assess whether combining different imaging modalities affects the results of a shape analysis, and if so, which modalities and how severely. A mandible was selected (*Cercocebus atys* #C13.21) which was available in all the modalities used in this study (Fig A2.1). This mandible had previously been scanned in both a MicroCT and a MedCT scanner. As this mandible forms part of the in-house collection at the Hull York Medical School, it was also possible to create a photogrammetry model and a surface scan model.

A landmark set representing key masticatory features was selected (Table A1.1). The selected mandible (C13.21) was landmarked in Avizo on 5 consecutive days in each modality. Additionally, MedCT scans of four other adult *Cercocebus atys* individuals (specimens 25626, c13.29, c13.12, c13.22) were landmarked once each, to provide a comparison. Landmarks were exported and analysed in R Studio (v1.1.383, RStudio Team, 2015) with the package Geomorph (v3.2.1, Adams et al., 2020). A procrustes registration was carried out, followed by a principal component analysis.

**Table A2.1 Landmarks used for sensitivity study.**

| Landmarks: Imaging modalities comparison | |
|---|---|
| # | Name and description |
| 1,2 | Gonion |
| 3,4 | Most superior point on coronoid process |
| 5,6 | Most posterior and inferior point of the coronoid process |
| 7,8 | Most anterior and inferior point of the coronoid process |
| 9,10 | Point where mandibular ramus meets alveolus laterally |
| 11,12 | Point posterior to the alveolus of the last maxillary molar T |
| 13,14 | Centre of last molar |
| 15,16 | Centre of first molar |
| 17,18 | Protocone of first premolar |
| 19,20 | Point between second incisor and canine on the alveolar bone |
| 21 | Infradentale |
| 22 | Most inferior point on mandibular symphysis |
| 23 | Point directly superior to lingual foramen |
| 24,25 | Most lateral point on the articular surface of the mandibular condyle |
| 26,27 | Most medial point on the articular surface of the mandibular condyle |
| 28,29 | Most posterior point on the articular surface of the mandibular condyle |
| 30,31 | Most anterior part on the mandibular condyle at the midpoint of the mediolateral curve |
| 32,33 | Fulcrum of the condyle |

Results of repeated landmarking on C13.21 in multiple modalities shows that while the surface scan, Medical CT, and MicroCT are primarily separated along the second PC (19% variance), photogrammetry is separated from other modalities along the first PC (25% of variance) (Fig. A2.2). Overall, the greatest overlap is between the surface scanner and the MicroCT. Plotting the comparison specimens reveals that all modalities very tightly cluster when compared with a broader sample even when that sample is composed of individuals of the same species (Fig. A2.3).

Results show that although there are some differences between modalities, most especially photogrammetry relative to the other modalities, the difference is relatively small and is overshadowed by shape differences with other individuals of the same species. As is advocated in past studies (Cooke and Terhune, 2015), caution must be taken on very precise and small-scale comparisons using these models. However, the four different imaging modalities will be used in a broad comparison between distantly related species, so there is no concern that the minor effect of using a combination of imaging modalities will influence results.
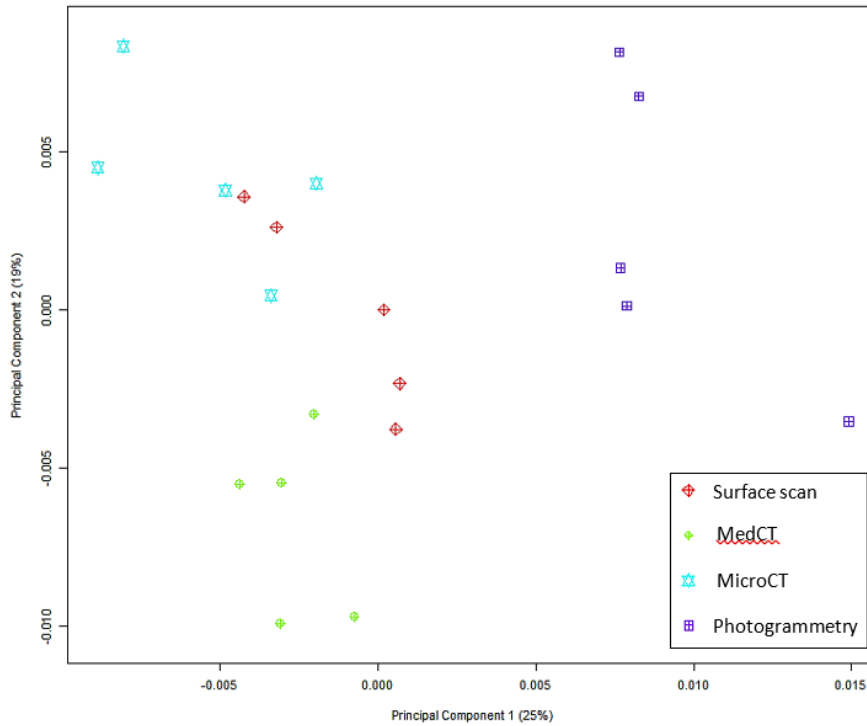
**Figure A2.2 Principal components plot for comparison of imaging modalities (PC1 and PC2), modalities in isolation. Showing PC1 (25% of variance) and PC2 (19% of variance).**
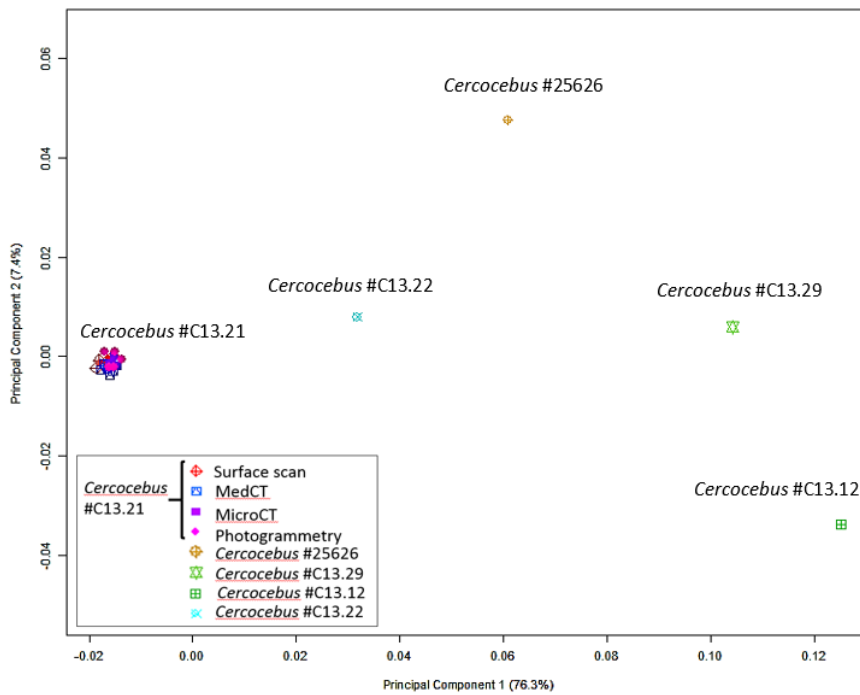


**Figure A2.3 Principal components plot for comparison of imaging modalities (PC1 and PC2), modalities and comparison specimens. Showing PC1 (76.3% of variance) and PC2 (7.4% of variance)**.

## A2.3 Sensitivity: Intraobserver error

A specimen with no damage to landmarked areas was selected (*Pithecia pithecia* specimen #38461, surface scan) to test for intraobserver error. Landmarks were placed for 5 consecutive days, then results were compared against two additional specimens (*Ateles* 39432 and *Pan* 383) using GMM methods. The landmark set (109 landmarks, 62 cranial and 39 mandibular) placed was larger than the set used for final data collection (Ch. 2, Table 2.3) with a larger number of Type II landmarks being included in this initial test which were removed following evidence of especially high intraobserver error. Unlike the final analysis, mandible and cranium were analysed separately here, in order to better appreciate problematic landmarks.

For both cranium and mandible, a Procrustes Anova with 999 permutations was carried out on the five repeats landmarking *Pithecia* in RStudio (v1.1.383, RStudio Team, 2015) using the package Morpho (v2.6, Schlager, 2017). Results were not significant in either case ($p = 0.638$ for the cranium, $p = 0.551$ for the mandible). A principal component analysis was then carried out for both the cranium and mandible, including the two comparison species. Results for both show the *Pithecia* repeats closely grouped and separated from the comparison species, although for the cranium there is some spread along the first principal component (Fig A2.).

The variability of each landmark was also assessed, ranking all landmarks from most to least variable for the mandible and cranium separately. Highly variable landmarks were assessed and, in a small number of cases, removed to increase overall study accuracy. For those landmarks which showed especially high variability but were essential to the study aims, a new protocol was developed to use during landmark placement. A reference guide was made with photographs of all landmarks in the view for which that landmark would be placed. The guide was used as a reference during all landmarking. The results of this test showed the intraobserver error to not be significant even before these adjustments, it is expected that these alterations further increased accuracy.
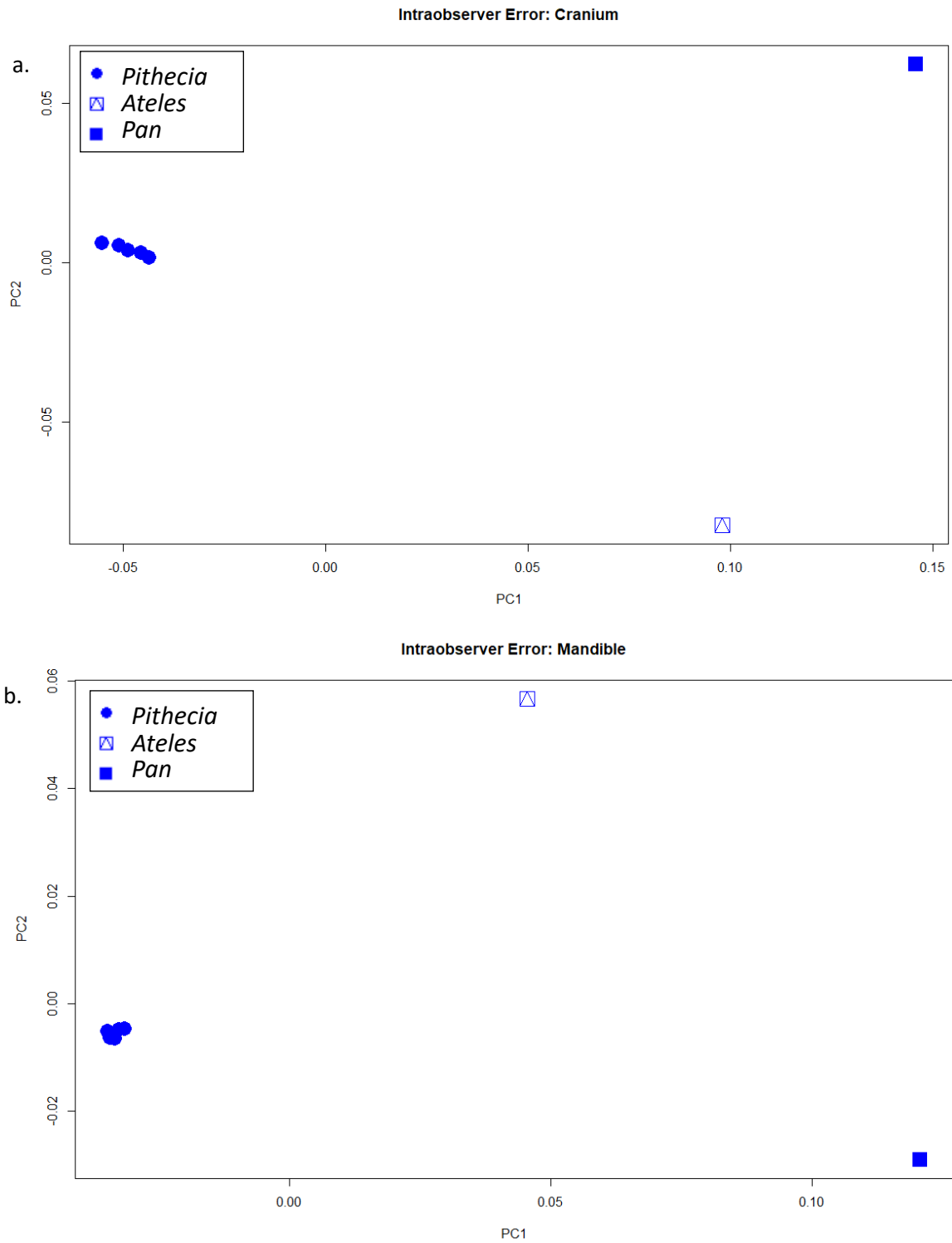
**Figure A2.4 Principal component plots showing test of intraobserver error after five landmarking repeats on** *Pithecia* **specimen as well as two comparison specimens. Results are for the cranium (above), showing PC1 (78.14% of variance) and PC2 (19.54% of variance), and the mandible (below), showing PC1 (83.26% of variance) and PC2 (15.82% of variance).**

# Appendix 3 - Sensitivity - Occlusal plane for vertical component in out-lever calculation

Given the broad range of jaw morphologies in the present sample, a sensitivity study was undertaken to estimate the effects of altering the occlusal plane used to calculate out-lever length. Three species were selected: *Mandrillus*, an African primate with a very flat occlusal plane, and both *Cacajao* and *Chiropotes*, two South American primates with very pronounced curvature of spee and procumbent incisors. For the sensitivity, mechanical advantage was calculated for each tooth along the dental row using out-lever lengths from three different orientations along the occlusal plane (A3.1, Fig A3.1).

**Table A3.1 Name and description of the three occlusal planes used in the sensitivity to generate out-lever lengths for the calculation of mechanical advantage.**

| Plane | Description |
|---|---|
| Full row plane | Occlusal plane was set from M3 to the centre between the first incisors. |
| Posterior row plane | Occlusal plane was set from M3 to the centre of PM2. |
| Two planes: Posterior and anterior planes | Two occlusal planes were set, a posterior plane from M3 to PM2 and an anterior plane from PM1 to the centre between the first incisors. Out-lever for the posterior teeth (M3 – PM2) was calculated using the posterior plane, and out-lever for the anterior teeth (PM1-incisor) was calculated using the anterior plane. |
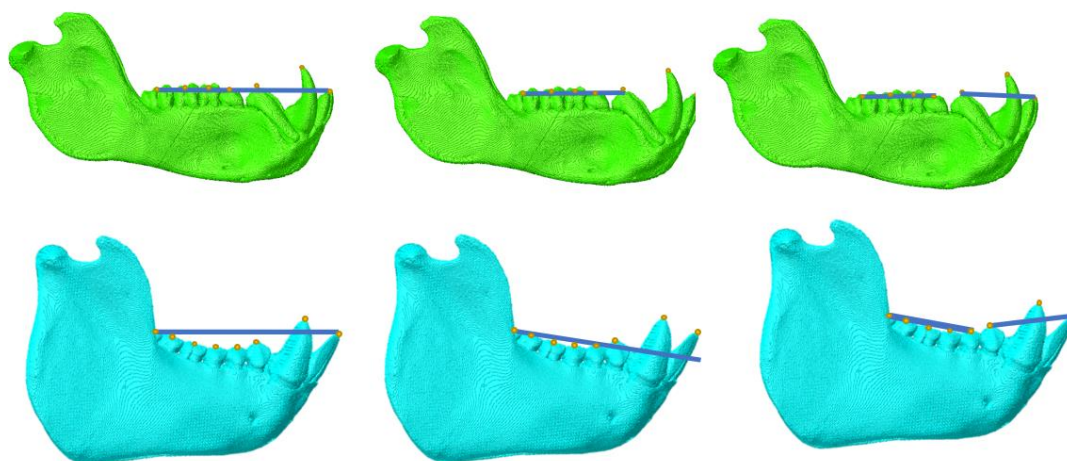


**Figure A3.1 The three occlusal plane options demonstrated on *Mandrillus* (above) and *Chiropotes* (below). Images not to scale. From left: full row plane (M3 – incisor); posterior row plane (M3 – PM2); and two plane, with separate anterior and posterior row planes (M3 – PM2 and PM1 – incisor).**

The methods detailed in Chapter 3 (3.3) were applied three times for each specimen, calculating mechanical advantage for each occlusal plane without modifying any other parameters. Results found that there are very pronounced differences between results using different occlusal planes for out-lever lengths for some species, but not for others (Fig. A3.2). Note that results calculated using the posterior plane and the two plane methods have the same orientation for M3 – PM2, so divergence between all three methods is only apparent from PM1 - incisor.

All three occlusal planes resulted in almost identical values for the mandrills, with very slight deviations on the first premolar (Fig. A3.2). However, both *Cacajao* and *Chiropotes* showed pronounced differences between planes, both following the same pattern: The full row plane results in a much higher mechanical advantage is much higher from M3 – PM2, however from PM1 – incisor there is little difference between the full row and posterior row planes. This indicates that for *Cacajao* and *Chiropotes* the full row plane results in a shorter out-lever, likely caused by the procumbent incisors tilting the plane upwards and shortening the distance to the condyle. The two-plane approach resulted in a very high mechanical advantage for the first premolar, which rises to a higher value on PM1 than PM2. This is illogical as PM2 is closer to the fulcrum than PM1. A separate anterior plane also results in higher values for mechanical advantage on canine and incisor, although to a lesser degree.

Overall, the selection of a plane has a far greater impact on some species than others, most especially on the last molars and first premolars. Results from the two-plane model were found to be inaccurate. The full row plane also risks a prominent effect from the anterior dentition, which are the most variable in their orientation. As such, the most conservative plane, the posterior row plane, was selected for the calculation of out-lever.
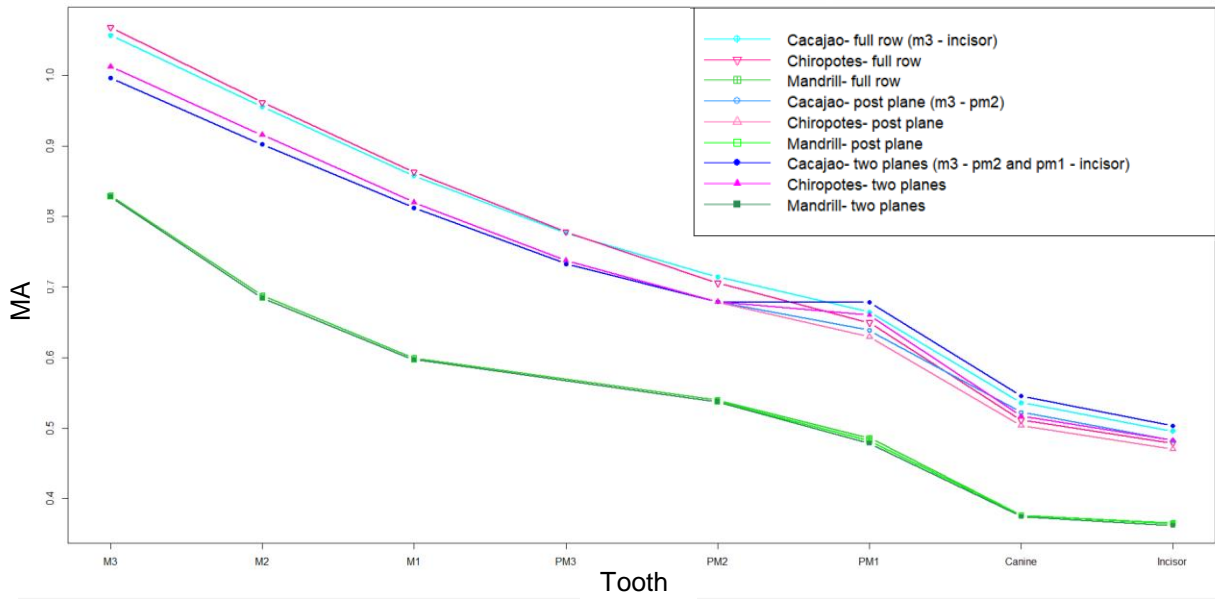
**Figure A3.2 Results of sensitivity study, showing mechanical advantage along the dental row of three primates,** *Cacajao* **(blue tones),** *Chiropotes* **(pink tones), and** *Mandrillus* **(green tones) for superior anterior masseter (SAM) at a gape of 10 mm. Mechanical advantage for three different occlusal planes is presented, note that M3 – PM2 results are identical in one set, hence the presence of three lines only on the anterior dentition.**

# Appendix 4 - Script for calculation of functional parameters (Ch. 3).

The following code was used in RStudio (v1.1.463, RStudio Team, 2018) to extract mechanical advantage at a series of gape heights as well as associated measurements. The code used the following packages: Arothron (Profico et al., 2015, v1.0.1), tcltk (R core team, 2018), linkR (Olsen, 2016, v1.1.1), MALDIquant (Gibb and Stimmer, 2012, v1.19.3), and stringr (Wickham, 2018, v1.3.1).

The code is divided into 4 scripts: a top-level script used to run all other three as functions, and three scripts which 1. Calculated out-levers, 2. Extracted and combined landmark coordinates for the and 3. Carried out all remaining calculations.

Note that any text following # is not executed so this is used for explanatory comments. Working directory names have been removed – a new user running this code would need to set working directories with their files.

Note also that values were calculated for more muscles and linear gape heights than were included in the thesis.

## Script 1: Top level

```
print("sourcing functions")
setwd()
source("OutLeverFunctions.R")
source("extract_coords.R")
source("calc_functions.r")

setwd()
dir <- getwd()
speciesfolderlist <- list.files()

for(species in speciesfolderlist){
  print(paste("extracting", species, "data"))
  setwd(paste(dir,"/",species,sep= ""))
  specimenList  <- list.files()
  extract_coords()

  #go into species folder

  for(specimen in specimenList){
    print(paste("calculating outlever for", species, specimen))
    setwd(paste(dir, "/",species,"/",specimen,sep = ""))
    secondlastletter <- substr(specimen, nchar(specimen)-1,nchar(specimen)-1)
    if(secondlastletter == "O"){
      OldWorldOutLeverFunction(paste(dir, "/",species,"/",specimen,sep = ""))
    } else if (secondlastletter == "N"){
      NewWorldOutLeverFunction(paste(dir, "/",species,"/",specimen,sep = ""))
    }
    print(paste("calculating mechanical advantage for", species, specimen))
    calculate_mechanical_advantage(getwd())
  }
}
```

# Script 2: Function for calculating out-levers

```
OldWorldOutLeverFunction <- function(foldername){

 library(Arothron)
 #out-lever length
 ##African and South American primates have different numbers of teeth so there are two sections run. At the time of coding I
abbreviated files with "Old world" and "New world" to refer to Africa and South America. I have since realised how inappropriate this
language is. Unfortunately, it was coded into all files. These terms were not included in the main body of text and will not be included in
future file naming in new projects.

 #in post occlusal plane
 mandible_set_p=read.amira.set("full_lms_post_plane.landmarkAscii", nland="auto")
 post_dent=read.amira.set("post_bitepoints_post_plane.landmarkAscii", nland="auto")
 #in ant occlusal plane (sensitivity)
 mandible_set_a=read.amira.set("full_lms_post_plane.landmarkAscii", nland="auto")
 ant_dent=read.amira.set("ant_bitepoints_post_plane.landmarkAscii", nland="auto")

 setwd(foldername)
 lastLetterOfWd <- substr(getwd(), nchar(getwd()),nchar(getwd()))
 if(lastLetterOfWd == "L"){
  ### LEFT HAND SIDE
  tmjpo <- mandible_set_p[89,1:3,1]
  tmjan <- mandible_set_a[89,1:3,1]
 } else  if(lastLetterOfWd == "R"){
  ### RIGHT HAND SIDE
  tmjpo <- mandible_set_p[90,1:3,1]
  tmjan <- mandible_set_a[90,1:3,1]
 }

 #specify the position of each dental landmark
 m3 <-post_dent[1,1:3,1]
 m2 <-post_dent[2,1:3,1]
 m1 <-post_dent[3,1:3,1]
 pm2 <-post_dent[4,1:3,1]
 pm1 <-ant_dent[1,1:3,1]
 canine <-ant_dent[2,1:3,1]
 inci <-ant_dent[3,1:3,1]

 #actual calculations
 ####M3
 out_m3<- (sqrt((((tmjpo[1]-m3[1])^2)+
           ((tmjpo[2]-m3[2])^2))))

 lm_position_m3 <- (c(1,2,3)[1:3])
 lm_position_m3[1]<- (m3[1])
 lm_position_m3[2]<- (m3[2])
 lm_position_m3[3]<- (tmjpo[3])

 ####M2
 out_m2<- (sqrt((((tmjpo[1]-m2[1])^2)+
           ((tmjpo[2]-m2[2])^2))))

 lm_position_m2 <- (c(1,2,3)[1:3])
 lm_position_m2[1]<- (m2[1])
 lm_position_m2[2]<- (m2[2])
 lm_position_m2[3]<- (tmjpo[3])

 ####M1
 out_m1<- (sqrt((((tmjpo[1]-m1[1])^2)+
           ((tmjpo[2]-m1[2])^2))))

 lm_position_m1 <- (c(1,2,3)[1:3])
 lm_position_m1[1]<- (m1[1])
 lm_position_m1[2]<- (m1[2])
 lm_position_m1[3]<- (tmjpo[3])

 ####PM2
 out_pm2<- (sqrt(((((tmjpo[1]-pm2[1])^2)+
           ((tmjpo[2]-pm2[2])^2))))
```

```
lm_position_pm2 <- (c(1,2,3)[1:3])
lm_position_pm2[1]<- (pm2[1])
lm_position_pm2[2]<- (pm2[2])
lm_position_pm2[3]<- (tmjpo[3])

####PM1
out_pm1<- (sqrt((((tmjan[1]-pm1[1])^2)+
          ((tmjan[2]-pm1[2])^2))))

lm_position_pm1 <- (c(1,2,3)[1:3])
lm_position_pm1[1]<- (pm1[1])
lm_position_pm1[2]<- (pm1[2])
lm_position_pm1[3]<- (tmjan[3])

####CANINE
out_can<- (sqrt((((tmjan[1]-canine[1])^2)+
          ((tmjan[2]-canine[2])^2))))

lm_position_can <- (c(1,2,3)[1:3])
lm_position_can[1]<- (canine[1])
lm_position_can[2]<- (canine[2])
lm_position_can[3]<- (tmjan[3])

####INCISOR
out_inci<- (sqrt((((tmjan[1]-inci[1])^2)+
          ((tmjan[2]-inci[2])^2))))

lm_position_inci <- (c(1,2,3)[1:3])
lm_position_inci[1]<- (inci[1])
lm_position_inci[2]<- (inci[2])
lm_position_inci[3]<- (tmjan[3])

####MATRIX OF THE DISTANCES, NAMED
out_levers <- matrix (c(out_m3, out_m2, out_m1, out_pm2, out_pm1, out_can, out_inci),
          nrow = 7, ncol =1)
rownames(out_levers) <- c("out_m3", "out_m2", "out_m1", "out_pm2",
             "out_pm1", "out_can", "out_inci")
write.table(out_levers, file="out_levers.txt", row.names=TRUE, col.names=FALSE)

}

NewWorldOutLeverFunction <- function(foldername){
 library(Arothron)
 #out-lever length ###NEW WORLD PRIMATES (with pm3)
 #tmj imported from the original mand set, other landmarks in relevant planes
 setwd(foldername)
 #in post occlusal plane
 mandible_set_p=read.amira.set("full_lms_post_plane.landmarkAscii", nland="auto")
 post_dent=read.amira.set("post_bitepoints_post_plane.landmarkAscii", nland="auto")
 #in ant occlusal plane
 mandible_set_a=read.amira.set("full_lms_post_plane.landmarkAscii", nland="auto")
 ant_dent=read.amira.set("ant_bitepoints_post_plane.landmarkAscii", nland="auto")

 lastLetterOfWd <- substr(getwd(), nchar(getwd()),nchar(getwd()))
 if(lastLetterOfWd == "L"){
  ### LEFT HAND SIDE
  tmjpo <- mandible_set_p[89,1:3,1]
  tmjan <- mandible_set_a[89,1:3,1]
 } else if(lastLetterOfWd == "R"){
  ### RIGHT HAND SIDE
  tmjpo <- mandible_set_p[90,1:3,1]
  tmjan <- mandible_set_a[90,1:3,1]
 }
 #specify the position of each dental landmark
 m3 <-post_dent[1,1:3,1]
 m2 <-post_dent[2,1:3,1]
 m1 <-post_dent[3,1:3,1]
 pm3 <-post_dent[4,1:3,1]
 pm2 <-post_dent[5,1:3,1]
 pm1 <-ant_dent[1,1:3,1]
```

```
canine <-ant_dent[2,1:3,1]
inci <-ant_dent[3,1:3,1]

#actual calculations
####M3
out_m3<- (sqrt((((tmjpo[1]-m3[1])^2)+
        ((tmjpo[2]-m3[2])^2))))

lm_position_m3 <- (c(1,2,3)[1:3])
lm_position_m3[1]<- (m3[1])
lm_position_m3[2]<- (m3[2])
lm_position_m3[3]<- (tmjpo[3])

####M2
out_m2<- (sqrt((((tmjpo[1]-m2[1])^2)+
        ((tmjpo[2]-m2[2])^2))))

lm_position_m2 <- (c(1,2,3)[1:3])
lm_position_m2[1]<- (m2[1])
lm_position_m2[2]<- (m2[2])
lm_position_m2[3]<- (tmjpo[3])

####M1
out_m1<- (sqrt((((tmjpo[1]-m1[1])^2)+
        ((tmjpo[2]-m1[2])^2))))

lm_position_m1 <- (c(1,2,3)[1:3])
lm_position_m1[1]<- (m1[1])
lm_position_m1[2]<- (m1[2])
lm_position_m1[3]<- (tmjpo[3])

####PM3
out_pm3<- (sqrt((((tmjpo[1]-pm3[1])^2)+
        ((tmjpo[2]-pm3[2])^2))))

lm_position_pm3 <- (c(1,2,3)[1:3])
lm_position_pm3[1]<- (pm3[1])
lm_position_pm3[2]<- (pm3[2])
lm_position_pm3[3]<- (tmjpo[3])

####PM2
out_pm2<- (sqrt((((tmjpo[1]-pm2[1])^2)+
        ((tmjpo[2]-pm2[2])^2))))

lm_position_pm2 <- (c(1,2,3)[1:3])
lm_position_pm2[1]<- (pm2[1])
lm_position_pm2[2]<- (pm2[2])
lm_position_pm2[3]<- (tmjpo[3])

####PM1
out_pm1<- (sqrt((((tmjan[1]-pm1[1])^2)+
        ((tmjan[2]-pm1[2])^2))))

lm_position_pm1 <- (c(1,2,3)[1:3])
lm_position_pm1[1]<- (pm1[1])
lm_position_pm1[2]<- (pm1[2])
lm_position_pm1[3]<- (tmjan[3])

####CANINE
out_can<- (sqrt((((tmjan[1]-canine[1])^2)+
        ((tmjan[2]-canine[2])^2))))

lm_position_can <- (c(1,2,3)[1:3])
lm_position_can[1]<- (canine[1])
lm_position_can[2]<- (canine[2])
lm_position_can[3]<- (tmjan[3])

####INCISOR
out_inci<- (sqrt((((tmjan[1]-inci[1])^2)+
        ((tmjan[2]-inci[2])^2))))
```

```
lm_position_inci <- (c(1,2,3)[1:3])
lm_position_inci[1]<- (inci[1])
lm_position_inci[2]<- (inci[2])
lm_position_inci[3]<- (tmjan[3])

####MATRIX OF THE DISTANCES, NAMED
out_levers <- matrix (c(out_m3, out_m2, out_m1, out_pm3, out_pm2, out_pm1, out_can, out_inci),
          nrow = 8, ncol =1)
rownames(out_levers) <- c("out_m3", "out_m2", "out_m1", "out_pm3", "out_pm2",
              "out_pm1", "out_can", "out_inci")
write.table(out_levers, file="out_levers.txt", row.names=TRUE, col.names=FALSE)
}
```

# Script 3: Function for landmark coordinate extraction and compilation

```
extract_coords <-function(){
library(Arothron)
library(tcltk)
#setwd('~')
#getwd()
# [1] "C:/Users/Root/Documents"
#dir <- tclvalue(tkchooseDirectory())  # opens a dialog window in 'My Documents'
#setwd(dir)

newdir<-getwd()
folderlist <- list.files()
for(folder in folderlist ){

 setwd(paste(newdir, "/",folder,sep = ""))

 lastLetterOfWd <- substr(getwd(), nchar(getwd()),nchar(getwd()))

 full=read.amira.set("full_lms_cond_plane.landmarkAscii", nland=90)
 added=read.amira.set("added_lms.landmarkAscii", nland="auto")

 array2list<-function (array)
 {
  thelist <- NULL
  for (i in 1:dim(array)[3]) {
   eli <- array[, , i]
   thelist <- c(thelist, list(eli))
  }
  if (is.null(dimnames(array)[[3]]) == F) {
   names(thelist) <- dimnames(array)[[3]]
  }
  return(thelist)
 }

 if(lastLetterOfWd == "L"){
  ###########  LEFT  #################
  #LEFT CRANIUM
  craniumL=as.matrix(full[c(5, 11, 50, 13, 15,48),1:3,])
  craniumL2=array(craniumL)
  cranium<-array2list(array(craniumL2,dim=c(6,3,1)))
  export_amira(cranium,path=getwd())
  file.rename("set 1.txt", "cranium.txt")
  #LEFT MANDIBLE
  mandFL=as.matrix(full[c(54, 52, 58, 60, 89),1:3,])
  mandAL=matrix(added, nrow=2, ncol=3)
  mandL=rbind(mandFL, mandAL)
  mandL2=array(mandL)
  mandible<-array2list(array(mandL2,dim=c(7,3,1)))
  export_amira(mandible,path=getwd())
  file.rename("set 1.txt", "mandible.txt")
  # LEFT DISTANCE
  distance_L=as.matrix(full[c(40,46),1:3,])
  distance_L2=array(distance_L)
  distance<-array2list(array(distance_L2,dim=c(2,3,1)))
  export_amira(distance,path=getwd())
  file.rename("set 1.txt", "distance.txt")
```

```
  }
  if (lastLetterOfWd == "R"){
   ###########  RIGHT  #################
   #RIGHT CRANIUM
   craniumR=as.matrix(full[c(6, 12, 51, 14, 16, 49),1:3,])
   craniumR2=array(craniumR)
   cranium<-array2list(array(craniumR,dim=c(6,3,1)))
   export_amira(cranium,path=getwd())
   file.rename("set 1.txt", "cranium.txt")
   #RIGHT MANDIBLE
   mandFR=as.matrix(full[c(55, 53, 59, 61, 90),1:3,])
   mandAR=matrix(added, nrow=2, ncol=3)
   mandR=rbind(mandFR, mandAR)
   mandR2=array(mandR)
   mandible<-array2list(array(mandR2,dim=c(7,3,1)))
   export_amira(mandible,path=getwd())
   file.rename("set 1.txt", "mandible.txt")
   #RIGHT DISTANCE
   distance_R=as.matrix(full[c(41,47),1:3,])
   distance_R2=array(distance_R)
   distance<-array2list(array(distance_R2,dim=c(2,3,1)))
   export_amira(distance,path=getwd())
   file.rename("set 1.txt", "distance.txt")

  }

# print(paste(dir, folder,sep = ""))

 }

#setwd(paste(dir, folder,sep = ""))

}
```

## Script 4: Function for calculate mechanical advantage and all other calculations

```
calculate_mechanical_advantage <- function(inSpecimenFolder){
 #setwd()
 setwd(inSpecimenFolder)

  #setwd()
 library(Arothron)
 library(linkR)
 library(MALDIquant)
 library(stringr)
 #IN-LEVER LANDMARKS
 cranium<- read.amira.set("cranium.txt", nland = "auto")
 mandible<- read.amira.set("mandible.txt", nland = "auto")
 cran_bitepoints <- read.amira.set("cran_bitepoints.landmarkAscii", nland="auto")
 mand_bitepointsP <- read.amira.set("post_bitepoints_cond_plane.landmarkAscii", nland="auto")
 mand_bitepointsA <- read.amira.set("ant_bitepoints_cond_plane.landmarkAscii", nland="auto")

 mand_bitepoints <- rbind(matrix(mand_bitepointsP,ncol = 3),matrix(mand_bitepointsA,ncol = 3)) ##read in out-levers - pre-calculated in
separate script!
 out_levers<-read.table("out_levers.txt", sep = "")

 distance_g <- read.amira.set("distance.txt", nland = "auto")
 distance_g <- matrix(distance_g, nrow = 2)
 ##measure the distance. is only in y!!
 distancey <- (sqrt((distance_g[1,2]-distance_g[2,2])^2))
 #thisToothResults = NULL
 full_results = NULL

 #and the CRAN landmarks
 SAM_cran <- matrix(cranium[1,,], ncol=3)
 AT_cran <- matrix(cranium[2,,], ncol=3)
```

```
  CT_cran <- matrix(cranium[3,,], ncol=3)
  PT_cran <- matrix(cranium[4,,], ncol=3)
  FAKETMJ <- NULL
  MP_cran <- matrix(cranium[5,,], ncol=3)
  SCM_cran <- matrix(cranium[6,,], ncol=3)

  #cran_array<- matrix(rbind(SAM_cran,AT_cran,CT_cran,PT_cran,MP_cran,MP_cran,SCM_cran), nrow=7,ncol=3, byrow = )#  position 5 is
a repeat for convenience later on
  cran_array<- matrix(rbind(SAM_cran,SCM_cran,CT_cran,PT_cran,PT_cran,AT_cran,MP_cran), nrow=7,ncol=3, byrow = )#  position 5 is a
repeat for convenience later on


  #calculate how many teeth we have
  numTeeth <- dim(mand_bitepoints)[1];
  #calculate if new or old world
  if(numTeeth == 7){
   world<-"old"
   cran_bitepoints <- as.matrix(cran_bitepoints[c(1:7),1:3,])
   toothnames <- c("m3", "m2","m1","pm2","pm1", "canine","incisor")

  } else if (numTeeth == 8){
   world <- "new"
   cran_bitepoints <- as.matrix(cran_bitepoints[c(1:8),1:3,])
   toothnames <- c("m3", "m2","m1","pm3","pm2","pm1", "canine","incisor")

  } else {
   print("ERROR: teeth number not 7 or 8")
  }


  for (i in 1:numTeeth){

   thisToothResults = NULL
   thisTooth <-toothnames[i]

   #INDEX
   ##calculate if this tooth is canine
   if(world ==  "old"){
    if(i == 6){
     canine<-TRUE
    } else {
     canine<- FALSE
    }
   } else if (world == "new"){
    if(i == 7){
     canine<-TRUE
    } else {
     canine<- FALSE
    }
   } else{
    print("ERROR")
   }

   #rotate tooth
   muscle_coords = NULL
   tooth_coords = data.frame(x=rep(0, 40), y=rep(0,40), z=rep(0,40))
   #make the mandible landmarks into a matrix
   mand_mat=as.matrix(mandible[c(1:7),1:3,])
   tooth_mat = matrix(mand_bitepoints[i,], nrow=1, ncol = 3)  ## this changes between teeth
   for (rot in 1:40){
    #rotate
    mand_mat <- mand_mat %*% rotationMatrixZYX(0, 0,  -0.0174533)
    muscle_coords = cbind(muscle_coords, matrix(mand_mat))
    tooth_mat <- tooth_mat %*% rotationMatrixZYX(0, 0, -0.0174533)
    tooth_coords[rot, ] <- c(tooth_mat[1,1], tooth_mat[1,2], tooth_mat[1,3])
    #print(mand_mat)
    #print(tooth_mat)
   }
   ###
   #now d contains all muscle values, out of order, so re-order
   x<- muscle_coords[1:7,1:40]
```

```
y<- muscle_coords[8:14,1:40]
z <- muscle_coords[15:21,1:40]
muscle_coords= array(1:9, c(7, 3, 40))  #nonsense numbers to fill array
muscle_coords[1:7,1,1:40]<- x
muscle_coords[1:7,2,1:40]<- y
muscle_coords[1:7,3,1:40]<- z
#muscle_coords #print to check if desired

d <- NULL
distance<- NULL

for (j in 1:40){
 d <- (sqrt(((tooth_coords[j,1]-cran_bitepoints[i,1])^2)+((tooth_coords[j,2]-cran_bitepoints[i,2])^2)+
       ((tooth_coords[j,3]-cran_bitepoints[i,3])^2)))
 distance[j] <- d[1:j]

}

if(canine){
 distance[1:(which.min(distance))] <- -1
}

#### CREATE BITE ARRAY
bitesizes<-(c(0,10,15,20,25,30,40,50,60,70,80,90,100,140,160))
bitenames<-c("occlusion", "bite_ten_mm", "bite_fifteen_mm",
      "bite_twenty_mm", "bite_twentyfive_mm"
      ,"bite_thirty_mm", "bite_fourty_mm","bite_fifty_mm",  "bite_sixty_mm",
      "bite_seventy_mm", "bite_eighty_mm", "bite_ninety_mm",
      "bite_onehundo_mm","bite_onehundfourty_mm","bite_onehundsixy_mm")
musclenames <-c("SAM","SCM","CT","PT","TMJ","AT","MP")
numBites <-match.closest(max(distance),bitesizes) #finds maximum bite and matches to list of bite sizes - index
#previous problem here- if top values are too close it can pair incorrectly.
maxBite <-bitesizes[match.closest(max(distance),bitesizes)] #uses above index to find maxbite value
bite_array<-NULL
rotation<-NULL
heights<-NULL

bite_array <- array(0,dim = c(7,3,match.closest(max(distance),bitesizes) + 4))
rotation <- matrix(0,nrow = c(match.closest(max(distance),bitesizes) + 4,ncol = 1))
heights <- matrix(0,nrow = c(match.closest(max(distance),bitesizes) + 4,ncol = 1))

bite_array[,,1] <- as.matrix(mandible[c(1:7),1:3,])  #original coords = in occlusion position
rotation[1] <- 0

for (j in 1:numBites){
 bite_array[,,j+1] <- muscle_coords[,,(which.min(abs(distance - bitesizes[j+1])))]
  rotation[j+1] <- (which.min(abs(distance - bitesizes[j+1])))
}

twenty_degrees <- muscle_coords[,,20]
fourty_degrees <- muscle_coords[,,40]

bite_array[,,numBites+1]<-muscle_coords[,,20]
bite_array[,,numBites+2]<-muscle_coords[,,40]
bite_array[,,numBites+3]<-muscle_coords[,,20]
bite_array[,,numBites+4]<-muscle_coords[,,40]
bite_array[,2,numBites+3]<-twenty_degrees[,2] + distancey
bite_array[,2,numBites+4]<-fourty_degrees[,2] + distancey

rotation[numBites+1]<-"20 deg"
rotation[numBites+2]<-"40 deg"
rotation[numBites+3]<- "20 deg trans"
rotation[numBites+4]<-"40 deg trans"

heights[0:numBites]<-bitesizes[0:numBites]
heights[(numBites+1):length(heights),] <- c("20 deg", "40 deg", "20 deg trans", "40 deg trans")

rownames(bite_array)<-c("SAM","SCM","CT","PT","TMJ","AT","MP")
colnames(bite_array)<-c("x","y","z")
dimnames(bite_array)[[3]] <- c(bitenames[0:numBites], "20 deg", "40 deg", "20 deg trans", "40 deg trans")
```

```
#dimnames(bite_array[,,])[[3]][1]
#dimnames(bite_array[,,])[[3]][numBites]

   out <-out_levers$V2[i]   ## so this is another bit that varies by tooth
tmj<-bite_array[5,,]
SAM_mand <-bite_array[1,,]
# if we want to transpose we do t(sam_mand)
#tmj[,x] where x is bite angle
in_lever <- NULL
mechanical_ad <- NULL
results_in <- NULL
results_MA <- NULL
#thisToothResults <- NULL


tempMuscOrder <- c(1,2,3,4,6,7)
#note there is no 5 this is important as 5 is a repeat for convenience so that the same index skips TMJ in the bite_array - do not change!
mo<- 1
numallbites<-numBites+4
for(m in tempMuscOrder){
 #print(musclenames[m])
 #cran_array[m]
 #tempnumbites<-numBites+4
 for (z in 1:numallbites){   #adjust for # of rotations!!! this will change with available bite heights
  #print(bitenames[z])
  in_lever <-
   (sqrt(((cran_array[m,1]-tmj[1,z])^2)+
       ((cran_array[m,2]-tmj[2,z])^2) +
       ((cran_array[m,3]-tmj[3,z])^2))) *
   (sin(acos(((((sqrt(((cran_array[m,1]-tmj[1,z])^2)+
              ((cran_array[m,2]-tmj[2,z])^2) +
              ((cran_array[m,3]-tmj[3,z])^2)))^2)
          +((sqrt(((cran_array[m,1]-bite_array[m,1,z])^2)+
              ((cran_array[m,2]-bite_array[m,2,z])^2) +
              ((cran_array[m,3]-bite_array[m,3,z])^2)))^2)
         -((sqrt(((bite_array[m,1,z]-tmj[1,z])^2)+
              ((bite_array[m,2,z]-tmj[2,z])^2) +
              ((bite_array[m,3,z]-tmj[3,z])^2)))^2))/
          (2 *
            ((sqrt(((cran_array[m,1]-tmj[1,z])^2)+
                ((cran_array[m,2]-tmj[2,z])^2) +
                ((cran_array[m,3]-tmj[3,z])^2)))) *
            ((sqrt(((cran_array[m,1]-bite_array[m,1,z])^2)+
                ((cran_array[m,2]-bite_array[m,2,z])^2) +
                ((cran_array[m,3]-bite_array[m,3,z])^2)))))))))

  mechanical_ad <- in_lever / out
  results_in[z] <- cbind(in_lever)[1:z]   ####export
  results_MA[z] <- cbind(mechanical_ad)[1:z]  #####export
  #print(in_lever_SAM)
  #print(mechanical_ad)
  #print(in_lever)
 }

 out_m3_rep <- matrix(out, nrow=numallbites)

    ##add colnames for the bites / muscles to the mechanical ad table.
 results <- matrix(results_MA, nrow=numallbites, ncol=1)

 rownames(results) <- heights
 #add the in-lever to the file
 inL <- matrix(results_in, nrow=numallbites, ncol= 1)
 #now calculate the distance between muscle landmarks
 m_d <- NULL
 mus_distance <- NULL
 for (h in 1:numallbites){  #note ALTER THE # for the different heights!!
  m_d <- (sqrt(((bite_array[m,1,h]-cran_array[m,1])^2)+((bite_array[m,2,h]-cran_array[m,2])^2)+
          ((bite_array[m,3,h]-cran_array[m,3])^2)))
  mus_distance[h] <- m_d[1:h]
 }
 #and add it as a matrix to the list..
 mus_distance_matrix <- matrix(mus_distance, nrow=numallbites, ncol=1)
```

```
#now calculate the % muscle stretch
muscle_stretch <- NULL
mu_s <- NULL
for (h in 1:numallbites) {
  mu_s <- (((mus_distance[h]-mus_distance[1])/mus_distance[1])*100)
  muscle_stretch[h] <- mu_s[1:h]
}
muscle_stretch_matrix <- matrix(muscle_stretch, nrow=numallbites, ncol=1)

#collate as results!!!
thisToothCol <-  (rep(toothnames[i],numallbites))
thisMuscCol <- (rep(musclenames[m],numallbites))
thisMuscleResults <- cbind(thisToothCol,thisMuscCol, heights, results, rotation, inL,out_m3_rep,
mus_distance_matrix,muscle_stretch_matrix)
colnames(thisMuscleResults)<- c("Tooth", "Muscle","Bite_height", "Mechanical_advantage", "Degrees_rotation", "In-lever", "Out-
lever",
                   "Muscle-length", "Perc_increase")
thisToothResults <-rbind(thisToothResults,thisMuscleResults)
mo<-mo+1
}
full_results<- rbind(full_results,thisToothResults)
#store these muscles and openings as a 3d overall tooth arra
}

locs = str_locate_all(pattern = '/', getwd())
species<-substring(getwd(),locs[[1]][length(locs[[1]])-1]+1,locs[[1]][length(locs[[1]])]-1)
specimen <-substring(getwd(),locs[[1]][length(locs[[1]])]+1,nchar(getwd()))
filename <- paste(species,"_",specimen,".txt", sep = "")
write.table(full_results, file = filename, sep="\t")
}
```

# Appendix 5 - Database of raw data for biomechanical measurements (Ch. 3)

[Please click here to access the spreadsheet of raw data for each specimen extracted for the analyses in Chapter 3.](#)

The link will take you to a spreadsheet uploaded as a google spreadsheet. No log-ins are required.

The spreadsheet lists the following values for each specimen in the sample by tooth (bite points, incisor, canine, PM1, M1): Muscle used for measurement; height of linear gape in mm, mechanical advantage; degrees jaw rotation at measurement including whether translated ("40 deg trans" values); in-lever length; out-lever length; muscle line of action length in mm, percentage increase in muscle length from occlusion, condyle height above occlusal plane, antero-posterior length of glenoid, specimen sex, side used for measurement.

# Appendix 6 - Data tables, Chapter 3 results

All values grouped means for the full sample except CSA are. CSA are values for single individuals. For absolute values see Appendix 5.

**Table A6.1 Percentage increase in muscle length with and without translation on incisor at 40 degrees rotation, for masseter and temporalis, in females. Change is untranslated value minus translated.**

| Species | Muscle % stretch | | | | | |
|---|---|---|---|---|---|---|
| | Masseter | | | Temporalis | | |
| | Untranslated | Translated | Change | Untranslated | Translated | Change |
| *Ateles* | 51.33 | 31.79 | 19.54 | 42.56 | 42.32 | 0.23 |
| *Cacajao* | 59.43 | 39.97 | 19.46 | 32.89 | 31.88 | 1.02 |
| *Chiropotes* | 48.12 | 31.12 | 17.00 | 32.22 | 30.38 | 1.84 |
| *Pithecia* | 54.78 | 39.58 | 15.20 | 34.61 | 33.79 | 0.82 |
| *Sapajus* | 51.66 | 33.62 | 18.04 | 30.96 | 30.64 | 0.32 |
| *Saimiri* | 49.29 | 24.54 | 24.74 | 30.26 | 29.17 | 1.09 |
| *Cercocebus* | 55.52 | 37.78 | 17.74 | 27.23 | 27.05 | 0.18 |
| *Mandrillus* | 57.66 | 42.79 | 14.87 | 25.30 | 31.09 | -5.79 |
| *Theropithecus* | 47.61 | 37.36 | 10.26 | 26.09 | 27.81 | -1.72 |
| *Pan* | 58.74 | 43.30 | 15.44 | 33.95 | 35.10 | -1.15 |

**Table A6.2 Percentage increase in muscle length with and without translation on incisor at 40 degrees rotation, for masseter and temporalis, in females and males. Change is untranslated value minus translated.**

| Species | Muscle % stretch | | | | | |
|---|---|---|---|---|---|---|
| | Masseter | | | Temporalis | | |
| | Untranslated | Translated | Change | Untranslated | Translated | Change |
| *Ateles* | 52.21 | 32.88 | 19.33 | 38.75 | 38.32 | 0.43 |
| *Cacajao* | 55.59 | 37.22 | 18.37 | 36.34 | 34.47 | 1.87 |
| *Chiropotes* | 47.86 | 31.94 | 15.93 | 33.30 | 31.78 | 1.52 |
| *Pithecia* | 60.70 | 42.02 | 18.68 | 36.57 | 35.36 | 1.21 |
| *Cebus* | 50.91 | 27.50 | 23.41 | 39.64 | 38.16 | 1.48 |
| *Sapajus* | 51.67 | 33.06 | 18.62 | 33.96 | 32.72 | 1.24 |
| *Saimiri* | 53.27 | 31.70 | 21.56 | 29.83 | 28.96 | 0.87 |
| *Cercocebus* | 49.26 | 33.37 | 15.89 | 25.95 | 27.19 | -1.24 |
| *Mandrillus* | 55.15 | 42.16 | 12.99 | 26.39 | 32.04 | -5.65 |
| *Theropithecus* | 46.49 | 36.94 | 9.55 | 25.90 | 27.37 | -1.47 |
| *Pan* | 57.46 | 42.21 | 15.26 | 36.37 | 37.32 | -0.96 |

**Table A6.3 Mechanical advantage at maximum gape in females, with and without anterior translation**

| Species | Tooth | 40° | 40° translated | 40° | 40° translated |
|---|---|---|---|---|---|
| | | MA for the masseter | | MA for the temporalis | |
| *Ateles* | Incisor | 0.333 | 0.255 | 0.287 | 0.218 |
| | Canine | 0.376 | 0.288 | 0.324 | 0.246 |
| | PM1 | 0.416 | 0.318 | 0.358 | 0.272 |

| | | | | | |
|---|---|---|---|---|---|
| | M1 | 0.539 | 0.413 | 0.464 | 0.353 |
| *Cacajao* | Incisor | 0.385 | 0.318 | 0.281 | 0.227 |
| | Canine | 0.470 | 0.388 | 0.343 | 0.277 |
| | PM1 | 0.536 | 0.442 | 0.391 | 0.315 |
| | M1 | 0.695 | 0.574 | 0.507 | 0.409 |
| *Chiropotes* | Incisor | 0.360 | 0.281 | 0.283 | 0.230 |
| | Canine | 0.433 | 0.337 | 0.340 | 0.277 |
| | PM1 | 0.501 | 0.391 | 0.394 | 0.320 |
| | M1 | 0.668 | 0.521 | 0.524 | 0.427 |
| *Pithecia* | Incisor | 0.384 | 0.314 | 0.281 | 0.227 |
| | Canine | 0.449 | 0.367 | 0.330 | 0.267 |
| | PM1 | 0.499 | 0.409 | 0.367 | 0.296 |
| | M1 | 0.661 | 0.541 | 0.485 | 0.392 |
| *Sapajus* | Incisor | 0.357 | 0.302 | 0.301 | 0.251 |
| | Canine | 0.392 | 0.332 | 0.331 | 0.276 |
| | PM1 | 0.446 | 0.378 | 0.376 | 0.314 |
| | M1 | 0.608 | 0.515 | 0.513 | 0.428 |
| *Saimiri* | Incisor | 0.298 | 0.248 | 0.252 | 0.205 |
| | Canine | 0.337 | 0.281 | 0.285 | 0.232 |
| | PM1 | 0.375 | 0.313 | 0.318 | 0.258 |
| | M1 | 0.510 | 0.426 | 0.433 | 0.351 |
| *Cercocebus* | Incisor | 0.361 | 0.283 | 0.211 | 0.154 |
| | Canine | 0.417 | 0.327 | 0.244 | 0.179 |
| | PM1 | 0.465 | 0.366 | 0.272 | 0.199 |
| | M1 | 0.602 | 0.473 | 0.352 | 0.259 |
| *Mandrillus* | Incisor | 0.313 | 0.229 | 0.155 | 0.097 |
| | Canine | 0.346 | 0.254 | 0.168 | 0.103 |
| | PM1 | 0.380 | 0.279 | 0.184 | 0.113 |
| | M1 | 0.483 | 0.355 | 0.234 | 0.144 |
| *Theropithecus* | Incisor | 0.346 | 0.259 | 0.203 | 0.155 |
| | Canine | 0.382 | 0.286 | 0.225 | 0.172 |
| | PM1 | 0.419 | 0.314 | 0.246 | 0.188 |
| | M1 | 0.513 | 0.384 | 0.301 | 0.230 |
| *Pan* | Incisor | 0.374 | 0.295 | 0.270 | 0.207 |
| | Canine | 0.430 | 0.339 | 0.311 | 0.238 |
| | PM1 | 0.490 | 0.387 | 0.355 | 0.271 |
| | M1 | 0.610 | 0.481 | 0.441 | 0.337 |

**Table A6.4 Mechanical advantage at maximum gape in males, with and without anterior translation**

| Species | Tooth | 40° | 40° translated | 40° | 40° translated |
|---|---|---|---|---|---|
| | | MA for the masseter | | MA for the temporalis | |
| *Ateles* | Incisor | 0.343 | 0.269 | 0.284 | 0.218 |
| | Canine | 0.392 | 0.307 | 0.324 | 0.250 |
| | PM1 | 0.437 | 0.342 | 0.361 | 0.278 |
| | M1 | 0.567 | 0.444 | 0.469 | 0.361 |
| *Cacajao* | Incisor | 0.390 | 0.324 | 0.320 | 0.270 |
| | Canine | 0.466 | 0.387 | 0.382 | 0.323 |
| | PM1 | 0.535 | 0.444 | 0.439 | 0.370 |
| | M1 | 0.682 | 0.566 | 0.559 | 0.472 |
| *Chiropotes* | Incisor | 0.384 | 0.299 | 0.307 | 0.251 |
| | Canine | 0.461 | 0.359 | 0.369 | 0.302 |

| Species | Tooth | | | | |
|---|---|---|---|---|---|
| | PM1 | 0.531 | 0.414 | 0.425 | 0.347 |
| | M1 | 0.686 | 0.535 | 0.550 | 0.449 |
| *Pithecia* | Incisor | 0.390 | 0.313 | 0.300 | 0.241 |
| | Canine | 0.451 | 0.363 | 0.347 | 0.278 |
| | PM1 | 0.506 | 0.407 | 0.389 | 0.312 |
| | M1 | 0.657 | 0.529 | 0.507 | 0.406 |
| *Cebus* | Incisor | 0.310 | 0.267 | 0.318 | 0.263 |
| | Canine | 0.349 | 0.301 | 0.358 | 0.297 |
| | PM1 | 0.401 | 0.346 | 0.412 | 0.341 |
| | M1 | 0.533 | 0.461 | 0.547 | 0.454 |
| *Sapajus* | Incisor | 0.371 | 0.312 | 0.349 | 0.295 |
| | Canine | 0.404 | 0.339 | 0.379 | 0.320 |
| | PM1 | 0.474 | 0.398 | 0.445 | 0.376 |
| | M1 | 0.634 | 0.532 | 0.595 | 0.502 |
| *Saimiri* | Incisor | 0.317 | 0.269 | 0.266 | 0.223 |
| | Canine | 0.352 | 0.299 | 0.296 | 0.249 |
| | PM1 | 0.398 | 0.338 | 0.335 | 0.281 |
| | M1 | 0.541 | 0.459 | 0.455 | 0.382 |
| *Cercocebus* | Incisor | 0.313 | 0.238 | 0.209 | 0.155 |
| | Canine | 0.360 | 0.275 | 0.241 | 0.180 |
| | PM1 | 0.408 | 0.312 | 0.274 | 0.205 |
| | M1 | 0.502 | 0.384 | 0.337 | 0.252 |
| *Mandrillus* | Incisor | 0.280 | 0.221 | 0.158 | 0.113 |
| | Canine | 0.314 | 0.248 | 0.177 | 0.127 |
| | PM1 | 0.374 | 0.295 | 0.211 | 0.151 |
| | M1 | 0.452 | 0.357 | 0.256 | 0.183 |
| *Theropithecus* | Incisor | 0.323 | 0.235 | 0.211 | 0.165 |
| | Canine | 0.353 | 0.256 | 0.230 | 0.181 |
| | PM1 | 0.420 | 0.305 | 0.274 | 0.215 |
| | M1 | 0.501 | 0.364 | 0.327 | 0.257 |
| *Pan* | Incisor | 0.362 | 0.283 | 0.277 | 0.211 |
| | Canine | 0.414 | 0.323 | 0.317 | 0.241 |
| | PM1 | 0.481 | 0.375 | 0.368 | 0.279 |
| | M1 | 0.599 | 0.467 | 0.458 | 0.348 |

**Table A6.5 Female mechanical advantage for the masseter, at linear gape heights ranging from occlusion (0 mm) to 40mm.**

| | | Occlusion | 10mm | 20mm | 30mm | 40mm |
|---|---|---|---|---|---|---|
| **Species** | **Tooth** | **Mechanical advantage** | | | | |
| *Ateles* | Incisor | 0.442 | 0.427 | 0.407 | 0.385 | 0.362 |
| | Canine | 0.499 | 0.459 | 0.431 | 0.401 | 0.376 |
| | PM1 | 0.552 | 0.522 | 0.491 | 0.454 | 0.417 |
| | M1 | 0.715 | 0.676 | 0.622 | 0.561 | NA |
| *Cacajao* | Incisor | 0.491 | 0.472 | 0.447 | 0.420 | 0.388 |
| | Canine | 0.599 | 0.536 | 0.494 | NA | NA |
| | PM1 | 0.683 | 0.640 | 0.588 | 0.532 | NA |
| | M1 | 0.885 | 0.826 | 0.737 | NA | NA |
| *Chiropotes* | Incisor | 0.467 | 0.445 | 0.414 | NA | NA |
| | Canine | 0.561 | 0.484 | 0.433 | NA | NA |
| | PM1 | 0.650 | 0.595 | 0.527 | NA | NA |
| | M1 | 0.866 | 0.791 | 0.673 | NA | NA |

| Species | Tooth | Occlusion | 10mm | 20mm | 30mm | 40mm |
|---|---|---|---|---|---|---|
| *Pithecia* | Incisor | 0.489 | 0.467 | 0.435 | 0.396 | NA |
| | Canine | 0.572 | 0.502 | 0.450 | NA | NA |
| | PM1 | 0.636 | 0.585 | 0.524 | NA | NA |
| | M1 | 0.841 | 0.771 | 0.665 | NA | NA |
| *Sapajus* | Incisor | 0.479 | 0.455 | 0.422 | 0.386 | 0.357 |
| | Canine | 0.526 | 0.467 | 0.424 | NA | NA |
| | PM1 | 0.599 | 0.549 | 0.495 | 0.448 | NA |
| | M1 | 0.816 | 0.738 | 0.637 | NA | NA |
| *Saimiri* | Incisor | 0.397 | 0.359 | 0.308 | NA | NA |
| | Canine | 0.449 | 0.376 | NA | NA | NA |
| | PM1 | 0.500 | 0.430 | NA | NA | NA |
| | M1 | 0.681 | 0.562 | NA | NA | NA |
| *Cercocebus* | Incisor | 0.471 | 0.457 | 0.438 | 0.415 | 0.391 |
| | Canine | 0.545 | 0.512 | 0.484 | 0.451 | 0.425 |
| | PM1 | 0.608 | 0.578 | 0.542 | 0.501 | 0.470 |
| | M1 | 0.787 | 0.738 | 0.679 | 0.616 | NA |
| *Mandrillus* | Incisor | 0.393 | 0.387 | 0.378 | 0.367 | 0.355 |
| | Canine | 0.436 | 0.426 | 0.413 | 0.399 | 0.382 |
| | PM1 | 0.479 | 0.470 | 0.455 | 0.437 | 0.417 |
| | M1 | 0.609 | 0.592 | 0.565 | 0.534 | 0.499 |
| *Theropithecus* | Incisor | 0.444 | 0.436 | 0.425 | 0.412 | 0.396 |
| | Canine | 0.491 | 0.473 | 0.456 | 0.439 | 0.418 |
| | PM1 | 0.539 | 0.526 | 0.507 | 0.486 | 0.462 |
| | M1 | 0.659 | 0.639 | 0.613 | 0.580 | 0.544 |
| *Pan* | Incisor | 0.487 | 0.479 | 0.468 | 0.455 | 0.442 |
| | Canine | 0.560 | 0.536 | 0.519 | 0.500 | 0.482 |
| | PM1 | 0.639 | 0.619 | 0.599 | 0.578 | 0.554 |
| | M1 | 0.794 | 0.770 | 0.741 | 0.708 | 0.672 |

**Table A6.6 Female mechanical advantage for the temporalis, at linear gape heights ranging from occlusion (0 mm) to 40mm.**

| | | Occlusion | 10mm | 20mm | 30mm | 40mm |
|---|---|---|---|---|---|---|
| **Species** | **Tooth** | **Mechanical advantage** | | | | |
| *Ateles* | Incisor | 0.395 | 0.379 | 0.360 | 0.338 | 0.315 |
| | Canine | 0.445 | 0.406 | 0.378 | 0.349 | 0.324 |
| | PM1 | 0.493 | 0.462 | 0.432 | 0.395 | 0.359 |
| | M1 | 0.638 | 0.599 | 0.546 | 0.486 | NA |
| *Cacajao* | Incisor | 0.407 | 0.382 | 0.351 | 0.320 | 0.285 |
| | Canine | 0.497 | 0.417 | 0.369 | NA | NA |
| | PM1 | 0.566 | 0.510 | 0.449 | 0.389 | NA |
| | M1 | 0.734 | 0.656 | 0.554 | NA | NA |
| *Chiropotes* | Incisor | 0.402 | 0.375 | 0.340 | NA | NA |
| | Canine | 0.483 | 0.394 | 0.340 | NA | NA |
| | PM1 | 0.560 | 0.494 | 0.421 | NA | NA |
| | M1 | 0.746 | 0.656 | 0.530 | NA | NA |
| *Pithecia* | Incisor | 0.407 | 0.375 | 0.337 | 0.294 | NA |
| | Canine | 0.476 | 0.386 | 0.331 | NA | NA |
| | PM1 | 0.530 | 0.461 | 0.392 | NA | NA |
| | M1 | 0.700 | 0.606 | 0.489 | NA | NA |

| Species | Tooth | | | | | |
|---|---|---|---|---|---|---|
| Sapajus | Incisor | 0.437 | 0.411 | 0.374 | 0.333 | 0.301 |
| | Canine | 0.481 | 0.414 | 0.366 | NA | NA |
| | PM1 | 0.548 | 0.491 | 0.430 | 0.371 | NA |
| | M1 | 0.746 | 0.658 | 0.545 | NA | NA |
| Saimiri | Incisor | 0.352 | 0.316 | 0.263 | NA | NA |
| | Canine | 0.398 | 0.326 | NA | NA | NA |
| | PM1 | 0.443 | 0.376 | NA | NA | NA |
| | M1 | 0.603 | 0.487 | NA | NA | NA |
| Cercocebus | Incisor | 0.329 | 0.311 | 0.291 | 0.266 | 0.241 |
| | Canine | 0.380 | 0.343 | 0.313 | 0.279 | 0.252 |
| | PM1 | 0.424 | 0.390 | 0.351 | 0.309 | 0.277 |
| | M1 | 0.549 | 0.492 | 0.431 | 0.367 | NA |
| Mandrillus | Incisor | 0.262 | 0.249 | 0.235 | 0.220 | 0.203 |
| | Canine | 0.287 | 0.268 | 0.247 | 0.228 | 0.207 |
| | PM1 | 0.315 | 0.298 | 0.274 | 0.250 | 0.225 |
| | M1 | 0.400 | 0.368 | 0.329 | 0.291 | 0.252 |
| Theropithecus | Incisor | 0.319 | 0.305 | 0.290 | 0.273 | 0.255 |
| | Canine | 0.353 | 0.325 | 0.303 | 0.284 | 0.261 |
| | PM1 | 0.387 | 0.366 | 0.341 | 0.316 | 0.289 |
| | M1 | 0.473 | 0.442 | 0.408 | 0.370 | 0.332 |
| Pan | Incisor | 0.403 | 0.393 | 0.378 | 0.363 | 0.346 |
| | Canine | 0.464 | 0.432 | 0.411 | 0.389 | 0.368 |
| | PM1 | 0.529 | 0.503 | 0.478 | 0.452 | 0.425 |
| | M1 | 0.657 | 0.626 | 0.590 | 0.551 | 0.510 |

**Table A6.7 Male mechanical advantage for the masseter, at linear gape heights ranging from occlusion (0 mm) to 40mm.**

| Species | Tooth | Occlusion | 10mm | 20mm | 30mm | 40mm |
|---|---|---|---|---|---|---|
| | | Mechanical advantage | | | | |
| Ateles | Incisor | 0.457 | 0.440 | 0.419 | 0.397 | 0.372 |
| | Canine | 0.522 | 0.458 | 0.426 | 0.396 | NA |
| | PM1 | 0.582 | 0.547 | 0.513 | 0.473 | 0.437 |
| | M1 | 0.754 | 0.710 | 0.651 | 0.585 | NA |
| Cacajao | Incisor | 0.503 | 0.486 | 0.463 | 0.436 | 0.405 |
| | Canine | 0.602 | 0.529 | 0.488 | NA | NA |
| | PM1 | 0.691 | 0.646 | 0.598 | 0.542 | NA |
| | M1 | 0.881 | 0.825 | 0.747 | 0.673 | NA |
| Chiropotes | Incisor | 0.494 | 0.476 | 0.447 | 0.412 | 0.384 |
| | Canine | 0.594 | 0.506 | NA | NA | NA |
| | PM1 | 0.684 | 0.633 | 0.570 | NA | NA |
| | M1 | 0.885 | 0.820 | 0.716 | NA | NA |
| Pithecia | Incisor | 0.493 | 0.470 | 0.440 | 0.404 | NA |
| | Canine | 0.570 | 0.501 | 0.454 | NA | NA |
| | PM1 | 0.639 | 0.593 | 0.536 | NA | NA |

| Species | Tooth | | | | | |
|---|---|---|---|---|---|---|
| | M1 | 0.831 | 0.769 | 0.676 | NA | NA |
| *Cebus* | Incisor | 0.410 | 0.391 | 0.366 | 0.338 | 0.310 |
| | Canine | 0.461 | 0.388 | 0.350 | NA | NA |
| | PM1 | 0.531 | 0.485 | 0.441 | 0.386 | NA |
| | M1 | 0.706 | 0.641 | 0.557 | NA | NA |
| *Sapajus* | Incisor | 0.498 | 0.475 | 0.446 | 0.416 | 0.381 |
| | Canine | 0.541 | 0.458 | 0.419 | NA | NA |
| | PM1 | 0.634 | 0.583 | 0.533 | 0.478 | NA |
| | M1 | 0.849 | 0.777 | 0.689 | NA | NA |
| *Saimiri* | Incisor | 0.420 | 0.381 | 0.330 | NA | NA |
| | Canine | 0.467 | 0.366 | NA | NA | NA |
| | PM1 | 0.528 | 0.453 | NA | NA | NA |
| | M1 | 0.717 | 0.599 | NA | NA | NA |
| *Cercocebus* | Incisor | 0.421 | 0.408 | 0.393 | 0.376 | 0.358 |
| | Canine | 0.481 | 0.422 | 0.398 | 0.378 | 0.360 |
| | PM1 | 0.546 | 0.520 | 0.491 | 0.460 | 0.427 |
| | M1 | 0.672 | 0.636 | 0.595 | 0.547 | 0.503 |
| *Mandrillus* | Incisor | 0.365 | 0.360 | 0.354 | 0.347 | 0.339 |
| | Canine | 0.409 | 0.366 | 0.355 | 0.344 | 0.331 |
| | PM1 | 0.487 | 0.475 | 0.462 | 0.447 | 0.433 |
| | M1 | 0.590 | 0.576 | 0.557 | 0.537 | 0.514 |
| *Theropithecus* | Incisor | 0.414 | 0.408 | 0.400 | 0.392 | 0.381 |
| | Canine | 0.453 | 0.409 | 0.395 | 0.379 | 0.363 |
| | PM1 | 0.538 | 0.525 | 0.511 | 0.494 | 0.476 |
| | M1 | 0.643 | 0.627 | 0.605 | 0.582 | 0.553 |
| *Pan* | Incisor | 0.475 | 0.467 | 0.456 | 0.445 | 0.432 |
| | Canine | 0.543 | 0.510 | 0.491 | 0.474 | 0.455 |
| | PM1 | 0.630 | 0.610 | 0.590 | 0.568 | 0.546 |
| | M1 | 0.785 | 0.762 | 0.731 | 0.701 | 0.665 |

**Table A6.8 Male mechanical advantage for the temporalis, at linear gape heights ranging from occlusion (0 mm) to 40mm.**

| | | Occlusion | 10mm | 20mm | 30mm | 40mm |
|---|---|---|---|---|---|---|
| **Species** | **Tooth** | **Mechanical advantage** | | | | |
| *Ateles* | Incisor | 0.400 | 0.382 | 0.361 | 0.338 | 0.313 |
| | Canine | 0.457 | 0.391 | 0.359 | 0.328 | NA |
| | PM1 | 0.509 | 0.473 | 0.439 | 0.398 | 0.361 |
| | M1 | 0.660 | 0.614 | 0.554 | 0.487 | NA |
| *Cacajao* | Incisor | 0.436 | 0.417 | 0.393 | 0.365 | 0.335 |
| | Canine | 0.521 | 0.445 | 0.404 | NA | NA |
| | PM1 | 0.597 | 0.550 | 0.501 | 0.445 | NA |
| | M1 | 0.762 | 0.703 | 0.622 | 0.564 | NA |
| *Chiropotes* | Incisor | 0.436 | 0.410 | 0.376 | 0.337 | 0.307 |
| | Canine | 0.524 | 0.417 | NA | NA | NA |
| | PM1 | 0.603 | 0.537 | 0.467 | NA | NA |
| | M1 | 0.780 | 0.696 | 0.581 | NA | NA |
| *Pithecia* | Incisor | 0.424 | 0.393 | 0.357 | 0.316 | NA |
| | Canine | 0.491 | 0.403 | 0.350 | NA | NA |

320

| Species | Tooth | | | | | |
|---|---|---|---|---|---|---|
| | PM1 | 0.550 | 0.488 | 0.422 | NA | NA |
| | M1 | 0.716 | 0.632 | 0.526 | NA | NA |
| *Cebus* | Incisor | 0.432 | 0.410 | 0.382 | 0.350 | 0.318 |
| | Canine | 0.486 | 0.403 | 0.360 | NA | NA |
| | PM1 | 0.559 | 0.508 | 0.457 | 0.402 | NA |
| | M1 | 0.744 | 0.671 | 0.574 | NA | NA |
| *Sapajus* | Incisor | 0.491 | 0.466 | 0.433 | 0.399 | 0.359 |
| | Canine | 0.534 | 0.440 | 0.396 | NA | NA |
| | PM1 | 0.626 | 0.568 | 0.512 | 0.450 | NA |
| | M1 | 0.837 | 0.757 | 0.657 | NA | NA |
| *Saimiri* | Incisor | 0.375 | 0.336 | 0.280 | NA | NA |
| | Canine | 0.417 | 0.311 | NA | NA | NA |
| | PM1 | 0.472 | 0.395 | NA | NA | NA |
| | M1 | 0.642 | 0.518 | NA | NA | NA |
| *Cercocebus* | Incisor | 0.333 | 0.317 | 0.298 | 0.278 | 0.258 |
| | Canine | 0.386 | 0.311 | 0.283 | 0.260 | 0.243 |
| | PM1 | 0.438 | 0.403 | 0.367 | 0.331 | 0.294 |
| | M1 | 0.539 | 0.492 | 0.441 | 0.386 | 0.338 |
| *Mandrillus* | Incisor | 0.258 | 0.251 | 0.243 | 0.234 | 0.224 |
| | Canine | 0.289 | 0.234 | 0.221 | 0.209 | 0.196 |
| | PM1 | 0.344 | 0.328 | 0.310 | 0.293 | 0.276 |
| | M1 | 0.416 | 0.397 | 0.373 | 0.348 | 0.322 |
| *Theropithecus* | Incisor | 0.325 | 0.313 | 0.300 | 0.288 | 0.274 |
| | Canine | 0.355 | 0.291 | 0.274 | 0.257 | 0.240 |
| | PM1 | 0.422 | 0.398 | 0.377 | 0.355 | 0.334 |
| | M1 | 0.504 | 0.476 | 0.444 | 0.414 | 0.381 |
| *Pan* | Incisor | 0.407 | 0.397 | 0.384 | 0.370 | 0.355 |
| | Canine | 0.466 | 0.424 | 0.402 | 0.382 | 0.361 |
| | PM1 | 0.541 | 0.515 | 0.490 | 0.465 | 0.439 |
| | M1 | 0.674 | 0.644 | 0.607 | 0.571 | 0.530 |

**Table A6.9 Female and male in- and out-lever lengths for masseter and temporalis at bite height of 20 mm on each tooth, lengths in mm.**

| Species | Tooth | Female | | | Male | | |
|---|---|---|---|---|---|---|---|
| | | In-lever masseter | In-lever temporalis | Out-lever | In-lever masseter | In-lever temporalis | Out-lever |
| *Ateles* | Incisor | 31.169 | 27.543 | 76.540 | 32.019 | 27.549 | 76.365 |
| | Canine | 29.274 | 25.650 | 67.839 | 28.506 | 23.982 | 66.854 |
| | PM1 | 30.143 | 26.524 | 61.345 | 30.803 | 26.303 | 59.968 |
| | M1 | 29.455 | 25.849 | 47.330 | 30.125 | 25.600 | 46.227 |
| *Cacajao* | Incisor | 27.506 | 21.624 | 61.483 | 30.811 | 26.142 | 66.575 |
| | Canine | 24.864 | 18.596 | 50.337 | 27.206 | 22.518 | 55.716 |
| | PM1 | 26.013 | 19.881 | 44.194 | 29.026 | 24.325 | 48.550 |
| | M1 | 25.145 | 18.915 | 34.110 | 28.426 | 23.720 | 38.084 |
| *Chiropotes* | Incisor | 21.260 | 17.475 | 51.356 | 24.714 | 20.773 | 55.220 |
| | Canine | 18.484 | 14.523 | 42.705 | NA | NA | 45.958 |
| | PM1 | 20.754 | 15.527 | 36.877 | 22.789 | 18.648 | 39.894 |
| | M1 | 18.626 | 18.164 | 27.677 | 22.154 | 17.967 | 30.855 |

| | | | | | | | |
|---|---|---|---|---|---|---|---|
| Pithecia | Incisor | 21.553 | 16.698 | 49.545 | 22.772 | 18.452 | 51.501 |
| | Canine | 19.057 | 14.006 | 42.303 | 20.278 | 15.683 | 44.540 |
| | PM1 | 19.939 | 14.931 | 38.040 | 21.375 | 16.867 | 39.706 |
| | M1 | 19.115 | 14.065 | 28.771 | 20.726 | 16.164 | 30.534 |
| Cebus | Incisor | NA | NA | NA | 21.494 | 22.444 | 58.735 |
| | Canine | NA | NA | NA | 18.271 | 18.756 | 52.136 |
| | PM1 | NA | NA | NA | 19.999 | 20.728 | 45.344 |
| | M1 | NA | NA | NA | 18.987 | 19.575 | 34.093 |
| Sapajus | Incisor | 23.503 | 20.804 | 55.651 | 28.087 | 27.249 | 62.811 |
| | Canine | 21.480 | 18.527 | 50.613 | 24.250 | 22.908 | 57.806 |
| | PM1 | 22.010 | 19.123 | 44.463 | 26.294 | 25.228 | 49.267 |
| | M1 | 20.807 | 17.790 | 32.645 | 25.434 | 24.253 | 36.854 |
| Saimiri | Incisor | NA | NA | 33.064 | 10.874 | 9.249 | 33.041 |
| | Canine | NA | NA | 29.229 | NA | NA | 29.687 |
| | PM1 | NA | NA | 26.265 | NA | NA | 26.225 |
| | M1 | NA | NA | 19.638 | NA | NA | 19.289 |
| Cercocebus | Incisor | 33.396 | 22.137 | 76.120 | 36.271 | 27.521 | 92.280 |
| | Canine | 31.943 | 20.653 | 65.895 | 32.251 | 22.977 | 81.102 |
| | PM1 | 32.057 | 20.726 | 59.036 | 35.079 | 26.226 | 71.495 |
| | M1 | 31.062 | 19.688 | 45.677 | 34.582 | 25.636 | 58.144 |
| Mandrillus | Incisor | 38.849 | 24.171 | 102.94 | 53.895 | 37.089 | 152.44 |
| | Canine | 37.668 | 22.575 | 91.437 | 48.198 | 30.155 | 136.34 |
| | PM1 | 37.828 | 22.793 | 83.416 | 52.689 | 35.532 | 114.20 |
| | M1 | 36.934 | 21.567 | 65.596 | 52.574 | 35.387 | 94.692 |
| Theropithecus | Incisor | 41.810 | 28.571 | 98.445 | 48.885 | 36.664 | 122.20 |
| | Canine | 40.595 | 27.047 | 89.141 | 44.156 | 30.659 | 111.85 |
| | PM1 | 41.117 | 27.680 | 81.244 | 48.046 | 35.459 | 94.049 |
| | M1 | 40.665 | 27.118 | 66.463 | 47.696 | 34.980 | 78.787 |
| Pan | Incisor | 56.084 | 45.333 | 119.87 | 56.946 | 47.902 | 124.81 |
| | Canine | 54.119 | 42.886 | 104.38 | 53.633 | 43.948 | 109.11 |
| | PM1 | 54.814 | 43.734 | 91.567 | 55.473 | 46.121 | 93.974 |
| | M1 | 54.499 | 43.367 | 73.554 | 55.239 | 45.833 | 75.487 |

**Table A6.10 Female bite force along the dental row at linear gape heights ranging from occlusion (0 mm) to 40mm.**

| | | Occlusion | 10mm | 20mm | 30mm | 40mm |
|---|---|---|---|---|---|---|
| Species | Tooth | Estimated bite force (N) | | | | |
| Ateles | Incisor | 103.31 | 98.35 | 92.85 | 87.03 | 103.31 |
| | Canine | 110.93 | 103.91 | 96.39 | 89.99 | 110.93 |
| | PM1 | 126.19 | 118.50 | 109.15 | 99.95 | 126.19 |
| | M1 | 163.38 | 149.94 | 134.62 | NA | 163.38 |
| Cacajao | Incisor | 89.68 | 84.17 | 78.19 | 71.42 | 89.68 |
| | Canine | 100.54 | 91.38 | NA | NA | 100.54 |
| | PM1 | 121.07 | 109.68 | 97.80 | NA | 121.07 |
| | M1 | 155.85 | 136.64 | NA | NA | 155.85 |
| Chiropotes | Incisor | 63.35 | 58.46 | NA | NA | 63.35 |
| | Canine | 68.11 | 60.26 | NA | NA | 68.11 |
| | PM1 | 84.28 | 73.78 | NA | NA | 84.28 |
| | M1 | 111.98 | 93.76 | NA | NA | 111.98 |

| Species | Tooth | | | | | |
|---|---|---|---|---|---|---|
| Pithecia | Incisor | 60.40 | 55.66 | 50.02 | NA | 60.40 |
| | Canine | 64.04 | 56.72 | NA | NA | 64.04 |
| | PM1 | 75.30 | 66.37 | NA | NA | 75.30 |
| | M1 | 99.10 | 83.69 | NA | NA | 99.10 |
| Sapajus | Incisor | 80.59 | 74.26 | 67.23 | 61.56 | 80.59 |
| | Canine | 82.19 | 73.90 | NA | NA | 82.19 |
| | PM1 | 96.96 | 86.43 | 76.88 | NA | 96.96 |
| | M1 | 130.11 | 110.62 | NA | NA | 130.11 |
| Saimiri | Incisor | 23.11 | 19.63 | NA | NA | 23.11 |
| | Canine | 24.08 | NA | NA | NA | 24.08 |
| | PM1 | 27.62 | NA | NA | NA | 27.62 |
| | M1 | 35.97 | NA | NA | NA | 35.97 |
| Cercocebus | Incisor | 130.11 | 123.86 | 116.03 | 107.99 | 130.11 |
| | Canine | 145.22 | 135.82 | 124.91 | 116.17 | 145.22 |
| | PM1 | 164.19 | 152.14 | 138.67 | 128.18 | 164.19 |
| | M1 | 208.64 | 189.40 | 168.56 | NA | 208.64 |
| Mandrillus | Incisor | 145.32 | 140.49 | 134.68 | 128.43 | 145.32 |
| | Canine | 158.85 | 151.45 | 144.21 | 135.88 | 158.85 |
| | PM1 | 175.66 | 167.02 | 157.87 | 148.15 | 175.66 |
| | M1 | 219.57 | 205.26 | 190.16 | 173.74 | 219.57 |
| Theropithecus | Incisor | 193.53 | 187.08 | 179.29 | 170.46 | 193.53 |
| | Canine | 208.58 | 198.71 | 189.41 | 178.15 | 208.58 |
| | PM1 | 233.11 | 221.68 | 210.02 | 196.91 | 233.11 |
| | M1 | 282.41 | 267.06 | 248.61 | 229.60 | 282.41 |
| Pan | Incisor | 293.77 | 284.95 | 275.51 | 265.48 | 293.77 |
| | Canine | 325.70 | 313.04 | 299.55 | 286.49 | 325.70 |
| | PM1 | 377.74 | 362.51 | 346.81 | 329.40 | 377.74 |
| | M1 | 470.28 | 448.18 | 424.14 | 398.26 | 470.28 |

**Table A6.11 Male bite force along the dental row at linear gape heights ranging from occlusion (0 mm) to 40mm.**

| | | Occlusion | 10mm | 20mm | 30mm | 40mm |
|---|---|---|---|---|---|---|
| Species | Tooth | Estimated bite force (N) | | | | |
| Ateles | Incisor | 126.90 | 120.53 | 113.65 | 106.03 | 126.90 |
| | Canine | 131.20 | 121.49 | 112.20 | NA | 131.20 |
| | PM1 | 157.65 | 147.21 | 134.80 | 123.73 | 157.65 |
| | M1 | 204.48 | 186.41 | 166.21 | NA | 204.48 |
| Cacajao | Incisor | 149.98 | 142.19 | 133.36 | 123.38 | 149.98 |
| | Canine | 161.98 | 148.68 | NA | NA | 161.98 |
| | PM1 | 198.64 | 182.86 | 164.56 | NA | 198.64 |
| | M1 | 253.83 | 227.93 | 205.99 | NA | 253.83 |
| Chiropotes | Incisor | 70.73 | 65.91 | 60.21 | 55.59 | 70.73 |
| | Canine | 74.12 | NA | NA | NA | 74.12 |
| | PM1 | 93.67 | 83.34 | NA | NA | 93.67 |
| | M1 | 121.27 | 104.43 | NA | NA | 121.27 |
| Pithecia | Incisor | 78.80 | 72.86 | 65.98 | NA | 78.80 |
| | Canine | 82.60 | 73.50 | NA | NA | 82.60 |
| | PM1 | 98.72 | 87.67 | NA | NA | 98.72 |
| | M1 | 127.98 | 109.98 | NA | NA | 127.98 |
| Cebus | Incisor | 77.49 | 72.40 | 66.56 | 60.78 | 77.49 |

| | | | | | |
|---|---|---|---|---|---|
| | Canine | 76.59 | 68.81 | NA | NA | 76.59 |
| | PM1 | 96.08 | 86.97 | 76.34 | NA | 96.08 |
| | M1 | 126.96 | 109.55 | NA | NA | 126.96 |
| *Sapajus* | Incisor | 153.50 | 143.58 | 133.16 | 120.96 | 153.50 |
| | Canine | 146.56 | 133.12 | NA | NA | 146.56 |
| | PM1 | 187.78 | 170.52 | 151.78 | NA | 187.78 |
| | M1 | 250.14 | 219.90 | NA | NA | 250.14 |
| *Saimiri* | Incisor | 25.18 | 21.48 | NA | NA | 25.18 |
| | Canine | 23.86 | NA | NA | NA | 23.86 |
| | PM1 | 29.82 | NA | NA | NA | 29.82 |
| | M1 | 39.35 | NA | NA | NA | 39.35 |
| *Cercocebus* | Incisor | 182.40 | 173.88 | 164.41 | 155.13 | 182.40 |
| | Canine | 184.68 | 171.63 | 160.95 | 152.13 | 184.68 |
| | PM1 | 231.85 | 215.79 | 199.35 | 181.87 | 231.85 |
| | M1 | 283.31 | 260.70 | 235.17 | 212.25 | 283.31 |
| *Mandrillus* | Incisor | 338.90 | 330.67 | 322.10 | 312.56 | 338.90 |
| | Canine | 332.14 | 318.86 | 306.20 | 292.64 | 332.14 |
| | PM1 | 445.00 | 428.11 | 410.83 | 394.07 | 445.00 |
| | M1 | 537.13 | 514.81 | 489.85 | 463.47 | 537.13 |
| *Theropithecus* | Incisor | 302.14 | 293.58 | 284.99 | 274.97 | 302.14 |
| | Canine | 293.74 | 280.72 | 267.05 | 253.40 | 293.74 |
| | PM1 | 387.18 | 372.41 | 356.18 | 339.91 | 387.18 |
| | M1 | 462.21 | 440.17 | 417.70 | 391.89 | 462.21 |
| *Pan* | Incisor | 401.03 | 390.01 | 378.80 | 366.30 | 401.03 |
| | Canine | 434.14 | 415.94 | 399.02 | 380.30 | 434.14 |
| | PM1 | 522.76 | 502.32 | 481.05 | 459.37 | 522.76 |
| | M1 | 652.73 | 622.20 | 592.10 | 557.22 | 652.73 |

# Appendix 7 - Comparison of different real seeds

Force to fracture was measured for a range of seeds (pecan, hazelnut, Brazil nut) to compare seed performance. A physical testing machine (Mecmesin MultiTest 2.5-*i*) was used. Data was collected in collaboration with another researcher, Mariana Fogaça. Seeds were measured on their longitudinal and transverse axes and the 'sulcus', the join between seed halves, was marked on one side. Seeds were placed on the centre of PM1 – PM2 on the specimen *Sapajus* 90010 (see Ch. 4, 4.3 for manufacture). The marked sulcus was aligned to this bite point for all seed types. As opposed to the main study (Ch 4), seeds were tested without gape, and dental rows were in a flat plane. The physical testing machine test program run was identical to that run in Ch 4 (see section 4.3.7.1). For each seed type n = 30 seeds were tested. Emperor (v.1.18-408, Mecmesin, UK) was used to record and export data, plots were made in RStudio (v1.1.442, RStudio Team 2016) with the package ggplot2 (Wickham, 2016). Results (A6.1) found differences between seed types. The Brazil nut required a much higher force to fracture (median 443.9N) than either the pecan or hazelnut, which were quite similar in median force (166.7N for pecan, 180N for hazelnut). However, the pecan had the most consistent results, with the hazelnut showing a broad spread (SD 98.6) and an even broader spread for the Brazil nut (SD 112.2).
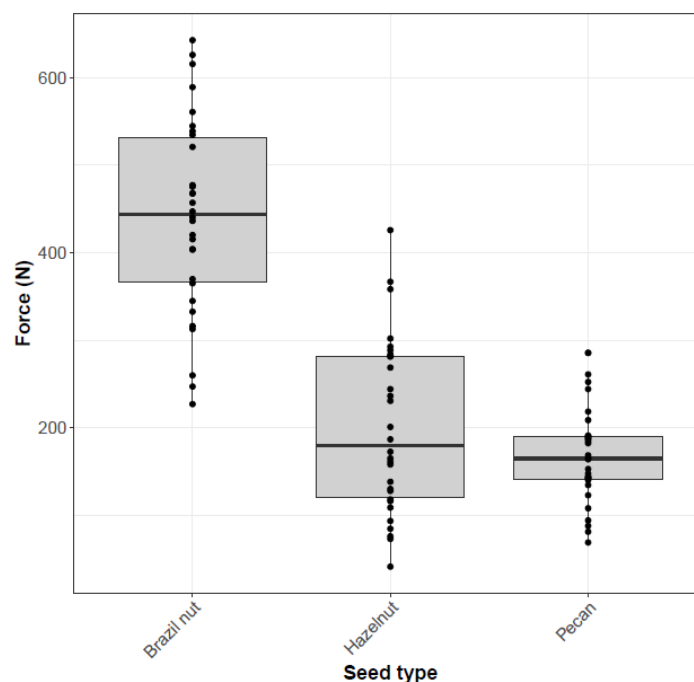


**Table A7.1 Boxplot comparing force to fracture for three seed types (Brazil nut, hazelnut, and pecan), with each point representing a single sample.**

# Appendix 8 - Displacement at fracture

Displacement (mm) at the point of fracture initiation was extracted for each tooth and specimen. Results as plotted (Figs. A7.1-A7.4 and tabulated, Table A7.1).
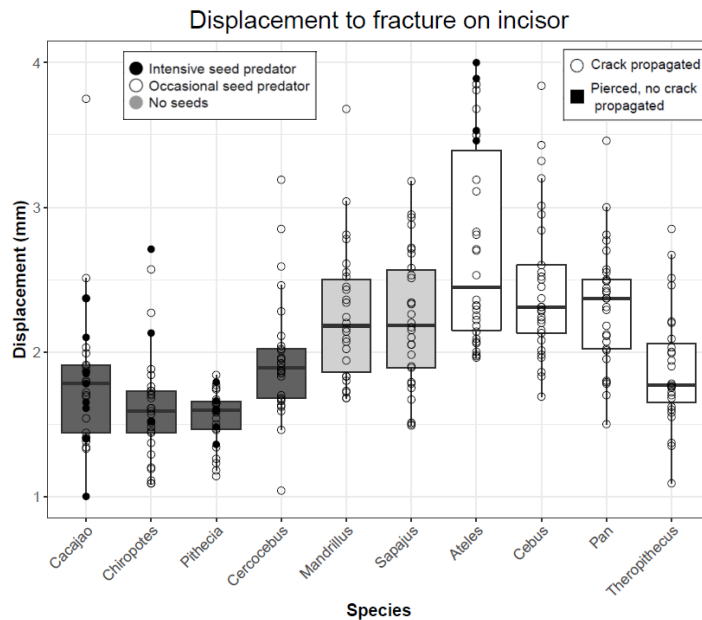


**Figure A8.1 Boxplot showing displacement at fracture on incisor for all species. Anterior seed predators are *Cacajao, Chiropotes,* and *Pithecia*. Posterior seed predators are *Cercocebus, Mandrillus* and *Sapajus.***
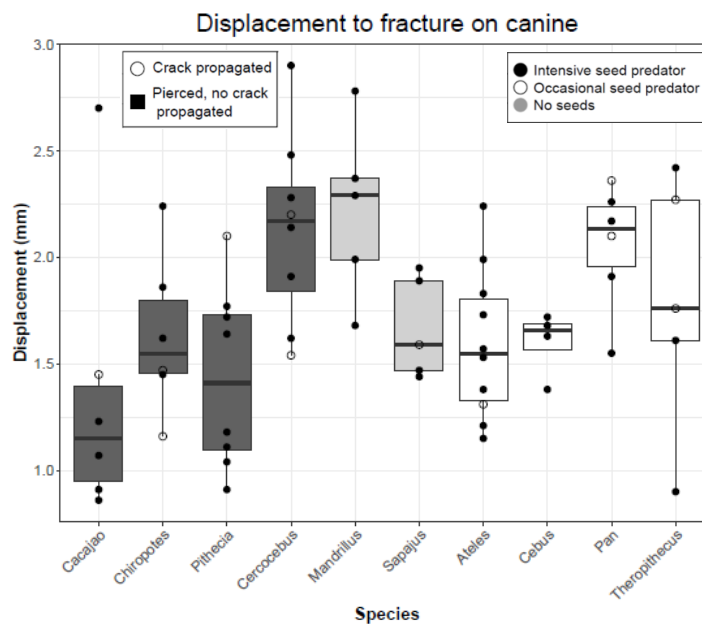


**Figure A8.2 Boxplot showing displacement at fracture on canine for all species. Anterior seed predators are *Cacajao, Chiropotes,* and *Pithecia*. Posterior seed predators are *Cercocebus, Mandrillus* and *Sapajus.***
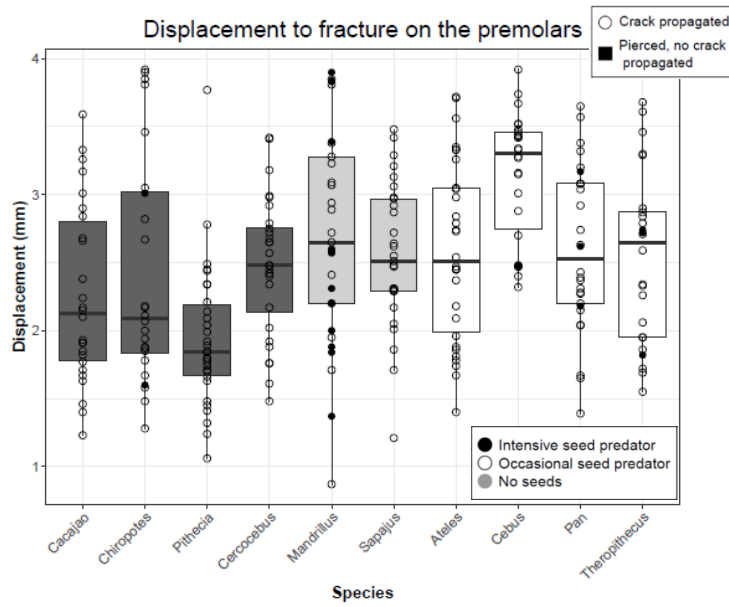
**Figure A8.3 Boxplot showing displacement at fracture on premolar bites for all species. Anterior seed predators are *Cacajao, Chiropotes,* and *Pithecia*. Posterior seed predators are *Cercocebus, Mandrillus* and *Sapajus.***
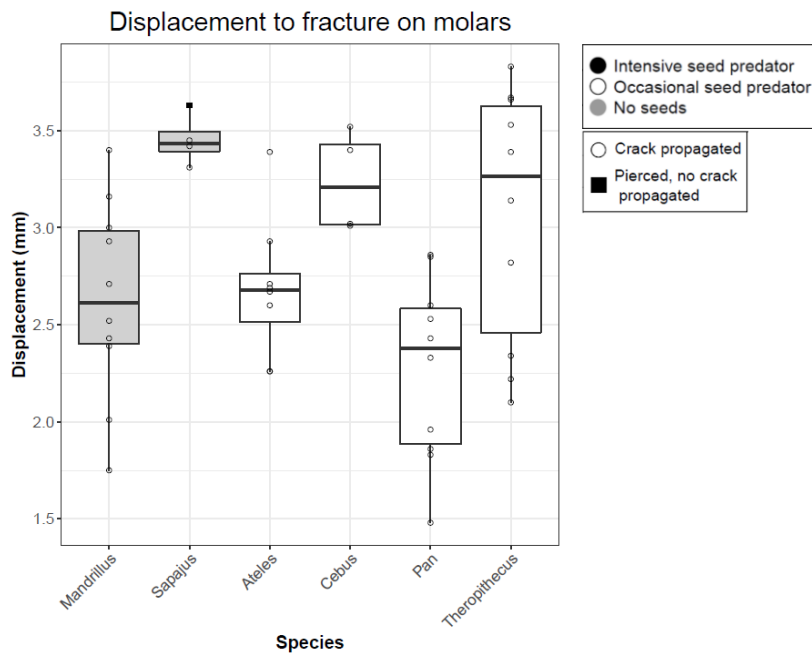


**Figure A8.4 Boxplot showing displacement at fracture on molar bites for all species. Anterior seed predators are *Cacajao, Chiropotes,* and *Pithecia*. Posterior seed predators are *Cercocebus, Mandrillus* and *Sapajus.***

**Table A8.1 Mean and median displacement at fracture (in mm), and standard deviation (SD) for each species on each bite point**.

| Species | Tooth | Displacement to initiate fracture | | |
|---|---|---|---|---|
| | | Mean (N) | Median (N) | SD |
| *Cacajao* | Incisor | 1.81 | 1.78 | 0.51 |
| | Canine | 1.37 | 1.15 | 0.69 |
| | Premolar | 2.26 | 2.13 | 0.66 |
| | Molar | NA | NA | NA |
| *Chiropotes* | Incisor | 1.63 | 1.59 | 0.40 |
| | Canine | 1.63 | 1.55 | 0.38 |
| | Premolar | 2.41 | 2.09 | 0.85 |
| | Molar | NA | NA | NA |
| *Pithecia* | Incisor | 1.54 | 1.60 | 0.19 |
| | Canine | 1.43 | 1.41 | 0.43 |
| | Premolar | 1.94 | 1.85 | 0.53 |
| | Molar | NA | NA | NA |
| *Cercocebus* | Incisor | 1.95 | 1.89 | 0.42 |
| | Canine | 2.13 | 2.17 | 0.45 |
| | Premolar | 2.48 | 2.48 | 0.51 |
| | Molar | NA | NA | NA |
| *Mandrillus* | Incisor | 2.26 | 2.18 | 0.47 |
| | Canine | 2.22 | 2.29 | 0.41 |
| | Premolar | 2.70 | 2.65 | 0.80 |
| | Molar | 2.63 | 2.62 | 0.51 |
| *Sapajus* | Incisor | 2.23 | 2.19 | 0.46 |
| | Canine | 1.67 | 1.59 | 0.24 |
| | Premolar | 2.56 | 2.51 | 0.53 |
| | Molar | 3.45 | 3.44 | 0.13 |
| *Ateles* | Incisor | 2.73 | 2.45 | 0.69 |
| | Canine | 1.59 | 1.55 | 0.35 |
| | Premolar | 2.58 | 2.51 | 0.66 |
| | Molar | 2.69 | 2.68 | 0.36 |
| *Cebus* | Incisor | 2.45 | 2.31 | 0.52 |
| | Canine | 1.60 | 1.66 | 0.15 |
| | Premolar | 3.14 | 3.31 | 0.47 |
| | Molar | 3.24 | 3.21 | 0.26 |
| *Pan* | Incisor | 2.31 | 2.37 | 0.42 |
| | Canine | 2.06 | 2.14 | 0.29 |
| | Premolar | 2.60 | 2.53 | 0.60 |
| | Molar | 2.27 | 2.38 | 0.47 |
| *Theropithecus* | Incisor | 1.89 | 1.77 | 0.41 |
| | Canine | 1.79 | 1.76 | 0.60 |
| | Premolar | 2.54 | 2.65 | 0.64 |
| | Molar | 3.07 | 3.27 | 0.66 |
| | | | | |